TETRA TECH EBA

OQM | Organizational Quality Management Program

PIGEON CREEK HAZARD ASSESSMENT

PRESENTED TO

TOWN OF CANMORE

NOVEMBER 2016
ISSUED FOR USE
FILE: 704-V13203145-01

CONSULTING ENGINEERS & SCIENTISTS · www.eba.ca

Tetra Tech EBA Inc.
Suite 1000 – 10th Floor, 885 Dunsmuir Street
Vancouver, BC V6C 1N5 CANADA
Tel 604.685.0275 Fax 604.684.6241

This page intentionally left blank.

EXECUTIVE SUMMARY

Objective

The main objective of this assessment is to establish a relation between the frequencies (or return period) and the magnitudes of flood and debris flood hazards that could potentially impact infrastructure, properties and people in the Pigeon Creek fan, with focus on the area known as Dead Man Flats. Hydraulic modeling was carried out to delineate hazard areas on the fan for floods with various return periods.

Background

A high intensity and long duration rainstorm event occurred in southwestern Alberta between June 19 and 21, 2013. This event resulted in high flows on the larger rivers, such as the Bow River, and floods and debris floods on many of its mountainous tributaries. Many of the alluvial fans of these tributaries experienced significant flooding, sediment influx, aggradation, erosion, and channel avulsions. Pigeon Creek was no exception. In response to the flood event, Tetra Tech was retained by the Town of Canmore to carry out a detailed hazard assessment on Pigeon Creek. Output data from the hazard assessment presented in this report was used on the preparation of the risk assessment by the Town of Canmore..

Geology

The Pigeon Creek study area is underlain by slightly metamorphosed sedimentary rocks of Carboniferous to Cretaceous age: mainly limestone, dolostone, siltstone and shale. Till, bedrock, and colluvium are present in the upper watershed, while alluvial fan sediments and Bow River flood deposits are found in the fan area.

Fan deposits appear to overlie glaciolacustrine clay, in at least in one location near the Bow River. Although the fans in the Bow Valley are all still active, most of the fan formation likely occurred from 12,000 to 6,000 years ago following deglaciation of the region, when vegetation was less extensive or nonexistent.

Watershed

Pigeon Creek is a third to fourth order stream flowing northward for 8 km from an elevation of 3,153 masl to the Bow River (elevation 1291 masl). The Pigeon Creek watershed upstream of the apex has an area of 55.1 km^2, and average gradient of 11 percent. The watershed contains three subcatchments. These are, from west to east: West Wind Creek; Wind Creek; and Pigeon Creek. Based on the Melton ratios, the Pigeon Creek watershed is likely dominated by flood events, although debris flood events can be expected within the occurrence of a flood event.

Review of historical air photographs suggested that most of the slide areas within the watershed were already established by 1947 which was the date of earliest air photos. These photos showed that the lower slopes in the watershed were covered with a thick layer of glacially-derived till that likely overlies bedrock. It is the periodic failures that happen in these sediments that are most important to fan development. The fresher appearance of slide areas and higher number of slides in the upper watershed in the 1950 air photographs compared to later years is considered to indicate that debris slide activity was a fairly recent phenomenon in 1950 and may have been preceded by a large, stand-replacing, fire.

The earliest photos illustrated that the upper watershed showed evidence of large, stand-replacing forest fires. Most of the area was covered with young conifers, with a few islands of older conifers. Older conifers are more common at high elevations as well. On the south valley wall of upper Pigeon Creek, stand variability shows evidence of a number of small fires. On the opposite side of the valley at this location, a large pale area showed a more recent fire, where bushes were just starting to regenerate on the landscape.

Exposed bedrock, rockfalls and rockslides at high elevations within the watershed are active, but do not contribute significantly to the debris that is incorporated in debris floods, as this debris appears to remain in the higher elevation areas. The lower slopes are covered with a thick layer of surficial material (till) overlying bedrock, which supplies most of the granular material for debris floods. Debris slides developed in these materials along the eastern slopes of Pigeon and Wind creeks are the most common form of mass movement.

Many of the debris slides evident in in the upper watershed in 1950 became quite overgrown prior to the June 2013 event. During the June 2013 event, many new slides formed, but these are not as extensive or as large as those visible on the 1950 photographs. Slides reactivated on the eastern slopes of Pigeon Creek during the 2013 event, but those on the eastern slope of Wind Creek remained stable. In 2013 slides on the west slope of Wind Creek reactivated much older slide surfaces instead.

Dendrochronology

Based on the determination of ages and growth patterns of trees, dendrochronology is an absolute method for evaluating the minimum age of the surface upon which the tree is growing and the frequency of various types of disturbance events over the last few hundred years.

On the fan, seventy-eight (78) percent of the aged trees (which represented the largest diameter trees in the sampled areas) are less than 100 years old and 73 percent are between 50 and 100-years old which suggests that the last major event occurred about 100 years ago. The relatively even age of the trees at the fan apex, excluding the island of older trees (>200 years), suggests that the last morphologically significant event on the fan was in excess of 80 years ago (older than 1934).

In the watershed, the age distribution of the cored trees indicates that 29 percent are in the 50-100 year class, 26 percent are in the 100-150 year class, 26 percent are in the 150-200 year class and 19 percent are older than 200 years. Field evidence of channel avulsions very similar to that observed upstream of large woody debris jams after the 2013 event suggests that there was a morphologically significant flood event about 63 to 64 years ago (early 1950's) based on the ages of trees growing on the bed of the abandoned channel. Inferred and reported flood events were identified on nearby watersheds between 1948 and 1956, so it is likely that there was an event on Pigeon Creek in that time frame. The aerial photographic analysis of the Pigeon Creek fan identified that there was a significant change in the creek alignment on the distal portion of the fan between 1950 and 1962. Since many trees adjacent to Pigeon Creek survived the 2013 flood, it is possible that a number survived this flood event as well.

Fan

Radiometric dating of organic materials found within watershed and fan sediments was used to determine limiting dates for older flood and debris floods, those beyond the reach of dendrochronological dating. The timing and frequency of debris floods in the watershed is generally unknown, but one radiocarbon date showed that one debris flood unit is less than 2010 years old.

Events on the west side of the fan in the vicinity of the 2013 debris flood appear to have occurred (in radiocarbon years BP): 520 years ago; between 520 and 850 years ago; between 880 and 1260 years ago; and, between 1260 and possibly 1820 years ago. Four debris flood events and one lower sediment concentration water flood event appear to have occurred in this time frame. Deposits close to the present Pigeon Creek alignment are thickest, which is interpreted to indicate that the deposits younger than 850 years old probably formed in floods that occurred in approximately the same location as the present creek alignment.

The eastern portion of the fan is older. Its debris flood deposits formed: <1820 years ago (possibly the same event as the western fan) >1260 to <1820 year event; >2510 to <2890 years ago; >2890 to <3280 years ago; >3280 to <3430 years ago; and, > 3430 years ago.

Landslide Damming by Bedrock Failure

Two possible deep-seated bedrock failure areas are found about 190 m upstream of the Pigeon Creek waterfall at a sharp bend in the creek. One is a smaller feature on the northwest side of the creek (Slide A) and the other (Slide B) is larger and is situated on the southeast side of the creek, surrounding the creek's outer bend. Both slides pre-date the 1950 air photos.

It is theoretically possible for the deep-seated bedrock failure to dam Pigeon Creek within its canyon located immediately upstream of the fan apex. No evidence of landslide debris dams were observed during the field investigation so it is not possible to accurately ascribe a frequency for such an event.

The estimated peak discharge from an outburst flood are in the order of 75 m^3/s. The volume of water released under such an event is orders of magnitude less that the estimated runoff volume from the 2013 event.

Fire History and Significance

The very common presence of charcoal and charred materials within the Pigeon Creek coarse fan deposits is interpreted to indicate that fires, both on the fans and in the contributing watersheds, may have been previously unrecognized drivers for the dated fan disturbance events. Because charcoal generally does not travel too far from its source, it may be a good indicator of past fire history in the area. Post-severe fire flood, debris flood and debris flow hazards, while common in the western United States, have only recently been recognized in Canada (Jordan, 2012).

The influence of fires on watershed processes is significant. The destruction of the plant canopy, litter and duff in forested watersheds and the development of hydrophobic soil properties following high severity burns that are typical of relatively infrequent (200-300 year recurrence intervals prior to effective fire suppression over the last 100- years) stand-replacing fires, can lead to significant increases in flood peaks and runoff volumes during post-fire rainfall events and significant increases in watershed erosion and sediment yield. Hydrological modeling was carried out simulating 95 percent water repellency of soil after a fire for 10 percent and 20 percent of the watershed area affected by a hypothetical fire to evaluate the potential impact of fire within the Pigeon Creek watershed. The model was run under various hydrological conditions including rainfall return periods ranging between 20 and 2500 years, as well as the June 2013 event. Using the hydrographs obtained for the hypothetical fire conditions, the potential sediment volume was calculated using a bedload transport equation. The modeling results indicate that the presence of fire could lead to substantial increases in clear water peak flows and sediment volumes. The changes would result in the augmented frequency of runoff events and the associated sediment loadings. Effective fire suppression over the last 100 years may have increased the probability of a high burn severity stand-replacing fire in the future.

Debris Flood Magnitude-Frequency Relationship

Test pit profiles were prepared based on test pit logs and stratigraphy was inferred. Debris flood deposit volumes were approximated from deposit thicknesses observed in test pits and inferred, approximate planimetric areas. Event deposit age ranges were derived from radiocarbon dates and a frequency-magnitude relationship for test pit data was established.

Additionally, a frequency magnitude relationship was established based on a sediment transport analysis using a calibrated hydrologic model.

Various methods were employed to ultimately establish a debris flood frequency-magnitude relationship for return periods up to 3000 years. The relationship combines data from; a sediment transport-based yield analysis for events with 10 year to the 300 year return periods, and data from the test pit/ radiocarbon dating analysis for events with more than 750 year return period. The validity of the frequency-magnitude relationship was checked using unit yield rates against data from Cougar Creek and Three Sisters Creek.

	Unit Sediment Yield (m^3/km^2)		Sediment Yield (m^3/km^2)	Total Sediment Yield (m^3)
	Three Sisters Creek	**Cougar Creek**	**Pigeon Creek**	**Pigeon Creek**
Drainage Area (km^2)	10	42.9	55	55
Return Period (Years)				
10-30	1,000	700	700	36,000
30-100	1,400	930	1,000	54,000
100-300	1,800	1,400	1,500	74,000
300-1000	2,200	3,730	2,000	100,000
1000-3000	2,600	6,000	2,500	131,000

Hydrological Modelling

A deterministic, distributed hydrological model of the Pigeon Creek watershed was developed using the PCSWMM software. The model was used to compute creek flows under various hydrological scenarios, which were then used to estimate sediment loadings from the watershed, as explained in Section 6.5.

The Pigeon Creek watershed, upstream of the fan, was subdivided into a number of subcatchments as shown in Figure 6.1. The model was discretized to represent small and large tributaries to Pigeon Creek. Subcatchment and creek slopes were obtained from the available LiDAR data. The model computes flows for each subcatchment for a given event, producing a hydrograph which is then hydraulically routed. Flows are accumulated in the downstream direction until reaching the outfall of the system. The model was extended to the Bow River.

The model was calibrated using data from the Marmot Creek watershed as well as observed high water marks located upstream of the fan apex. For the 2013 event at the Pigeon Creek watershed in the channel immediately upstream of the waterfall the model computed a peak flow of 108 m^3/s.

Summary of June 2013 Event

Comparison of LiDAR data from 2008 and 2013 estimated that the June 2013 event deposited approximately 70,000 m^3 of debris and sediment on the fan following the flood. Using the combined frequency-magnitude relationship the June 2013 debris flood event can be assigned a return period of between 100 and 200 years.

This return period is comparable with return periods derived by BGC (2014 a,b) for the June 2013 events for both the Three Sisters and Cougar Creek watersheds and fans (about 300 years). Regardless of the estimated return period of the events in the three watersheds, it is clear that the hydro-geomorphic events on the fans, while substantial, were the result of significant rainfall and were not the result of periodic catastrophic events, such as landslide dam failures or stand-replacing fires.

Hydraulic Modeling

Using the LiDAR estimate of approximately 70,000 m^3 debris deposited on the fan during the June 2013 event, the mean sediment concentration was estimated to be 4 percent.

Debris flood modelling was carried out using PCSWMM which is a 2-dimensional volume conservation model that conveys a flood within defined channel segments and as overland flow. Five scenarios were modelled corresponding to each return period class from 10 to 3000 years. The model outputs, which includes the 2013 event, illustrate the area of potential inundation on the fan under the various scenarios. The inundated area is classified into flow depths of <1, 1-2.5 and >2.5 m as well as high, medium and low flood intensity.

PCSWMM modeling was used to evaluate fan inundation for the 2013 event and for 5 other scenarios. These 5 scenarios correspond to return period classes from 10 to 3000 years. The results suggest that during the 10 to 30 year event, most of the flows would be conveyed by highway culverts, with some flow diverted to the west and east. The model predicts some flow overtopping of George Biggy Sr. Road and continuing north through minor highway culverts and east towards the animal underpass. Moderate flood intensity is expected in the creek channel and may impact existing properties on the lower fan, including the River's Bend development project.

Under the current channel alignment, the highway culverts do not have the hydraulic capacity to convey the 30 to 100 year event. Under this scenario, water will flow west along the ditchline adjacent to highway off-ramp. Again, the model shows overtopping of George Biggy Sr. Road.

During the 100 to 300 year event the highway culverts are overwhelmed, causing a significant amount of water, sediment and debris to flow west along the ditchline. The model indicates the highway will overtop along the western edge of the fan. Some flow will go east along the highway as water and sediment crosses George Biggy Sr. Road. Under the 300 to 1000 year and 1000 to 3000 year scenarios a larger portion of the fan will be inundated. Modelling of the 2013 event shows similarities to what was observed in the field; discrepancies are explained in Table 9.3.

Risk Assessment

The results of this hazard assessment were used to complete the risk assessment which is prepared as a separate report.

TABLE OF CONTENTS

1 INTRODUCTION 1
1.1 Previous Reports 1

2 WATERSHED CHARACTERIZATION 1
2.1 Bedrock Geology 2
2.2 Surficial Geology 2

3 DEBRIS FLOOD PROCESSES 3
3.1 Terminology 3
3.2 Watershed Morphology 4

4 FREQUENCY ANALYSIS 4
4.1 Aerial Photography Interpretation 5
4.1.1 Methods 5
4.1.2 Results 6
4.1.2.1 1947 6
4.1.2.2 1950 6
4.1.2.3 1958 8
4.1.2.4 1962 to 1972 8
4.1.2.5 1984 8
4.1.2.6 1997 9
4.1.2.7 2008 9
4.1.3 Limitations 9
4.1.4 Summary 10
4.2 Dendrochronology 11
4.2.1 Introduction 11
4.2.2 Methods 11
4.2.3 Results 12
4.3 Radiocarbon Dating 16
4.3.1 Methods 16
4.3.2 Results 17
4.3.2.1 Coal Contamination 17
4.3.2.2 Ages and Interpretation 17
4.3.2.3 Summary 18
4.3.3 Limitations 19
4.4 Fire History 19
4.4.1 Discussion 20
4.4.2 Limitations 20

5 MAGNITUDE ANALYSIS 20
5.1 Peak Flow Estimates for the Event of June 19-22, 2013 based on Field Observations 21
5.1.1 Bulking Factor 21
5.1.2 Assessment of Clear Water Flows through Hydrological Modelling 22
5.1.3 Model Calibration 23

5.1.4 Pigeon Creek Hydrological Model 30
5.1.5 Assessment of 2013 Clear Water Flows at Pigeon Creek Using Watershed Model 31
5.1.6 Assessment of Pigeon Creek Clear Water Peak Flows 31
5.1.7 Assessment of Clear Water Flows Under Climate Change 35
5.2 Assessment of the 2013 Debris Flood Event Using LIDAR Data 38
5.2.1 Information Sources and Methods 39
5.2.2 Results 39
5.2.2.1 Thunderstone Quarry 40
5.2.2.2 Other areas 40
5.2.3 Limitations 40
5.2.4 Findings from BGC (2016) 40
5.3 Volume Estimates from Test Pit Profiles 41
5.3.1 Methods 41
5.3.2 Results 41
5.3.3 Limitations 42
5.4 Magnitude Estimates Using Empirical Relationships 42
5.4.1 Methods 42
5.4.2 Results 42
5.4.3 Limitations 43
5.5 Sediment Volume Estimates Using Modified Bedload Transport Equations 44
5.5.1 Methods 44
5.5.2 Results 45

6 FIRE HISTORY AND EFFECTS 48
6.1 Association with Landslides and Erosion 48
6.2 Influence of Climate 49
6.3 Influence of Local Factors 49
6.3.1 Elevation 49
6.3.2 Aspect 49
6.4 Fire Suppression 50
6.5 Timing 50
6.5.1 Return Periods 50
6.5.2 High Fire Frequency Periods 50
6.5.3 Potential Effects of Forest Fires on the Hydrological Response of the Pigeon Creek Watershed 50
6.5.4 Limitations 52

7 LANDSLIDE DAMMING BY BEDROCK FAILURE 52
7.1.1 Dam Outburst Flood 53

8 FREQUENCY-MAGNITUDE RELATIONSHIPS 54
8.1 Introduction 54
8.2 Frequency Magnitude from Sediment Yield Analysis 54
8.3 Frequency-Magnitude Estimates from Test Pit Analysis 54
8.3.1 Method 54
8.3.2 Results 55

8.3.3 Limitations 56
8.4 Combined Frequency-Magnitude Analysis 57
8.5 Comparison of Unit Sediment Yield 58

9 DEBRIS FLOOD MODELLING 59
9.1 Sediment Concentration and Bulked Flows 59
9.2 Debris Flood Modelling 60
9.2.1 Model Input 60
9.2.2 Hydraulic Structures 60
9.2.3 Model Runs and Results 61
9.2.3.1 Scenario 1 61
9.2.3.2 Scenario 2a 62
9.2.3.3 Scenario 2b 62
9.2.4 Limitations 62

10 CONCLUSIONS 62

11 CLOSURE 64

12 REFERENCES 65

LIST OF TABLES IN TEXT

Table 3.1: Classifications of Flows by Sediment Concentration (modified from O'Brien, 1986) 4
Table 3.2: Morphology Data for the Three Subcatchment Areas 4
Table 4.1: Pigeon Creek Fan and Watershed Historical Aerial Photographs 5
Table 4.2: Watershed Tree Establishment and Disturbance Events 15
Table 5.1: Comparison of Key Characteristics Between Marmot and Pigeon Creek Watershed 25
Table 5.2: Infiltration Parameters (Green&Ampt Method) Based on Surficial Geology Mapping 26
Table 5.3: Summary of 3-day storm volumes (Kananaskis Station) for various return periods and corresponding computed clear water peak flows 32
Table 5.4: Summary of 24-hr storm intensities (Kananaskis Station) for various return periods and corresponding computed clear water peak flows 34
Table 5.5: Climate Change Monthly Adjustment Factors** 36
Table 5.6: Summary of computed peak flows under climate change scenario for 3-day storms 37
Table 5.7: Intensity Duration Frequency Rainfall (mm/hr) under Climate Change – Scenario RCP 8.5 37
Table 5.8: Summary of computed peak flows under climate change scenario for 24-hr storms 38
Table 5.9: Pigeon Creek Fan: Summary of Differential Surface using LIDAR from 2008 and 2013 40
Table 5.10: Debris Flood Event Volumes Estimated from Test Pit Interpretation 41
Table 5.11: Estimated Sediment Volumes Using BGC (2014) Equation Applied to Watershed 43
Table 5.12: Estimated Sediment Volumes Using BGC (2014) Equation Applied to Subcatchments 43
Table 5.13: Bedload Transport Sediment Volume 46
Table 5.14: Summary of Bulked Peak Flows 48
Table 5.15: Potential Effects of Fire in the Hydrological Response of Pigeon Creek Watershed 51
Table 7.1: Volume of deep-seated slide material 53
Table 7.2: Estimated Peak Discharge resulting from Dam Outburst Flood 53

Table 8.1: Estimated Magnitude-Frequencies for all Events in Test Pit Data Set 55
Table 8.2: Frequency Magnitude Relationship of Debris Flood Events in the Pigeon Creek Watershed 57
Table 8.3: Estimate of Sediment Yield for Pigeon Creek 59
Table 9.1: Highway Culvert – Twin – Details 60
Table 9.2: Highway Culvert – Downstream – Details 60

LIST OF FIGURES IN TEXT

Figure 4.9. Age Classes of Sampled Trees in the Pigeon Creek Watershed. 14
Figure 4.10. Frequency of Release-Type Events in the Pigeon Creek Watershed 15
Figure 5.1. Marmot Creek and Pigeon Creek Watersheds 24
Figure 5.2. Pigeon Creek and Marmot Creek Watersheds Aspect 25
Figure 5.3. Precipitation Data for the Event of June 19 to 21, 2013 at 3 stations at the Marmot Creek Research Basin.(Figure provided by the University of Saskatchewan through BGC Engineering and the Town of Canmore) 26
Figure 5.4. Marmot Creek Hydrograph: Observed vs. Computed Flows 28
Figure 5.5. Marmot Creek Calibration Scattered Plot to Compare Observed vs. Computed Peak Flows 29
Figure 5.6. Pigeon Creek Watershed – Model Discretization 30
Figure 5.7. Computed Clear Water Hydrographs for various 3-day Return Period Rainfall Events 32
Figure 5.8. Intensity Duration Frequency (IDF) Curve for the Kananaskis Station (Environment Canada Station 3053600) 33
Figure 5.9. Computed Clear Water Hydrographs for various 24-hr Return Period Rainfall Events 33
Figure 5.10. Computed Clear Water Hydrographs for various 12-hr Return Period Rainfall Events 34
Figure 5.11. Computed Clear Water Hydrographs for various 6-hr Return Period Rainfall Events 35
Figure 5.12. Climate Change Adjustment Factors for the Canmore Area. Monthly Temperature Adjustments for Near Term Projections (2020 to 2049) 36
Figure 5.13. Computed Clear Water Hydrographs for various 24-hr Return Period Rainfall Modified to Account for Climate Change Scenario RCP 8.5 38
Figure 5.17. Computed Sediment Loads using Modified Bedload Transport Equations 46
Figure 5.18. 2013 Event – Computed Bulked Flows and Sediment Concentrations 47
Figure 5.19. Pigeon Creek Bulked Flows 47
Figure 8.1. Pigeon Creek Frequency-Magnitude Data Points from Test Pit Analysis with a Logarithmic Curve Fitted to Circle Symbol Data Points, Three Sisters Creek and Cougar Creek Curves approximated from BGC reports (2014a and 2014b) 56
Figure 8.2. Frequency-Magnitude of Debris Flood Events in the Pigeon Creek Watershed 58
Figure 9.9. Critical culverts in the Pigeon Creek Fan 61

APPENDIX SECTIONS

TABLES

Table 4.3 Radiocarbon ages obtained at Pigeon Creek
Table 4.4 Comparison of Radiocarbon Dating and Dendrochronology to known Climate Trends and Fire Histories of Adjacent Areas
Table 9.3 Summary of Model Runs Corresponding to Each Hazard Class
Table 9.4 Summary of Model Runs Corresponding to Each Hazard Class – Scenario 1
Table 9.5 Summary of Model Runs Corresponding to Each Hazard Class – Scenario 2a
Table 9.6 Summary of Model Runs Corresponding to Each Hazard Class – Scenario 2b

FIGURES

Figure 1.1 Project Location
Figure 1.2 Pigeon Creek Fan
Figure 1.3 LIDAR Contours on the Pigeon Creek Fan
Figure 2.1 Geology of the Pigeon Creek Area
Figure 2.2 Surficial Geology of the Pigeon Creek Area
Figure 4.1 Location of Selected Photos in the Watershed
Figure 4.2 Location of Selected Photos on the Fan
Figure 4.3 June 2013 Event – Fan Inundation and Aggradation Impacted Area
Figure 4.4 Geomorphic Features in the Watershed
Figure 4.5 Geomorphic Features on the Fan
Figure 4.6 Historic Alignments of Pigeon Creek on the Fan
Figure 4.7 Tree Core Locations and Age on the Fan
Figure 4.8 Tree Core Locations and Age in the Watershed
Figure 4.11 Sampled Natural Exposure Site Locations in the Watershed
Figure 4.12 Sampled Test Pit and Exposure Locations on the Fan
Figure 4.13 Test Pit Profiles on the Fan – Lower Fan
Figure 5.14 LiDAR derived DEM Elevation Differences Between 2008 and 2013 of Pigeon Creek Fan
Figure 5.15 Test Pit Profiles on the Fan – Lower Fan
Figure 5.16 Test Pit Profiles on the Fan – Upper Fan and North - South
Figure 9.1 Mesh Grid Used for Two Dimensional Modeling
Figure 9.2 Flood Intensity and Flood Depth – 10-30 yr Return Period
Figure 9.3 Flood Intensity and Flood Depth – 30-100 yr Return Period
Figure 9.4 Flood Intensity and Flood Depth – 100-300 yr Return Period
Figure 9.5 Flood Intensity and Flood Depth – 300-1000 yr Return Period
Figure 9.6 Flood Intensity and Flood Depth – 1000-3000 yr Return Period
Figure 9.7 Flood Intensity and Flood Depth – June 19-21, 2013
Figure 9.8 Composite Flood Intensity and Flood Depth – Return Period Classes
Figure 9.10 Flood Intensity and Flood Depth – 10-30 yr Return Period – Scenario 1
Figure 9.11 Flood Intensity and Flood Depth – 30-100 yr Return Period – Scenario 1
Figure 9.12 Flood Intensity and Flood Depth – 100-300 yr Return Period – Scenario 1
Figure 9.13 Flood Intensity and Flood Depth – 300-1000 yr Return Period – Scenario 1

Figure 9.14 Flood Intensity and Flood Depth – 1000-3000 yr Return Period – Scenario 1
Figure 9.15 Flood Intensity and Flood Depth – June 19-21, 2013 – Scenario 1
Figure 9.16 Composite Flood Intensity and Flood Depth – Return Period Classes – Scenario 1
Figure 9.17 Flood Intensity and Flood Depth – 10-30 yr Return Period – Scenario 2a
Figure 9.18 Flood Intensity and Flood Depth – 30-100 yr Return Period – Scenario 2a
Figure 9.19 Flood Intensity and Flood Depth – 100-300 yr Return Period – Scenario 2a
Figure 9.20 Flood Intensity and Flood Depth – 300-1000 yr Return Period – Scenario 2a
Figure 9.21 Flood Intensity and Flood Depth – 1000-3000 yr Return Period – Scenario 2a
Figure 9.22 Flood Intensity and Flood Depth – June 19-21, 2013 – Scenario 2a
Figure 9.23 Composite Flood Intensity and Flood Depth – Return Period Classes – Scenario 2a
Figure 9.24 Flood Intensity and Flood Depth – 10-30 yr Return Period – Scenario 2b
Figure 9.25 Flood Intensity and Flood Depth – 30-100 yr Return Period – Scenario 2b
Figure 9.26 Flood Intensity and Flood Depth – 100-300 yr Return Period – Scenario 2b
Figure 9.27 Flood Intensity and Flood Depth – 300-1000 yr Return Period – Scenario 2b
Figure 9.28 Flood Intensity and Flood Depth – 1000-3000 yr Return Period – Scenario 2b
Figure 9.29 Flood Intensity and Flood Depth – June 19-21, 2013 – Scenario 2b
Figure 9.30 Composite Flood Intensity and Flood Depth – Return Period Classes – Scenario 2b

APPENDICES

Appendix A Engineering Reports Review
Appendix B Test Pit Natural/Manmade Exposure Logs
Appendix C Photographs
Appendix D Bedload Transport Analysis
Appendix E Pigeon Creek: Airborne Lidar Change Detection Analysis, BGC Engineering Inc
Appendix F Tetra Tech EBA's General Conditions

LIST OF ABBREVIATIONS

BGC	BGC Engineering Inc.
IDF	Intensity Duration Frecuency.
masl	Meters above sea level.
DBH	Diameter of the individual tree.
^{14}C years BP	Radiocarbon years before present.
DEM	Digital elevation model.
BF	Bulking factor.
USEPA	United States Environmental Protection Agency.
WCRP	World Climate Research Programme.
CMIP3	WCRP Coupled Model Intercomparison Project Phase 3.
C Yrs BP	Radiocarbon dates.
Cal BP	Calibrated years before 1950.

LIST OF VARIABLES

Q_B	Bulked discharge.
Q_W	Peak clear water discharge.
Q_S	Peak volumetric sediment discharge.
C_v	Sediment concentration in percent volume (sediment volume/total volume).
C_w	Sediment concentration by weight (sediment weight/total weight).
γ	Specific weight of water.
γ_s	Specific weight of the sediment.
Φ_b	Dimensionless bedload transport.
D_x	Grain size for which x percent of the material is finer.
θ	Dimensionless shear stress.
θ_c	Critical dimensionless shear stress at the initiation of bedload transport.
Fr	Froude number.
s	Ratio of solid to fluid density.
q_b	Bedload transport rate per unit of channel width.
q	Unit discharge.
q_c	Critical unit discharge.
S	Total energy slope.
S_{red}	Energy slope reduced.
n_0	Base-level Manning's number.
n_{tot}	Total Manning's number, including stream macro-roughness.

LIMITATIONS OF REPORT

This report and its contents are intended for the sole use of the Town of Canmore and their agents. Tetra Tech EBA Inc. (Tetra Tech EBA) does not accept any responsibility for the accuracy of any of the data, the analysis, or the recommendations contained or referenced in the report when the report is used or relied upon by any Party other than the Town of Canmore, or for any Project other than the proposed development at the subject site. Any such unauthorized use of this report is at the sole risk of the user. Tetra Tech EBA's General Conditions are provided in Appendix F of this report.

1 INTRODUCTION

A high intensity, long duration rainfall event occurred in southwestern Alberta between June 19 and 21, 2013. This event resulted in high flows on the larger rivers such as the Bow River, and debris floods on many of the mountainous tributaries. The alluvial fans of these tributaries experienced significant flooding, sediment transport, aggradation, erosion and large morphologic changes. Pigeon Creek, a tributary to the Bow River located 12 km south of the Town of Canmore, was no exception. In response to the flood event, Tetra Tech was retained by the Town of Canmore (the Town) to conduct a detailed hazard assessment on Pigeon Creek, the subject of thisreport.

Figure 1.1 shows the project location and the Pigeon Creek watershed, including its alluvial fan ("the fan"). Figure 1.2 focusses on the fan area. Figure 1.3 presents the contours derived from the 2013 LiDAR data collected after the June 2013 event. The event altered the stream alignment and damaged infrastructure and private property on the fan.

Impacts to public infrastructure and private property included the following:

- Water and debris damaged or destroyed buildings at the Thunderstone Quarry (the quarry);
- Large volumes of stockpiled materials at the quarry were transported downstream and deposited further downstream on the lower fan, or into the Bow River;
- The alignment of Pigeon Creek upstream of the highway crossings shifted east and now occupies the previous ditchline of George Biggy Sr. Road;
- Sections of George Biggy Sr. road were eroded, and the road was overtopped near the quarry;
- Highway culverts were partially plugged with sediment, causing a portion of the flood to be diverted along Highway 1;
- The twin culverts at the Dead Man's Flat access road were washed out;
- The abutment of the 2 Avenue bridge collapsed;
- The area immediately east of Pigeon Creek that was being developed as residential properties was flooded and was the location of significant sediment deposition;
- Highway 1 was temporarily closed.

1.1 Previous Reports

Following the June 2013 event and prior to either the short term mitigation assessment and the detailed hazard and risk assessment, two other assessments/reports were carried out on Pigeon Creek. A preliminary hazard assessment for Pigeon Creek was completed by BGC Engineering Inc. (BGC 2013). M. Miles and Associates (Miles 2014a, b) completed a reconnaissance assessment. A summary of these reports is provided in Appendix A. Field work carried out by Tetra Tech for both the short term mitigation and the hazard and risk assessment confirmed field observations presented by BGC and M. Miles and Associates.

2 WATERSHED CHARACTERIZATION

Figure 1.1 shows the Pigeon Creek watershed and tributaries. Pigeon Creek is a third to fourth order stream flowing northward for 8 km from an elevation of 3,153 masl to the Bow River (elevation 1291 masl). The Pigeon Creek watershed has an area of 55.1 km^2, and average gradient of 11 percent. The watershed contains three subcatchments. These are, from west to east:

- West Wind Creek;
- Wind Creek; and
- Pigeon Creek.

2.1 Bedrock Geology

This section describes bedrock geology for the Pigeon Creek watershed area. Regional geology is described by BGC's (2014a). Geological maps of the Canmore area (Price 1970a, b) show that limestone, dolostone, siltstone and shale are the dominant rock types in the Pigeon Creek watershed (Figure 2.1).

On the north side of Pigeon Mountain, from north to south, the Mississippian Livingstone and Mount Head Formations and the Permian-Pennsylvanian Rocky Mountain Group make up the bedrock units. The Livingstone Formation consists of calcareous sandstone, limestone, cherty limestone and dolostone. The Mount Head Formation is similar; it is made up of grey and black limestone, argillaceous limestone, dolostone, silty dolostone and cherty dolostone. Grey sandstone, dolomitic sandstone, silty dolostone and chert make up the Rocky Mountain group. The Triassic Spray River Group (Sulphur Mountain Formation) is found on the south and west flanks of Pigeon Mountain. It comprises grey dolomitic siltstone and sandstone; red, green and brown mudstone and siltstone; as well as limestone and dolostone breccia.

Pigeon Creek is underlain by the Jurassic Fernie Group, which consists of dark grey to black shale; dark grey siltstone and sandstone; argillaceous limestone; and brown limonitic sandstone. In its northern reaches immediately south of the fan, the Sulphur Mountain Formation outcrops. Grey and black carbonaceous mudstone, shale and coal of the Jura-Cretaceous Kootenay formation underlie the Wind Creek, West Wind Creek and Wind Ridge area.

2.2 Surficial Geology

Till covers the upper watershed, and also underlies a few wetlands. A large number of debris slide deposits derived from shallow failures of the till flank from Pigeon and Wind creeks. Bedrock, visible at higher elevations, is associated with rockfall/rock slide material where it is exposed. Dead Man's Flats rests on an alluvial fan. Debris flood deposits dominate the fan; Bow River flood deposits are present around its outer edge. Glaciolacustrine clay was found at depth at one site within the fan near its distal margin.

The glacial history outlined in BGC (2014a) also applies to the Dead Man's Flats area. Please refer to that report for a detailed discussion of the glacial history of the Bow Valley area. The surficial geology map for the Pigeon Creek area is shown in Figure 2.2.

Most alluvial fan formation in the region is thought to have occurred between 12,000 and 6,000 years BP (BGC 2014a). Although the fans in the Bow Valley are all still active, as evidenced by the 2013 event, it is likely that they are less active now than they were immediately following deglaciation, both as a result of the decline in unit sediment yield over time within the paraglacial sedimentation cycle (Church and Ryder 1972; Church and Slaymaker 1989) and due to a lack of vegetation at that time (Kostaschuk et al. 1986).

Rockslides, most of which originated at high elevations, are common in the Kananaskis area to the south; these have been modifying mountain landscapes for the last 10,000 years (Cruden and Eaton 1987).

3 DEBRIS FLOOD PROCESSES

3.1 Terminology

Mountain creeks can experience different hydro-geomorphological processes ranging from floods to debris floods to debris flows. Distinction between these processes is important, as they differ in flow mechanics and potential consequences. Transitions between processes are common within space and time during an event, with floods transitioning into debris floods and eventually debris flows through progressive sediment entrainment. Conversely, dilution of a debris flow through partial sediment deposition and tributary injection of water can lead to a transition towards debris floods and eventually floods. Definitions of these processes are listed below:

- *Flood:* For the practical purposes of this study, floods are defined as water flows with sediment concentrations up to 10 percent by volume (i.e. selected threshold to debris flood); however, others may use a threshold up to 20 percent (FLO-2D, 2015). Sediment in floods is transported as suspended load and bed load.

- *Debris Flood:* Debris floods can be defined as “a very rapid, surging flow of water, heavily charged with debris in a steep channel” (Hungr et al. 2001). Debris floods typically occur on creeks with channel gradients between 3 and 30 percent. The term “debris flood” is similar to the term “hyperconcentrated flow”, defined by Pierson (2005) on the basis of sediment concentration as “a type of two-phase, non-Newtonian flow of sediment and water that operates between normal streamflow (water flow) and debris flow (or mudflow)”. Transitions from flood to debris flood/hyperconcentrated flow and vice versa occur at minimum volumetric sediment concentrations of 3 to 10 percent. See also Table 3.1 based on O’Brien (1986) for a classification of different flows based on sediment concentrations. Debris floods (as defined by Hungr) have slightly lower sediment concentrations than hyperconcentrated flows (as defined by Pierson), but this range depends on overall grain size distribution and the ability to acquire yield strength (i.e. internal resistance of sediment mixture to shear stress deformation; it is the result of friction between grains and cohesion (Pierson 2005)). This definition is consistent with terminology used in the BGC (2014a) report for Cougar Creek.

- *Debris Flow:* A debris flow can be defined as: “a very rapid to extremely rapid flow of non-plastic debris in a steep channel” (Hungr et al., 2001). Debris-flow material is typically saturated, however, unlike debris floods, the movement is colluvial (gravity transported) rather than fluvial (water transported). As such, debris flows typically require slopes between 25 and 30° to mobilize (Iverson, 2014). To maintain material transport, flows require an established channel or confined path. Hungr et al. (2001) suggest the maximum width to depth ratio of 5 to 1 to adequately maintain this constriction. When debris flows exit the confines of canyons, significant deposition occurs at the apex of their fans. Boulder lobes often observed at the front of debris flows may create levees that channelize the flow and lead to greater run-out distances on the fan surface. Often, debris flows occur in multiple surges with flood dominated transport mechanisms in between (Hungr et al., 2001). This can lead to multiple types of deposits in the channel and on the fan surface. The boulder front and surging behaviour results in up to 40 times higher peak discharges than those of (water) floods. (Hungr et al., 2001) suggest the use of peak discharge as the most reliable criterion to distinguish between debris flows and debris floods (i.e. two to three times higher than floods). Debris flows typically require a channel gradient in excess of some 15° for transport over long distances and have volumetric sediment concentrations typically in excess of 50-60 percent. This definition is consistent with terminology used in the BGC (2015) report for Stone Creek.

A *Landslide Dam Outbreak Flood* is a hazard that occurs when a landslide or debris flow from a tributary blocks a creek or river and water starts to impound behind the landslide dam. If the landslide dam fails, it may lead to downstream flooding. Sediment concentrations in an outbreak flood depend on sediment entrainment of the landslide material itself and entrainment along the flood path.

Table 3.1: Classifications of Flows by Sediment Concentration (modified from O'Brien, 1986)

Bulking Factor							
0	1.11	1.25	1.43	1.67	2.00	2.50	>3.33
Sediment Concentration , % by weight (100% by WT = 1 x 10^6 ppm)							
0	23	40	52	63	72	80	87- 100
Sediment Concentration, % by Volume (specific gravity = 2.65)							
0	10	20	30	40	50	60	70-100
	Normal Stream Flow		Hyperconcentrated Flow		Debris Flow / Mud Flow	Landslide	

3.2 Watershed Morphology

The Melton ratio (R) is used to distinguish between watersheds that are prone to debris flows, as opposed to debris floods (Jackson et al. 1987, Wilford et al. 2004). Overall, the Melton ratio has shown to be one of the more robust morphometric variables used to classify basin by process, with a number of studies identifying similar critical threshold values of R for hydrogeomorphic phenomena in different regions (e.g. Jackson et al., 1987; Bovis and Jakob, 1999; de Scally and Owens, 2004; Wilford et al., 2004). The Melton ratio (R) is defined as the relative relief of a catchment area divided by the square root of the catchment area. Melton ratios between 0.3 and 0.6 indicate that watersheds or catchment areas are prone to debris floods.

Table 3.2: Morphology Data for the Three Subcatchment Areas

Catchment Area	Approximate Relief (m)	Area (km^2)	Melton Ratio (R)	Dominant Hazard Type	Gradient of Upper Slopes (%)	Gradient of Lower Slopes (%)
Pigeon Creek	1300	18.5	0.30	Debris Flood	20-60	3-20
Wind Creek	1400	16.7	0.34	Debris Flood	50-90	2-10
West Wind Creek	1730	19.9	0.39	Debris Flood	40-65	10-20

Details on the catchment topography are shown in Table 3.2.The calculated R values of 0.30 for Pigeon Creek and 0.34 for Wind Creek are near the lower threshold between floods and debris floods (0.3) and are significantly below the threshold between debris floods and debris flows (0.6).which may explain why there is little evidence of debris flow deposits on and within the Pigeon Creek fan. Table 3.2 also lists slope gradients to give an idea of the topography of each subcatchment. The entire Pigeon Creek watershed has an R of 0.25.

Based on the Melton ratios, the Pigeon Creek watershed is likely dominated by debris floods events.

4 FREQUENCY ANALYSIS

Tetra Tech investigated the occurrence of previous debris flood events in the Pigeon Creek watershed in order to estimate their frequency. Given the complexity of the processes and the lack of monitoring data, the problem was addressed from three different angles, which are described in more detail in the following sub-sections:

- Aerial photography interpretation;
- Dendrochronology; and
- Radiocarbon Dating.

The above included field investigations on foot and by helicopter which were conducted in August and September, 2014. An overview helicopter flight was completed during the August investigation for reconnaissance purposes and to acquire photographs of the area. Field investigations on foot included numerous traverses of the fan, and traverses of Pigeon, Wind and West Wind Creek. LiDAR data from the post-flood period in 2013 was added to a GIS map and database for the area.

Numerous sites on the fan and in the upper watershed were investigated. Descriptive notes and photographs were taken at all sites. A collection of photos identifying the most notable features on the fan and watershed are provided in Appendix C. The locations of these selected photos are shown on Figure 4.1 for the watershed and Figure 4.2 for the fan. The notable features include large eroding banks, aggradation areas, channel avulsions, sediment wedges, landslides, log jams, and impacted trees.

The field team mapped the extent of flooding and aggradation resulting from the June 2013 event. Figure 4.3 delineates the approximate extent of the sediment deposition after the 2013 flood on the fan.

4.1 Aerial Photography Interpretation

Historical aerial photographs of the study area were analyzed using PurVIEW™ technology to evaluate changes in the local terrain since 1947 (the earliest year for which aerial photographs are available). The aerial photographs used for the interpretation of relevant features in the study area are shown in Table 4.1.

Digital aerial photographs were provided to Tetra Tech by the Town for most of the years shown in Table 4.1. Some of these did not cover the Dead Man's Flats and Pigeon Creek watershed areas. Missing aerial photographs were searched for at the University of Calgary and University of Alberta libraries; however, too few photographs were available to consider borrowing them from the two libraries. The missing photos were purchased as high resolution digital files from the air photo library at Alberta Environment and Sustainable Resources Development (AESRD) in Edmonton.

Although more photo years were available, a selection of these was taken to cover a reasonable time frame between photo years, with closer spacing in the early years, when more undisturbed land was present. Most of the aerial photography that is available does not cover the southern portion of the watershed, but all of the photographs cover the fan. Only the 2013 aerial photographs provide full coverage. The 1950 photographs are from a set that is dated 1950-52; the ones of the fan area are actually from 1950. Digital air photos from 1947 were obtained from the Town of Canmore.

Table 4.1: Pigeon Creek Fan and Watershed Historical Aerial Photographs

Year	Roll	Photo #	Scale	Date
1947	A10908	107	1:30,000	unknown
1950	AS168	136-140	1:40,000	unknown
1958	AS745	152-161; 197-203	1:15,840	unknown
1962	AS830	53-55	1:31,680	September 18
1962	AS831	149-154	1:31,680	September 18
1972	AS1184	315-321	1:21,120	July 8
1972	AS1185	6-9	1:21,120	July 8
1984	AS3085	7-12; 41-46	1:20,000	August 22
1997	AS4824	26-29; 46-49	1:15,000	July 19
2008	AS5450N	170-175; 193-197;217-222	1:30,000	August 18, September 4
2013	DS2013020	1010-1020; 1039-1053; 1121-1127	1:24,000	July, August

4.1.1 Methods

Tetra Tech used the PurVIEW™ system for air photo interpretation. The system incorporates 3D visualization and ArcGIS technologies, which allow the mapper to view traditional aerial photography in a digital environment with the aid of specialized 3D glasses. Ideally, aerial photographs are scanned or provided as digital images at 2,400 dpi using a high resolution scanner. Next, they are georeferenced, merged with DEM data, and uploaded to a computer.

With this system, the mapper can zoom in and out to observe and map the landscape in detail. Traditional aerial photographs captured at 1:60,000 scale, for example, can be viewed in the PurVIEW™ system at scales as large as 1:2,000 or greater, which allows for greater accuracy when identifying and delineating critical landscape features such as landslides and debris floods deposits.

Additionally, since all of the aerial photographs are digitally georeferenced in 3D (with the exception of the 1947 photo, which was georeferenced in 2D), the mapping for each year is spatially accurate (somewhat less so for 1947). This is critical for comparing landslides and other features from year to year.

Old fan channels, wetland/grasslands and mass movement features within the lower elevation areas of the watershed were mapped, along with any other relevant features. Mapping began with the 1950 aerial photographs and proceeded forward in time to the 2013 photographs. Mapped features were assigned a colour for each photo year and a line type for each feature type, so that changes from year to year could be easily identified.

4.1.2 Results

Results of the air photo interpretation are shown on Figures 4.4 and 4.5. A number of trends and changes can be identified from year to year as discussed below and illustrated on the figures.

4.1.2.1 1947

The 1947 air photo is of lower resolution than photos from the other years and covers only the fan and lowest part of the upper watershed. However, a number of cleared areas and old channels were visible. The location of Pigeon Creek and its floodplain was mapped. One large and a few small grasslands visible on the fan in 1947 are probably human-cleared areas.

Most of the fan's trees were deciduous, with some conifers along the east side of Pigeon Creek, some in the Bow River floodplain areas, and a few tall conifers on the upper fan east of the apex. This could be due either to fan activity or fire.

4.1.2.2 1950

The 1950 air photos are of higher resolution and cover more of the study area. Debris slides in the upper watershed were identified on these photos. The higher resolution and perhaps different sun angle allowed more old channels to be delineated on the fan. These no doubt pre-date 1947, as there is good tree cover along the channels.

Most slide areas within the watershed were already established by 1950. Some of the apparently new ones visible on the 1962 aerial photographs may be older but were simply difficult to identify on the 1950 photographs. The higher elevations in the watershed are characterized by exposed bedrock, and rockfalls and rockslides originating on the steep bedrock slopes feed colluvial cones or thinner, blocky material below. As these are extensive throughout the watershed, they were not mapped. The lower slopes are covered with a thick layer of till that likely overlies bedrock. It is the failures that happen in the tills that are most important to fan development. Some of the areas mapped as debris slides or debris flows appear to have formed via a combination of debris slide and rockfall/rock slide activity or debris slide/debris flow movements. These were much less common than simple debris slides along the valley walls of Pigeon and Wind Creeks. Most of the active failures visible in the 1950 photographs have formed on the eastern slopes of these two narrow valleys. Although most of the debris slides appear to initiate in till, two deep-seated slides immediately south of the current location of the fan apex waterfall may involve the movement of bedrock. The relevance of these deep-seated slides is further explored in Section 7. Rills on the lower till slope in the southeastern portion of the watershed indicate that till is thick and clay-rich in this area, which explains why debris flows and slides are more common in this area.

The fresher appearance of slide areas and higher number of slides in the watershed in the 1950 air photographs compared to later years is considered to indicate that debris slide activity was a fairly recent phenomenon in 1950. However, it is unknown when the triggering event actually occurred, or how long the slide recovery process takes.

A right of way crosses southeastward from an area west of the fan into the upper watershed area and trails are present on the valley slope south of the fan between the right of way, Pigeon Creek and the fan. The highway is not yet present.

Older channels are difficult to identify in all of the photo years; most were identified on the 1947 and 1950 photographs because human disturbance had not yet obliterated their signatures. The position of Pigeon Creek and its floodplain changed very little since 1947, so it was not mapped, in order to reduce map complexity.

The watershed showed evidence of large, stand-replacing forest fires. The vast majority of the area was covered with young conifers, with a few islands and patches of older conifers present locally. Older conifers were more common at high elevations. The obvious difference in height between the large areas of young conifers and the small patches of older conifers was easily identified on the 1950 aerial photography. The young trees were also more widely spaced than the older ones – the forest floor could be seen between many of them, while it could not in the older stands. Colluvial fans/cones in the West Wind Creek area were covered with a mix of deciduous and coniferous trees, the deciduous trees indicative of more recent fan activity. Unfortunately, a two-dimensional image of the upper watershed area did not allow the differences in the conifer stands to be seen easily, so a figure is not provided. Viewing in 3D is required to see the height differential of the trees.

The pre-1950 fire appears to have jumped over Wind Creek valley. While younger conifers were visible on the east slope, this is the slope containing failures. The more stable west slope was densely covered with older coniferous trees. Down creek, south of where Wind Creek joins West Wind Creek, deciduous trees and young conifers marked the former locations of the Wind Creek floodplain. An isolated stand of older conifers was present on the floodplain where the narrow valley ends and the floodplain starts.

The fire did not appear to have skipped over Pigeon Creek. While slides on the eastern valley wall either expose bare soil or have a mix of deciduous and conifer trees that are even smaller than the young ones on the till surfaces to the east and west, this is probably due to sliding and not fire. Trees on the western slope were the same size as the ones above on the gently sloping till surfaces. However, on the narrow floodplain in the upper creek area, older conifers make up about 40 percent of the trees, with the rest being young conifers and a few deciduous trees. Older conifers make up about 10 percent of the very narrow floodplain area in the space immediately north of the steep valley walls and at the confluence of Pigeon Creek with West Wind Creek. The remainder are deciduous trees of various sizes and young conifers, both of which dominate the gentler slopes on either side of the floodplain. The reason for the presence these older outlier trees is not certain. They may have survived the fire or may have been missed by the fire, but the presence of the younger trees implies some activity. Since the trees are on the floodplain, this activity could be due to debris floods or floods. Unfortunately, the absence of ages of the various size classes of trees identified within the watershed does not permit fire chronology in the watershed to be determined from these observations.

On the south valley wall of upper Pigeon Creek, stand variability shows evidence of a number of small fires and some seepage areas. On the opposite side of the valley at this location, a pale area shows a more recent fire, where bushes are just starting to regenerate on the landscape.

4.1.2.3 1958

The 1958 and 1962 photographs are virtually identical where mappable features are concerned, so the few drainage channels evident on the fan in 1958 were added to the 1962 map layer to simplify the mapping. The highway was built and three areas cleared for aggregate extraction by 1958. A number of trails were present on the fan and in the upper watershed. A very straight looking trail that crosses the fan and Pigeon Creek and extends into the upper watershed is likely a seismic line clearance.

Pigeon Creek was straightened and culverted in the highway area. Its location is virtually identical to that of 1962, so only the 1958 position was mapped. However, this shows up as the 1962 position on Figure 4.6 (again to simplify the mapping). The creek position deviated from the 1950 location in the lower reaches of the creek (Figure 4.6). There is an extra channel cut into the grassland, and a couple of channels head northward and die out. The grassland channel becomes the main channel in future years.

Evidence of the large fire in the upper watershed is easier to see on the 1958 photographs. The bushes in the recently burnt part of the upper Pigeon Creek area are more numerous in 1958.

4.1.2.4 1962 to 1972

More development was underway by 1962. Buildings on the former grassland on the western portion of the fan, the beginnings of a ski hill and the campground, and a road to the upper watershed had been built by this time and a few small areas had been cleared of trees. The three gravel pits appear to have been in use at this time and probably served as aggregate resources for the highway and other development. Old channels become increasingly difficult to see as development progresses.

Pigeon Creek was culverted in a few more areas by 1972 as the highway was expanded with an interchange and new road area, and the Thunderstone Quarry area and shooting range upslope of the highway are now present. The gravel pit on the eastern part of the fan downslope of the highway has expanded to a much larger area. There is little change in the creek alignment between 1962 and 1972. Human changes made by 1972 in the watershed include ski hill development and some cleared areas near it, more trails and some new seismic lines. By 1962, small conifers were becoming more numerous on the western portion of the fan and by 1972 they had spread to the central fan area.

It is more difficult to identify the older burn areas in the upper watershed as the younger trees are becoming taller in both years. Conifers are now colonizing the upper Pigeon burn area. Colluvial fans in the West Wind Creek area are still covered with a mix of deciduous and coniferous trees. The debris slides that were so evident in 1950 are now fairly grown in with conifers and a few deciduous trees. Some exposed slopes are still present in the lower Pigeon Creek valley.

4.1.2.5 1984

The Thunderstone Quarry site has one rock stockpile and there are a few more cleared areas on the fan. Transmission lines are now present within the fan and upper watershed right of ways. There are now more trails in the upper watershed, but they do not appear to have initiated any slides. Coniferous trees in the central and western fan area have grown but have not expanded much. The eastern half of the fan is still dominated by deciduous trees, although some conifers are present.

Many of the debris slides evident in 1950 are now overgrown, but a few fresh ones have formed. The upper Pigeon burn area was about 60 percent covered with coniferous trees and the young conifers from the large burn areas were almost as tall as the older trees. The colluvial fans of West Wind Creek were dominated by conifers.

4.1.2.6 1997

Rock was being quarried at Thunderstone and steep quarry rock faces were evident. The sewage ponds had been constructed on the northern part of the fan and the campground appeared to be more developed. Condominiums were present on the west bank of Pigeon Creek and many small buildings had been added at the bottom of the ski hill.

In the upper watershed, more of the older debris slides had grown in, but a few freshly exposed slopes were present. A few of the debris slides had expanded upward by 1997. The wetlands in the West Wind Creek area were growing in with conifers and three areas had been cleared on a gentle slope northwest of them. Some of the older trails were becoming grown over as well. Former burn areas were not possible to identify; the upper Pigeon burn area was not covered by this set of photographs. The eastern fan area still appeared to be dominated by deciduous trees.

4.1.2.7 2008

These were the first aerial photographs to extend the airphoto coverage to the south watershed, although they do not cover quite all of the area. Development on the fan continued with the addition of more condominiums adjacent to the first set. Much rock had been removed from the Thunderstone Quarry site and steep quarry walls were present near the fan apex waterfall, which was first identifiable in 1984. The Highway Wildlife underpass had been added in the eastern fan area. Pigeon Creek's alignment is very similar to that of 1997 so it was not mapped. Conifers were more evident on the eastern portion of the fan.

Even more of the debris slides in the upper watershed were grown over. On the higher slopes, rockfall and rockslide evidence was visible, but avalanche tracks were also identifiable. There is a bit of hummocky till, which was not failing, in one of the cirque basins.

The upper Pigeon burn area had completely grown over and there was no visible evidence of fire in the rest of the watershed. It appears that the site had re-vegetated 58+ years after the fire.

The 2013 photographs were flown in August and therefore show the post-June 2013 flood condition of the study area. Pigeon Creek straightened its course within Thunderstone Quarry, which had expanded significantly toward the west since 2008. A bridge over the new creek position must be new construction. Temporary berms are present along Pigeon Creek in the western fan area. Roads for a new subdivision have been built in the central fan area but there is little other significant development.

More coniferous trees are evident in the eastern fan area but there are still many deciduous trees. There are numerous debris slides along Pigeon and Wind creeks; however, these are not as extensive as those evident in the 1950 photographs. Most slides are on the eastern slope of Pigeon Creek, while most are on the western slope of Wind Creek. This is different from 1950, when most slides along Wind Creek were on the east side.

4.1.3 Limitations

Photograph scale is not an issue when using PurVIEW for analysis and thus does not limit interpretations for this study. However, the results of smaller magnitude floods or debris floods that do not cause forest damage cannot be seen on aerial photographs due to tree cover. Development on the fan in later years obscures the evidence of former floods and debris floods. For this reason, shorter time periods between photographs were chosen for the earliest years available.

4.1.4 Summary

Historical disturbance evidence was identified by air photo analysis using PurVIEW. Most of the earlier events were identified on the 1947 and 1950 photography, when development had not yet hindered the interpretation of natural features. Rockfalls and rockslides in exposed bedrock areas at high elevations within the watershed are active, but do not contribute significantly to the debris that is incorporated in debris floods, as this debris appears to remain in the higher elevation areas. The lower slopes are covered with a thick layer of surficial material (till) overlying bedrock, which supplies most of the granular material for subsequent transport during floods and debris floods. Debris slides developed in these materials along the eastern slopes of Pigeon and Wind creeks are the most common form of mass movement. Former flood channels and various alignments of Pigeon Creek were mapped on the fan to help identify past debris flood activity and location and to identify any recent (post-1950) morphologic changes on the fan.

Most of the mapped paleochannels, identified by differences in tree size and type, are visible on the aerial photographs, but some were only visible in the field (see Figures 4.5. and 4.6). Fining of deposits from the proximal (bouldery) to distal (sandy) fan is evident, but varies across the fan. The current Pigeon Creek channel is incised into the older proximal to mid-fan area, probably the result of historic sand and gravel mining, and spreads to multiple shallow channels and then depositional areas on the distal fan. Two main facies are evident: Facies 1 (Debris Flood) and Facies 2 (fluvial or maybe finer distal debris flood). These consist of sandy pebble to boulder gravel (Facies 1) and sand/silt/organic beds (Facies 2).

Deciduous trees on the fan are interpreted to imply that either the fan had been quite active in the recent past, or it had been affected by fire. Adjacent areas within Bow Valley support coniferous forest; the fan stands out from its surroundings, especially in the 1947/50 aerial photography, because of the predominance of deciduous trees. As coniferous trees form the climax forest in the region, the entire fan must have experienced some kind of disturbance in the past. Extensive fires were reported in the Bow Valley and in the vicinity of Dead Man's Flats in 1936 (77 years ago). Evidence of large, stand-replacing fires was identified in the watershed, one of which was quite recent on the 1950 photographs. By 2008, the forest there had returned to a more normal state in which evidence of the pre-1950 fires was no longer visible.

Many of the debris slides evident in in the upper watershed in 1950 became quite overgrown by 2008, with the exception of a few fresh slides occurring locally in some years. Wetlands near West Wind Creek began to grow in and a few of the debris slides had expanded upward by 1997. During the June 2013 event, many new slides formed, but these are not as extensive or as large as those visible on the 1950 photographs. In 2013, slides reactivated on the eastern slopes of Pigeon Creek, but those on the eastern slope of Wind Creek remained stable. The 2013 event reactivated much older slide surfaces on the west slope of Wind Creek instead.

A likely reason for the less extensive sliding in 2013 is that the slide trigger was several days of very wet weather. In contrast, the pre-1950 slides may have been preceded by a very large fire that affected most of the upper watershed. Avulsion of the lower reach of Pigeon Creek on the distal portion of the fan between 1950 and 1962 and the presence of avulsed channels in the watershed in the same period indicate that an event occurred in the watershed in that time frame.

4.2 Dendrochronology

4.2.1 Introduction

Tree coring was completed at select locations on both the fan and watershed. These samples underwent dendrochronological analysis. Dendrochronology, based on the determination of ages and growth patterns of trees, is an absolute method for evaluating the minimum age of the surface upon which the tree is growing and the frequency of various types of disturbance events over the last few hundred years. The method provides temporal data for the interval between historic observations and radio-isotope dating methods such as radiocarbon dating (Kondolf and Piegay, 2003). Tree-ring dating involves the observation of the number or character of tree rings to date the occurrence of an event that influenced the establishment or growth of the tree. This method takes advantage of the long life of many trees, the annual nature of tree rings in many species in temperate regions, and the fact that the macro- and micro-anatomy of wood are influenced in predictable ways by disturbances of interest, such as floods, droughts, and ice impact (Merigliano et al., 2013). The number of annual rings in a tree core or cross section is an estimate of the number of years since the establishment of the tree (Stokes and Smiley, 1968). Disturbance events recorded within tree ring growth patterns can be due to floods, debris floods, debris flows, slides or fires. The annual growth rings reflect the disturbance from floods or debris floods/flows in a number of ways, including impact scars, increases or decreases in growth rates as a result of changes in water/nutrient availability, deposition of resin ducts as a result of trauma, and production of denser and darker reaction wood to counter tilting (BGC, 2014a). The evidence for fires includes the presence of fire scars near the base of the tree resulting from heat killing part of the tree cambium and releases which reflect sudden increases in growth rates that persist for ten years or more as a result of dramatically reduced competition for light and nutrients (Rogeau, 2005).

4.2.2 Methods

Seventy (70) trees on the Pigeon Creek fan and thirty three (33) trees within the Pigeon Creek watershed were sampled with a 4 mm increment borer between September 8 and September 14, 2014 (Figures 4.7 and 4.8). Coniferous tree species sampled included lodgepole pine, Engelmann spruce, white spruce and Douglas fir, which are typical of the species found growing in the Montane and Subalpine zones of the Bow River Valley (Rogeau, 2005; Walkinshaw, 2008). The cores were extracted at breast height (typically about 1.4 m above the ground surface) and the diameter of the individual tree (DBH) at the height of the core and the ground surface condition (i.e. had the tree base been buried since it became established) were also measured and recorded. In addition, the diameters of 22 un-cored trees on the fan were measured. Although of fairly low precision, tree diameter vs. age relations can be used to estimate the ages of un-cored trees. The locations of the cored and measured trees were recorded with an iPad. The individual trees were also photographed and were inspected for the presence of impact or fire scars.

The retrieved cores were glued and mounted on a slotted board and then sanded to a high finish using 200- 400 grit sand paper and then lightly oiled to emphasize the growth rings. The cores were then examined under a binocular microscope with 40-50x magnification and the growth rings and growth patterns were counted and identified. The ages of the trees and the timing of growth anomalies were determined by counting tree rings back from the outermost ring which corresponds to current (2014) growth. While at the site, observations were made to note the age of sapling spruce, lodgepole pine and Douglas fir trees at 1.4 m (DBH) above ground level. Age was determined by counting the whorl of branches produced each year to a height of 1.4 m. On average, the age at a height of 1.4 m across the species was about eight years, and thus this value was added to the ages determined from the tree ring counts to determine the approximate year of establishment of the tree and thus the minimum age for the surface upon which the tree became established.

The watershed tree cores are most likely to directly reflect disturbance events because the trees were all sampled on channel margins. Thus, the widths of individual 10-year blocks of rings along the length of these cores were measured and unitized by dividing the length of the 10-year block by the total length of the core. A cumulative growth curve was then established by summing the percentage values for each 10-year block of rings and plotting it against the time since the tree became established. Upward inflections in the curve were assumed to reflect disturbance events within the watershed that released the trees and promoted accelerated growth over a decadal period (Rogeau, 2005).

4.2.3 Results

The estimated ages of the trees on the fan and the watershed are shown on Figures 4.7 and 4.8, respectively. The ages on the fan were determined directly by counting the tree rings (70 trees) or by estimating the age from the measured tree diameter (22 trees) using the following equation where Y is the predicted age (years) and X is the measured diameter (cm):

$$Y = 2.1062X + 6.7354 \qquad (R^2 = 0.31)$$

An age-diameter relationship was also established for the trees growing in the watershed above the fan:

$$Y = 2.6245X + 43.845 \qquad (R^2 = 0.32)$$

A single tree age was estimated from this equation (W26) because the recovered core was unreadable due to rot. Comparison of the two equations indicates that the tree growth rates on the fan are quite a bit higher than those in the watershed. For example, a 40 cm diameter tree on the fan is estimated to be about 91 years old, whereas a tree with the same diameter in the watershed is estimated to be about 149 years old. The difference in age could reflect environmental conditions or it could also reflect the fact that most of the trees cored on the fan were white spruces with some Douglas firs, while the watershed group were dominated by lodgepole pine and Engelmann spruce.

The distribution of tree ages across the proximal, medial and distal portions of the fan can be seen on Figure 4.7. The youngest aged trees are located on the medial and distal portions of the fan from roughly the center of the fan to the eastern margin. A significant number of the trees located on this part of the fan are deciduous aspens that were identified on the 1947 and 1950 aerial photographs (Section 4.1). The presence of the aspens clearly indicates that a large scale disturbance took place on the fan prior to 1947 (Kostaschuk et al., 1986), but it is unknown whether the disturbance was the result of a flood/sedimentation event or a fire. Extensive fires occurred in the Bow River Valley in 1936, so it is possible that the eastern portion of the fan burned at that time (78 years ago). The cored tree ages indicate that the coniferous trees in that area became established about 50-60 years ago (1964-1974) and they are replacing the aspens, which is a typical plant successional trend in the absence of recent fires (Walkinshaw, 2008) that can be seen on the time sequential aerial photography (Section 4.1). At the fan apex, the tree ages are grouped.

On the eastern side of George Biggy Senior Road immediately downstream of Thunderstone Quarry there is a group of older trees (>200 years). Immediately down-fan of this group on the eastern side of the road, the trees are older than 100 years. Farther to the east, among a number of former channels on the fan surface, the trees are about 80 years old, which is the same age as most of the trees on the fan apex below the quarry and to the west of the road. This suggests that the fan apex area has been relatively stable for the last approximately 80 years and may not have burned in the 1936 fires. As can be seen on the 1950 aerial photographs (this study), the center portion of the fan from the apex to the Bow River is occupied by coniferous trees and the ages of these trees from the tree core data are on the order of 90-115 years. To the west of this belt of older trees, including the location of Pigeon Creek in 1950 (Figures 4.7 and 4.8), the vegetation appears to be a mixture of coniferous and deciduous trees. Tree ages are generally less than 100-years.

Interpretation of the tree core data on the fan is complicated by the fact that the distribution of the tree species and the tree ages could be the result of fires, flood events or some mixture of floods and fires. There is also an unquantified lag time between the occurrence of events and tree establishment. If fires are eliminated from consideration, the tree age data might suggest that the active portion of the fan was located on the eastern side of the fan until there was a flood event about 80 years ago that caused an avulsion towards the west side of the fan and resulted in the channel of Pigeon Creek being located in the 1950 position (Figures 4.7 and 4.8).

The mixed deciduous and coniferous tree species visible on the west side of the fan in 1950 (about 100 years old) might suggest that the channel avulsed back to an area that had been active prior to the occupation of the east side of the fan. It would appear that the central portion of the fan where the trees are predominantly conifers has been stable for a relatively long period of time (>100 years). The widespread ages of the trees across the fan means that it is unlikely that the distribution of the trees on the Pigeon Creek fan can be unambiguously correlated with specific flood events even though large floods were recorded on the Bow River in the early 1900's (1902, 1912, 1916) and again in 1932 (BGC, 2014b).

Seventy-eight (78) percent of the aged trees on the fan are less than 100 years old and 73 percent are between 50 and 100-years old which suggests that the last major event occurred about 100 years ago. The relatively even age of the trees at the fan apex, excluding the island of older trees (>200 years), suggests that the last morphologically significant event on the fan was in excess of 80 years ago (older than 1934). Based on the aerial photographic record prior to 2013, there has not been a morphologically significant flood event on the Pigeon Creek fan since the avulsion of the lower part of the Pigeon Creek channel on the distal margin of the fan between 1950 and 1962 (50-63 years) even though there have been flood events inferred from tree ring data in the post-1947 period in nearby watersheds in the Bow River Valley, including Three Sisters, Heart, Jura, Harvie and Cougar Creeks (BGC, 2014b).

The locations of the 38 cored trees and their estimated ages within the watershed of Pigeon Creek upstream of the bedrock waterfall at the apex of the fan are shown in Figure 4.8. The sampled trees were all located on the margins of either Pigeon Creek or Wind Creek. Impact scars from the 2013 event were identified on some of the trees, generally in the vicinity of log jams (up to 2.5 m above the bed of the channel), but in the main there was little evidence of impact damage to the channel margin trees even though there was evidence of overbank flow and in some cases overbank coarse sediment deposits. A few of the older trees showed evidence of pre-2013 event scars. Spatially, the oldest trees (>200 years) tend to be located towards the upper reaches of the creeks, but some older trees are also located in the lower watershed all the way to the fan apex.

The age distribution of the cored trees in the watershed indicates that 29 percent are in the 50-100 year class, 26 percent are in the 100-150 year class, 26 percent are in the 150-200 year class and 19 percent are older than 200 years (Figure 4.9). In fact, about 46 percent of the aged trees along the channels within the watershed are older than 150 years which suggests they may have become established after the major regional fires in the 1860's. Field evidence of channel avulsions very similar to that observed upstream of large woody debris jams after the 2013 event, suggests that there was a morphologically significant flood event about 63 to 64 years ago (early 1950's), based on the ages of trees growing on the bed of the abandoned channel. A number of other trees in this general age range were also located along Pigeon Creek. Inferred and reported flood events were identified on nearby watersheds between 1948 and 1956 by BGC (2014a), so it is likely that there was an event of unknown magnitude on Pigeon Creek in that time frame. The aerial photographic analysis of the Pigeon Creek fan identified that there was a significant change in the lower creek alignment between 1950 and 1962 (Figure 4.6).

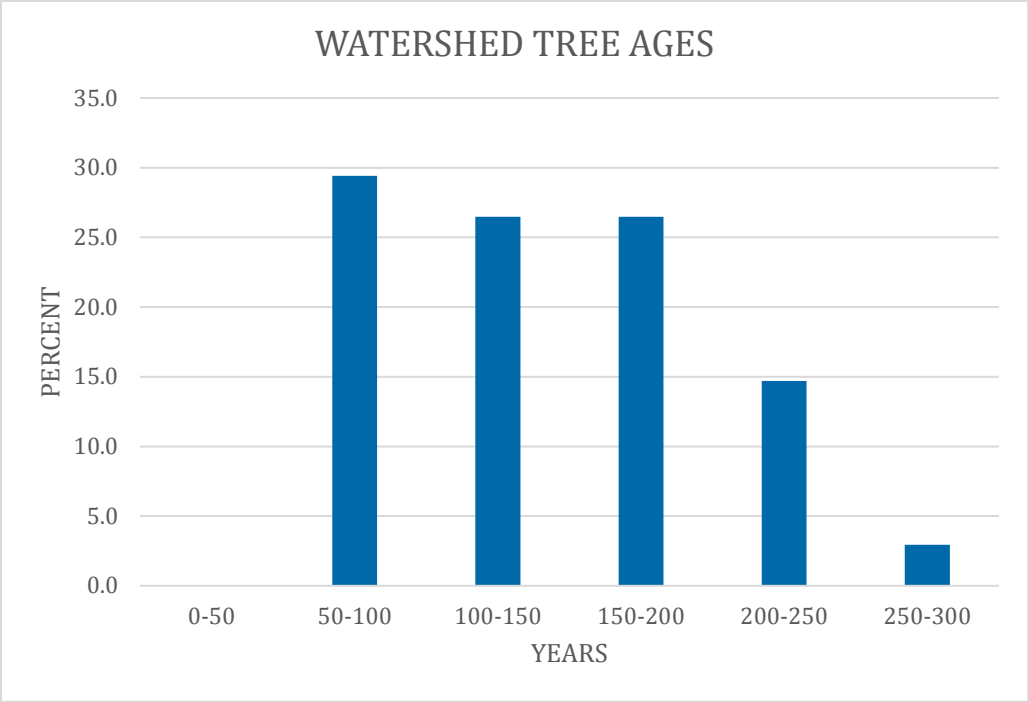

Figure 4.9. Age Classes of Sampled Trees in the Pigeon Creek Watershed.

Analysis of the tree ring growth patterns on the cored trees (Table 4.2) using 10-year growth increments indicated that release–type events prior to 1940 may have occurred on about the same frequency (30-100 years) as that reported for non-stand-replacing fires (White, 1985) (Figure 4.10). Widespread fires in the Bow River Valley were reported to have occurred in the late 1800's, early 1900's and in 1936 (Walkinshaw, 2008). Prior to 1936, fires in parts of the Pigeon Creek watershed occurred in 1867, 1864, 1833, 1765 and 1740 with recurrence intervals of between about 20 and 70 years (Rogeau, 2005). Since the 1930's there have been no fires reported in the Pigeon Creek watershed (Rogeau, 2005). The presence of a number of trees in excess of 200 years in age within the watershed suggests that there may not have been a stand-replacing fire for at least that period of time which would be in accord with White's (1985) estimate for the historical recurrence interval (200-300 years) for stand-replacing fires at that range of elevations. If it is assumed that the stand-replacing fires are associated with significant increases in runoff volume and sediment yield from the watershed (Meyer et al., 1995; Cannon et al, 2010), it suggests that the recurrence interval for very large, fire-induced, morphologically significant events on the fan may be on the same order of magnitude. However, in the immediate post-fire period, the magnitude and recurrence interval for the associated hydrologic event can be relatively small and frequent, respectively (Cannon et al., 2010) because of the significantly increased runoff in the post-fire period. The Holocene fire record from both the Cougar Creek (BGC, 2014) and Pigeon Creek fans, if complete, tends to support the fire-related recurrence interval for geomorphically significant events on the fans (240-250 years). Fire suppression since about 1910 has resulted in an increase in the age of trees in the watershed and increased susceptibility to mountain pine beetle attack and potentially to an increased fire severity risk (Walkinshaw, 2008) that could result in a large, morphologically significant, event on the fan during extreme climatically forced dry periods.

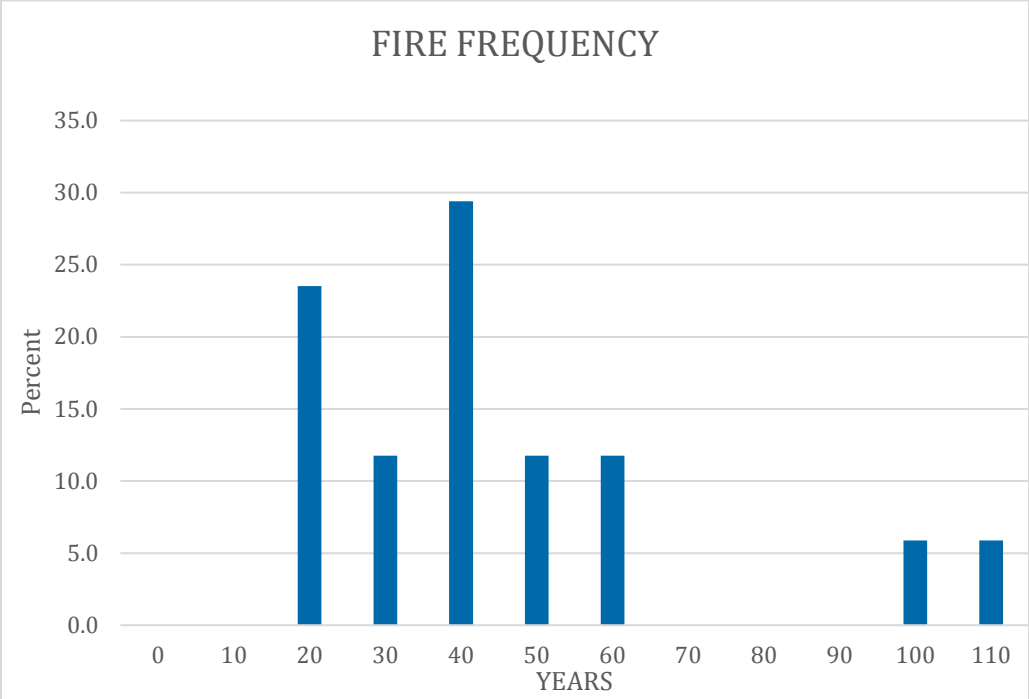

Figure 4.10. Frequency of Release-Type Events in the Pigeon Creek Watershed

Table 4.2: Watershed Tree Establishment and Disturbance Events

Core ID	Estimated Year of Establishment	Estimated Fire Disturbance Years			
W-35	1814		1872	1912	
W-34	1841		1859	1909	
W-30	1828		1886	1906	
W-29	1736	1794	1894		1934
W-28	1789		1877		
W-27	1826		1874		1934
W-24	1797			1915	
W-23	1799			1915	
W-22	1877		1895		1935
W-21	1846		1894		1934
W-19	1779	1807		1917	
W-18	1764		1892	1912	
W-17	1847		1895	1915	1935
W-15	1819		1877	1907	
W-13	1815		1883		1933
W-10	1863		1891		1931
W-4	1810		1878		1938
W-1	1872			1910	1940

4.3 Radiocarbon Dating

The dating of organic materials found within watershed and fan sediments can be used to determine limiting dates for older depositional events (floods and debris floods), those beyond the limits of dendrochronological dating. The general method is described in BGC (2013).

Because coal is present in the Jura-Cretaceous Kootenay formation that underlies Wind Creek and West Wind Creek, dating soil is less ideal than dating wood or charcoal. Although no coal was seen in bedrock exposures in the field, coal dust that cannot be separated out could be present in a paleosol sample and could create an erroneously old age for the soil.

4.3.1 Methods

Samples were acquired from natural creek exposures (banks) in the watershed (Figure 4.11) and from excavated trenches (test pits) and a few natural exposures on the fan (Figure 4.12). Test trenches were dug with a hydraulic excavator between September 8 and 16, 2014. The excavated face was examined and documented, and samples, suitable for radiocarbon dating, were collected. A number of natural exposures were also described and select exposures were sampled. The sides of the test pits were sloped to allow safe access to the trench. The vertical face that was used for logging was stepped. The vertical face was cleaned for analysis using a shovel and/or a trowel and each unit was logged separately using standard geological descriptions, including clast type, size and quantity, as well as structures identifiable within the different units. Logged details of each exposure and test pit as well as photos are provided in Appendix B. Samples were taken with a trowel and stored in plastic bags and the best samples for dating purposes selected. Samples were dated from most of the exposures and test pits on the fan and lower watershed. Figure 4.13 shows the location, depth and age of the samples. Those containing both charcoal/wood and organic sediment were washed in distilled water and sieved in Tetra Tech's Edmonton lab to isolate the charcoal and/or wood. The charcoal or wood was then sent for AMS radiocarbon dating at Beta Analytic Laboratories in Miami, Florida. A few samples were sent as organic sediment because charcoal was not immediately evident. A small amount of charcoal in two of these (PCFTR35b and PCFTR43a) was separated out at Beta Analytic and the charcoal dated instead of the sediment. Dating of all samples collected was not possible due to budget constraints. The samples with the highest likelihood of providing useful data were selected from the sample set.

Two samples from natural exposures in the upper watershed were sent for dating after the initial fieldwork in August 2014 (Samples PCUR13 and PCFR27). These came from depths of 1.17 m and 0.83 m, respectively, below the ground surface. The young dates from these samples (90±30 yrs BP and 210±30 yrs BP, respectively) helped direct our selection of the remaining samples to be sent for radiocarbon dating, operating on the assumption that the upper metre or so of deposits are fairly recent and less ideal options for radiocarbon dating (due in part to the general uncertainty in radiocarbon age of samples dating to the last 300 years and in part to being able to get more accurate ages from tree ring dating).

Generally the samples that could provide the most useful ages, including the oldest age, or samples that bracketed the age of a debris flood were chosen for analysis. Apart from avoiding sending samples from the upper metre of sediment for the most part, other samples were not selected for dating for a variety of reasons. Some samples were vertically close together in the exposure or test pit; these were suspected to all be of similar age and only the deepest one was thus selected. This assumption was tested and found to be valid by submitting all four samples from Test Pit PCFT36.

Test Pit PCFT37 did not contain any debris flood deposits. This site is located just within the Bow River floodplain (Figure 4.13) and it was determined that dating these samples would give the age of various Bow River floods, which may or may not have coincided with depositional events on the fan. These samples were therefore also not sent for dating.

4.3.2 Results

Radiocarbon dating results are shown in Appendix B and on Figure 4.13. Table 4.3 details the analytical results.

4.3.2.1 Coal Contamination

Contamination of samples by old carbon is a possibility in the region as coal is present locally in bedrock. Staff at Beta Analytic Laboratories identified small pieces of possible coal in two of the samples (PCFTR34a and PCFTR35b). Tetra Tech requested that the pieces most resembling charcoal be cleaned and dated. However, some coal contamination (from local bedrock) does appear to have affected Sample 35b, resulting in an unreliable age for this sample. Sample 34a seems to have a reasonable radiocarbon age, but it is possible it is slightly too old due to minor coal contamination. A lack of overlying and underlying age information means that it is not certain whether this sample is contaminated or not. However, the age fits well within the context of the increasing ages from west to east across the fan (Figure 4.13). Also, it fits well with the stratigraphic correlations made in Section 4.3.2.2. For the purposes of this report, Sample PCFTR34a is presumed to be uncontaminated. Although no contamination was identified in Sample PCFTR36c, it was the only sample where a bulk soil sample was dated due to a lack of visible charcoal in the sample. It thus appears that coal dust has contaminated this sample, as the age is anomalous compared to others on the fan and also falls into an age range where glacier ice is likely to have been present (BGC 2014a). The anomalous and potentially anomalous radiocarbon ages are shown in red on Figure 4.13.

4.3.2.2 Ages and Interpretation

All ages in this section are given in radiocarbon years before present (^{14}C years BP), without the error factor for ease of discussion. Error factors are shown in Appendix B and on Figure 4.13. Sample PCFTR38 was determined to be modern (1950 or later). The 2013 flood deposit is 3.9 m thick at this location and the sampled wood was found at 2.51 m (Figure 4.13). The modern date shows that the sampled wood is from a tree root related to the old floodplain surface. This test pit is located in the Thunderstone Quarry area and is near the fan apex where aggradation from the 2013 event is much thicker than elsewhere on the fan. Tree ring data are important in this area, as the other nearby test pit (PCFT39) and the nearby exposure (PCF40) did not contain datable material.

The youngest ages come from PCUR13 (lower watershed) and PCFR27 (lower fan). These fall into the questionable calendar age period for radiocarbon dating, but it is fair to assume that samples from close to 1 m depth are less than 300 years old. Sample PCFTR31b (lower fan), the only bone fragment sample, returned an age of about 520 years BP from a depth of 1.25 m, which provides an approximate age for the flood unit in which the bones were found (Figure 4.13) and a minimum age for the overlying debris flood unit.

Three samples on the lower western portion of the fan returned ages of 850 to 880 years BP (Figure 4.13). These provide a maximum age for overlying debris flood deposits at all three sites and a minimum age for underlying debris flood units.

The next oldest radiocarbon age is about 1260 years BP, from Sample PCFTR43b. This and sample PCFTR43a are in close vertical proximity to a debris flood unit for which they provide a bracketing age. This flood event appears to correlate with other debris flood deposits at PCFT31 and 36. A date of about 2010 years BP from exposure PCU40 in the watershed does not appear to match any of the debris flood dates on the fan. This site provides a maximum date for the overlying deposit at PCU40; it is possible that it relates to the 1820 year event or perhaps a younger one, but this cannot be confirmed by the radiocarbon date alone.

Two dates from a sand layer at PCFT35 (Figure 4.13) date the sand layer at about 2500 years old and provide a maximum age for an overlying debris flood unit and a minimum age for the underlying one. Sample PCFTR35d gives an age of 2890 years BP for a sand lens within a debris flood unit, which is interpreted to suggest that the unit actually represents two flood units – one older than 2890 years BP below the sand lens and one younger above it.

The oldest radiocarbon ages are 3280 and 3430 years BP from PCFT33 (eastern portion of the fan). The first gives a maximum age of 3280 years for two debris flood deposits whose surfaces are at 0.4 and 2.18 m depths. Burrows in the soil above the sampled material show that intervening deposits did not experience flooding for some time as this sample came from a depth of 3.69 m. It may be the same event as the one that is older than 2890 and its actual age is likely closer to 2890 than to 3280. The lower sample brackets the age of the overlying debris flood unit as having occurred between 3280 and 3420 years ago and gives a maximum age for the underlying one of 3430 years ago.

Rates of fan aggradation during the Holocene have been determined for the Cougar Creek and Three Sisters Creek alluvial fans based on assumptions regarding historic fan topography developed from the results of excavations on the fans (BGC, 2014a, b). For the former, a rate of 1.6 mm/year was estimated and for the latter rates of between 0.6 mm/year and 0.8 mm/year. Based on the depths of burial of dated charcoals in the pits located across the fan, Holocene aggradation rates on the Pigeon Creek fan range from 0.7 mm/year (PCFTR34) to 7.5 mm/year (PCFR27). The wide range of values reflect the local variation in deposition on the fan during discrete events.

4.3.2.3 Summary

The frequency of debris floods in the watershed is generally unknown, but one radiocarbon date shows that one debris flood unit is less than 2010 ^{14}C years old. The erosive nature of debris flows and debris floods in the watershed and the depositional nature in the fan area are likely the reason little is known about the frequency of events in the watershed compared to that of the fan. Events on the west side of the fan in the vicinity of the 2013 debris flood appear to have occurred (in ^{14}C years BP):

- 520 years ago;
- >520 to <850 years ago;
- >880 to <1260 years ago; and
- >1260 to possibly <1820 years ago.

Four debris flood events and one lower sediment concentration water flood event appear to have occurred in this time frame. Although the upper debris flood unit at PCFT43 is correlated with an older unit at PCFT31, it is quite possible that it could actually correlate to the upper younger debris flood unit. There is enough dating evidence to have more confidence in the remaining correlations, with the exception of the oldest units, which lack lower bounding dates.

Deposits close to the present Pigeon Creek alignment are thickest, which is interpreted to indicate that the deposits younger than 850 years old probably formed in floods that occurred in approximately the same location as the present creek alignment.

The eastern portion of the fan is older. Its debris flood deposits formed:

- <1820 years ago (possibly the same event as the western fan >1260 to <1820 year event;
- >2510 to <2890 years ago;
- >2890 to <3280 years ago;
- >3280 to <3430 years ago; and
- > 3430 years ago.

These five events include two events at the base of test pit PCFT35, which contain a sand lens with organic material indicating a hiatus in debris flood deposition.

These results are in general agreement with the chronology of formation of the Cougar Creek fan in the last few thousand years (BGC 2014a).

The nature of stratigraphy on the fan and the locations of radiocarbon dates does not allow an absolute chronology of fan sedimentation to be made (e.g. a date of less than 1820 years on the eastern part of the fan could correlate to any of the earlier dated events on the western portion of the fan or possibly even a different one).

4.3.3 Limitations

Limitations of radiocarbon dating are fully discussed in BGC (2014a).

4.4 Fire History

The abundance of charcoal rather than wood in the fan deposits indicates that forest fires have occurred through time and based on the review of fire impacts literature (Section 3) that they may have some relationship to debris flood deposits. In addition, charcoal found in the modern soil (e.g. at site PCU09) suggests that fires have also occurred in fairly recent times, which is supported by the reported fire history of the Bow Valley (Hawkes 1979; Walkinshaw 2008).

Results of the analysis of fire history data from this report were compared to BGC's Cougar Creek data (2014a) and to other available literature as shown in Table 4.4. Radiocarbon dates from charred material only have been converted to median age calendar years for ease of presentation and comparison to non-radiocarbon dates.

Although climatic periods and glacial advances for western Canada have been updated with new data, some are still somewhat equivocal (Clague et al. 2009), these are included in Table 4.4 for reference. The table shows colder climatic periods with light blue backgrounds and warmer ones with orange. High frequency fire periods are shown in red, medium frequency periods in lighter red and low frequency in green. These colours cover ranges of dates. Single numbers indicate the end dates of a range or a single fire data point. Variability in ages is expected due to the error factor of radiocarbon dates and the fact that the median age has been chosen for Table 4.4. Fires and fire frequencies from nearby areas described in the literature have been added for comparison.

The approximate timing of fire history for the Pigeon Creek area is broadly correlative with the fire history of the Cougar Creek area (Table 4.4). Differences may be due either to localized fires in each area and/or the lesser number of radiocarbon dates for the Pigeon Creek area.

Timing correlates with overall climate events fairly well for the last 800 years. Fires occurred just before the start of the Little Ice Age, and around the timing of short warm periods that occurred within the overall span of time regarded as the Little Ice Age. A major fire appears to have occurred between 85 and 100 years ago in the Bow Valley, Kananaskis and subalpine Kootenay National Park areas. This appears to represent a fire that occurred prior to 1936, possibly the 1910, 1915, or 1919 fires, which were fairly large events in the Kananaskis region (Rogeau 2005).

Prior to 1000 years ago, fires do not appear to relate to climate at all for the Pigeon/Cougar Creek region, unlike other areas, such as the Kootenay Valley and northern Montana. The First Millenium Glacial Advance has been recognized only recently, and how it relates to climate may not be as clear as the Tiedemann-Peyto Advance or the Little Ice Age, which have been extensively studied. Despite this, it appears that fires have occurred in the Cougar and Pigeon Creek areas during both warm and cold climatic periods, which suggests that local factors may have played a more important role in fire frequency for this time period.

4.4.1 Discussion

As debris floods may be related to fire episodes (Section 3), determination of a forest fire return period may be an important parameter for the Pigeon Creek watershed and fan. From Table 4.4, the return period for Cougar Creek appears to be 100 to 200 years from 1570 to 590 years BP, and about 200-300 years from 3405 to 2490 years.

At Dead Man's Flats, the record appears to be less complete. The return period is about 50 years for the last 250 years, and about 100-200 years prior to that, if one assumes that the fire history record is incomplete. However, if it assumed that the record is complete, then 14 fires occurred over the last 3405 or 3510 years with an average recurrence interval of about 250 years for the Pigeon Creek and 243 years for the Cougar Creek area.

4.4.2 Limitations

Morphologically significant disturbance events on the Pigeon Creek fan can be due to either relatively infrequent hydrologically-driven floods as happened in June 2013 (approximately 150-year recurrence interval, see Section 6) or to infrequent fire-flood events (>200 year recurrence interval) that may be associated with moderate rainfall events or snowmelt (Jordan, 2012) following a high severity, stand-replacing fire in the watershed. In contrast to the situation in Cougar Creek (BGC 2014b), there appears to be little potential for landslide dam-break flooding and resulting sedimentation in Pigeon Creek, probably because of the differences in watershed geology (BGC 2014a) and topography (refer to Section 6.6). Fire suppression since about 1910 has altered the frequency of fire events in the watershed and therefore, the historical recurrence interval of stand-replacing fires (200-300 years) may not be representative of future risk. If the fire record (i.e. charcoal) preserved in the Pigeon Creek fan deposits is complete, it appears that the last major fire-flood event occurred about 200 years ago (Table 4-4). Because of effective fire suppression, future fires may be less frequent but more severe with consequent effects on runoff and sediment volumes.

5 MAGNITUDE ANALYSIS

This section presents a magnitude analysis of previous debris flood events in the Pigeon Creek watershed. The potential effects of climate change and post-fire hydrology are also considered. Sediment volumes and peak flows, for various conditions are provided. This information was used to determine the extent of flooding and potential downstream impacts. Sediment transport processes in the Pigeon Creek watershed are dominated by fluvial processes, and have a strong dependency with the watershed's hydrological response. In Section 8, both frequency and magnitude are integrated to produce frequency-magnitude relationships, which is an instrumental input for the hazard assessment.

As noted in Section 3.2, the nature of flooding events in the Pigeon Creek watershed is dominated by flood processes with episodes of debris floods. For this reason, both floods and debris flood events were investigated.

In order to develop estimates of clear water flood and sediment volume deposition, various methods were used. A hydrologic and hydraulic model of the watershed was developed to understand the hydrological response of the Pigeon Creek watershed under various climatological conditions, including historical data and projected climate change. The hydrographs produced by the model were used as a driver in the sediment yield analysis. Other analyses are also provided, including the following:

- Peak flow estimate based on field observations,
- Hydrological modeling to quantify clear water flows;
- Comparison of the 2008 and 2013 digital elevation models (DEM) from LiDAR data of the Pigeon Creek fan;
- Estimation of sediment contributions from the Thunderstone Quarry during the 2013 event;

- Analysis of data and information obtained from test pits and carbon dating;
- Analysis of data obtained from dendrochronology;
- Sediment yield using empirical methods; and
- Sediment bedload transport methods.

5.1 Peak Flow Estimates for the Event of June 19-22, 2013 based on Field Observations

BGC identified a high water mark, and made measurements at a cross section upstream of the waterfall. Using this observation, BGC calculated a maximum peak flow of 105 m³/s. The level of bulking that could have occurred throughout the event is studied in further sections of the report. Bulking is the increasing of clear water flows due to high sediment concentrations. The extent of sediment deposition and woody debris documented by Miles, and BGC, and also observed by Tetra Tech in the fan, suggests that during peak conditions the clear water flows were increased by sediment and debris loadings. Based on their forensic investigations, BGC suggested that the Pigeon Creek event upstream of the falls could be classified as a flood event. On the other hand, Miles (2013) suggested that a significant volume of sediment came from the upper watershed. BGC also acknowledged in the forensic analysis report that the overall event could be considered as a debris flood event, taking into account sediment contributions from the stockpiled material that was at the quarry during the event. To account for sediment and debris loads, clear water flows are increased using a bulking factor (BF). Next section discusses the BF and presents a plausible range to be applied to the Pigeon Creek event of 2013.

5.1.1 Bulking Factor

Bulking is the increasing of flows due to high sediment concentrations. Woody debris is another contributing factor to the bulking effect. West Consultants (2011) conducted a literature review of bulking practices in California. As summarized by the authors, the total bulked flow can be represented as

$$Q_B = Q_W + Q_S$$

Where Q_B is the bulked discharge and Q_W and Q_S are the peak clear water discharge and peak volumetric sediment discharge. The bulking factor (BF) then is the ratio between the bulked and clear water discharges.

$$BF = \frac{Q_W + Q_S}{Q_W}$$

The bulked discharge can then be defined as

$$Q_B = BF * Q_W$$

And the BF can be computed based on the sediment concentration in the flow with:

$$BF = \frac{1}{1 - \frac{C_v}{100}}$$

Where C_v is the sediment concentration in percent volume (sediment volume/total volume)

In order to convert sediment concentration by volume into concentration by weight, O'Brien (2006) provided the following equation:

$$C_v = \frac{C_w \gamma}{\gamma_s - C_w(\gamma_s - \gamma)}$$

Where C_w is the sediment concentration by weight (sediment weight/total weight)

γ is the specific weight of water, and

γ_s is the specific weight of the sediment

Although actual sediment concentrations were not measured in Pigeon Creek during the 2013 event, some inferences can be made based on Miles, BGC and Tetra Tech observations. Generally, the size of sediment deposits from the point of discharge of Pigeon into the Bow River all the way up to the watershed apex, was observed by Miles to increase from fine sand, to gravels, to cobbles. Miles concluded that although sediment volumes washed-off from the quarry piles were substantial, sediment volumes coming from the upper watershed were also significant. Based on all observations, it appears that the event could be categorized as both a flood with episodes of debris flood (or hyperconcentrated flow). Based on these observations, and recommendations from O'Brien (1986) as shown in Table 3.1, a bulking factor range between 1.20 and 1.30 is considered appropriate for the event of 2013 for Pigeon Creek flows. This range, then provides a clear water peak flow range between 81 m³/s and 87.5 m³/s based on BGC's peak flow estimates. This range is refined in further sections.

5.1.2 Assessment of Clear Water Flows through Hydrological Modelling

An understanding of the hydrological behaviour of the Pigeon Creek watershed is required as part of the hazard and risk assessment. The heavy rainfall and a rapidly melting snowpack in June of 2013 resulted in extreme flows that led to the flooding experience on Pigeon Creek. These extreme flows triggered the mobilization of a large volume of sediment and woody debris, most of which deposited in the fan.

On a regional basis, Pomeroy et al. (2013) provided an assessment of the event mechanisms, as well as causes of the flooding triggered by the 2013 event. To quote Pomeroy et al.: "The event was an intense and slow-moving moist upper low that parked itself over southern Alberta delivering heavy rains". Regarding the principal flood processes, Pomeroy et al. concluded that although the flood was generated through several mechanisms, the primary one was rainfall-runoff in the foothills and lower elevations in the front ranges.

In the Pigeon Creek watershed, several processes in the upper watershed colluded to produce the sediment and debris that were transported downstream. These included sheet erosion, gully erosion, channel bed scour and bank erosion, slides, and debris flows.

In the absence of flow monitoring data for Pigeon Creek, it was necessary to develop an alternative method for estimating the peak flow and total volume of runoff that was generated during the 2013 event. Pomeroy et al. (2013) discussed the relevance of using physically based models to predict flows in ungauged basins. For the purposes of this project, a hydrological model was developed to evaluate watershed hydrological response under various climatic conditions. Historical conditions, including the 2013 event, as well future climate change scenarios, and post-fire conditions were assessed.

The hydrology of cold regions in Canada, as described by Pomeroy et al. (2007), is characterized by low to moderate precipitation, cold winters, and significant water storage by the seasonal snowpack, and the seasonally or perennial frozen ground.

A deterministic, distributed hydrological model of the Pigeon Creek watershed was developed using the PCSWMM software. The model computed creek flows under various hydrological scenarios. The computed flows were subsequently used to estimate sediment loadings from the watershed, as detailed in Section 6.5.

PCSWMM is a commercial package that uses the EPA SWMM5 (SWMM5) model as its main computational engine. SWMM5 was developed by the Environmental Protection Agency of the United States (EPA, 2010). SWMM5 is a dynamic model that accounts for various hydrologic processes that produce runoff from watershed areas.

These include:

- Time-varying rainfall;
- Evaporation of standing surface water;
- Snow accumulation and melting;
- Rainfall interception from depression storage;
- Infiltration of rainfall into unsaturated soil layers;
- Percolation of infiltrated water into groundwater layers;
- Interflow between groundwater and the drainage system, and
- Nonlinear reservoir routing of overland flow.

Spatial variability in these processes is achieved by dividing a study area into a collection of smaller, homogeneous sub-catchment areas, each containing its own hydrologic parameters to represent the processes listed above. The model reads precipitation and climatic inputs, distributes rainfall and snowfall volumes on time step by time step basis, and accounts for snowpack accumulation, water retained at the surface, infiltration, shallow groundwater interactions, evapotranspiration, and runoff generation and routing. Generated flows are then hydraulically routed through tributary channels using the Saint-Venant equations. The model reports a runoff hydrograph for each sub-catchment and flow hydrographs at any location in the watershed. The Pigeon Creek model was developed and then calibrated as explained in the next section.

5.1.3 Model Calibration

Model calibration is the iterative adjustment of model parameters until an acceptable agreement between computed model outputs and monitoring data, usually flows, is achieved. In the absence of flow monitoring data from Pigeon Creek, an alternative methodology was implemented.

Marmot Creek is a neighbouring watershed with available flow monitoring data. We developed a hydrological model for Marmot Creek and calibrated the model against the observed flow data. The hydrological parameters employed in the Marmot Creek model were then transferred to the Pigeon Creek model. A map of the two watersheds is provided in Figure 5.1.

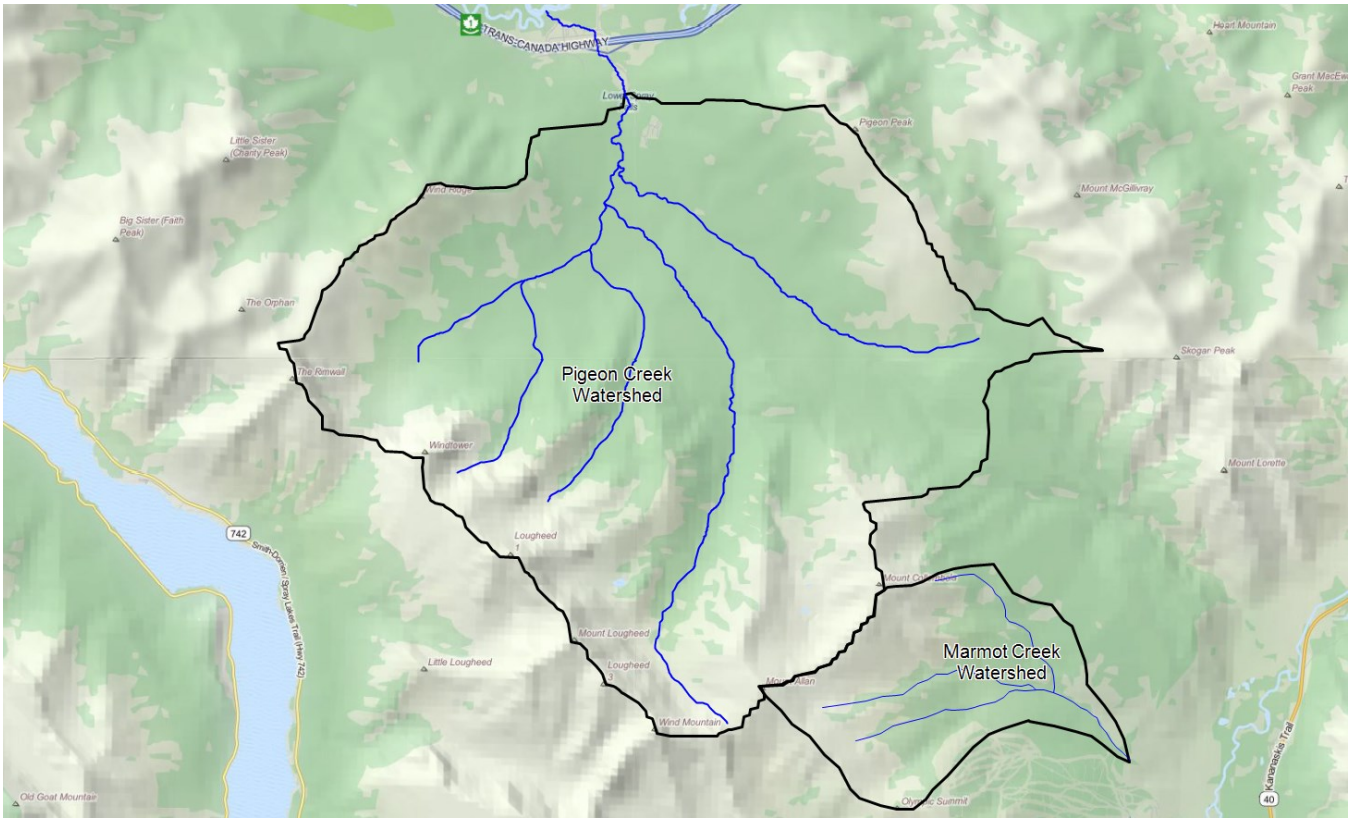

Figure 5.1. Marmot Creek and Pigeon Creek Watersheds

Marmot Creek is a research basin that has been the subject of hydrological studies since 1962, and it is currently managed by the University of Saskatchewan. Research has been conducted on mountain hydrology, including snowmelt, infiltration in frozen soils, hydrological modelling and streamflow generation amongst other research topics. A physically based model called the *Cold Regions Hydrological Model* was developed and validated using long term data from the research (Pomeroy et al., 2007). Key findings from the Research Basin, as summarized by Pomeroy et al., are:

- Spring snowmelt is usually responsible for the annual peak flow;
- Freshet is sensitive to antecedent soil moisture and ground ice conditions; and
- The effect of heavy summer rainfall is highly variable, except for intense convective rainfall.

Marmot Creek watershed has an area of approximately 9.4 km² and elevations that range from 1,600 m to 2,825 m at the peak of Mount Allan. A comparison of key watershed characteristics of Marmot Creek and Pigeon Creek is presented in Table 5.1. Figure 5.2 shows the aspect for both watersheds.

There are three precipitation gauges in the Marmot Creek watershed: Hay Meadow (Elev. 1,436 m), Upper Clearing (Elev. 1,844 m), and Fisera Ridge (Elev. 2,325 m). The June 2013 event was captured by the three stations. Figure 5.3 presents the recorded rainfall volumes, per station. for the 19th, the 20th and the 21st of June, as well as the cumulative for the three-day event.

Table 5.1: Comparison of Key Characteristics Between Marmot and Pigeon Creek Watershed

Characteristic	Marmot Creek Watershed	Pigeon Creek Watershed
Area (Km²)	9.4	55.1
Length of Main Stem Stream (Km)	4.85	10.7
Average Watershed Width (Km)	2	5
Ratio Length/Width	2.4	2.14
Average slope from top to the apex (%)	23	16
Highest/Lowest Elevation - apex (masl)	2,825/1,671	3,153/1,348
Aspect	South East Facing	North Facing
Orientation	North West to South East	South to North

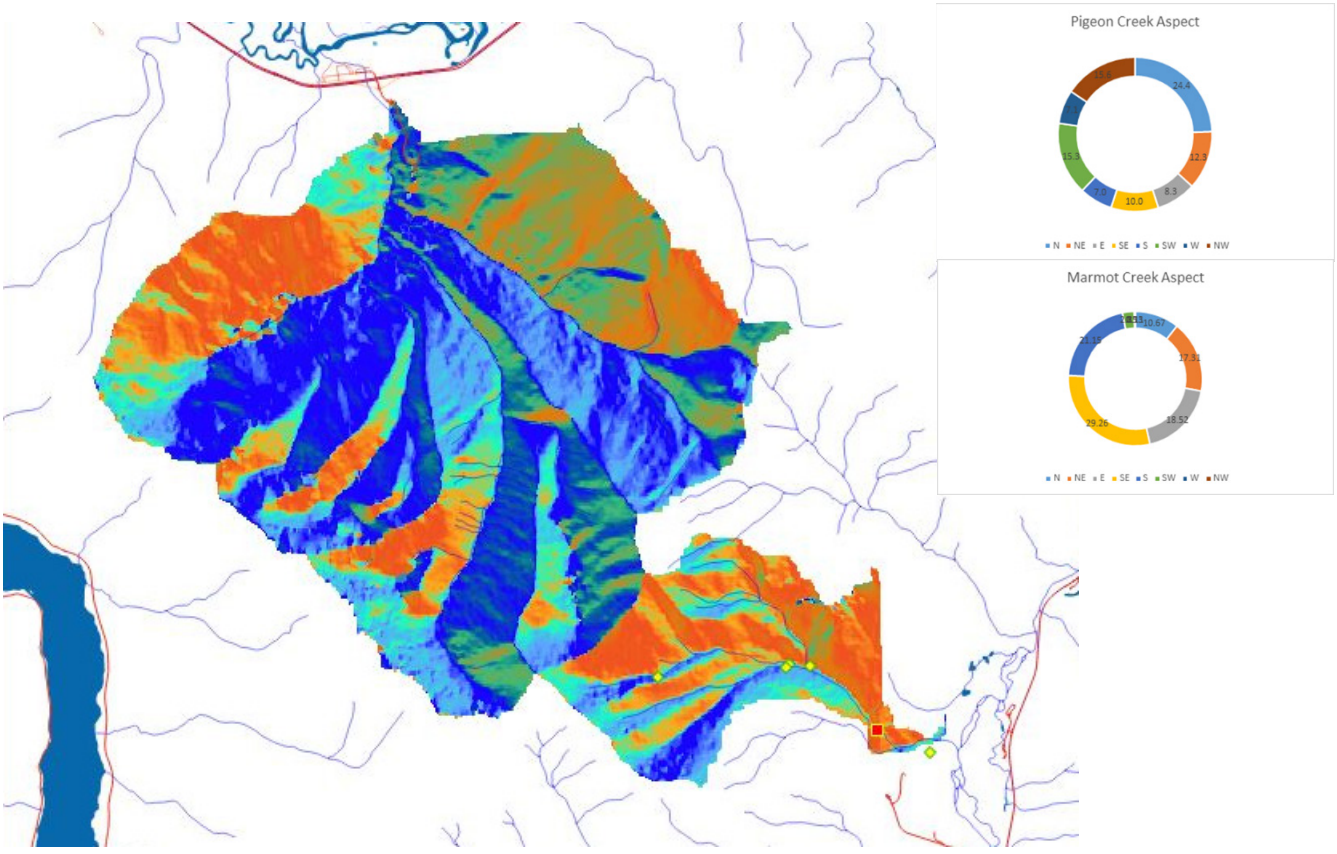

Figure 5.2. Pigeon Creek and Marmot Creek Watersheds Aspect

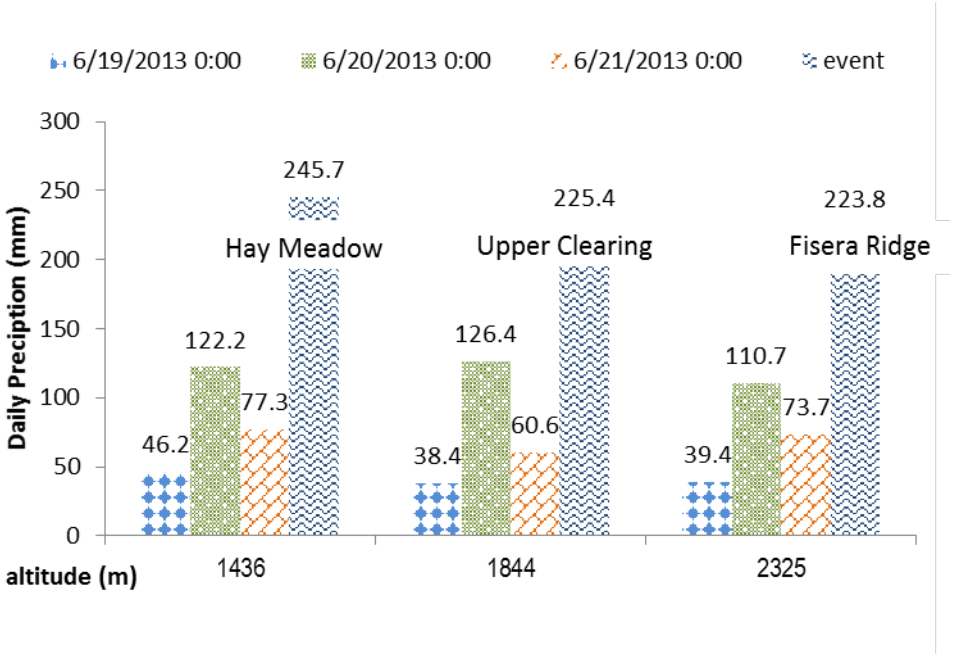

Figure 5.3. Precipitation Data for the Event of June 19 to 21, 2013 at 3 stations at the Marmot Creek Research Basin.(Figure provided by the University of Saskatchewan through BGC Engineering and the Town of Canmore)

The surficial geology map obtained online from the Alberta Government was used to generate infiltration parameters for the Green and Ampt infiltration method. For each soil texture within the Pigeon and Marmot Creek watersheds, infiltration parameters were assigned, as shown in Table 5.2. Using GIS tools in PCSWMM, a weighted spatial average was performed that calculated the infiltration parameters for each model sub-catchment.

Table 5.2: Infiltration Parameters (Green&Ampt Method) Based on Surficial Geology Mapping

Soil Texture	Hydraulic Conductivity (mm/hr)	Suction Head (mm)
Poorly- to well-sorted, stratified-to-massive sand, gravel, silt, clay and organic sediments occurring in channel and overbank deposits.	60	60
Till a mixture of clay, silt, sand and minor pebbles, cobbles and boulders. Locally, this unit may contain blocks of bedrock, pre-existing stratified sediment and till, and/or lenses of glaciolacustrine and/or glaciofluvial sediment.	0.5	250
May contain pre-existing bedrock, till, glaciolacustrine, glaciofluvial and/or eolian sediments, generally poorly sorted.	1	250
Bedrock	0.1	300

Parameters for snowmelt, groundwater, depression storage, surficial roughness were also assigned for each sub-catchment. Long term temperature records were obtained from the Kananaskis Climate Station (Environment Canada ID 3053600).

Monthly factors were assigned to account for seasonal variability of the hydraulic conductivity, frozen ground during winter months, and increased infiltration capacity during warmer months. Season variability was also considered in the depression storage parameter to account for seasonal variability in surface depressions and interception. Monthly evapotranspiration values were obtained from research conducted in Marmot Creek by Munn and Storr (1967).

The Marmot Creek model was calibrated using 10 years of flow data, from 2001 to 2010. Figure 5.4 presents the computed and observed peak flows. These values were compared with the scatter plot shown in Figure 5.5. The objective of the calibration is to bring the computed peak flows as close to the observed values in order to minimize the distance from the 45 degree line. We note that most computed peak flows were within the 15% error band.

The outcome of the calibration is considered acceptable for the purposes of this project: the model is able to properly simulate key hydrologic watershed processes, including snow accumulation, snowmelt, infiltration, soil moisture, depression storage, runoff generation, and streamflow routing.

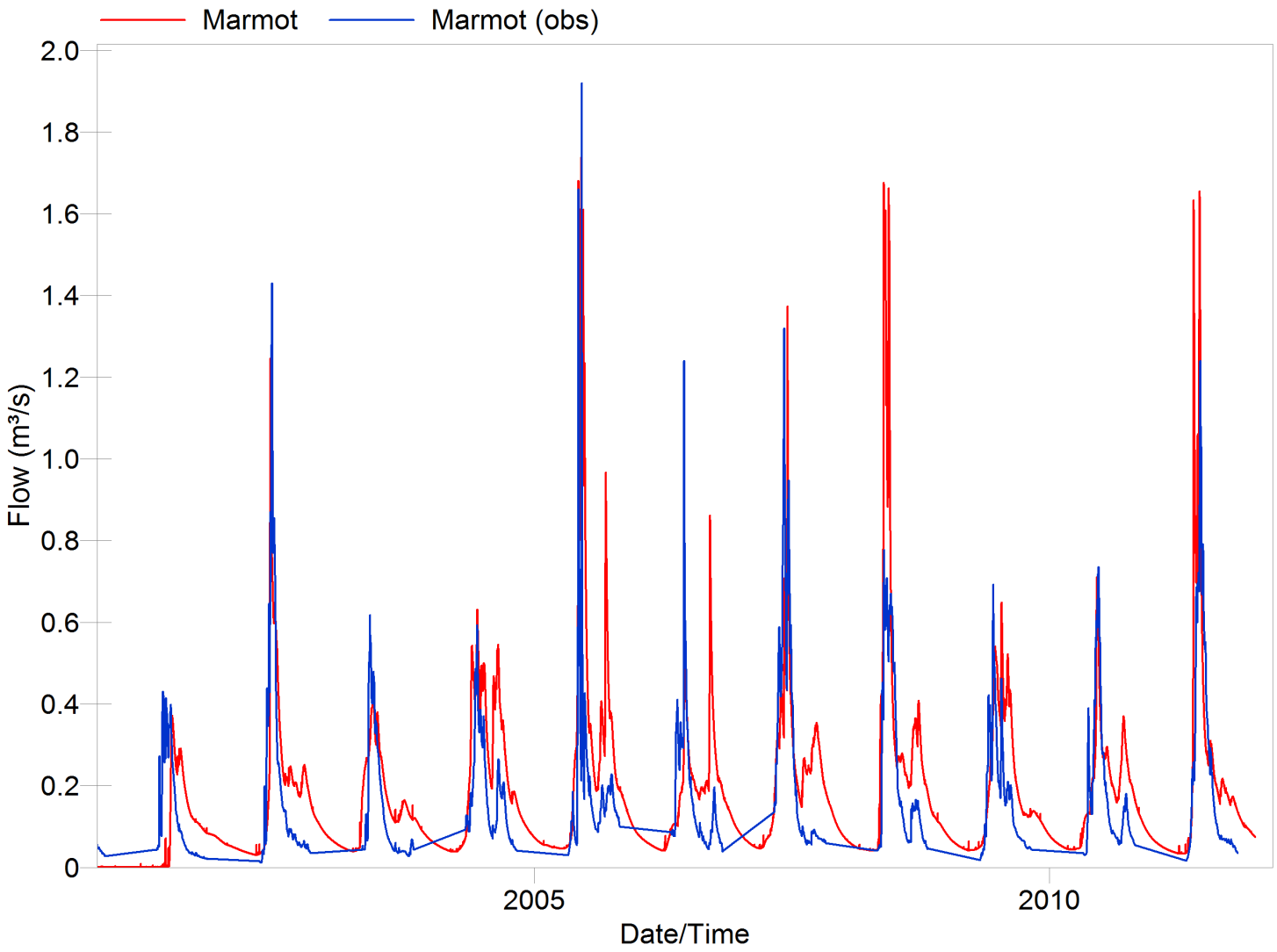

Figure 5.4. Marmot Creek Hydrograph: Observed vs. Computed Flows

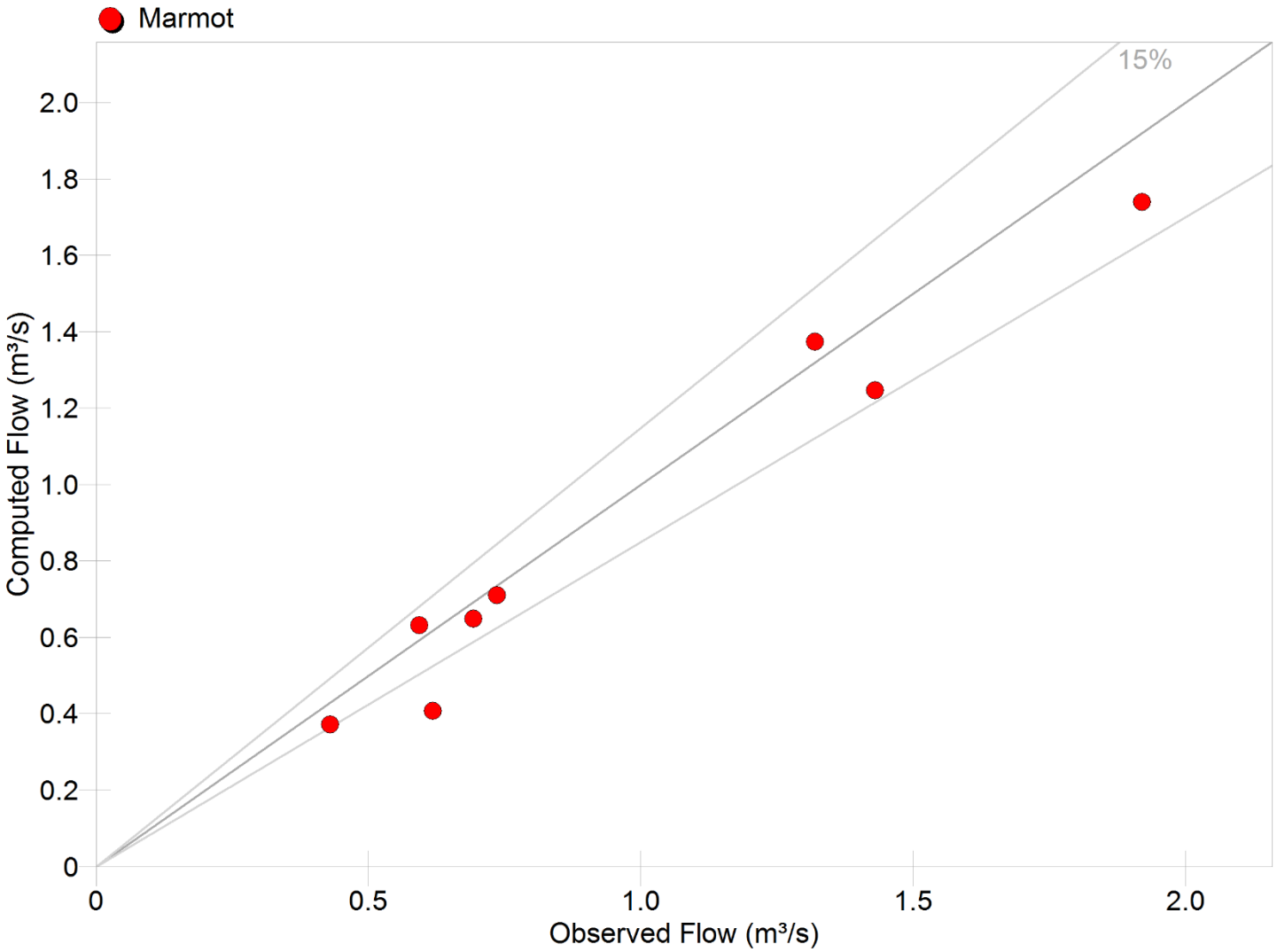

Figure 5.5. Marmot Creek Calibration Scattered Plot to Compare Observed vs. Computed Peak Flows

5.1.4 Pigeon Creek Hydrological Model

Although the Pigeon Creek watershed is about 6 times larger in area, and flatter than the Marmot Creek watershed, their similarities in surficial geology and vegetation cover, and the fact that they are located in the same climatic region, makes it reasonable for the transfer of hydrologic parameters from the calibrated model. Infiltration parameters for Pigeon were calculated using the same method applied for Marmot, based on the surficial geology.

The Pigeon Creek watershed, upstream of the fan, was subdivided into sub-catchments as shown in Figure 5.6. The model was discretized to represent small and large tributaries to Pigeon Creek. Sub-catchment (overland) and channel slopes were obtained from the available LIDAR data. The model computes flows for each sub-catchment for a given event, producing a hydrograph which is then hydraulically routed. Flows are accumulated in the downstream direction until they reach the outlet of the system. The model was extended to the Bow River.

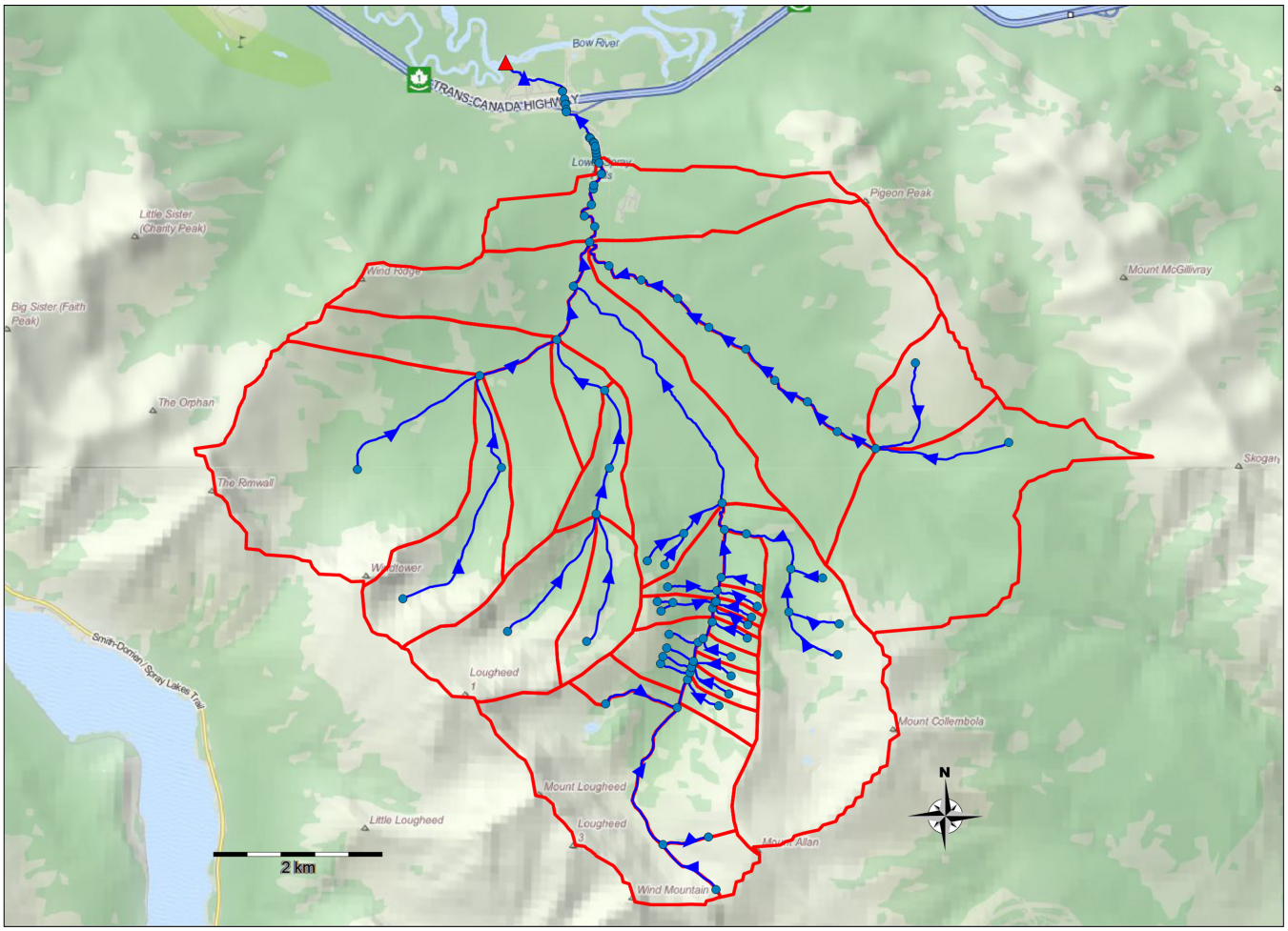

Figure 5.6. Pigeon Creek Watershed – Model Discretization

5.1.5 Assessment of 2013 Clear Water Flows at Pigeon Creek Using Watershed Model

The Pigeon Creek watershed model was used to assess the clear water peak flow for the event of June 2013. As noted before, based on field observations of high water marks, a bulked peak flow of 105 m³/s was first established. Assuming a bulking factor range between 1.2 and 1.3, clear water peak flows between 80.7 m³/s and 87.5 m³/s were determined. The objective of the modelling exercise is to provide a tool able to calculate flows within that range. This was achieved by modeling the event of June 2013 under different antecedent conditions. Antecedent soil moisture conditions can have a significant effect on the hydrological response of a watershed. An extreme rainfall event will produce result in a larger peak flow if the soil is saturated. Available snowpack will also affect hydrograph characteristics such as volume and peak flow. To assess the effects of antecedent conditions in the Pigeon Creek watershed, the hyetograph of the June 19 to 21, 2013 event was inserted in every year of the 10 year rainfall record from 2001 to 2010. The modified rainfall timeseries was then used as input to the watershed model. This was done to assess possible scenarios in terms of streamflow generation that could be observed in the watershed under various antecedent conditions. Every one of the years had different soil moisture and snowpack conditions before June 19. As some years are drier than others, and warmer than others this exercise provides valuable information regarding possible flow scenarios.

Results from the modelling show that if the event of 2013 would have happened in any of those years, clear water peak flows between 72 m³/s and 112 m³/s could have been observed. The year with the most severe antecedent conditions was 2005. This finding confirms the order of magnitude of peak flows based on high water marks; and because it confirms that it is possible that the higher end of the established peak flow based on high water marks could have occurred. *Based on the latter, for the purposes of the hazard and risk assessment, a bulked peak flow of 105 m³/s is considered to be plausible*.

5.1.6 Assessment of Pigeon Creek Clear Water Peak Flows

The Pigeon Creek model was used to assess the hydrological response of the watershed under various storm conditions. BGC (2014) presented a summary of 3-day storm volumes for the Kananaskis station for various return periods, as summarized in Table 5.3. The hyetograph of the June 2013 event was used to distribute the rainfall volumes for each of those events. Those hyetographs were inserted in the 2005 rainfall annual timeseries. The 2005 dataset was employed because it had the most precipitation and the most severe (wettest) antecedent conditions. The event was inserted starting June 19, replicating the starting day and time in 2013. The model was run for the entire year with the inserted hyetograph, for all events. Peak flows for clear water conditions obtained from the model for each storm event are summarized in Table 5.3 and shown in Figure 5.7.

Furthermore, the hydrological response of the watershed for various 24-hr duration events was assessed. Data was obtained from the Kananaskis Station IDF curve shown in Figure 5.8. Similarly, rainfall intensities from the IDF were inserted in the 2005 rainfall record as a constant value for the entire day on June 19th. Results from the 24-hr storms are summarized in Figure 5.9 and Table 5.4. Flows for the 12-hr and 6-hr duration storms were also computed and are shown in Figures 5.10 and 5.11.

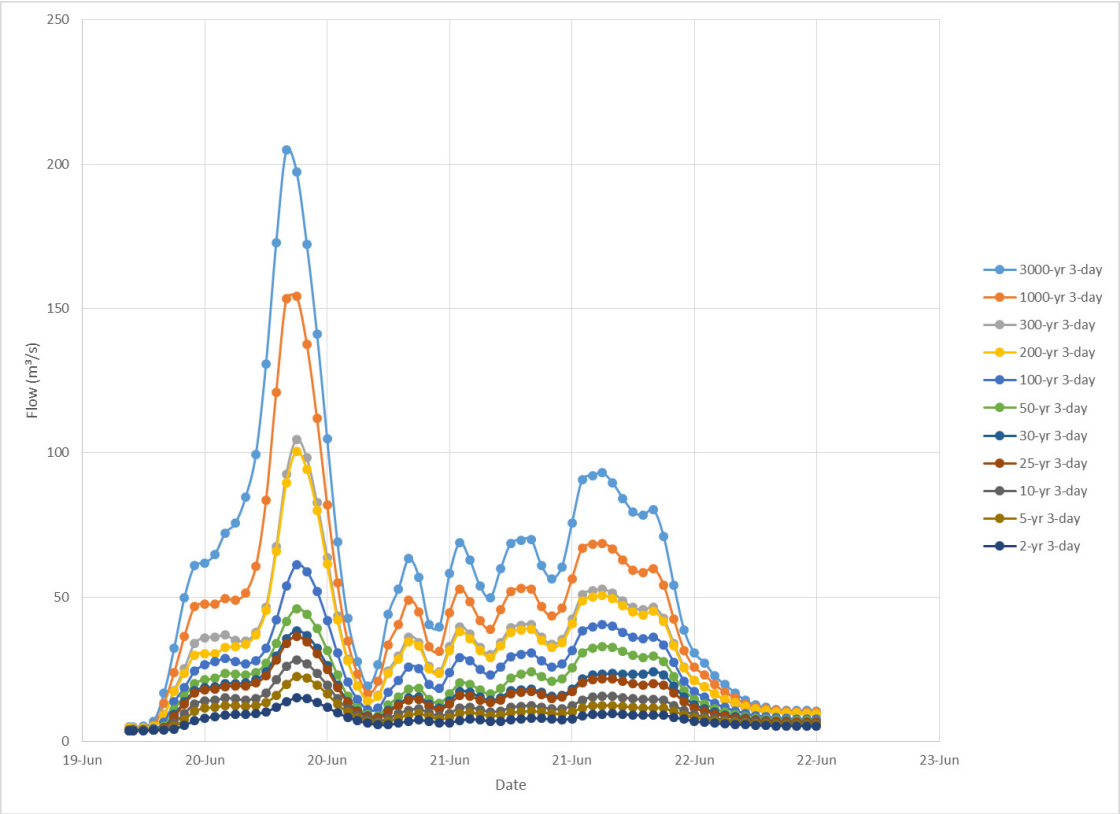

Figure 5.7. Computed Clear Water Hydrographs for various 3-day Return Period Rainfall Events

Table 5.3: Summary of 3-day storm volumes (Kananaskis Station) for various return periods and corresponding computed clear water peak flows

Return Period (years)	Rainfall (mm)	Clear Water Peak Flow (m^3/s)
2	61	15.03
5	85	22.42
10	104	28.31
25	132	36.46
30	138	38.41
50	156	46.03
100	182	61.2
200	212	85.5
300	231	104.6
1000	296	154.2
3000	368	205

Rainfall Frequency analysis at Kananaskis Station (BGC,2014).

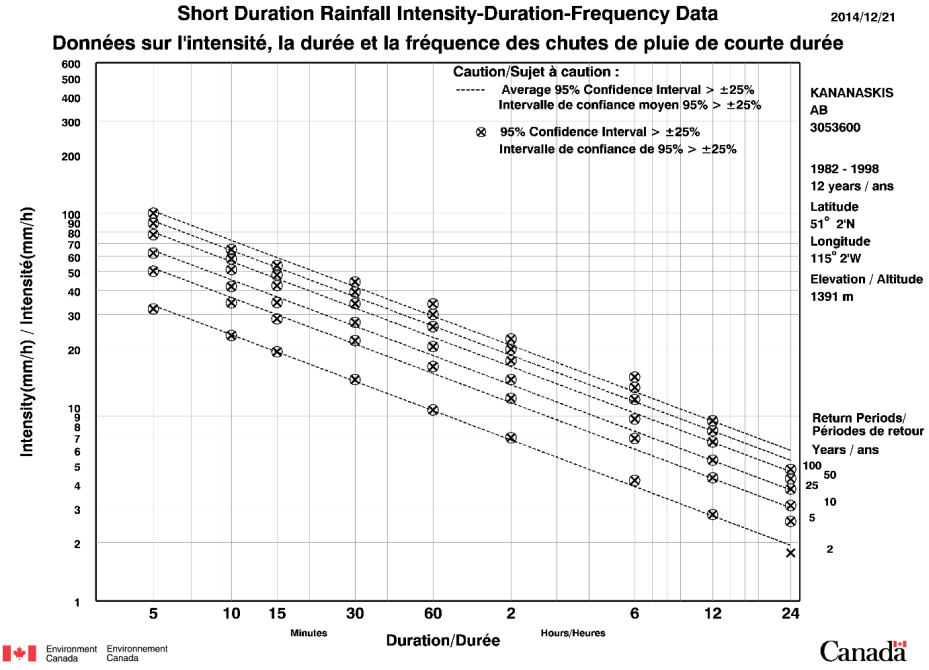

Figure 5.8. Intensity Duration Frequency (IDF) Curve for the Kananaskis Station (Environment Canada Station 3053600)

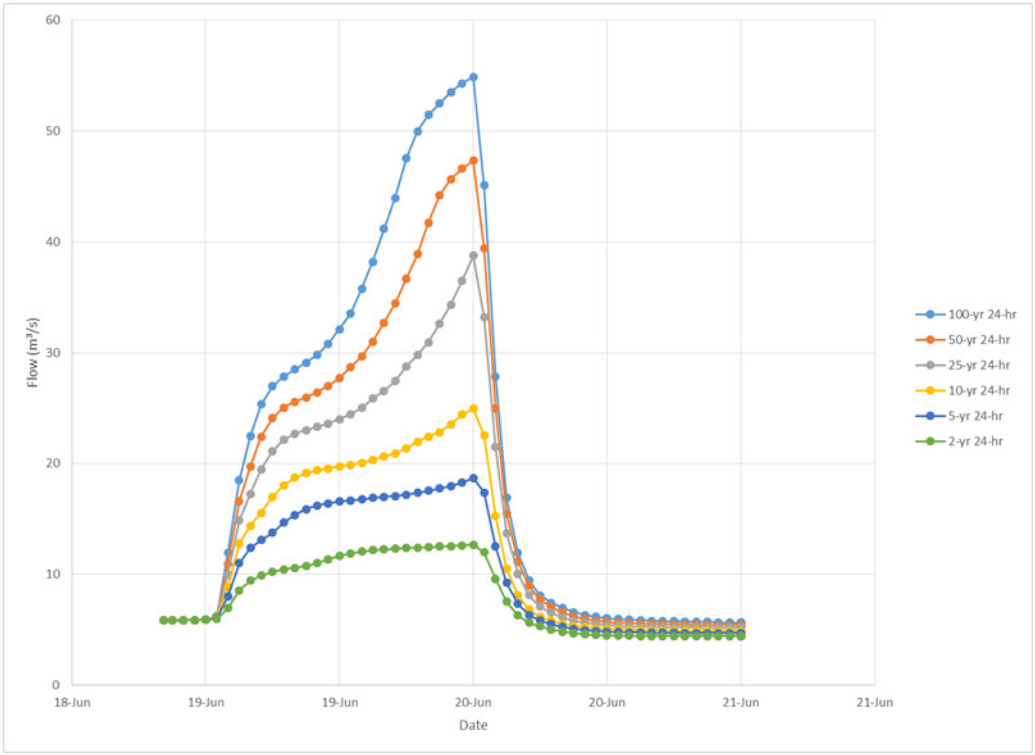

Figure 5.9. Computed Clear Water Hydrographs for various 24-hr Return Period Rainfall Events

Table 5.4: Summary of 24-hr storm intensities (Kananaskis Station) for various return periods and corresponding computed clear water peak flows

Return Period (years)	Rainfall Intensity (mm/hr)	Clear Water Peak Flow (m^3/s)
2	1.8	12.7
5	2.6	18.7
10	3.1	25.0
25	3.8	38.8
50	4.3	47.3
100	4.8	54.9

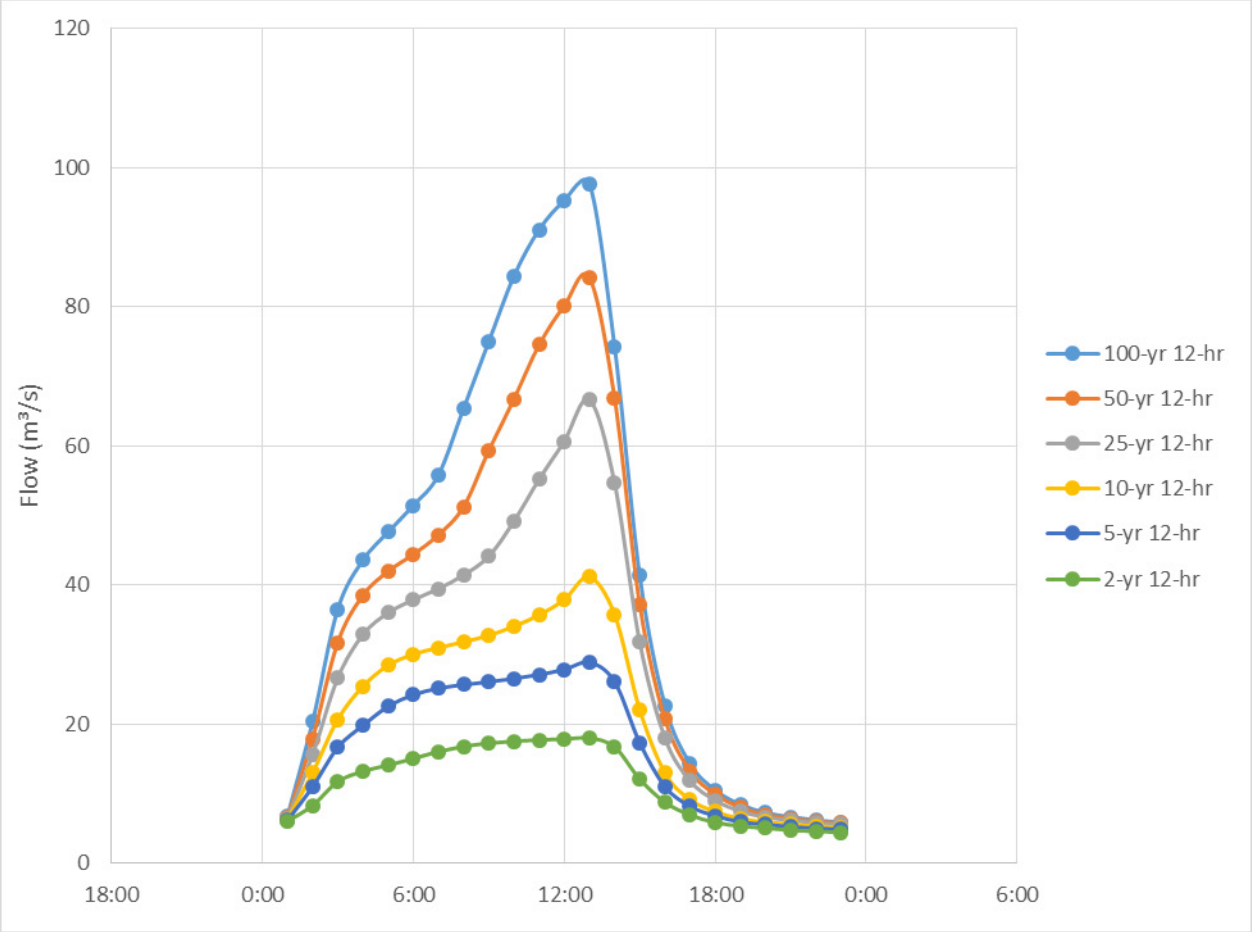

Figure 5.10. Computed Clear Water Hydrographs for various 12-hr Return Period Rainfall Events

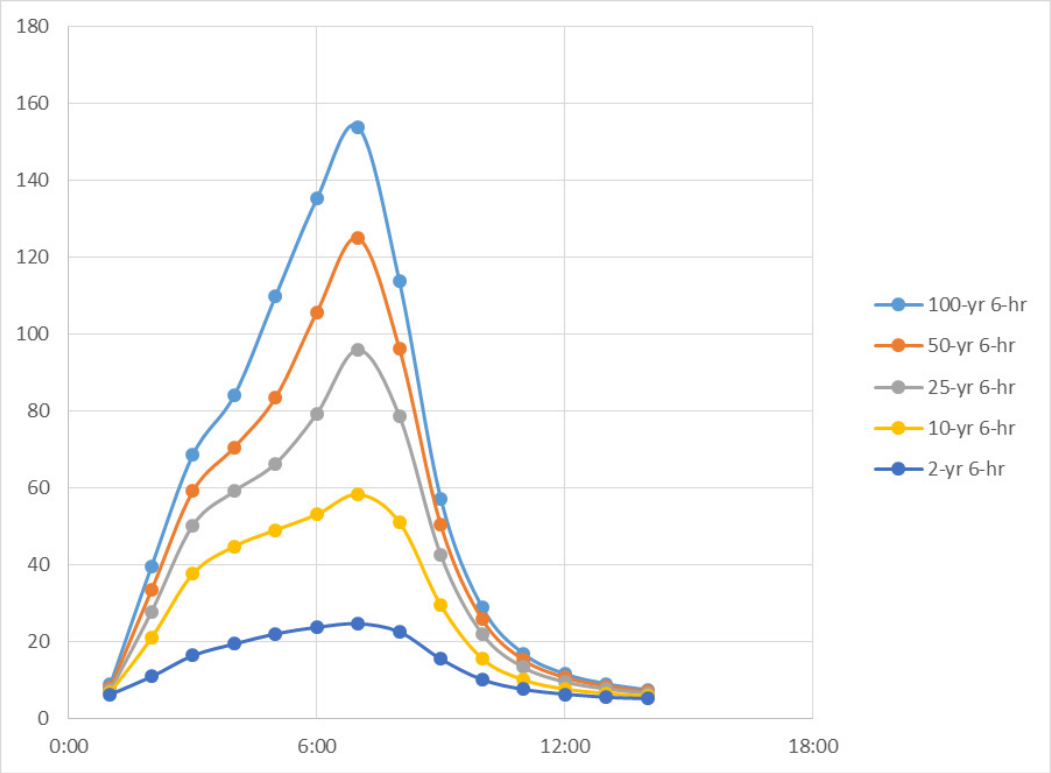

Figure 5.11. Computed Clear Water Hydrographs for various 6-hr Return Period Rainfall Events

5.1.7 Assessment of Clear Water Flows Under Climate Change

Climate change in the Canadian Rockies is expected to impact hydrological processes, more notably, increases in temperature will affect temperature sensitive snow processes (Zhang et al., 2000). Generally, average warming in western Canada from the year 1900 to 1998 has resulted in increased temperatures between 0.5C to 1.5C (Zhang et al., 2000). As a consequence, the ratio between rainfall and snow is expected to increase (Zhang et al., 2000). With a reduced snowpack, there will be more energy available for evapotranspiration which would in turn lead to drier soils and reduced groundwater recharge in the summer (Hayashi and Van der Kamp, 2009). On the other hand, groundwater recharge may increase in the spring due to increase in infiltration capacity due to less frozen ground area.

Expected changes in temperature, evapotranspiration and precipitation for various climate change scenarios can be obtained from available tools. For instance the United States Environmental Protection Agency (USEPA) developed a tool called SWMM-CAT, which calculates location-specific climate change adjustments. These adjustments are produced in a format that can be easily imported into a PCSWMM input file. Such adjustments are applied on a monthly basis to air temperature, evaporation rates, and precipitation, as well as to the 24-hour design storm at different recurrence intervals. The source of these adjustments are global climate change models run as part of the World Climate Research Programme (WCRP) Coupled Model Intercomparison Project Phase 3 (CMIP3) archive. Downscaled results from this archive were generated and converted into changes with respect to historical values by USEPA's CREAT project (http://water.epa.gov/infrastructure/watersecurity/climate/creat.cfm).

SWMM-CAT was run for the Canmore area and climate change adjustment parameters were obtained. Figure 5.12 shows a screenshot of the tool and Table 5.5 shows the monthly adjustment for temperature, evaporation and rainfall for near term (2020 – 2049) climate change projections. All adjustments were saved and imported in to the PCSWMM input files which were then run. Peak flows obtained are summarized in Table 5.6.

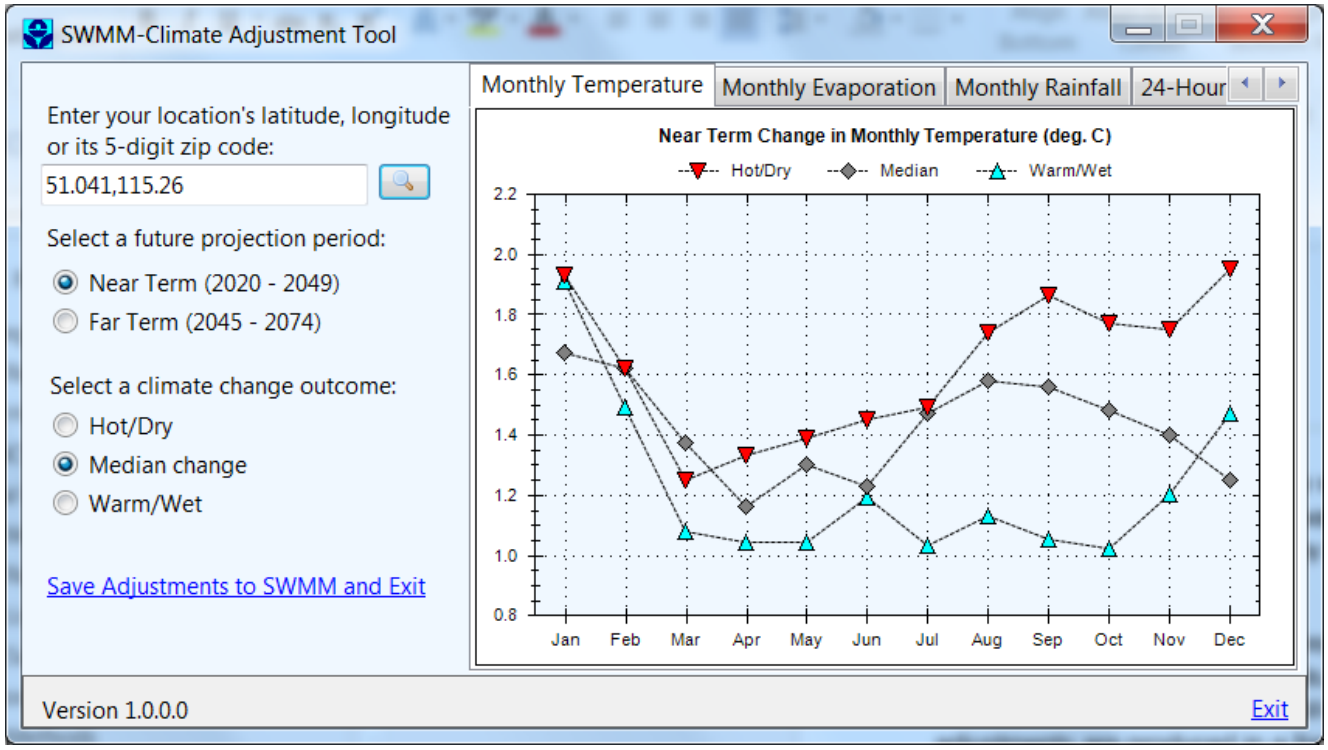

Figure 5.12. Climate Change Adjustment Factors for the Canmore Area. Monthly Temperature Adjustments for Near Term Projections (2020 to 2049)

Table 5.5: Climate Change Monthly Adjustment Factors**

Month	Temperature	Evaporation (mm/day)	Rainfall
January	3.06	0.0762	1.199
February	2.97	0.1270	1.154
March	2.50	0.2540	1.153
April	2.11	0.2794	1.082
May	2.39	0.3556	1.069
June	2.25	0.3302	1.036
July	2.70	0.3810	1.006
August	2.89	0.3556	0.874
September	2.85	0.2540	0.939
October	2.72	0.2032	1.089
November	2.56	0.1524	1.104
December	2.29	0.0762	1.102

**Adjustments are +/- changes to temperature and evaporation and multiplier for rainfall that can vary by month of the year.

Table 5.6: Summary of computed peak flows under climate change scenario for 3-day storms

Return Period (years)	Clear Water Peak Flow (m^3/s)	Clear Water Peak Flows CMIP3 (m^3/s)
2	15.03	16.01
5	22.42	21.37
10	28.31	26.28
25	36.46	38.92
30	38.41	42.03
50	46.03	51.73
100	61.2	71.16
200	85.5	100.6
300	104.6	117.2
1000	154.2	165.3
3000	205	214.4

In addition to SWMM-CAT, the Computerized Tool for the Development of Intensity-Duration-Frequency Curves under Climate Change developed by Srivastav and Simonovic (2014), was used to assess hydrological changes due to climate change. This computerized web-based IDF tool is able to generate possible future change using a combination of global climate modeling outputs and locally observed weather data. For this project, the tool was used to generate IDF curves for the Kananaskis Station under various climate change scenarios. Table 5.7 presents the modified IDF values. Models for these conditions were run. Peak flows are summarized in Table 5.8 and results shown in Figure 5.13.

Table 5.7: Intensity Duration Frequency Rainfall (mm/hr) under Climate Change – Scenario RCP 8.5

T (years)	2	5	10	25	50	100
5 min	42.24	65.45	80.63	98.84	112.13	125.33
10 min	29.3	43.81	53.09	64.22	72.35	80.41
15 min	24.17	36.19	43.88	53.1	59.84	66.52
30 min	18.39	28.75	35.53	43.66	49.59	55.48
1 h	13.34	21.73	27.12	33.62	38.39	43.13
2 h	9.26	14.55	18.01	22.17	25.2	28.21
6 h	5.69	9.16	11.4	14.09	16.07	18.03
12 h	3.64	5.58	6.85	8.38	9.49	10.6
24 h	2.19	3.24	3.91	4.71	5.3	5.88

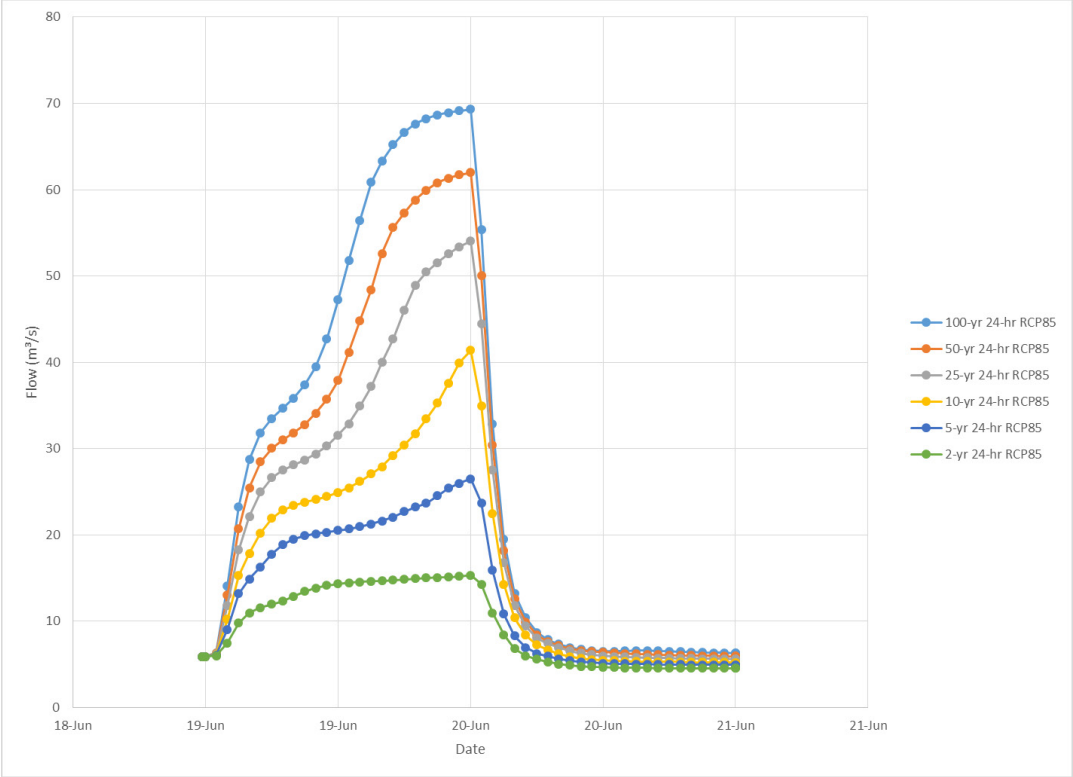

Figure 5.13. Computed Clear Water Hydrographs for various 24-hr Return Period Rainfall Modified to Account for Climate Change Scenario RCP 8.5

Table 5.8: Summary of computed peak flows under climate change scenario for 24-hr storms

Return Period (years)	Clear Water Peak Flow (m^3/s)	Clear Water Peak Flow RCP8.5 (m^3/s)
2	12.7	15.3
5	18.7	26.5
10	25.0	41.4
25	38.8	54.0
50	47.3	62.0
100	54.9	69.3

5.2 Assessment of the 2013 Debris Flood Event Using LIDAR Data

The quantity of material deposited, removed and re-positioned on the Pigeon Creek fan is difficult to estimate. One method that can be used for this estimate is to complete a differential surface analysis using pre-event and post-event LiDAR based surface information. BGC (2016) conducted a separate change detection analysis using the same Airborne LiDAR Scanning (ALS) datasets used by Tetra Tech. The following sections describe the work conducted by Tetra Tech, and BGC (2016) report is included in Appendix E.

5.2.1 Information Sources and Methods

Post-event LiDAR information was acquired on June 28, 2013, six days after the June 21-22 event. A digital elevation model (DEM) was developed for the fan from LiDAR point cloud. The raster surface created from the 2013 elevation data contained a single source of LiDAR xyz point cloud data. The extensive set of LiDAR data encompassed both the boundaries of the Pigeon Creek Fan and Watershed. This information was provided by the Town of Canmore.

The most recent pre-event surface elevation data was composed from two data sets. LiDAR, in the form of xyz point cloud data, was provided by Ms. Julia Eisl from the Town of Canmore. Contour line data (0.5 m interval) was provided by the Municipal District of Bighorn. The extent of each set coincides with the municipal boundary of the Town and Municipal District. For the Pigeon Creek Fan, the boundary runs parallel to and just north of the Trans-Canada Highway. While issued in 2009, both sets of data were acquired in 2008.

The analysis was conducted using ESRI ARCGIS 10.2 with 3D Analyst and Spatial Analyst extensions. QGIS Desktop 2.8.1. The process that was adopted can be summarized as follows:

- 1m cell size DEM rasters were created in ArcGIS 3D Analyst and QGIS using the contour and point cloud LiDAR data for the 2008 data, and the point cloud data for the 2013 data. Both of the resultant DEM .tif files were clipped to the fan boundary in order to retain the data that is relevant to the study;
- Hillshades of the 1m DEM rasters were created in ArcGIS Spatial Analyst for mapping interpretation and figure creation;
- A comparison of the 2008 and 2013 DEMs was created by developing a 1m cell size .tif difference raster in ArcGIS Spatial Analyst. For any cell in the raster, a value of +1 would mean that the cell is 1m higher in 2013 compared to 2008. Conversely, a value of -1 denotes that the cell in question has lost 1m in elevation in 2013 compared to 2008;
- The difference output was analyzed, and zones of interest were drawn onto a hardcopy print and digitized back into the GIS using ArcGIS with names for identification. Included with these zones are 3 locations where elevation changes would not be expected. These were used to verify the data between the 2008 and 2013 datasets; and
- Zonal statistics was run in ArcGIS Spatial Analyst to generate statistics for the ‘zones of interest’ polygons. The sum of the 1m difference cells in the zone represents the volume of the zone. Because the size of the cell is 1m, a value of 1 in the difference cell is 1 cubic metre.

5.2.2 Results

The pre- and post-event surfaces were analysed using GIS, based on a 1m x 1m grid size. Changes in elevation were computed and the results are presented in Figure 5.14. Negative values represent a lower elevation post-event; material was removed. Positive values represent an increased elevation; material was deposited.

To estimate the amount and location of material deposited, removed or re-distributed during the event, we isolated areas on the fan where inspections and analysis indicated changes had occurred (i.e. documented areas of deposition or avulsion) as a result of the June 2013 event. For discussion, we have grouped these areas based on location and/or land use. Table 5.9 presents a summary of the differential surface analysis.

Overall, the differential surface analysis estimated that 123,000 m^3 was deposited on the Pigeon Creek fan and 33,000 m^3 was entrained or eroded from the fan, resulting in a net deposition of 90,000 m^3.

Table 5.9: Pigeon Creek Fan: Summary of Differential Surface using LIDAR from 2008 and 2013

Location	Area (ha)	Difference (m^3)	Ave Deposition (m)	Total Deposition (m^3)	Total Erosion (m^3)
Quarry-Site	3.360	-97	0.00	21,085	21,182
Quarry - Downstream	3.683	27,405	0.74	34,754	7,349
Channel Fan	9.478	49,589	0.52	49,589	0
Central Fan	0.963	4,002	0.42	5,161	1,158
West Fan	3.961	7,387	0.19	8,956	1,569
East Fan	4.112	24,407	0.59	25,942*	1,535
Downstream East Fan	0.278	3,271	1.18	3,271	0
TOTAL:	25.835	115,964	0.45	148,758	32,793

*After careful examination of aerial photos taken after the 2013 event, included in Miles (2014), we have determined that the volume of deposition was insignificant in the area east of George Biggy Road, called East Fan in the analysis.

5.2.2.1 Thunderstone Quarry

Much speculation has occurred about the relative contribution of entrained stockpiled materials present on the quarry property at the time of the storm. The Thunderstone Quarry is in the business of mining, storing and transporting material. Calculating the amount of material contributed from stockpiles present when the storm occurred is not possible from the available LiDAR information. Significant change must have occurred at the site since 2008, and in the interceding six days between the storm event and the 2013 LiDAR capture during clean-up operations.

The above caveat noted, our differential surface analysis estimates that 21,200 m^3 of material was entrained from the quarry site. The entrainment was primarily from where we noted stockpiles were located in 2008 and 2012 imagery, and where they did not exist in the 2013 LiDAR imagery. An almost equal amount of material was deposited on the quarry site, presumably transported from the upper watershed.

5.2.2.2 Other areas

Large deposition areas included the area immediately downstream of the quarry bounded by the highway off-ramp and George Biggie Senior Road (27,000 m^3), the channel and immediate vicinity downstream of the highway (49,000 m^3), and the area immediately east of George Biggie Senior Road (24,000 m^3).

Aside from the stockpiled material at the quarry, entrainment occurred where new channels were formed, primarily along George Biggie Senior Road and along the southern ditch of Highway 1.

5.2.3 Limitations

The LiDAR comparison of the unaffected parts of the fan during the 2013 event shows some aggradation which may bias the volume calculation upwards: in other words this would make the volume estimate for the 2013 event conservative.

5.2.4 Findings from BGC (2016)

Appendix E includes the report from BGC (2016). BGCs analysis indicates that the net sediment volume deposition in the fan was in the order of 70,000 m^3. After discussions with the Town of Canmore, it was decided that BGCs findings are likely more representative of the actual deposition that took place and adopted as the value to be used in the report.

5.3 Volume Estimates from Test Pit Profiles

5.3.1 Methods

The following methods were applied for estimation of debris flood magnitudes from test pit interpretation:

- Test pit logs (Appendix B) were plotted in Figures 5.15 and 5.16. Stratigraphic units were identified based on deposit type and age from radiocarbon dating (Section 4.3.2.2);
- This information was used to draw polygons on the fan to estimate a planimetric area for each unit. The extent of the polygons was informed by the extent of stratigraphic units in Figures 5.15 and 5.16. It was assumed that the polygons would start near the fan apex;
- Deposit thickness of a stratigraphic unit was derived from the test pit logs and Figures 5.15 and 5.16. Depths were averaged for stratigraphic units that included more than one test pit;
- The following geometric assumptions were made for the volumetric shape of the deposit: First a constant deposit thickness was multiplied by the planimetric area of the deposit to derive a volume of a prism. However, the deposit thickness is assumed to thin out to zero from the leading edge of the deposition lobe towards the fan apex. This was approximated by a pyramid laying on its side with a rectangular base area towards the leading edge of the deposition lobe and the tip pointing towards the fan apex. By geometric relationship the volume of a pyramid is equal to 2/3 of the prism. Hence, the volume for the pyramid geometry was calculated as 2/3 of the prism volume; and
- Some stratigraphic units included sub-units of the same deposit type. This is interpreted as multiple events that occurred in the same stratigraphic unit, except for the 2013 event; where based on field observations the three sub-units in PCFT 38 and the top most unit of PCFT39 are interpreted as one event. For all other cases with sub-units the event magnitude is estimated proportional to the event thickness observed in a unit.

5.3.2 Results

Table 5.10 presents the debris flood event volumes calculated. Volumes are for deposited solids. A unit yield rate was calculated by dividing the event volume by the watershed area.

Table 5.10: Debris Flood Event Volumes Estimated from Test Pit Interpretation

Event Name	Volume (m^3)	Unit Yield (m^3/km^2)
Debris Flood (2013)	93,000*	1,700
Debris Flood (Modern 5)	4,000	80
Debris Flood (Modern 6)	13,000	240
Debris Flood (Modern 7)	13,000	240
Debris Flood (210 - 520 C yrs)	35,000	640
Debris Flood (Present - 880 C yrs)	258,000	4,690
Debris Flood (520 - 850 C yrs) aA	40,000	730
Debris Flood (520 - 850 C yrs) bA	191,000	3,460
Debris Flood (Present - 1820 C yrs) aA	318,000	5,790
Debris Flood (Present - 1820 C yrs) bA	38,000	690
Debris Flood (2890 C yrs) aA	574,000	10,440
Debris Flood (2890 C yrs) bA	143,000	2,600

Notes: A) Volumes of units including more than 1 event are broken out proportionally to event depths in test pits.
* The estimated volume for 2013 is less than the estimate from the LiDAR comparison

5.3.3 Limitations

The uncertainty in the shape and extent of the polygons drawn to estimate plan-view areas is high. Beyond the test pit information and the fan boundary, no evidence of the exact event deposit shape is at hand making this method imprecise. The large spacing between test pits, often on the order of several hundred metres, introduces error for delineation of planimetric polygons. This analysis likely contains only a subset of events that may lead to overestimation of event volumes.

Interpretation of deposit age and deposit types from individual test pits into stratigraphic units introduces some unavoidable uncertainty due to the judgement required for this task. Details about interpretation of stratigraphic units are described in Section 4.3.2.2.

There may be more events contained in a stratigraphic unit than identified in this analysis. Generally, this would cause the results to be too high.

Thickness of a deposit is known to vary substantially on fans. The thicknesses derived from the test pits may lead to under- or overestimation of volumes.

Overall confidence in the results is relatively low due to the nature of the estimate. However, the results do at least provide a means of estimating the volumes of historic events, even if the results are of low precision.

5.4 Magnitude Estimates Using Empirical Relationships

5.4.1 Methods

Rickenmann and Koschni (2010) summarized a large dataset obtained in Switzerland from several debris-flow and debris flood events. BGC (2014) separated the data for events driven by fluvial processes to develop an empirical equation that correlates sediment volume to runoff volume and channel gradient (as shown below), and a second equation that correlates sediment volume to runoff volume. These set of equations have been used by BGC (2014, 2015) for the estimation of sediment volumes for Cougar Creek, Jura Creek, as well as for many other mountain river systems in the Canadian Rocky Mountain.

$$logVs = -1.55 + 0.877LogVr + 0.019S, \quad R^2 = 0.81 \qquad \text{BGC (2014, 2015)}$$

Where

Vs: total sediment volume displaced,

VR: total runoff, and

S: channel slope.

5.4.2 Results

The equation presented above was applied to the Pigeon Creek watershed in two ways. First, using the total runoff volume for the entire watershed, as computed by the model at the point upstream of the waterfall (apex). Given that the sediment volumes correlated well to the stream gradient, a second approach was implemented which calculates the sediment yield separately for each subcatchment (see Figure 5.6), using the subcatchment's slope and runoff volume computed by the model. Sediment yield is then aggregated for all subcatchments to obtain the total for the watershed. Runoff volumes were obtained for all the three day events for return periods from the 2-year to the 3000-year events (Kananaskis station - AB 3053600).

Calculated sediment volumes for the first scenario, using an average watershed slope of 14% (i.e. runoff volume at watershed apex) are summarized in Table 5.11. Sediment volumes calculated using the second approach, based on runoff volumes per subcatchment are summarized in Table 5.12. It is observed that although the runoff volumes shown in Table 5.11 are larger than those shown in Table 5.12, the total sediment volumes are higher in the latter given that some of the subcatchments are steeper than the watershed average, resulting in a larger sediment yield.

Table 5.11: Estimated Sediment Volumes Using BGC (2014) Equation Applied to Watershed

Return Period	Rainfall	Runoff Volume (Vr)	Calculated Sediment Volume
(Years)	(mm)	(m^3)	(m^3)
2	61	2,481,000	20,650
5	85	3,035,000	24,673
10	104	3,518,000	28,105
25	132	4,401,000	34,232
30	138	4,663,000	36,030
50	156	5,501,000	42,400
100	182	6,791,000	50,292
200	212	8,895,000	63,770
300	231	9,170,000	65,484
1000	296	12,270,000	84,400
3000	368	15,940,000	106,307

Table 5.12: Estimated Sediment Volumes Using BGC (2014) Equation Applied to Subcatchments

Return Period	Rainfall	Runoff Volume (Vr)	Calculated Sediment Volume
(Years)	(mm)	(m^3)	(m^3)
2	61	786,419	23,201
5	85	1,257,508	35,202
10	104	1,677,394	45,868
25	132	2,429,215	65,171
30	138	2,664,786	71,420
50	156	3,420,124	90,348
100	182	4,579,721	117,910
200	212	6,288,268	156,664
300	231	6,737,906	166,368
1000	296	9,571,560	226,715
3000	368	13,104,340	299,994

5.4.3 Limitations

The use of empirical formulae, obtained from a given dataset, to estimate debris flood volumes for a watershed outside of the used dataset can lead to significant error as geological and hydrological conditions may be substantially different in the subject study area. Antecedent conditions can significantly affect the hydrological response of the watershed as well as the sediment yield. As such, caution is required in the use and interpretation of volumes obtained from such formulae. The validity of the equation applied to individual subcatchments in the watershed is questionable. Values are presented for context of potential sediment loadings that could be generated, and not used for the hazard assessment. It is noted that some of the sediment generated at steep subcatchments in the upper watershed may not reach the apex during a given event.

5.5 Sediment Volume Estimates Using Modified Bedload Transport Equations

5.5.1 Methods

Bedload transport methods are often used to assess sediment transport processes in river systems. The application of such methods in steep mountain terrain has been criticized because they tend to over-predict the sediment loadings by several orders of magnitude (Rickenmann, 2001; Nitsche et al., 2011). It has been argued that they are limited in their ability to account for the effects of macro-roughnesses, such as large boulders or step-pool channel sequences (Nitsche et al., 2012). To overcome this limitation, various authors have evaluated the use of bedload transport equations coupled with flow resistance equations to account for macro-roughness in steep mountain streams (Nitsche et al., 2011; Rickenmann, 2001; Rickenmann et al., 2006). For instance, Nitsche et al. (2011) used several flow resistance partitioning methods to estimate a reduced energy slope as a basis for modified bedload transport calculations. This approach significantly improved the bedload transport calculations when compared to observed bedload volumes. Nitsche et al (2011) applied this method using the Swiss dataset mentioned in Section 5.4. Other authors, have developed sediment routing models for steep mountain channel networks (Heimann, E.U.M. et al, 2015; Rickenmann et al., 2006).

In this section, sediment loadings from Pigeon Creek watershed are assessed using bedload transport equations coupled with an energy slope correction factor.

Rickenmann (1991) proposed a bedload transport equation, for a slope range of 0.0004 to 0.2. The equation is presented below:

$$\Phi_b = \frac{3.1\left(\frac{D_{90}}{D_{30}}\right)^{0.2}\sqrt{\theta}(\theta-\theta_c)Fr^{1.1}}{\sqrt{(s-1)}}$$

Where

Φ_b is the dimensionless bedload transport;

D_x is the grain size for which x percent of the material is finer;

θ is the dimensionless shear stress;

θ_c is the critical dimensionless shear stress at the initiation of bedload transport;

Fr is the Froude number; and

s is the ratio of solid to fluid density.

For quartz particles in water with a relative density s = 2.68, Rickenmann (2001) simplified the above equation to

$$\Phi_b = 2.5\sqrt{\theta(\theta-\theta_c)}F_r$$

For practical comparison with field data, Rickenmann further simplified the equation to

$$q_b = 1.5(q-q_c)S^{1.5}$$

Where

q_b is the bedload transport rate per unit of channel width;

q is the unit discharge; and

q_c is the critical unit discharge, calculated with

$$q_c = 0.065(s-1)^{1.67}\sqrt{g}D_{50}^{1.5}S^{-1.12}$$

The hydrological and hydraulic models developed for Pigeon Creek were used to compute the required flows to be used as input for the bedload transport equation. The bedload transport equation was run first in an Excel spreadsheet with the flows for the 2013 event computed by PCSWMM.

Based on field observations, a D_{50} of 25 mm was used for the bedload transport analysis. These values are consistent with field observations made by Miles (2013).

Results were compared with the sediment volume estimate from the comparative LIDAR analysis discussed in Section 6-2 It was found that the model over-estimated the 2013 volume. Following Nitsche et al (2011) approach, the energy slope was corrected using the following equation:

$$S_{red} = S\left(\frac{n_0}{n_{tot}}\right)^{1.5}$$

Where

S_{red} is the energy slope reduced;

S is the total energy slope;

n_0 is the base-level Manning's number; and

n_{tot} is the total Manning's number, including stream macro-roughness.

The value for n_{tot} was varied until an agreement between the computed sediment volume and the estimated sediment volume in Section 5-2 was achieved.

5.5.2 Results

The 'calibrated' bedload transport model was then used to compute sediment volume under various hydrological scenarios, using the 3-day rainfall pattern of the event of June 2013. Input hydrographs for all of these scenarios was obtained from the PCSWMM model of Pigeon Creek. Results from the bedload transport equation are presented in Table 5.13 and the corresponding plots for sediment loads for each event are shown in Figure 5.17, including the event of June 2013. Appendix D shows the spreadsheet developed for the bedload transport analysis.

Furthermore, the bulking factor (BF) for the event of June 2013 is presented in Figure 5.18 along with the bulked flows. It can be observed that there the BF fluctuates, further corroborating that the event transitions from flood to debris flood during the event. Bulked flows for all events are shown in Figure 5.19 and peak flows for both bulked and clear water flows summarized in Table 5.14.

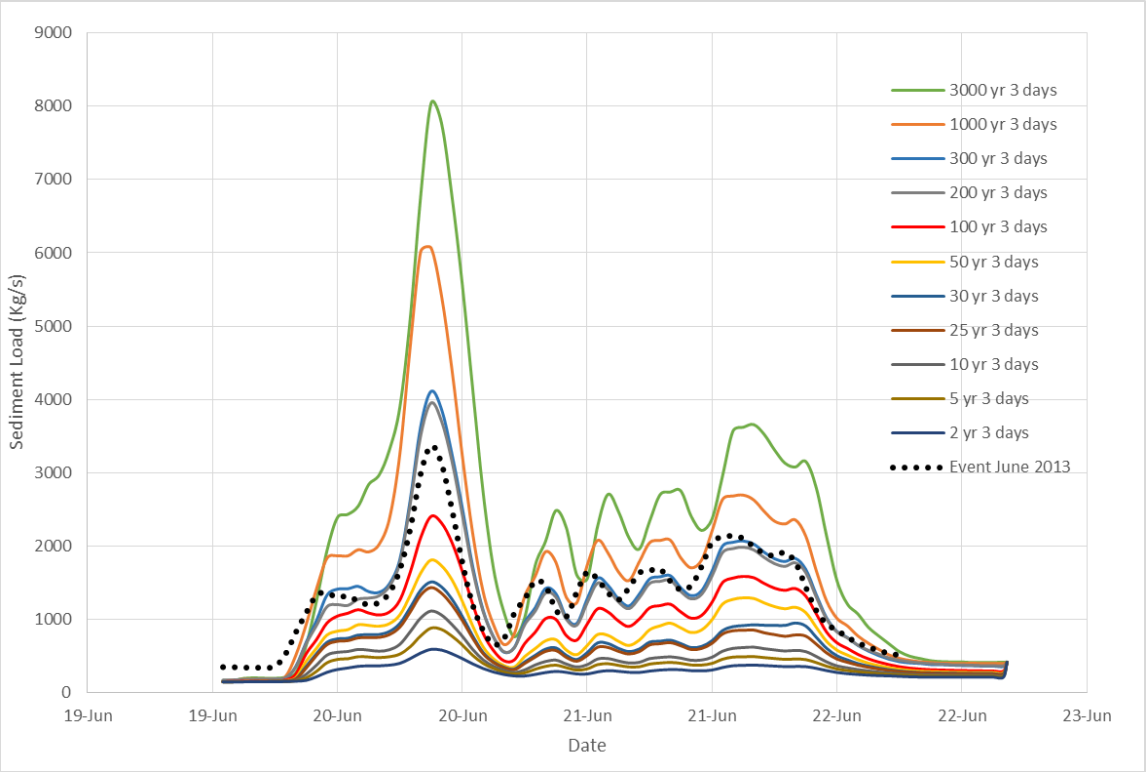

Figure 5.17. Computed Sediment Loads using Modified Bedload Transport Equations

Table 5.13: Bedload Transport Sediment Volume

Return Period (years)	Rainfall (mm)	Clear Water Peak Flow (m^3/s)	Sediment Volume (Vs) in m^3
25	132	36.46	33,937
30	138	38.41	36,161
50	156	46.03	43,282
100	182	61.2	54,218
200	212	85.5	71,569
300	231	104.6	74,156
1000	296	154.2	99,805
3000	368	205	131,107
Event June 2013**	230	85.8	70,652

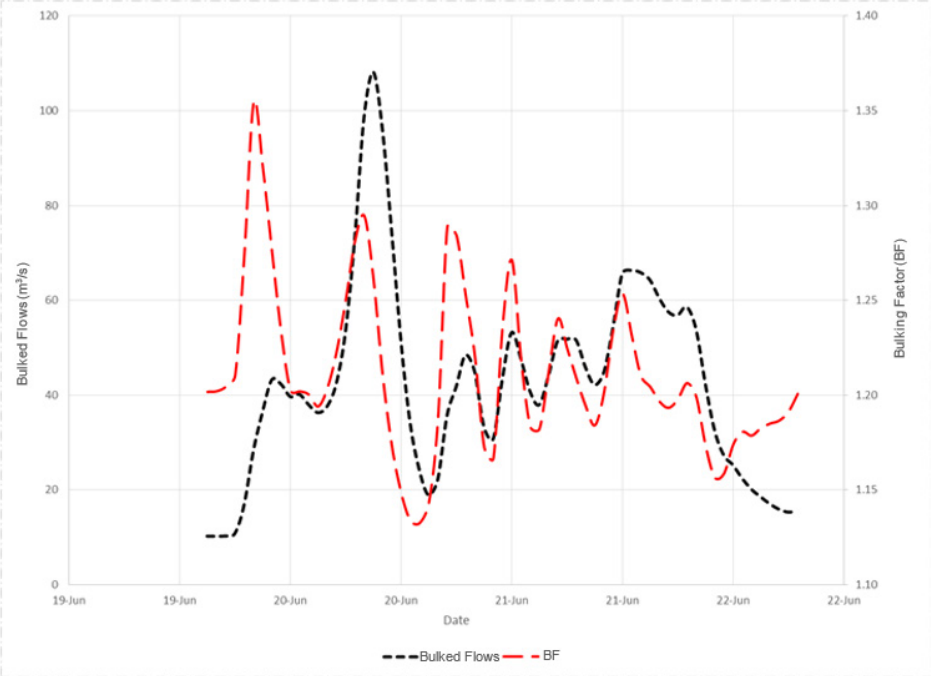

Figure 5.18. 2013 Event – Computed Bulked Flows and Sediment Concentrations

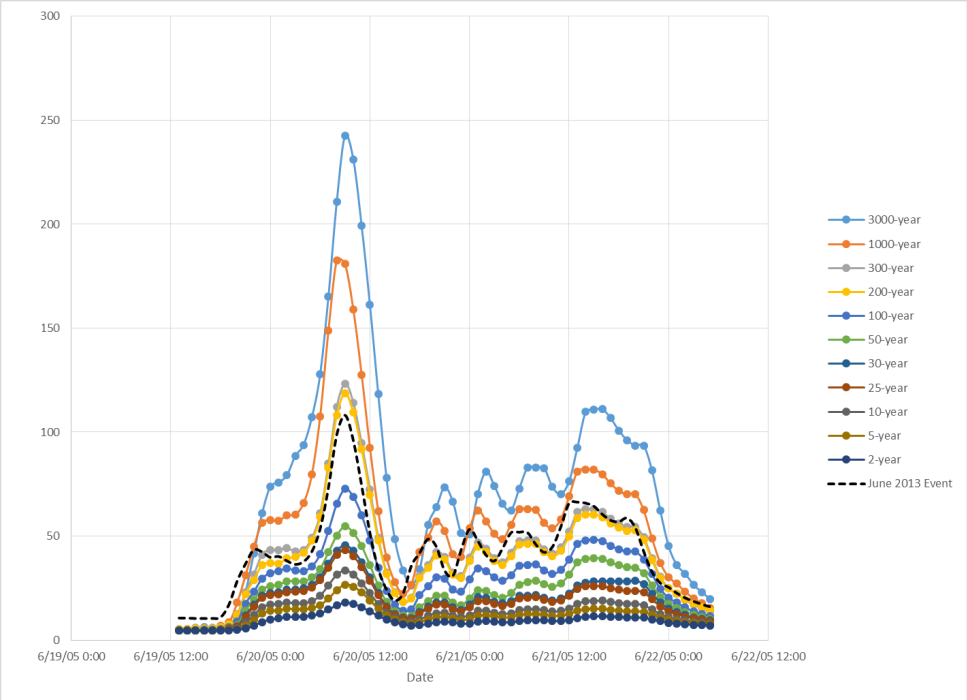

Figure 5.19. Pigeon Creek Bulked Flows

Table 5.14: Summary of Bulked Peak Flows

Return Period (years)	Rainfall (mm)	Bulked Peak Flow (m^3/s)	Clear Water Peak Flow (m^3/s)
2	61	17.9	15.03
5	85	26.7	22.42
10	104	33.5	28.31
25	132	43.2	36.46
30	138	45.6	38.41
50	156	54.6	46.03
100	182	72.6	61.2
200	212	118.7	85.5
300	231	123.4	104.6
1000	296	182.7	154.2
3000	368	242.7	205
Event June 2013**	230	108.2	85.8

6 FIRE HISTORY AND EFFECTS

BGC (2014a, b) used radiocarbon dating of predominantly charred material samples recovered from pits excavated into the Three Sisters Creek and Cougar Creek fans to develop chronologies for historic disturbance events on the two fans. BGC interpreted the presence of coarse grained deposits on the fans that contained charcoal to be the result of either extreme rainfall events or landslide dam failures. Charcoal samples were also acquired for dating purposes in this investigation of the Pigeon Creek area. The very common presence of charcoal and charred materials within the Pigeon Creek coarse fan deposits as well as within the Three Sisters and Cougar Creek fan deposits is interpreted to indicate that fires, both on the fans and in the contributing watersheds, may have been previously unrecognized drivers for some of the dated fan disturbance events (Jordan 2012). Because charcoal generally does not travel too far from its source (Hallett et al., 2003), it is a good indicator of past fire history in the area, which in the Canadian Rocky Mountains has been documented in a number of studies (Tande 1979; White, 1985; Arno et al., 2000; Rogeau 2005; Mori and Lertzman 2011; Power et al. 2011).

6.1 Association with Landslides and Erosion

The destruction of the plant canopy, litter and duff in forested watersheds and the development of hydrophobic soil properties (De Bano, 1981; Laird and Harvey, 1986; Letey, 2001; Jordan 2012) can lead to significant increases in flood peaks and runoff volumes during post-fire rainfall events (Veenhuis, 2002; Gallaher and Koch, 2004; Jordan 2012) and significant increases in watershed erosion and sediment yield (Laird and Harvey, 1986; Heede et al., 1988; Wells, 1987; Moody and Martin, 2001a, 2001b; Hallett et al., 2003; Sanborn et al. 2006; Jordan 2012; Tetra Tech, 2013). Depending on the burn severity, Post-fire increases in peak flows of up to 160 times the pre-fire values (Veenhuis, 2002) and increases in runoff volumes between 4 and 8 times the pre-fire condition have been measured in Ponderosa pine and Douglas fir-covered watersheds (Gallaher and Koch, 2004). Suspended sediment yields in excess of an order of magnitude higher than background have been measured up to four years after fires (Gallaher and Koch, 2004).

Following fires in many regions of the western U.S.A. and Canada, earth slides (Sanborn et al. 2006), debris flows and debris floods have been documented (Cannon et al., 2008, 2009; DeGraff et al., 2011; Goode et al., 2012; Tillery et al., 2011; Jordan, 2012; Tetra Tech, 2013). The debris flows have formed primarily as a result of downstream sediment bulking (Cannon et al., 2003; Cannon and Gartner, 2005; Cannon et al., 2010; Jordan 2012) rather than as a result of post-fire slope failures. Following fires in Yellowstone National Park in 1988, Meyer et al. (1995) described a process of debris flow generation by progressive bulking of runoff by sediment eroded from hillslopes and channels, rather than discrete hillslope failures. Similar observations following fires were made by Cannon and Gartner (2005) and Cannon et al. (2008), where debris flows were initiated by short duration storms with low recurrence intervals (<2-10 years) and by Jordan (2012) who reported that post-fire debris flows and debris floods were generated by both high-intensity storms as well as prolonged snowmelt following high severity burns in British Columbia. Although infiltration-triggered landslides can occur in burned basins, most landslide failures occur in response to prolonged and long-recurrence interval rainfall events years to decades after the fire (Sanborn et al. 2006), and they typically contribute a small proportion of the total volume of the material transported from the basin in the post-fire period (Cannon et al., 2010).

6.2 Influence of Climate

There is a general association of higher fire frequency in warmer climatic periods in British Columbia (BC) and Alberta (AB), but the timing of these varies across the two provinces. In this section, we discuss only the literature related to areas in or near the southern Canadian Rockies so that our data may be compared to other areas that have experienced similar climate fluctuations in the past.

Forest fires in southeastern BC commonly occur during periods of warm, dry weather followed by intermittent thunderstorms, which ignite the dry timber; these conditions may be associated with El Niño weather patterns (Jordan 2012; Courtney Mustaphi and Pisaric 2014). Large fires are generally more common during glacial retreat periods (warmer climate), less common during glacial advances (colder climate) (Courtney Mustaphi and Pisaric 2014) and are also more common during dry periods (Mori and Lertzman 2011). However, local site factors such as elevation and aspect complicate this picture.

6.3 Influence of Local Factors

Local site conditions, including elevation, aspect, fuel conditions and abundance, forest patch connectivity, lightning frequency and topography can all contribute to local variations in fire frequency (Mori and Lertzman 2011; Courtney Mustaphi and Pisaric 2014). Increased biomass resulting in greater fuel availability has been related to fire frequency in some areas (Courtney Mustaphi and Pisaric 2014).

6.3.1 Elevation

Higher elevation areas such as the Pigeon Creek watershed are more responsive to long term climate change because fires are commonly less frequent there (White, 1985; Power et al. 2011). High elevation (subalpine) sites in the Rocky Mountains generally have low frequency-high severity stand-replacing fire regimes, while low elevation sites such as the Pigeon Creek fan have high frequency-mixed severity fire regimes (Tande 1979; White, 1985; Arno et al., 2000; Rogeau 2005; Mori and Lertzman 2011; Power et al. 2011). However, not all studies have been able to corroborate this (Masters 1990; Rogeau 2005), possibly due to the influence of other factors.

6.3.2 Aspect

In the last 5000 years, south-facing slopes have experienced more fires than north-facing ones in some areas (Courtney Mustaphi and Pisaric 2014, Tande 1979) but not in others (Rogeau 2005). In general, north-facing and higher elevation slopes such as those in the Pigeon Creek watershed tend to have less frequent fires, which allows more fuel to accumulate, and results in more severe fires (Tande 1979). This produces even-aged stands in these areas. However, no such relationship is evident in other areas (Masters 1990).

6.4 Fire Suppression

Fire suppression activities since the early 19th century have affected fire frequency in some areas, but not others (Johnson and Fryer 1986; Masters 1990, Mori and Lertzman 2011). Within the Bow Valley, fire suppression has been very effective in the last approximately 100 years which has allowed biofuels to accumulate (Hawkes 1979; Walkinshaw 2008).

6.5 Timing

6.5.1 Return Periods

Median forest fire return periods are about nine years for the Kananaskis area (Rogeau 2005), 66 years for the Jasper area (Tande 1979), 177 years for Kootenay Valley (Hallett and Hills 2006) and 216 years for southeastern BC (Courtney Mustaphi and Pisaric 2014). This wide variation in return frequency may be attributable to the size of the studies and what is considered a large enough fire to calculate a return period for, as well as the fact that return periods are shorter for valleys than for higher elevation alpine areas.

In the Bow River Valley, the pre-1880 natural fire regime had 30-100 year return periods with varying intensity and severity, and tended to kill fire-susceptible species but allowed fire tolerant species to survive (Arno et al., 2000). Periodic stand-replacing fires with return periods on the order of 200-300 years also occurred at higher elevations (White, 1985).

6.5.2 High Fire Frequency Periods

Periods of high fire frequency vary from place to place, even within the southern Canadian Rockies. Although many large fires occurred in the early to middle Holocene, the period relevant to the study area ranges from 3750 calendar years ago to the present.

Fire suppression beginning in the first half of the 19th century decreased the number, intensity and extent of fires in southeastern BC and Jasper (Tande 1979, Courtney Mustaphi and Pisaric 2014). Larger fires occurred 256, 167, and 125 calendar years ago in Jasper (Tande 1979) and 95 to 179 years ago in the Canmore area (Rogeau 2005). The current high biomass accumulating in the forests due to over 100 years of fire suppression increases the likelihood of high severity fires in the future and thus increases the probability of fire-induced sedimentation events on the fans (Jordan, 2012).

The burn patterns in the Canmore area over the last 150 years may not be natural (Rogeau 2005). In the post-1880 period prior to effective fire suppression, fires in the Bow River Valley occurred more frequently due to construction of the railroad and early land use practices (White, 1985). Stand origin dates from the Alberta Vegetation Inventory database indicate that approximately 76 percent of the area is greater than 80 years of age and over 50 percent of the area is in the 81 to 140 year age class; the distribution can be related to large wildfires in the late 1890's and early 1900's (Walkinshaw, 2008). Nearly 19 percent of the area is in the 61-80 year age class which is attributable to the large wildfires of 1936 (Walkinshaw, 2008).

6.5.3 Potential Effects of Forest Fires on the Hydrological Response of the Pigeon Creek Watershed

The presence of charcoal in the test pits indicates that fires have occurred in the watershed over the past few thousand years. No evidence of more recent fires was found from the review of aerial photographs (post-1947), probably due to the very effective fire suppression that has occurred for the last 100 years (Walkinshaw, 2008). Yet, the literature review reveals that the potential effects of partial watershed fires can be devastating in terms of increased runoff rates and sediment loadings. This section discusses the potential effects that hypothetical fire events could have on the hydrological response of the watershed.

West Consultants (2011) provided a summary of potential changes that could be expected in a watershed after experiencing a fire, including:

- Reduced evapotranspiration;
- Reduced interception and initial losses;
- Reduced soil moisture storage capacity;
- Reduced infiltration rates;
- Reduced overland flow surface roughness;
- Reduced surface roughness for channels;
- Reduced interflow (shallow groundwater);
- Reduced watershed lag time due to decrease in surface roughness.

For the purposes of this report, it was assumed that 10 percent and 20 percent of the watershed area was affected by a hypothetical fire. The effect of fire was simulated by:

- Reduced soil reducing the hydraulic conductivity of the soil that controls infiltration, by 95 percent, simulating water repellency after a fire;
- Reduced depression storage by 50%;
- Reduced surface (overland runoff) Manning's number by 50%;

The model was run under various 3-day storms including the 100, 200, 300, 1000, and 3000 year rainfall return periods, as well as the June 2013 event. Results from this analysis are summarized in Table 5.15.

Table 5.15: Potential Effects of Fire in the Hydrological Response of Pigeon Creek Watershed

Return Period (years)	Clear Water Peak Flows - % of Fire Affected Watershed Area (m^3/s)		
	No Fire	10%	20%
2	15.03	18.8	22.7
5	22.42	27.9	33.9
10	28.31	35.1	42.8
25	36.46	45.3	55.3
30	38.41	47.6	58.2
50	46.03	56.5	68.7
100	61.2	73.7	87.9
200	85.5	94.4	110.8
300	104.6	110.4	123.5
1000	154.2	157.1	167.5
3000	205	207.3	212.5

6.5.4 Limitations

There are many uncertainties associated with selection of the total area that would be affected by fire and also on the hydrological changes that may be expected in the watershed after the fire occurs. The analysis presented in this section illustrates the relative change, compared to non-fire conditions, of the expected impact of fire on the hydrology of the watershed. The modeling results indicate that the presence of fire could lead to substantial increases in clear water peak flows and consequently on sediment volumes. The changes would result in an augmented frequency of larger runoff events and the associated sediment loadings.

7 LANDSLIDE DAMMING BY BEDROCK FAILURE

Two possible deep-seated bedrock failure areas are found about 190 m upstream of the Pigeon Creek waterfall at a sharp bend in the creek (Figures 4.4 and 4.5). One is a smaller feature on the northwest side of the creek (Slide A) and the other (Slide B) is larger and is situated on the southeast side of the creek, surrounding the creek's outer bend. Both slides pre-date the 1950 air photos and bedrock exposed in the creek bed dips gently to the southwest.

Slide A includes a bedrock slope and two arcuate terraces. Although both terrace surfaces are covered with a mix of deciduous and coniferous trees in the 1950 air photos, a possible scarp face above is well covered with coniferous trees indicating that it is an older feature. A lower fluvial terrace of sand (adjacent to the creek floodplain, which is narrow in this location) is situated below an upper terrace of bedrock. The slope was not examined in detail, but the bedrock terrace appears to be a slide block derived from the bedrock slope above, which is interpreted to infer that this feature is a deep-seated bedrock slide.

Slide B was mostly well vegetated with coniferous trees in 1950, but deciduous trees on its eastern slope indicate more recent debris slide activity on the surface of the slide zone. In 1962, there was some localized reactivation of this debris slide. An arcuate terrace with an irregular surface is situated at the bottom of the slide, flanking the creek. The arcuate terrace consists of fluvial sand overlain by debris slide material derived from the bedrock above. Abundant and large pieces of charcoal in the upper portion of the debris slide material and within the topsoil indicate that a relatively recent fire has occurred in this area. At Field Site PCU10, colluvium is exposed on the slope within a small debris slide. The bedrock, which consists of sandstone and siltstone, is quite easily weathered compared to the limestone visible elsewhere, and forms rocky colluvium consisting of very angular flat clasts and silt. A narrow strip of siltstone is exposed at the top of the debris slide and there are tension cracks above it which extend to the top of the slope. These, along with jack-strawed and pistol grip trees, indicate ongoing instability of the slope surface. This area is therefore interpreted as a bedrock slope with weathered bedrock that is forming surface debris slides. However, it is possible that the arcuate terrace at the base of the slide is underlain by a bedrock slide block. The bare earth LiDAR image shows a distinct block that does appear to be a slide block given its size and shape. Further study is warranted to determine if it is indeed a slide block of bedrock.

For modelling purposes, Slide B is likely to introduce only small amounts of surface debris to the creek in the form of weathered bedrock, likely much less frequently than the debris slides in surficial sediments (because of the time required to weather the bedrock at the slide surface). If it is indeed a deep-seated bedrock slide, then a second failure involving a slide block above it could conceivably occur. Slide A could also fail again along a bedrock slip surface in the same manner. Although these slides could be significant in size, they would introduce large pieces of bedrock, probably of the size of the slide blocks already formed, which could form a bedrock dam on Pigeon Creek. However, more in depth study is required to determine if these features are indeed both deep-seated bedrock slides and whether they pose a risk to the Pigeon Creek fan.

LiDAR data shows that the creek has an elevation of 1352 to 1356 masl along the length of the possible slide blocks. The upper portion of the potential slide block at Slide A ranges from 1360 to 1368 masl. A new slide slip surface would move this block into the creek and form another bedrock terrace above it (in the style of a rotational slide). There would be some downward movement of the lower slide block, with a possible damming scenario at an elevation of approximately 1360 to 1365 masl. Similarly, movement of the lower possible slide block further into the valley by formation of another block above and behind it would result in damming at elevations of approximately 1355 to 1358 masl for Slide B (its possible slide block has elevations ranging from 1353 to 1361 masl). An important assumption for these dam elevation estimates is that the slide is not so large that it pushes material upward against the opposite valley slope or upward above the new slide block and thus these elevation estimates are very approximate. Better constrained scenarios could be determined by more detailed study.

The size of the two slide blocks is shown in Table 7.1. The average thickness was obtained by determining the majority of elevations present on each slide block, rather than by calculating a mean. Area was determined by drawing a polygon around each slide block in ArcGIS.

Table 7.1: Volume of deep-seated slide material

Slide	Area (m^2)	Average Thickness (m)	Volume (m^3)
A	3270	10	32,700
B	1676	2	3352

7.1.1 Dam Outburst Flood

It is theoretically possible for a deep-seated bedrock failure to dam Pigeon Creek within its canyon located immediately upstream of the fan apex. No evidence of landslide debris dams were observed during the field investigation so it is not possible to accurately ascribe a frequency for such an event.

We have estimated the potential magnitude of a peak flow resulting from the catastrophic failure of a landslide dam. LiDAR of the area was used to estimate the volume of impounded water for various landslide dam heights. Costa and Schuster (1988) developed a regression equation for estimation of the peak discharge resulting from a failure of the landslide dam. The formula relies on the potential energy of the impounded water expressed as function of dam height and volume of impounded water. The estimated peak flows for various dam heights are presented in Table 7.2.

Table 7.2: Estimated Peak Discharge resulting from Dam Outburst Flood

Elevation	Max Height (m)	Impounded Volume (m^3)	Q_p (m^3/s)
1360	8.3	21033	119
1359	7.3	14759	97
1358	6.3	9702	77

The estimated peak discharge from an outburst flood are of the same order as the event of record (2013 flood ~ 70 m^3/s). The volume of water released under such an event is orders of magnitude less that the estimated runoff volume from the 2013 event (~3M m^3). It is assumed that the potential volume of entrained material below the dam would be small because the valley is bedrock constrained.

8 FREQUENCY-MAGNITUDE RELATIONSHIPS

8.1 Introduction

This section presents a combined analysis on the frequency and magnitude of debris flood events in the Pigeon Creek watershed based on results from Sections 5 and 6.

8.2 Frequency Magnitude from Sediment Yield Analysis

Assuming that the sediment volumes computed with the bedload transport equation discussed in Section 6.5 are reasonable, the results from this analysis were used for the frequency-magnitude analysis of small events, from 20 to 200-year return periods.

8.3 Frequency-Magnitude Estimates from Test Pit Analysis

8.3.1 Method

Event ages were estimated in the following manner:

- Debris flood event 'Modern 5' was assigned an age of 60 calendar years based on air photo and dendrochronology evidence of an event occurring between 1950 and 1962. For the other two modern events, where no date was available, a nominal age of 100 calendar years was assigned based on the general tree ages on the fan; and
- Radiocarbon dates (i.e. C Yrs BP) of events were converted to calendar years using Table 5-3. Cal BP are calibrated years before 1950. Where multiple date ranges were determined through calibration, a range of possible oldest to possible newest date were used. Years before 2014 are calculated as Cal BP plus 64 years. The mid-point between possible oldest and newest date is used as best estimate of event age.

Volume estimates from test pit analysis were converted into unit yield rates (m^3/km^2) for comparison with estimates from other watersheds (BGC, 2014a,b).

The yield rates in the data set are ranked from smallest to largest number. For each yield rate in the data set the return period was calculated as a weighted estimate using Eq. 1:

$$T = \frac{years\ of\ observation}{number\ of\ events \geq threshold} \qquad \text{(Eq. 1)}$$

Since the calculated return period is somewhat sensitive to the duration of the observation period, this process was carried out for four sub-data sets with the following observation periods:

- Present to 3100 calendar years before 2014 (i.e. all events in data set);
- Present to 1100 calendar years before 2014;
- Present to 500 calendar years before 2014; and
- Present to 100 calendar years before 2014.

8.3.2 Results

Table 8.1 lists the estimated magnitude-frequencies for all events in the test pit data set for an observation period from present (i.e. 2014) to 3100 calendar years.

Table 8.1: Estimated Magnitude-Frequencies for all Events in Test Pit Data Set

Event Name	Threshold Volume (m^3)	Threshold Unit Yield (m^3/km^2)	Number of events ≥ threshold (-)	Return period (Calendar years)	Years before 2014 (Best Estimate) (Calendar years)
Debris Flood (Modern 5)	4,000	80	12	260	60
Debris Flood (Modern 6)	13,000	240	11	280	100
Debris Flood (Modern 7)	13,000	240	10	310	100
Debris Flood (210 - 520 C yrs)	35,000	640	9	340	370
Debris Flood (Present - 1820 C yrs) b[A]	38,000	690	8	390	980
Debris Flood (520 - 850 C yrs) b[A]	40,000	730	7	440	720
Debris Flood (2013)	93,000	1,700	6	520	-
Debris Flood (2890 C yrs) b[A]	143,000	2,600	5	620	3,110
Debris Flood (880 - 1260 C yrs)	191,000	3,460	4	780	1,070
Debris Flood (520 - 850 C yrs) a[A]	258,000	4,690	3	1,030	720
Debris Flood (Present - 1820 C yrs) a[A]	318,000	5,790	2	1,550	980
Debris Flood (2890 C yrs) a[A]	574,000	10,440	1	3,100	3,110

Notes:

A) Volumes of units including more than 1 event are broken out proportionally to event depths in test pits.
B) Modern age for 'Modern 5' assigned 60yrs based on evidence of an event between 1950-1962 (airphotos, dendrochronology). 'Modern 6 and 7' approximated as 100 years.
C) Cal BP are calibrated years before 1950. Where multiple date ranges were determined through calibration, a range of possible oldest to possible newest date are given. Radiocarbon date calibration results are given in Table 5.3 of this report.
D) Years before 2014 are calculated as Cal BP plus 64 years. The mid-point between possible oldest and newest date is used as best estimate.

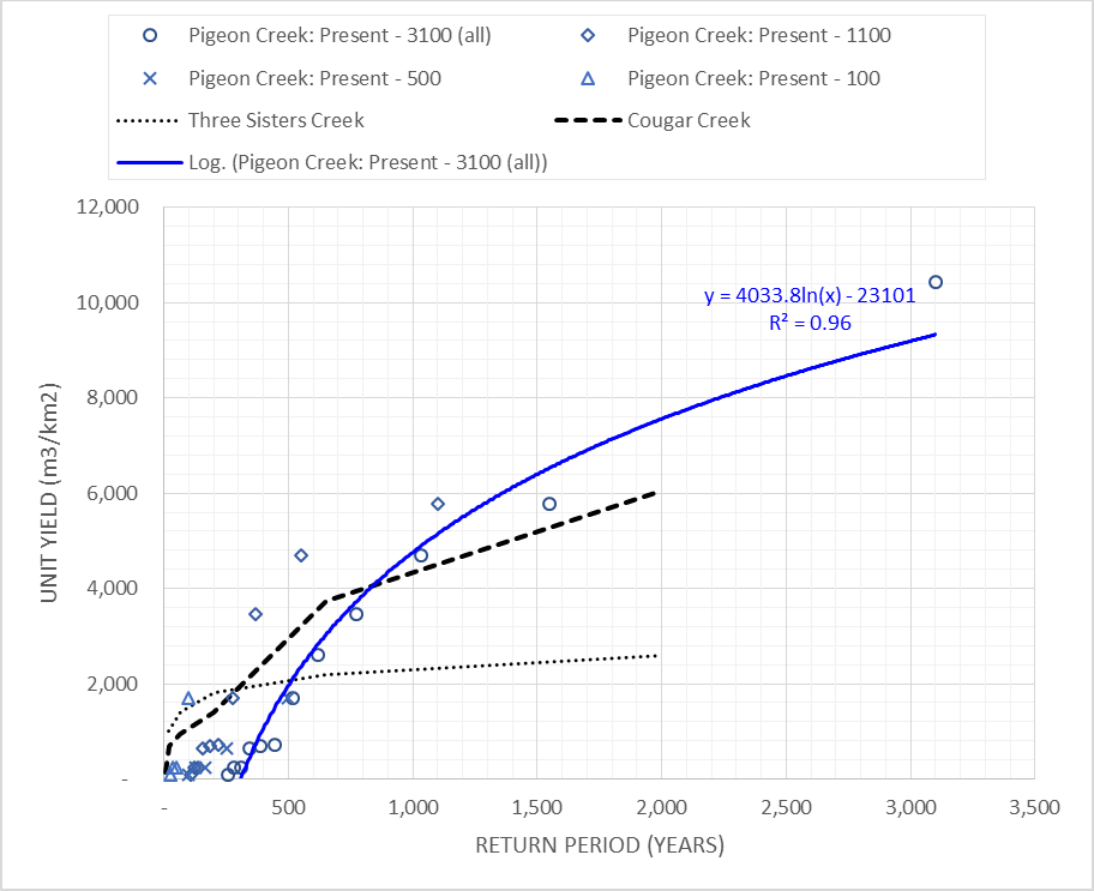

Figure 8.1. Pigeon Creek Frequency-Magnitude Data Points from Test Pit Analysis with a Logarithmic Curve Fitted to Circle Symbol Data Points, Three Sisters Creek and Cougar Creek Curves approximated from BGC reports (2014a and 2014b)

8.3.3 Limitations

Approximation of the return periods using weighted estimates is a relatively simple method. With only 12 data points for volume and age in the data set more sophisticated approaches such as rank order statistics (e.g. Hazen method or Weibull method) requiring at least 30 data points were not applied.

Figure 8.1 presents the Pigeon Creek frequency-magnitude data points from test pit analysis. The data points for the entire data set (Table 8.1) with an observation period of 3100 years (circle symbols) is the most comprehensive set available. A logarithmic curve is fitted to these data points for discussion purposes only. The test pit data set does likely not contain all events that occurred within the observation period. This would mean that the actual frequency of debris flood events is underestimated and the true curve would lie further left in Figure 8.1.

The other data points (diamond, cross and triangle symbol) illustrate the range of return periods resulting from use of shorter observation periods. Interestingly using shorter return periods would move a fitted curve closer to the point of origin.

The data point for 3100 years return period may be an outlier and overestimate the actual yield rate.

Test pit volumes may have been over- or underestimated, so the true curve could lie above or below the estimated best fit curve.

Comparison of unit yield rates between watersheds for Pigeon, Cougar and Three Sisters Creeks is discussed in Section 8.5.

8.4 Combined Frequency-Magnitude Analysis

Using both datasets, a combined frequency-magnitude relationship is summarized in Table 8.2. The upper range provided is based on the test pit analyses. Evidence suggests that debris volume estimated for the 750 year and higher return periods were likely associated with fire events. For the 1000 and 3000 year return periods the higher value in the provided range of debris volume is based on the findings from the test pits, and thus assumed to have been influenced by fire. Although this information is valuable as it provides estimates of extreme historical events, the processes that currently dominate the movement of sediment and debris are different than those that occurred thousands of years ago. Furthermore, the extrapolation techniques using data from the test trenching are associated with very significant error, which could be reduced by adding more data from many more test trenches. For this reason, the frequency-magnitude relationship shown in Figure 8.2 is based on the findings from the fluvial sediment transport analyses. Accordingly, the hazard mapping was developed using the debris volumes estimated with the fluvial sediment transport analysis (see Table 5.13). The return period of the June 2013 debris flood event was estimated to be between 100 and 200 years. This return period was informed from both data sets, for small and large debris flood events.

Table 8.2: Frequency Magnitude Relationship of Debris Flood Events in the Pigeon Creek Watershed

Return Period	Debris Volume (m^3) Based on current watershed processes	Upper Range of Debris Volume (m^3) Based on Test Pit data
10-30	36,000	61,000
30-100	54,000	92,000
100-300	74,000	126,000
300-1000	100,000	258,000
1000-3000	131,000	555,00

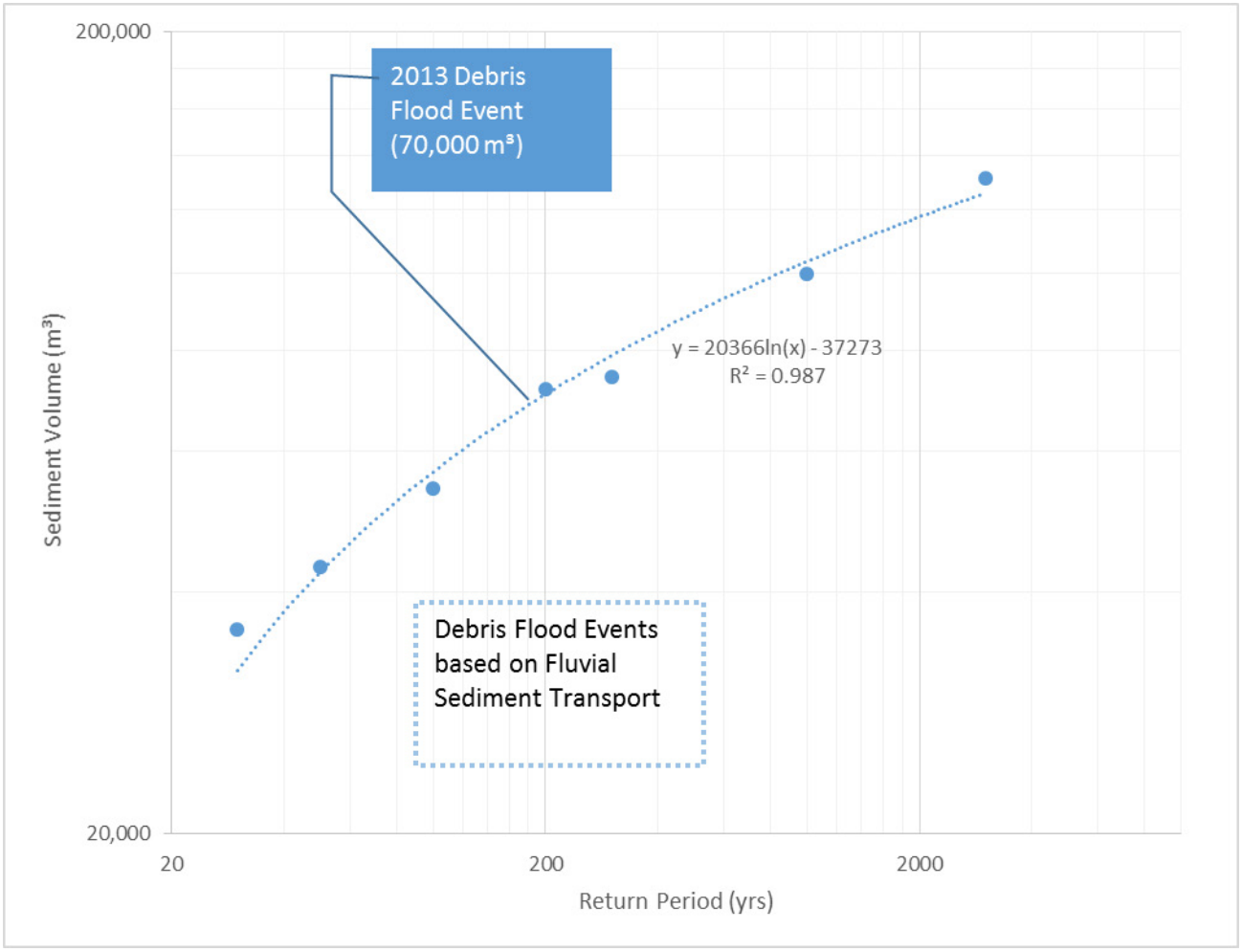

Figure 8.2. Frequency-Magnitude of Debris Flood Events in the Pigeon Creek Watershed

8.5 Comparison of Unit Sediment Yield

The sediment volume estimates in the Pigeon Creek watershed were calculated based on the bedload transport method described in Section 5-5 for a range of events (10-year to 3000-year return period), and from test pit data as described in Section 5-3. For comparison purposes, sediment yield results from Pigeon Creek were compared with those from adjacent watersheds, including Three Sisters Creek and Cougar Creek (BGC, 2014 a,b). The total sediment yields for each hazard class are summarized in Table 8-3. As discussed in Section 8.1.3.3, there are limitations with sediment volumes obtained with the test pit data used for the large events. These estimates are likely conservative but are considered appropriate for the hazard and risk assessment.

Table 8.3: Estimate of Sediment Yield for Pigeon Creek

	Unit Sediment Yield (m^3/km^2)		Sediment Yield (m^3/km^2)	Total Sediment Yield (m^3)
	Three Sisters Creek	Cougar Creek	Pigeon Creek	Pigeon Creek
Drainage Area (km^2)	10	42.9	55	55
Return Period (Years)				
10-30	1,000	700	700	36,000
30-100	1,400	930	1,000	54,000
100-300	1,800	1,400	1,500	74,000
300-1000	2,200	3,730	2,000	100,000
1000-3000	2,600	6,000	2,500	131,000

As shown by BGC's (2014a, b) magnitude-frequency data for the Three Sisters and Cougar Creeks, for more frequent events (<100-yr) the smallest watershed has a higher unit yield because there is limited storage potential for sediment within the watershed (Chorley et al. 1984) and its sediment yields probably reflect the current watershed erosion rate rather than those earlier in the paraglacial sedimentation cycle (Church and Ryder 1972: Church and Slaymaker 1989). However, for the more extreme events the unit yields increase for the larger watersheds because the sediment yield reflects erosion from both the watershed and from valley bottom storage (Schumm 1977; Church and Slaymaker 1989).

9 DEBRIS FLOOD MODELLING

A two dimensional hydraulic model of the Pigeon Creek fan was built and run under various scenarios using the PCSWMM software. This section presents a summary of the modelling results including hazard maps for various events. Prior to selecting PCSWMM for the analysis, FLO-2D was considered and tested for the hydraulic modeling. FLO-2D is able to simulate flows with high sediment concentrations where the rheological properties of the fluid are different than those of clear water. Given that sediment concentrations at Pigeon Creek are not particularly high during most of the flood events, the rheological properties of the water-sediment mix are similar to clear water flows. On the other hand, FLO-2D has a limitation related to the grid size. Because the entire grid in FLO-2D has to be the same size, in order to properly represent key prominent areas, either a smaller grid needs to be selected, or linear features (e.g. road embankment) added to the model. Selecting a smaller grid results in longer computational times, and adding the linear features resulted in model instability challenges. On the other hand, with PCSWMM it is possible to have a variable size mesh grid, which is useful for better representing key areas such as the highway and the creek corridor and also it is possible to explicitly model hydraulic structures such as culverts. Culverts in FLO-2D are modeled with the use of rating curves. For the development of hazard mapping, the flexibility provided by PCSWMM was the main factor for selecting this tool for the two dimensional hydraulic modeling.

9.1 Sediment Concentration and Bulked Flows

Section 5-2 summarized the surface differential analysis of the fan, using LIDAR data from 2008 and 2013 (post-event). The analysis suggests that approximately 70,000 m^3 of sediment produced by the watershed were deposited on the fan. Assuming the upper end of the given range was the total volume of sediment produced by the watershed, and assuming uniform distribution throughout the entire range of the flood event, an average volumetric concentration of less than 4 percent. This tends to confirm BGC's (2013) preliminary assessment that the 2013 event in the Pigeon Creek watershed was a relatively low sediment concentration flood event rather than a debris flood event. Furthermore, sediment concentrations were calculated using bedload transport equations, as described in Section 5.

9.2 Debris Flood Modelling

PCSWMM is a 2-dimensional hydraulic model that conveys a flood within defined channel segments and as overland flow. PCSWMM has the ability to route a hydrograph through a system of open channels, culverts, pipes, hydraulic structures, and simulate flood conditions that include overtopping of the channel and overland flood routing. PCSWMM allows to have a variable size mesh which allows the simulation of areas of interest in more detail than others. As noted in Section 5, Pigeon Creek is flood dominated with fluvial sediment transport processes that allow the entrainment of sediment loads, making the flood to transition to debris flood during high sediment loading episodes within the flood. As PCSWMM simulates clear water flows, bulked hydrographs were used for the modeling (See Figure 5.18).

9.2.1 Model Input

The 2013 LiDAR data, taken after the flood event, was used to create a digital elevation model (DEM) with 1 meter resolution. This DEM was used to create a hexagonal mesh grid, in turn used for the two dimensional hydraulic model as shown in Figure 9.1. Approximately 3.5 km^2 area was modelled using 5 m X 5 m grid mesh for the Pigeon Creek channel and highway areas, and a 10 m x 10 m sized grid mesh for the rest of the fan. Sudden changes in topographic relief, such as roads and buildings, were better represented with the smaller size grid mesh. In addition, obstructions represented by the buildings and the sewage lagoons in the fan were captured in the development of the grid. The model was built as a combination of a 1-dimensional model that represented the main creek stem and culverts, linked with 2 dimensional elements that represent overland areas subject to flooding.

The LiDAR data does not include any stream channel bathymetry. As such, the flood routing analysis assumes water-surface from the LiDAR as the bed of the channel for subsequent modeling.

9.2.2 Hydraulic Structures

Culverts under the Highway were modelled in PCSWMM by providing culvert dimensions and invert elevations as specified in Tables 9.1 and 9.2.

Table 9.1: Highway Culvert – Twin – Details

Type	Twin Arch	Unit
Culvert Length	58	m
Manning's N	0.027	
Span	4.3	m
Rise	2.7	m
U/S Invert	1308.16	m
D/S Invert	1307	m

Table 9.2: Highway Culvert – Downstream – Details

Type	Arch	Unit
Culvert Length	14	m
Manning's N	0.027	
Span	4.3	m
Rise	2.7	m
U/S Invert	1305.91	m
D/S Invert	1305.63	m

9.2.3 Model Runs and Results

Four different scenarios were modelled. For each of these, every return period class from 10 to 3000 years was considered, plus the June 2013 event. The benchmark scenario represents the ideal conditions in the fan; thus, it does not consider culvert blockage. On the other hand, the other 3 scenarios anticipate different culvert obstruction situations. Figures 9.2 to 9.7 illustrate the model results for different return period events under the benchmark scenario. Each figure shows the maximum flood depth and flood intensity, which is determined as a function of flow depth and velocity squared at a specific location. The intensity level was categorized to define the destruction potential of modelled flows. Table 9-3 summarizes the key results including a brief description of areas impacted. Figure 9.8 shows a composite flood intensity map which combines all return period classes for the benchmark scenario.

Figure 9.9 shows the location of critical culverts within the Pigeon Creek Fan. Different culvert blockage combinations are considered in Scenarios 1, 2a, and 2b; as described below.

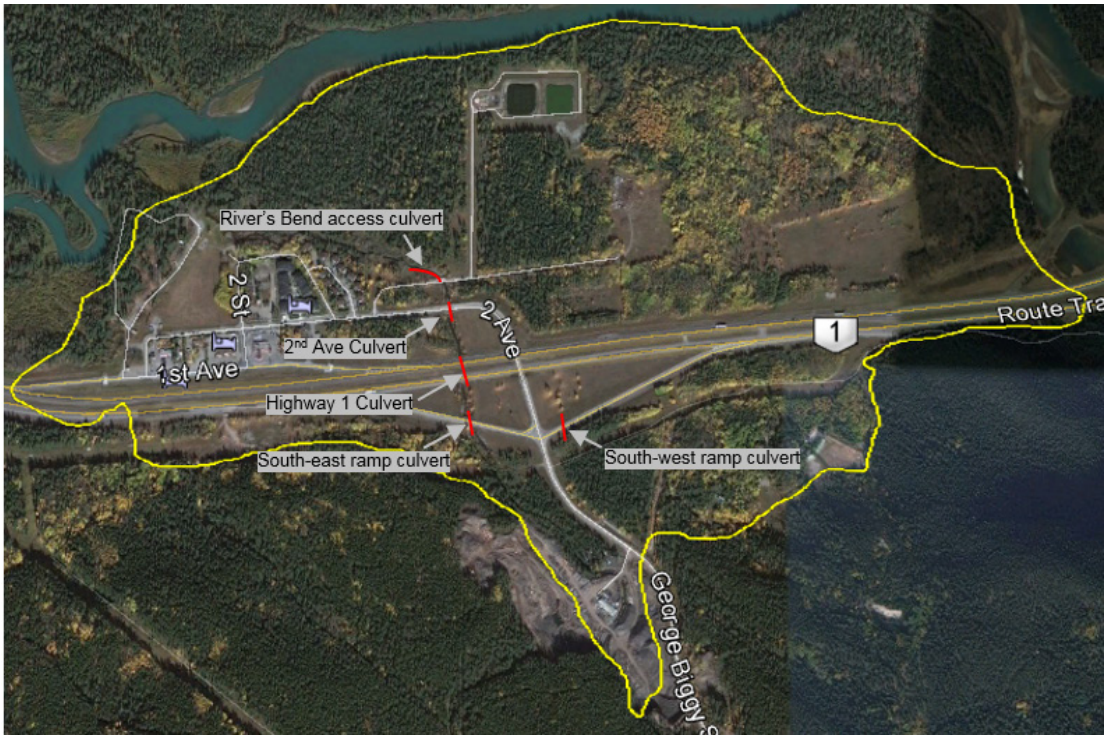

Figure 9.9. Critical culverts in the Pigeon Creek Fan

9.2.3.1 Scenario 1

Scenario 1 assumes full blockage of South-east ramp, South-west ramp and Highway 1 culverts. Figures 9.10 to 9.15 illustrate the model results for different return period events under this scenario. Each figure shows the maximum flood depth and flood intensity, which is determined as a function of flow depth and velocity squared at a specific location. The intensity level was categorized to define the destruction potential of modelled flows. Table 9-4 summarizes the key results including a brief description of areas impacted. Figure 9.16 shows a composite flood intensity map which combines all return period classes for this scenario.

9.2.3.2 Scenario 2a

Scenario 2a assumes full blockage of 2nd Ave. and River's Bend access culverts, while Highway 1 and South-west ramp culverts remain open. Figures 9.17 to 9.22 illustrate the model results for different return period events under this scenario. Each figure shows the maximum flood depth and flood intensity, which is determined as a function of flow depth and velocity squared at a specific location. The intensity level was categorized to define the destruction potential of modelled flows. Table 9-5 summarizes the key results including a brief description of areas impacted. Figure 9.23 shows a composite flood intensity map which combines all return period classes for Scenario 2a.

9.2.3.3 Scenario 2b

Scenario 2b assumes full blockage of 2nd Ave. and River's Bend access culverts, but contrary to Scenario 2a, Highway 1 and South-west ramp culverts are assumed to be partially blocked. Figures 9.24 to 9.29 illustrate the model results for different return period events under this scenario. Each figure shows the maximum flood depth and flood intensity, which is determined as a function of flow depth and velocity squared at a specific location. The intensity level was categorized to define the destruction potential of modelled flows. Table 9-6 summarizes the key results including a brief description of areas impacted. Figure 9.30 shows a composite flood intensity map which combines all return period classes for Scenario 2b.

9.2.4 Limitations

The modeling results presented for the 2013 event are not intended to replicate exactly what happened during the event given that the surface used for the modeling was the post-flood condition. Significant morphological changes occurred during the event, including channel avulsion and significant sediment deposition. Under the post-flood conditions, the model shows that some of the flooding would be diverted to the east. Although during the 2013 event some flows and sediment volumes overtopped the George Biggy Sr. Road, the extent of the flooding was not as shown by the model. The results indicate the current hazards with the existing topography.

10 CONCLUSIONS

Based on its morphometric characteristics (Melton Ratio), the Pigeon Creek watershed appears to be a flood-dominated rather than debris flood dominated system. However, it is likely that that debris flood episodes will occur within a flood event. This conclusion is substantiated by the small volumetric sediment concentrations estimated for the 2013 event as well as for other return period events.

The very common presence of charcoal and charred materials within the Pigeon Creek coarse fan deposits is interpreted to indicate that severe, stand-replacing fires, with a natural return period of 200-400 years in the contributing watersheds, may have been previously unrecognized drivers for the dated fan disturbance events. Modeling of the effects of fires in the Pigeon Creek watershed indicates that peak flows and sediment yields increased by factors of 2 and 3, respectively for the lower magnitude, higher frequency events (20 yr) when 20 percent of the watershed was burned. If a similar fire had preceded the 2013 event, the magnitudes of the peak flows and sediment volumes would have increased by a factor of about 1.5. Because of very effective fire suppression over the last 100 years, it is likely that fuel loading in the watershed is increasing and the probability of a stand-replacing severe fire event has increased.

Review of historical air photographs shows that most of the slide areas within the Pigeon Creek watershed were already established by 1950, which was the date of earliest aerial photography analyzed in this study. Debris slide activity was a fairly recent phenomenon in 1950. These earliest photos illustrate that the upper watershed shows evidence of large, stand-replacing forest fires of uncertain age. Extensive fires were reported in the Bow Valley in the early 1900's. Deciduous trees present on the fan are interpreted to imply that either the fan had been quite active in the recent past, or it had been affected by fire. It is possible that the fan was burned in the widespread fires of the early 1900's or possibly the 1936 fire.

Evidence from dendrochronology analysis suggests that the last morphologically significant event on the fan occurred more than 80 years ago (before 1934). Based on the aerial photographic record prior to 2013, there has not been a morphologically significant flood event on the Pigeon Creek fan since at least 1950 (63 years). Field evidence of channel avulsions within the watershed, very similar to that observed upstream of large woody debris jams after the 2013 event, suggests that there was a morphologically significant flood event in the watershed about 63 to 64 years ago (early 1950's) based on the ages of trees growing on the bed of the abandoned channel. Inferred and reported flood events occurred in the same timeframe in other local watersheds.

Landslide dam breaks have been identified as a hazard in the neighboring Cougar Creek watershed. There is no evidence of historic landslide dam break flood events in the Pigeon Creek watershed, probably because the geology is dominated by glacial till deposits rather than steeply-dipping bedrock exposures. However, the potential for a bedrock failure-induced landslide dam break was investigated in the lower reach of Pigeon Creek above the fan apex where two possible bedrock failures were identified. The peak flow from a dam break at this location would have a magnitude on the order of the 2013 event (~75m^3/s).

Various methods were employed to ultimately establish a debris flood frequency-magnitude relationship for return periods up to 3000 years. The relationship combines data from; a sediment transport-based yield analysis for events with 10 year to the 300 year return periods, and data from the test pit/ radiocarbon dating analysis for events with more than 750 year return period. The validity of the frequency-magnitude relationship was checked using predicted unit sediment yield rates against data from Cougar Creek and Three Sisters Creek.

Based on the analysis conducted by BGC (2016), a comparison of LiDAR data from 2008 and 2013 estimated the June 2013 Event Deposited approximately 70,000 m^3 of debris and sediment on the fan during the flood event. Using the combined frequency-magnitude relationship the June 2013 debris flood event can be assigned a return period between 100 and 200 years. This return period is comparable with return periods derived by BGC (2014 a,b) for the June 2013 events for both the Three Sisters and Cougar Creek watersheds and fans (about 300 years). Regardless of the estimated return period of the events in the three watersheds, it is clear that the hydro-geomorphic events on the fans, while substantial, were the result of significant rainfall and were not the result of periodic catastrophic events, such as landslide dam failures or stand-replacing fires.

PCSWMM modeling was used to evaluate fan inundation for the 2013 event and for 5 other scenarios. These 5 scenarios correspond to return period classes from 10 to 3000 years. The results suggest that during the 10 to 30 year event, most of the flows would be conveyed by highway culverts (provided they are cleaned periodically), with some flow diverted to the west and east. The model predicts some flow overtopping of George Biggy Sr. Road and some flow continuing north through minor highway culverts and east towards the animal underpass. Moderate flood intensity is expected in the creek channel and may impact existing properties on the lower fan, including the River's Bend development project.

Under the current channel alignment, the highway culverts do not have the hydraulic capacity to convey the 30 to 100 year event. Under this scenario, water will flow west along the ditchline adjacent to the highway off-ramp. Again, the model shows overtopping of George Biggy Sr. Road.

During the 100 to 300 year event the highway culverts are overwhelmed, causing a significant amount of water, sediment and debris to flow west along the ditchline. The model indicates the highway will overtop along the western edge of the fan. Some flow will go east along the highway as water and sediment crosses George Biggy Sr. Road. Under the 300 to 1000 year and 1000 to 3000 year scenarios a larger portion of the fan will be inundated. Modelling of the 2013 event shows similarities to what was observed in the field; discrepancies are explained in Table 9.3.

The results of this hazard assessment were used to complete the risk assessment which is prepared as a separate report.

11 CLOSURE

This work was undertaken under the attached General Conditions in Appendix F. We trust this report meets your present requirements. If you have any questions or comments, please contact the undersigned.

Respectfully submitted,
Tetra Tech EBA Inc.

Prepared by:
Mauricio Herrera, Ph.D., P.Eng.
Hydrotechnical Engineer
Direct Line: 604.608.8612
Mauricio Herrera@tetratech.com

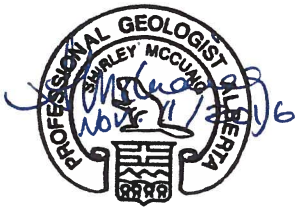

Prepared by:
Shirley McCuaig, Ph.D., P.Geol.
Senior Terrain Scientist
Direct Line: 780.451.2130 x705
Shirley.Mccuaig@tetratech.com

Prepared by:
Doug Johnston, P.Eng.
Senior Hydrotechnical Engineer
Direct Line: 778.945.5808
Doug.Johnston@tetratech.com

Prepared by:
Matthias Busslinger, M.A.Sc., P.Eng.
Geotechnical Engineer
Direct Line: 604.608.8611
Matthias.Busslinger@tetratech.com

Reviewed by:
Mike Harvey, Ph.D., P.G
Sci. Program Manager
Direct Line: 970.222.1710
Mike.Harvey@tetratech.com

/db

12 REFERENCES

Arno, S.F., and Sneck, K.M. 1977. A method for determining fire history in coniferous forests of the Mountain West. USDA Forest Service General Technical Report, INT-42.

BGC Engineering Inc. (BGC). 2013. BGC Project Memorandum: Pigeon Creek, Forensic analysis and Short-Term Debris Flood Mitigation. Memorandum prepared for the Town of Canmore.

BGC Engineering Inc. (BGC). 2014a. Cougar Creek, Debris Flood Hazard Assessment. Report prepared for the Town of Canmore.

BGC Engineering Inc. (BGC). 2014b. Three Sisters Creek Debris flood Hazard Assessment. Report prepared for the Town of Canmore.

BGC Engineering Inc. (BGC). 2015. Stone Creek Debris-Flow Hazard Assessment. Report prepared for the Town of Canmore. Final Report, dated January 16th, 2015, Project No. 1261-008, Document No. TC13-010.

Bisson, M., Favalli, M., Fornaciai, A., Mazzarini, F., Isola, I., Zanchetta, G. and Pareschi, M.T. (2005). "A rapid method to assess fire-related debris flow hazard in the Mediterranean region: An example from Sicily (southern Italy)". International Journal of Applied Earth Observation and Geoinformation, 7 (3): 217-231

Bovis, M.J. and Jakob, M. (1999)."The role of debris supply conditions in predicting debris-flow activity". Earth Surface Processes and Landforms, 24: 1039-1054

Cannon, S.H. and Gartner, J.E., 2005. Wildfire-related debris flow from a hazard perspective. Chapter 15, in Jakob, Mathias and Hungr, Oldrich, eds, Debris-flow hazards and related phenomena. Chichester, Springer-Praxis Books in Geophysical Sciences, 321-344.

Cannon, S.H. and Renneau, S.L. 2000. Conditions for the generation of fire-related debris flows, Capulin Canyon, New Mexico. Earth Surface Processes and Landforms 25, 1103-1121.

Cannon, S.H., Gartner, J.E. and Michael, J.A. 2007. Methods for the emergency assessment of debris-flow hazards from basins burned by the fires of 2007, southern California. USGS Open-File Report 2007-1384.

Cannon, S.H., Gartner, J.E., Bowers, J.C. and Laber, J.L. 2008. Storm rainfall conditions for floods and debris flows for recently burned areas in southeastern Colorado and southern California. Geomorphology 96, 250-269.

Cannon, S.H., Gartner, J.E., Parrett, C., and Parise, M. 2003. Wildfire-related debris-flow generation through episodic progressive sediment-bulking processes, western U.S.A. In Ricenmann, D. and Chen, C. (eds), International Conference on Debris-Flow Hazard Mitigation—Mechanics, Prediction and Assessment, 3rd Davos, Switzerland, September, 10-12, 2003, Proceedings. Milpress, Rotterdam, 71-82.

Cannon, S.H.; Gartner, J.E.; Rupert, M.G.; Michael, J.A.; Rea, A.H.; Parrett, C. 2010. Predicting the probability and volume of postwildfire debris flows in the intermountain western United States. Geological Society of America Bulletin 122, 127-144.

Cheng, W., Wang, X. and Zhou, X. (1999). "Research on some characteristics of two-phase hyperconcentrated flow". In: Jayawardena, A.W., Lee, J.H. and Wang, Z.Y. (eds) (1999). River Sedimentation: Theory and applications. Rotterdam, A.A. Balkema.

Chorley, R.J., Schumm, S.A. and Sugden, D.E., 1984. Geomorphology. Methuen, London, 326p.

Church M., Ryder J.M., 1972. Paraglacial sedimentation: consideration of fluvial processes conditioned by glaciation. Geological Society of America Bulletin 83, 3059-3072.

Church M., Slaymaker O., 1989. Disequilibrium of Holocene sediment yield in glaciated British Columbia. Nature 337, 452-454.

Clague, J.J., Menounos, B., Osborn, G., Luckman, B.H. and Koch, J. 2009. Nomenclature and resolution in Holocene glacial chronologies. Quaternary Science Reviews 28, 2231-2238.

Costa, J.E., and Schuster, R.L., 1988, The formation and failure of natural dams: Geological Society of America Bulletin, v. 100, p. 1054-1068

Costa, J. E. (1988). Rheologic, geomorphic, and sedimentologic differentiation of water floods, hyperconcentrated flows, and debris flows.*Flood Geomorphology. John Wiley & Sons New York. 1988.*

Courtney Mustaphi, C.J. and Pisaric, M.F.J. 2014. Holocene climate-fire-vegetation interactions at a subalpine watershed in southeastern British Columbia, Canada. Quaternary Research 81, 228-239.

Cruden, D.M. and Eaton, T.M. 1987. Reconnaissance of rockslide hazards in Kananaskis Country, Alberta. Canadian Geotechnical Journal 24, 414-429.

De Bano, L.F. 1981. Water-repellent soil: A State-of-the-art. USDA Forest Service General Technical Report PSW-46, Berkeley, PSWFRES.

DeGraff, J.V., Wagner, D., Gallegos, A.J., DeRose, M., Shannon, C., and Ellsworth, T. 2011. The remarkable occurrence of large rainfall-induced debris flows at two different locations on July 12, 2008, Sierra Nevada, California. Landslides 8, 343-353.

De Scally, F.A., Slaymaker, O. and Owens, I.F. (2001). “Morphometric controls and basin response in the Cascade Mountains”. Geografisca Annaler, 83A (3):117-130

FloFLO-2D Software, 2015. Reference Manual. http://www.flo-2d.com/download/ Last accessed 20 March, 2015.

FloFLO-2D Software, 2009. Flod-2D Mapper Manual.

FloFLO-2D Software, 2009. Simulating Mud Flow.

Gallaher, B.M. and Koch, R.J. 2004. Cerro Grande Fire Impacts to Water Quality and Stream Flow near Los Alamos National Laboratory: Results of Four Years of Monitoring. Los Alamos National Laboratory Report LA-14177.

Gallaway, J.M., Martin, Y.E. and Johnson, E.A. 2009. Sediment transport due to tree root throw: integrating tree population dynamics, wildfire and geomorphic response. Earth Surface Processes and Landforms 34, 1255-1269.

Gartner, J.E. Cannon, S.H., Bigio, E.R., Davis, N.K., Parrett, C., Pierce, K.L., Rupert, M.G., Thurston, B.L., Trebish, M.J., Garcia, S.P. and Rea, A.H. 2005. Compilation of data relating to the erosive response of 606 recently burned areas. USGS Open-File Report 2005-1218.

Goode, R.G., Luce, C.H., and Buffington, J.M. 2012. Enhanced sediment delivery in a changing climate and in semi-arid mountain basins: Implications for water resource management and aquatic habitat in the northern Rocky Mountains. Geomorphology 139-140: 1-15.

Gomez, B., & Church, M. (1989). An assessment of bed load sediment transport formulae for gravel bed rivers. *Water Resources Research*, *25*(6), 1161-1186.

Hallett, D.J. and Hills, L.V. 2006. Holocene vegetation dynamics, fire history lake level and climate change in the Kootenay Valley, southeastern British Columbia, Canada. Journal of Paleolimnology 35, 351-371.

Hallett, D.J., Lepofsky, D.S., Mathewes, R.W. and Lertzman, K.P. 2003. 11,000 years of fire history and climate in the mountain hemlock rain forests of southwestern British Columbia based on sedimentary charcoal. Canadian Journal of Forest Research 33, 292-312.

Harder, P., 2008. Hydroclimatological Trends in the Kananaskis Valley. Centre for Hydrology Internal Report, University of Saskatchewan, Saskatoon.

Hayashi, M., & van der Kamp, G. (2009). Progress in Scientific Studies of Groundwater in the Hydrologic Cycle in Canada, 2003-2007. Canadian Water Resources Journal, 34(2), 177-186.

Hawkes, B.C., 1979. Fire history and fuel appraisal study of Kananaskis Provincial Park, Alberta. Report prepared for Resource Assessment and Management Section Planning and Design Branch, Parks Division, Alberta Recreation and Parks and the Department of Forest Science, University of Alberta, Edmonton.

Heede, B.H., Harvey, M.D. and Laird, J.F. 1988. Sediment delivery linkages in a chaparral watershed following fire. Environmental Management 12, 349-358.

Heimann, E.U.M., Rickenmann, D., Turowski, J.M., Kirchner, J.W. 2015. SedFlow – A tool for simulating fractional bedload transport and longitudinal profile evolution in mountain streams. Earth Surf. Dynam. 3, 15-34, 2015.

Hungr, O., Evans, S.G., Bovis, M.J., and Hutchinson, J.N. (2001) A review of the classification of landslides of the flow type. Environmental and Engineering Geoscience, Volume 7(3): 221-238.

Iverson, R.M. 2014. Debris flows: behavior and hazard assessment. Geology Today 30(1): 15-20.

Jackson, L.E. Jr, Kostaschuk, R.A. and MacDonald, G.M. (1987). "Identification of debris-flow hazard on alluvial fans in the Canadian Rocky Mountains". Reviews in Engineering Geology 7: 115-124

Jakob, M. (2005). Debris-flow Hazard Analysis. In M. Jakob and O. Hungr (eds). Debris-flow Hazards and Related Phenomena. © Praxis. Springer Berlin Heidelberg 2005.

Jakob, M., Bovis, M. and Oden, M. (2005). "The significance of channel recharge rates for estimating debris-flow magnitude and frequency". Earth Surface Processes and Landforms, 30: 755-766

Johnson, E.A. and Fryer, G.I. Historical vegetation change in the Kananaskis Valley, Canadian Rockies. Canadian Journal of Botany 65, 853-858.

Kondolf, G.M. and Piegay, H. 2003. Tools in Fluvial Geomorphology. John Wiley and Sons, Ltd., Chichester, England.

Kostaschuk, R.A., MacDonald, G.M. and Putnam, P.E. 1986. Depositional process and alluvial fan-drainage basin morphometric relationships near Banff, Alberta, Canada. Earth Surface Processes and Landforms 11, 471-484.

Laird, J.R. and Harvey, M.D. 1986. Complex-response of chaparral drainage basin to fire. Proceedings of the International Symposium on Drainage Basin Sediment Delivery, IAHS Special Publication. 159, 165-184.

Letey, J. 2001. Causes and consequences of fire-induced soil water repellency. Hydrological Processes 15, 2867-2875.

M. Miles and Associates Ltd. (Miles) 2014a. Pigeon Creek near Canmore, Alberta: Initial Hydrotechnical Assessment, Compendium of Ground Photos and Field Notes, November 30 - December 2, 2013. Unpublished report prepared for the Town of Canmore and the Municipal District of Bighorn, volumes 1 and 2.

M. Miles and Associates Ltd. (Miles) 2014b. Pigeon Creek near Canmore, Alberta: Initial Hydrotechnical Assessment, Helicopter Inspection Imagery and Notes, November 30, 2013. Unpublished report prepared for the Town of Canmore and the Municipal District of Bighorn.

Masters, A.M. 1990. Changes in forest fire frequency in Kootenay National Park, Canadian Rockies. Canadian Journal of Botany 68, 1763-1767.

Merigliano, M.; Friedman, J.M.; Scott, M.L. 2013. Tree Ring Records of Variation in Flow and Channel Geometry. In: Shroder, J.F. et al. (eds), Treatise in Geomorphology, Vol. 12, Academic Press, pp. 145-164.

Meyer, G.A., Wells, S.G. and Jull, A.J.T. 1995. Fire and alluvial chronology in Yellowstone National Park – Climatic and intrinsic controls on Holocene geomorphic processes. Geological Society of America Bulletin 107, 1211-1230.

Moody, J.A. and Martin, D.A. 2001a. Initial hydrologic and geomorphic response following a wildfire in the Colorado Front Range. Earth Surface Processes and Landforms 26, 1049-1070.

Moody, J.A. and Martin, D.A. 2001b. Hydrologic and sedimentologic response of two burned watersheds in Colorado. USGS Water-Resources Investigations Report 01-4122.

Montane Forest Management Ltd. 2008. Kananaskis Country Vegetation Management Strategy. Report prepared for Sustainable Resource Development and Tourism, Parks, Recreation and Culture.

Mori, A.S. and Lertzman, K.P. 2011. Historic variability in fire-generated landscape heterogeneity of subalpine forests in the Canadian Rockies. Journal of Vegetation Science 22, 45-58.

Munn, R. E., & Storr, D. (1967). Meteorological studies in the Marmot Creek Watershed, Alberta, Canada, in August 1965. Water Resources Research, 3(3), 713-722.

Mussetter Engineering, Inc. 2008. Cornet Creek Drainage Maintenance and Flood Mitigation Study, Colorado. Report prepared for the Town of Telluride Department of Public Works. March 2008.

Mussetter Engineering, Inc. 2009. Cornet Creek Watershed and Alluvial Fan Debris Flow Analysis. Prepared for the Town of Telluride Department of Public Works.

Nietsche, M., Rickenmann, D., Turowski, J., Badoux, A., Kirchner, J. 2011. Evaluation of bedload transport predictions using flow resistance equations to account for macro-roughness in steep-mountain streams. Water Resources Research, Vol. 47.

Nitsche, M., Rickenmann, D., Kirchner, J. W., Turowski, J. M., & Badoux, A. (2012). Macroroughness and variations in reach-averaged flow resistance in steep mountain streams. *Water Resources Research*, *48*(12).

O'Brien, J.S. 1986. Physical Processes, Rheology, and Modeling of Mud Flows. Ph.D. Dissertation, Colorado State University, Fort Collins, Colorado.

Pierson, T.C. Hyperconcentrated flow – transitional process between water flow and debris flow. In Jakob, M. and Hungr, O. (eds.), Debris-flow Hazards and Related Phenomena, Springer, Berlin, 2005.

Pomeroy, J.W., Spence, C., Whitfield, P.H..Putting Prediction in Ungauged Basins into practice. Ottawa: Canadian Water Resources Association, 2013.

Pomeroy, J. W., Gray, D.M., Brown, T., Hedstorm, N.R., Quinton, W.L., Granger, R.J., and Carey, S.K. "The cold regions hydrological model: a platform for basing process representation and model structure on physical evidence." Hydrological Processes 21.19 (2007): 2650-2667.

Power, M.J. Whitlock, C. and Bartlein, P.J. 2011. Postglacial fire, vegetation, and climate history across an elevational gradient in the Northern Rocky Mountains, USA and Canada. Quaternary Science Reviews 30, 2520-2533.

Price R.A. 1970a. Geology, Canmore (east half). Geological Survey of Canada Map 1265A, scale 1:50,000.

Price R.A. 1970b. Geology, Canmore (west half). Geological Survey of Canada Map 1266A, scale 1:50,000.

Rickenmann, D. 1991. Hyperconcentrated flow and sediment transport at steep slopes, J. Hydr. Engng, ASCE 117(11), 1419-1439.

Rickenmann, D. 1999. Empirical Relationships for Debris Flows. Natural Hazards 19: 47-77, 1999.

Rickenmann, D. 2001. Comparison of bed load transport in torrents and gravel bed streams. Water Resources Research, Vol. 37, No. 12, pages 3295-3305, December, 2001.

Rickenmann, D., Chiari, M., Friedl, K. 2006. SEATRAC – A sediment routing model for steep torrent channels. River Flow, 2006. – Ferreira, Alves, Leal & Cardoso (eds).

Rogeau, M-P. 2005. Fire History Study, Kananaskis District, Alberta, 2004 Field Results. Report Prepared for Spray Lake Sawmills Ltd., Alberta Community Development and Alberta Sustainable Resource Development.

Sanborn, P., Geertsema, M. Jull, A.J.T. and Hawkes, B. 2006. Soil and sedimentary charcoal evidence for Holocene forest fires in an inland temperate rainforest, east-central British Columbia, Canada. The Holocene 16, 415-427.

Schumm, S.A., 1977. The Fluvial System. Wiley, New York.

Srivastav, A. S. R., & Simonovic, (2014) S. P. GENERALIZED TOOL FOR UPDATING INTENSITY-DURATION-FREQUENCY CURVES UNDER CLIMATE CHANGE.

Stokes, M.A., Smiley, T.L., 1968. An Introduction to Tree-ring Dating. University of Arizona Press, Tucson, AZ

Tande, G.F. 1979. Fire history and vegetation pattern of coniferous forests in Jasper National Park, Alberta. Canadian Journal of Botany 57, 1912-1931.

Tetra Tech, Inc. 2013. Santa Clara Creek, Rio Ariba County, New Mexico, Post Las Conchas Fire Geomorphic Assessment. Report prepared for U.S. Army Corps of Engineers, Albuquerque District.

Tillery, A.C., Darr, M.J., Cannon, S.H. and Michael, J.A, 2011. Post wildfire preliminary debris flow hazard assessment for the area burned by the 2011 Las Conchas Fire in north-central New Mexico. USGS Open-File Report 2011-1308.

Town of Canmore (2015). Personal Communication. Email from Ms. Julia Eisl.

Veenhuis, J.E. 2002. Effects of wildfire on the hydrology of the Capulin and Rito De Los Frijoles Canyons, Bandelier National Monument, New Mexico. USGS Water Resources Investigations Report 02-4152.

Walkinshaw, S. 2008. Kananaskis Country Vegetation Management Strategy. Report prepared for Alberta Sustainable Resource Development and Tourism, Parks, Recreation and Culture by Montane Forest Management Ltd.

Wells, H.G. 1987. The effects of fire on the generation of debris flows in Southern California. In Costa .J.E. and Wieczorek, G.F., (eds), Debris flows/avalanches – Process, recognition and mitigation. Geological Society of America Reviews in Engineering Geology 7, 105-114.

West Consultants. 2011. Sediment/Debris Bulking Factors and Post-fire Hydrology for Ventura County. Final Report. Prepared for Ventura County Watershed Protection District. June 2011. Contract No. AE09-G20. Task Order No. PW09-171.

White, Cliff. 1985. Wildland Fires in Banff National Park 1880-1980. National Parks Branch, Parks Canada, Environment Canada.

Zhang, X., Vincent, L. A., Hogg, W. D., & Niitsoo, A. (2000). Temperature and precipitation trends in Canada during the 20th century. Atmosphere-ocean, 38(3), 395-429.

TABLES

Table 4.3 Radiocarbon ages obtained at Pigeon Creek
Table 4.4 Comparison of Radiocarbon Dating and Dendrochronology to known Climate Trends and Fire Histories of Adjacent Areas
Table 9.3 Summary of Model Runs Corresponding to Each Hazard Class
Table 9.4 Summary of Model Runs Corresponding to Each Hazard Class – Scenario 1
Table 9.5 Summary of Model Runs Corresponding to Each Hazard Class – Scenario 2a
Table 9.6 Summary of Model Runs Corresponding to Each Hazard Class – Scenario 2b

RADIOCARBON DATES

Table 4.3: Radiocarbon ages obtained at Pigeon Creek

Trench ID	Depth [1] (m)	Dated Materials	Context [2]	Conventional Radiocarbon age ^{14}C yr BP[3]	2 Sigma Calibrated Age (Cal yr BP)	Lab No.
PCUR13	1.17	Charred material	Watershed creek bank	90 +/- 30 BP	Cal AD 1685 to 1735 (Cal BP 265 to 215) and Cal AD 1805 to 1930 (Cal BP 145 to 20) and Post AD 1950 (Post 0)	389538
PCFR27	0.83	Charred material	Western fan deposits	210 +/- 30 BP	Cal AD 1645 to 1685 (Cal BP 305 to 265) and Cal AD 1735 to 1805 (Cal BP 215 to 145) and Cal AD 1930 to Post 1950 (Cal BP 20 to Post 0)	389537
PCFTR31B	1.25	Bone	Western fan deposits	520 +/- 30 BP	Cal AD 1330 to 1340 (Cal BP 620 to 610) and Cal AD 1395 to 1440 (Cal BP 555 to 510)	393181
PCFTR31C	4.1	Charred material	Western fan deposits	870 +/- 30 BP	Cal AD 1048 to 1086 (Cal BP 902 to 864) and Cal AD 1123 to 1138 (Cal BP 287 to 812) and Cal AD 1150 to 1223 (Cal BP 800 to 727	393182
PCFTR33B	3.69	Charred material	Eastern fan deposits	3280 +/- 30 BP	Cal BC 1625 to 1498 (Cal BP 3575 to 3448)	393183
PCFTR33D	4.81	Charred material	Eastern fan deposits	3430 +/- 30 BP	Cal BC 1870 to 1845 (Cal BP 3820 to 3795) and Cal BC 1810 to 1800 (Cal BP 3760 to 3750) and Cal BC 1775 to 1660 (Cal BP 3725 to 3610)	393184
PCFTR34A	1.26	Charred material	Central fan deposits	1820 +/- 30 BP	Cal AD 125 to 255 (Cal BP 1825 to 1695) and Cal AD 300 to 315 (Cal BP 1650 to 1635)	393185
PCFTR35A	2.25	Charred material	Eastern fan deposits	2520 +/- 30 BP	Cal BC 790 to 730 (Cal BP 2740 to 2680) and Cal BC 690 to 660 (Cal BP 2640 to 2610) and Cal BC 650 to 540 (Cal BP 2600 to 2490	393186
PCFTR35B	2.47	Charred material	Eastern fan deposits	3780 +/- 30 BP	Cal BC 2290 to 2135 (Cal BP 4240 to 4085)	393187
PCFTR35C	2.57	Charred material	Eastern fan deposits	2510 +/- 30 BP	Cal BC 790 to 540 (Cal BP 2740 to 2490)	393188
PCFTR35D	5.99	Charred material	Eastern fan deposits	2890 +/- 30 BP	Cal BC 1190 to 1175 (Cal BP 3140 to 3125) and Cal BC 1160 to 1145 (Cal BP 3110 to 3095) and Cal BC 1130 to 1000 (Cal BP 3080 to 2950)	393189
PCFTR36B	1.58	Wood	Western fan deposits	850 +/- 30 BP	Cal AD 1155 to 1255 (Cal BP 795 to 695)	393190
PCFTR36C	4.06	Organic sediment	Western fan deposits	14380 +/- 50 BP	Cal BC 15685 to 15475 (Cal BP 17635 to 17425)	393191
PCFTR38	2.51	Wood	Upper fan deposits	101.1 +/- 0.3 pMC	Modern	393192
PCUR40	1.32	Charred material	Watershed creek bank	2010 +/- 30 BP	Cal BC 85 to 75 (Cal BP 2035 to 2025) and Cal BC 55 to AD 60 (Cal BP 2005 to 1890)	394159
PCFTR43A	1.61	Charred material	Central fan deposits	880 +/- 30 BP	Cal AD 1045 to 1097 (Cal BP 905 to 853) and Cal AD 1119 to 1220 (Cal BP 831 to 730)	393193
PCFTR43B	2.18	Charred material	Central fan deposits	1260 +/- 30 BP	Cal AD 670 to 775 (Cal BP 1280 to 1175) and Cal AD 790 to 800 (Cal BP 1160 to 1150)	393194

Table 4.4 Comparison of Radiocarbon Dating and Dendrochronology to known Climate Trends and Fire Histories of Adjacent Areas

Source	General Study Area	Calendar years BP (median age)																							
Climate (Clague et al. 2009)		warmer		150	Little Ice Age					800	warmer			1st Millenium Adv			warmer	Tiedemann - Peyto Glacial Advances							
(Clague et al. 2009)	Warm periods within LIA					250		600	700																
BGC (2014)[1,2]	Cougar Creek	94						590	700	870		1000	1150	1350	1570				2490	2640	3020	3205	3405		
									740			1040								2760	2990				
***Tetra Tech EBA (this report)*[1,2]**	Pigeon Creek							550	750	810							1960			2630	3100		3430	3510	
Establishment age of oldest trees					200	250				820			1210							2770					
Disturbance on established trees		100		150																					
Literature																									
Rogeau 2005	Canmore area	94		179																					
Rogeau 2005	Upper Kananaskis Foothills	95		150																					
Masters 1990	Kananaskis area	86	medium freq.		226	236		506																	
Mori and Lertzman 2011	Subalpine Kootenay National Park	88		174		244																			
Hallett and Hills 2006	Kootenay Valley			150	lower frequency			600		800	medium high fire frequency				1600			2000	low fire frequency					3500	
Tande 1979			125	167		256																			
Power et al. 2011	High elevations northern Montana		High fire frequency					500							1600										
Power et al. 2011	Low elevations northern Montana									High but variable fire frequency						1800		2200							
Colour fill indicates a range of time																									
[1]Black: calendar years converted from ^{14}C dates																									
[2] Blue: calender years from tree core data																									

Table 9.3: Summary of Model Runs Corresponding to Each Hazard Class

Run ID	Return Period (year)	Assumptions	Results
1	10-30	Debris flood, culverts perform to capacity	▪ Inundation area in the treed area within River's Bend Development property and north of the condo complexes. ▪ Moderate flood intensity in the main channel along 3 Avenue. Existing buildings and infrastructure would be impacted. ▪ Overtopping of George Biggy Sr. Road occurs.
2	30-100	Debris flood, culverts perform to capacity	▪ The majority of the flow goes through the highway twin culverts. Some of the flooding spreads out across the River's Bend Development property and the area north of the condo complex. ▪ Overtopping occurs at George Biggy Sr. Road upstream of the highway off ramp. Overflow splits into two directions: flowing northwards through the highway culverts and flowing eastwards along Bow Corridor Link Trail and crossing Hwy 1 through the animal underpass. ▪ Due to increased flood depth at the inlet of the twin culverts at the highway off ramp, the channel overflows to the west along the highway upslope ditch. This is due to unfavorable culvert inlet conditions, i.e. the 90 degree angle to the inflow direction. ▪ Moderate flood intensity in the main channel along 3 Avenue. Existing buildings and infrastructure would be impacted.
3	100-300	Debris flood, culverts perform to capacity	▪ Increased flow through the highway twin culverts results in greater inundation area to the River's Bend Development property and property of the condo complexes. ▪ Increased amount of overtopping at George Biggy Sr. Road, sends flow east through the animal underpass. Greater flood intensity on the eastern fan area. ▪ The twin highway culverts hit capacity. More overflow to the west along the off ramp ditch due to backwater effect at the culvert inlets. As the depth builds up in the low lying fan area along the western edge of the fan, overtopping occurs at the highway west of the Esso gas station. Inundation also occurs in the treed area west of the Esso gas station.
4	300-1000	Debris flood, culverts perform to capacity	▪ Most developed areas and areas under development would be inundated in this scenario. ▪ Over 1.5 km of Hwy 1, 0.3 km of George Biggy Sr Rd, and all the access road to local business would be impacted. ▪ Inundation of the Thunderstone Quarry and the proposed River's Bend development site occurs. ▪ Pigeon Creek Condos, Copperstone Resort, Pigeon Creek Motel, Husky House, Big Horn Motel, Bandoleers, Kiska Inn and Esso gas station would be impacted.
5	1000-3000	Debris flood, culverts perform to capacity	▪ Similar to Run 4 with larger inundation area and greater flood depth.
6	2013 Event	Debris flood, culverts perform to capacity	▪ Extent of inundation in this scenario is similar to Run 3 with the majority of the flow going north through the twin culverts and going east and avulsing over George Biggy Sr. Road and inundating a large portions of the eastern fan area. ▪ Note that while the model reflected the impacted area downstream of the twin culverts there are discrepancies between the modelled results and field observations. The model over estimated flooding to the eastern fan area and under estimated flooding to the west fan area west of the Esso gas station. ▪ Possible explanations on the discrepancies may be the difference in the pre- and post-event topography. The hydraulic model was constructed using post-flood topography where a new channel has formed along the George Biggy Sr. Road. Under the current condition, the road embankment is more prone to overtopping due to close vicinity to the creek channel. From a mass balance point of view, this also explains the underestimated inundation area to the western fan area. The sequence of events that occurred during the 2013 event were also not included in the model, for instance sediment deposition during the event plays a role in the flow distribution. The presence of an excavator cleaning sediment built-up upstream of the highway culverts was not included in the model. During the 2013 event, the twin culverts flowed at capacity before blockage occurred, which directed more flow to the west. In the PCSWMM model, the gradual reduction of culvert capacity was not accounted for. Lastly, extensive deposition from the 2013 debris flood event increased floodplain elevation at certain areas by approximately 0.3 m. This may increase the risk of future flooding to the areas that were outside the 2013 inundation zone (i.e. Pigeon Mountain Condos, Copperstone Resort).

FIGURES

Figure 1.1 Project Location
Figure 1.2 Pigeon Creek Fan
Figure 1.3 LIDAR Contours on the Pigeon Creek Fan
Figure 2.1 Geology of the Pigeon Creek Area
Figure 2.2 Surficial Geology of the Pigeon Creek Area
Figure 4.1 Location of Selected Photos in the Watershed
Figure 4.2 Location of Selected Photos on the Fan
Figure 4.3 June 2013 Event – Fan Inundation and Aggradation Impacted Area
Figure 4.4 Geomorphic Features in the Watershed
Figure 4.5 Geomorphic Features on the Fan
Figure 4.6 Historic Alignments of Pigeon Creek on the Fan
Figure 4.7 Tree Core Locations and Age on the Fan
Figure 4.8 Tree Core Locations and Age in the Watershed
Figure 4.11 Sampled Natural Exposure Site Locations in the Watershed
Figure 4.12 Sampled Test Pit and Exposure Locations on the Fan
Figure 4.13 Test Pit Profiles on the Fan – Lower Fan
Figure 5.14 LiDAR derived DEM Elevation Differences Between 2008 and 2013 of Pigeon Creek Fan
Figure 5.15 Test Pit Profiles on the Fan – Lower Fan
Figure 5.16 Test Pit Profiles on the Fan – Upper Fan and North - South
Figure 9.1 Mesh Grid Used for Two Dimensional Modeling
Figure 9.2 Flood Intensity and Flood Depth – 10-30 yr Return Period
Figure 9.3 Flood Intensity and Flood Depth – 30-100 yr Return Period
Figure 9.4 Flood Intensity and Flood Depth – 100-300 yr Return Period
Figure 9.5 Flood Intensity and Flood Depth – 300-1000 yr Return Period
Figure 9.6 Flood Intensity and Flood Depth – 1000-3000 yr Return Period

Figure 9.7 Flood Intensity and Flood Depth – June 19-21, 2013
Figure 9.8 Composite Flood Intensity and Flood Depth – Return Period Classes
Figure 9.10 Flood Intensity and Flood Depth – 10-30 yr Return Period – Scenario 1
Figure 9.11 Flood Intensity and Flood Depth – 30-100 yr Return Period – Scenario 1
Figure 9.12 Flood Intensity and Flood Depth – 100-300 yr Return Period – Scenario 1
Figure 9.13 Flood Intensity and Flood Depth – 300-1000 yr Return Period – Scenario 1
Figure 9.14 Flood Intensity and Flood Depth – 1000-3000 yr Return Period – Scenario 1
Figure 9.15 Flood Intensity and Flood Depth – June 19-21, 2013 – Scenario 1
Figure 9.16 Composite Flood Intensity and Flood Depth – Return Period Classes – Scenario 1
Figure 9.17 Flood Intensity and Flood Depth – 10-30 yr Return Period – Scenario 2a
Figure 9.18 Flood Intensity and Flood Depth – 30-100 yr Return Period – Scenario 2a
Figure 9.19 Flood Intensity and Flood Depth – 100-300 yr Return Period – Scenario 2a
Figure 9.20 Flood Intensity and Flood Depth – 300-1000 yr Return Period – Scenario 2a
Figure 9.21 Flood Intensity and Flood Depth – 1000-3000 yr Return Period – Scenario 2a
Figure 9.22 Flood Intensity and Flood Depth – June 19-21, 2013 – Scenario 2a
Figure 9.23 Composite Flood Intensity and Flood Depth – Return Period Classes – Scenario 2a
Figure 9.24 Flood Intensity and Flood Depth – 10-30 yr Return Period – Scenario 2b
Figure 9.25 Flood Intensity and Flood Depth – 30-100 yr Return Period – Scenario 2b
Figure 9.26 Flood Intensity and Flood Depth – 100-300 yr Return Period – Scenario 2b
Figure 9.27 Flood Intensity and Flood Depth – 300-1000 yr Return Period – Scenario 2b
Figure 9.28 Flood Intensity and Flood Depth – 1000-3000 yr Return Period – Scenario 2b
Figure 9.29 Flood Intensity and Flood Depth – June 19-21, 2013 – Scenario 2b
Figure 9.30 Composite Flood Intensity and Flood Depth – Return Period Classes – Scenario 2b

615000
620000
625000
630000

5660000
5655000
5650000

CANMORE
Bow River
Hwy 1A
Hwy 1
Pigeon Creek Fan
(1.47 km²)
West Wind Creek
Wind Creek
Pigeon Creek
Pigeon Creek Watershed
(57.3 km²)

N
W
E
S

ALBERTA
Fort McMurray
Grande Prairie
Edmonton
Site Location
Calgary

LEGEND

- Pigeon Creek Fan
- Pigeon Creek Watershed
- Road
- Watercourse
- Waterbody

NOTES
Base data source:
Imagery from Google; DigitalGlobe (2013).

STATUS
ISSUED FOR USE

PIGEON CREEK HAZARD ASSESSMENT

Project Location

PROJECTION UTM Zone 11	**DATUM** NAD83			**CLIENT** Town of CANMORE
Scale: 1:70,000 (1 0.5 0 1 Kilometres)				TETRA TECH EBA
FILE NO. V13203145-01_Figure01-1_SiteLocation.mxd				
PROJECT NO. V13203145-01	**DWN** SL	**CKD** MEZ	**APVD** JS	**REV** 0
OFFICE Tt EBA-VANC	**DATE** December 2016			**Figure 1.1**

Q:\Vancouver\GIS\ENGINEERING\V13203145-01_PigeonCreek\Maps\HazardAssessment\V13203145-01_Figure01-1_SiteLocation.mxd modified 12/8/2014 by stephanie.leusink

621500 622000 622500 623000

5656500 5656000 5655500 5655000

Bow River

Sewage Treatment Ponds

Pigeon Creek Condo Complex

Copperstone Condo Complex

Three Sisters Campground

River's Bend Development

Pigeon Creek

Dead Man's Flats

Trans-Canada Hwy

George Biggy Sr. Rd

Highway Animal Underpass

Thunderstone Quarry

Fan Apex (Waterfall)

N W E S

LEGEND

- Pigeon Creek Fan
- Pigeon Creek Watershed
- Road
- Intermediate Contour (1 m)
- Index Contour (5 m)
- Watercourse

NOTES
Base data source:
Imagery provided by Colbert Tam.
LiDAR data provided by the Town of Canmore.

STATUS
ISSUED FOR USE

PIGEON CREEK HAZARD ASSESSMENT

Pigeon Creek Fan

PROJECTION	DATUM	CLIENT
UTM Zone 11	NAD83	Town of CANMORE

Scale: 1:7,000
100 50 0 100
Metres

TETRA TECH EBA

FILE NO.				
V13203145-01_Figure1-2_Fan.mxd				
PROJECT NO.	**DWN**	**CKD**	**APVD**	**REV**
V13203145-01	SL	MEZ	JS	0
OFFICE	**DATE**			
Tt EBA-VANC	December 2016			

Figure 1.2

Q:\Vancouver\GIS\ENGINEERING\V13\V13203145-01_PigeonCreek\Maps\HazardAssessment\V13203145-01_Figure1-2_Fan.mxd modified 12/8/2014 by stephanie.leusink

621500 622000 622500 623000

5656500 5656000 5655500 5655000

N W E S

Bow River

Sewage Treatment Ponds

Pigeon Creek Condo Complex

Copperstone Condo Complex

Three Sisters Campground

River's Bend Development

Pigeon Creek

Dead Man's Flats

Trans-Canada Hwy

Highway Animal Underpass

George Biggy Sr. Rd

Thunderstone Quarry

Fan Apex (Waterfall)

LEGEND

- Pigeon Creek Fan
- Pigeon Creek Watershed
- Road
- Intermediate Contour (1 m)
- Index Contour (5 m)
- Watercourse

NOTES
Base data source:
LiDAR data provided by the Town of Canmore.

STATUS
ISSUED FOR USE

PIGEON CREEK HAZARD ASSESSMENT

LiDAR Contours on the Pigeon Creek Fan

PROJECTION	DATUM	CLIENT
UTM Zone 11	NAD83	Town of CANMORE

Scale: 1:7,000
100 50 0 100
Metres

TETRA TECH EBA

FILE NO.				
V13203145-01_Figure1-3_FanContours.mxd				
PROJECT NO.	**DWN**	**CKD**	**APVD**	**REV**
V13203145-01	SL	MEZ	JS	0
OFFICE	**DATE**			
Tt EBA-VANC	December 2016			

Figure 1.3

Q:\Vancouver\GIS\ENGINEERING\V13\V13203145-01_PigeonCreek\Maps\HazardAssessment\V13203145-01_Figure1-3_FanContours.mxd modified 12/8/2014 by stephanie.leusink

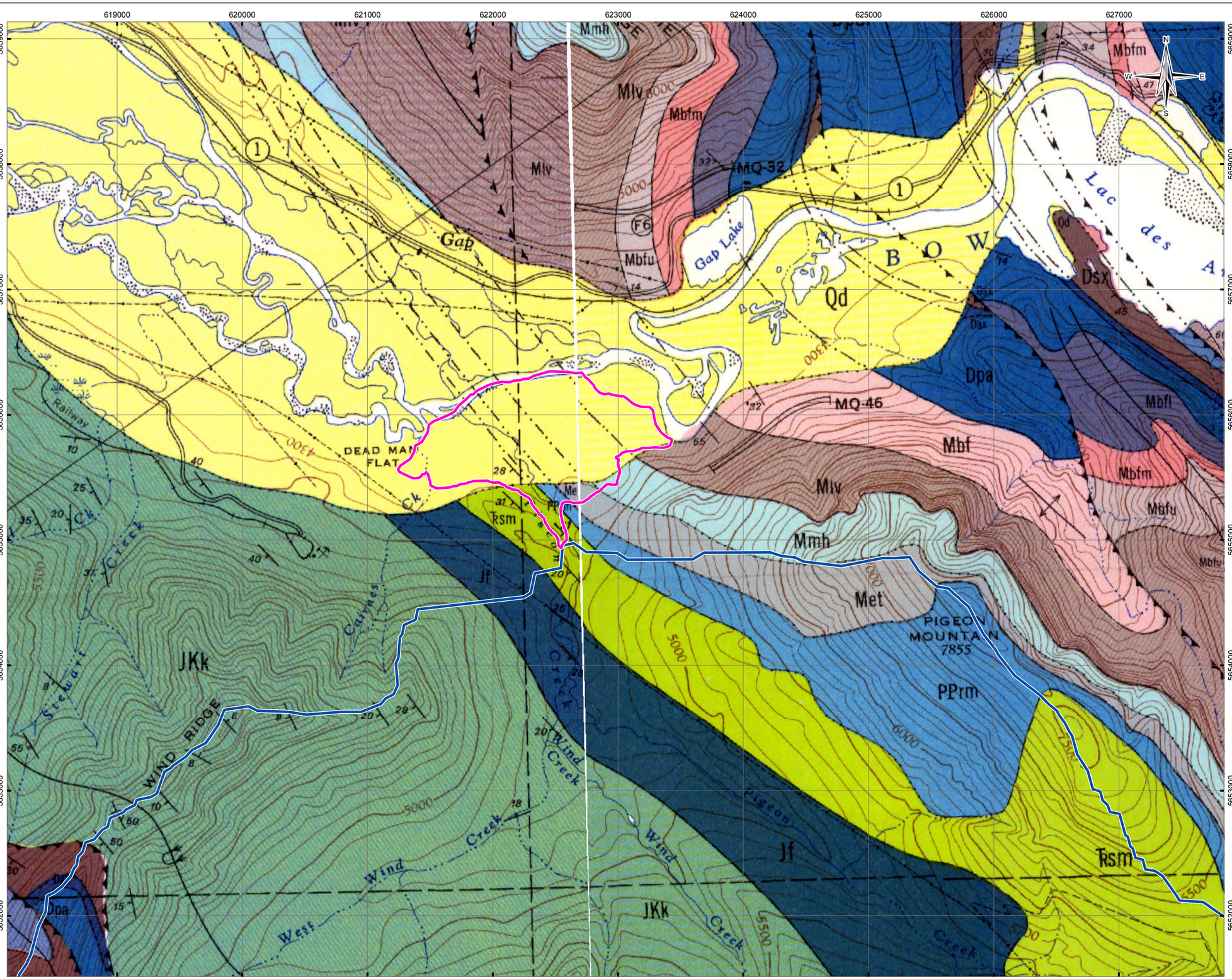

Q:\Vancouver\GIS\ENGINEERING\V13203145-01_PigeonCreek\Maps\HazardAssessment\V13203145-01_Figure02-1_Geology.mxd modified 12/8/2014 by stephanie.leusink

LEGEND

- Pigeon Creek Fan
- Pigeon Creek Watershed

Geology

- Qd - Till, alluvium, colluvium
- JKk - Kootenay Formation
- Jf - Fernie Group
- TRsm - Sulphur Mountain Formation
- PPrm - Rocky Mountain Group
- Met - Etherington Formation
- Mmh - Mount Head Formation
- Mlv - Livingstone Formation
- Mbfu - Exshaw and Banff Formations; Upper Part
- Mbfm - Exshaw and Banff Formations; Middle Part
- Mbfl - Exshaw and Banff Formations; Lower Part
- Dpa - Palliser Formation
- Dax - Alexo Formation
- Dsx - Southesk Formation
- Dcn - Cairn Formation
- Cpk - Pika Formation
- Cel - Eldon Formation

NOTES
Base data source:
Geology from Map 1265A (Canmore East Half) and Map 1266A (Canmore West Half). 1970. Geological Survey of Canada.

STATUS
ISSUED FOR USE

PIGEON CREEK HAZARD ASSESSMENT

Geology of the Pigeon Creek Area

PROJECTION UTM Zone 11		**DATUM** NAD83		**CLIENT** Town of CANMORE
Scale: 1:30,000 — 500 250 0 500 Metres				TETRA TECH EBA
FILE NO. V13203145-01_Figure02-1_Geology.mxd				
PROJECT NO. V13203145-01	**DWN** SL	**CKD** MEZ	**APVD** SMC	**REV** 0
OFFICE Tt EBA-VANC	**DATE** December 2016			**Figure 2.1**

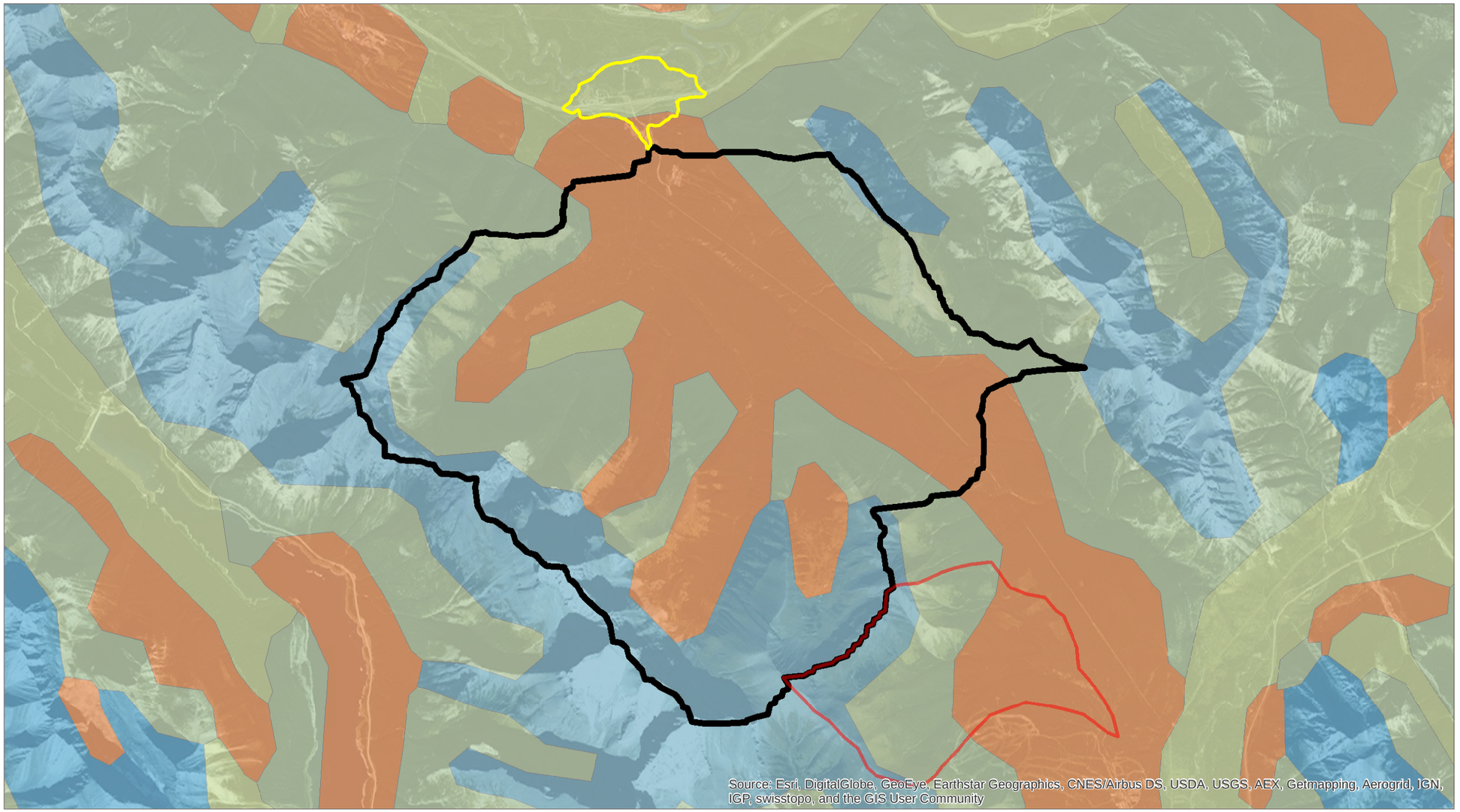

N
W
E
S

TEXTURE

- Bedrock
- Ice with minor boulders to clay sized sediment.
- Includes offshore sand, silt and clay, minor organic deposits; may also include minor littoral (nearshore) beaches and bars composed of sand, silt and minor gravel.
- May contain pre-existing bedrock, till, glaciolacustrine, glaciofluvial and/or eolian sediments, generally poorly sorted. In places includes a significant component of fluvial deposits, as these two units are inseparable at 1 million scale.
- Poorly- to well-sorted, stratified-to-massive sand, gravel, silt, clay and organic sediments occurring in channel and overbank deposits. In places includes a significant component of colluvial deposits as these two units are inseparable at 1 million map
- Predominantly well-sorted quartzite and chert gravel and cobbles with minor sand; Cordilleran source.
- Sediment is mainly till but locally includes stratified glaciolacustrine or glaciofluvial sediments.
- Sediment is mainly till may locally include stratified glaciolacustrine and/or glaciofluvial sediments.
- Sediment may include syngenetic till, as well as masses of pre-existing sediments and/or bedrock.
- Sediment ranges from massive to stratified, poor- to well-sorted, coarse- to fine- grained. In places, this unit includes till. May show evidence of ice melting (slumped structures).
- Till a mixture of clay, silt, sand and minor pebbles, cobbles and boulders. Locally, this unit may contain blocks of bedrock, pre-existing stratified sediment and till, and/or lenses of glaciolacustrine and/or glaciofluvial sediment.
- Well-sorted, medium- to fine-grained sand and minor silt; generally massive to locally cross-bedded or ripple-laminated; includes both active and vegetated dunes and sand sheets.
- Woody to fibrous muck; commonly underlain by fine-grained, poorly drained glaciolacustrine or lacustrine deposits; in some places underlain by till.
- a) Offshore sediment; rhythmically laminated to massive fine sand, silt and clay, locally debris released from floating ice. b) Littoral and nearshore sediments; massive to stratified, well-sorted silty sand, pebbly sand and minor gravel.
- Watershed- Marmot
- Watershed- Pigeon
- Pigeon Creek Fan

STATUS
ISSUED FOR USE

PIGEON CREEK HAZARD ASSESSMENT

Surficial Geology
Pigeon and Marmot Creek Watersheds

PROJECTION: UTM Zone 11	DATUM: NAD83	CLIENT: Town of CANMORE	
Scale: 1:68,887 (1 cm = 688.87 Metres)			
FILE NO.: V13203145-01_Figure2.2_surficialgeology.mxd		TETRA TECH EBA	
PROJECT NO.: V13203145-01	DWN: MH / CKD: MEZ / APVD: DJ / REV: 0		Figure 2.2
OFFICE: Tt EBA-VANC	DATE: December 2016		

Q:\Vancouver\Engineering\V13203145 Pigeon Cr Hazard and Risk\GIS\Report Figures\V13203145-01_Figure2.2_surficialgeology.mxd modified 1/31/2016 by mauricio.herrera

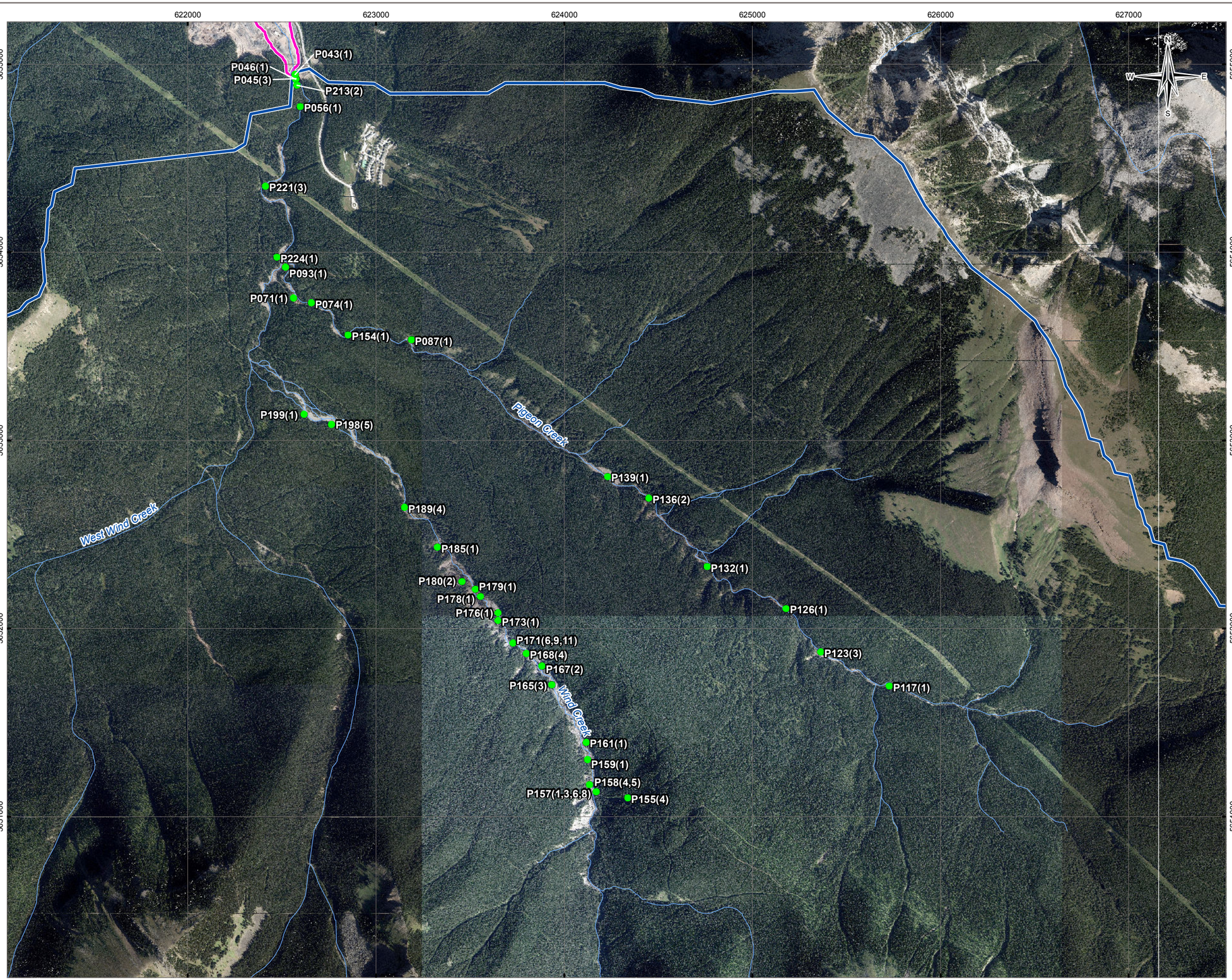

LEGEND

- Photo Location (P#)
- Pigeon Creek Fan
- Pigeon Creek Watershed
- Watercourse

NOTES
Base data source:
Imagery provided by Colbert Tam.

STATUS
ISSUED FOR USE

PIGEON CREEK HAZARD ASSESSMENT

Location of Selected Photos in the Watershed

PROJECTION UTM Zone 11	**DATUM** NAD83			**CLIENT** Town of CANMORE
Scale: 1:20,000 (400 200 0 400 Metres)				TETRA TECH EBA
FILE NO. V13203145-01_Figure04-1_WatershedPhotos.mxd				
PROJECT NO. V13203145-01	**DWN** MEZ	**CKD** SL	**APVD** JS	**REV** 0
OFFICE Tt EBA-VANC	**DATE** December 2016			**Figure 4.1**

Q:\Vancouver\GIS\ENGINEERING\V13\V13203145-01_PigeonCreek\Maps\HazardAssessment\V13203145-01_Figure04-1_WatershedPhotos.mxd modified 12/8/2014 by stephanie.leusink

621500 622000 622500 623000

5656500 5656000 5655500 5655000

P036(1)
P034(1)
P111(1)
Pigeon Creek
P7130
P7125
P7137
P045(3)
P046(1)
P043(1)
P213(2)
P056(1)

N W E S

LEGEND

- Photo Location (P#)
- Pigeon Creek Fan
- Pigeon Creek Watershed
- Watercourse

NOTES
Base data source:
Imagery provided by Colbert Tam.

STATUS
ISSUED FOR USE

PIGEON CREEK HAZARD ASSESSMENT

Location of Selected Photos on the Fan

PROJECTION	DATUM	CLIENT
UTM Zone 11	NAD83	Town of CANMORE

Scale: 1:7,000
100 50 0 100
Metres

TETRA TECH EBA

FILE NO. V13203145-01_Figure04-2_FanPhotos.mxd

PROJECT NO.	DWN	CKD	APVD	REV
V13203145-01	MEZ	SL	JS	0

OFFICE	DATE
Tt EBA-VANC	December 2016

Figure 4.2

Q:\Vancouver\GIS\ENGINEERING\V13203145-01_PigeonCreek\Maps\HazardAssessment\V13203145-01_Figure04-2_FanPhotos.mxd modified 12/8/2014 by stephanie.leusink

621500 622000 622500 623000

5656500 5656000 5655500 5655000

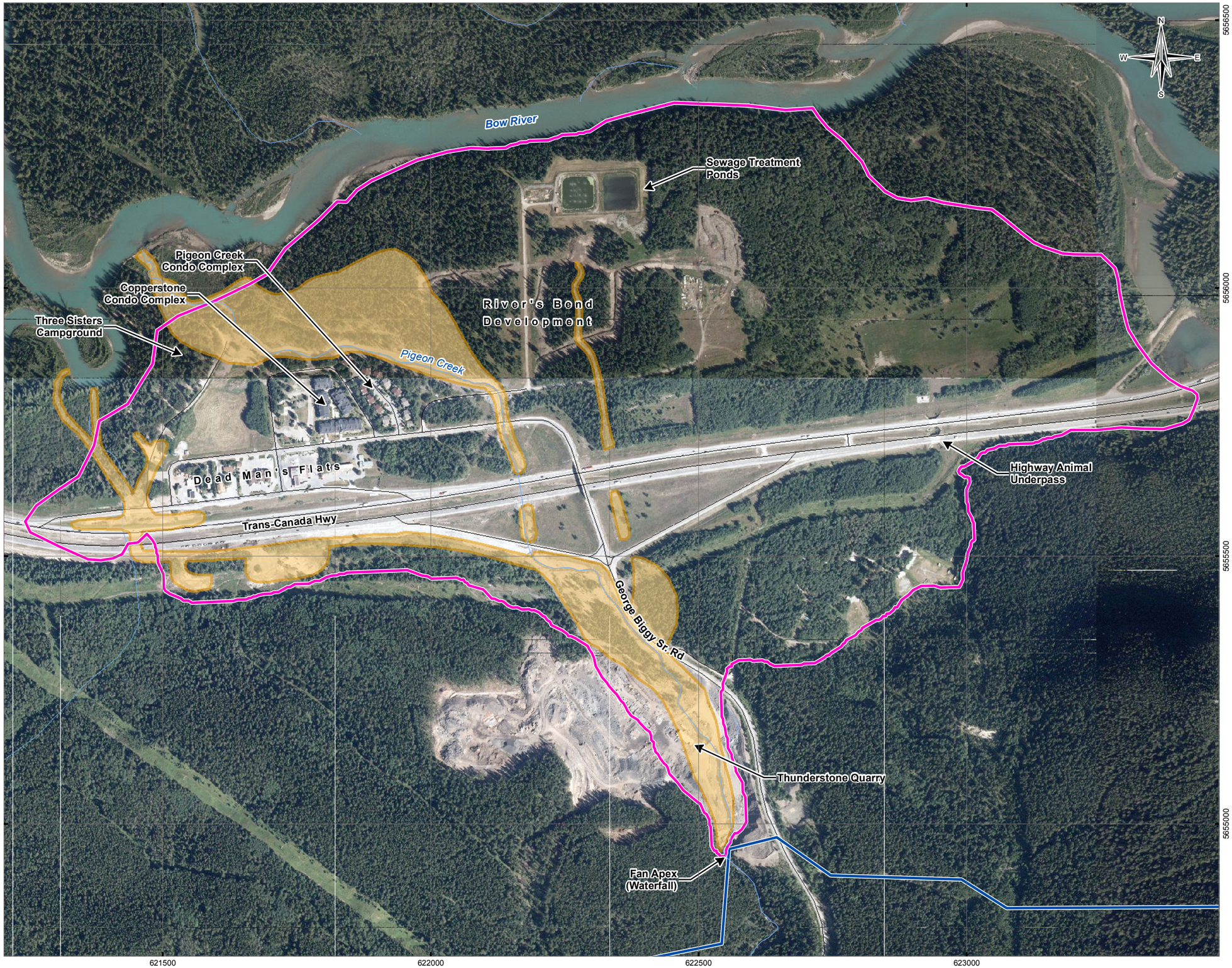

LEGEND

- Fan Inundation and Aggradation Area (0.198 km^2)
- Pigeon Creek Fan (1.47 km^2)
- Pigeon Creek Watershed
- Road
- Watercourse

NOTES
1. Base data source:
Imagery provided by Colbert Tam.
2. Impacted area based on post event field observations.

STATUS
ISSUED FOR USE

PIGEON CREEK HAZARD ASSESSMENT

June 2013 Event - Fan Inundation and Aggradation Impacted Area

PROJECTION UTM Zone 11	**DATUM** NAD83			**CLIENT** Town of CANMORE
Scale: 1:7,000 — 100 50 0 100 Metres				TETRA TECH EBA
FILE NO. V13203145-01_Figure04-3_DebrisExtent.mxd				
PROJECT NO. V13203145-01	**DWN** SL	**CKD** MEZ	**APVD** JS	**REV** 0
OFFICE Tt EBA-VANC	**DATE** December 2016			**Figure 4.3**

Q:\Vancouver\GIS\ENGINEERING\V13203145-01_PigeonCreek\Maps\HazardAssessment\V13203145-01_Figure04-3_DebrisExtent.mxd modified 12/8/2014 by stephanie.leusink

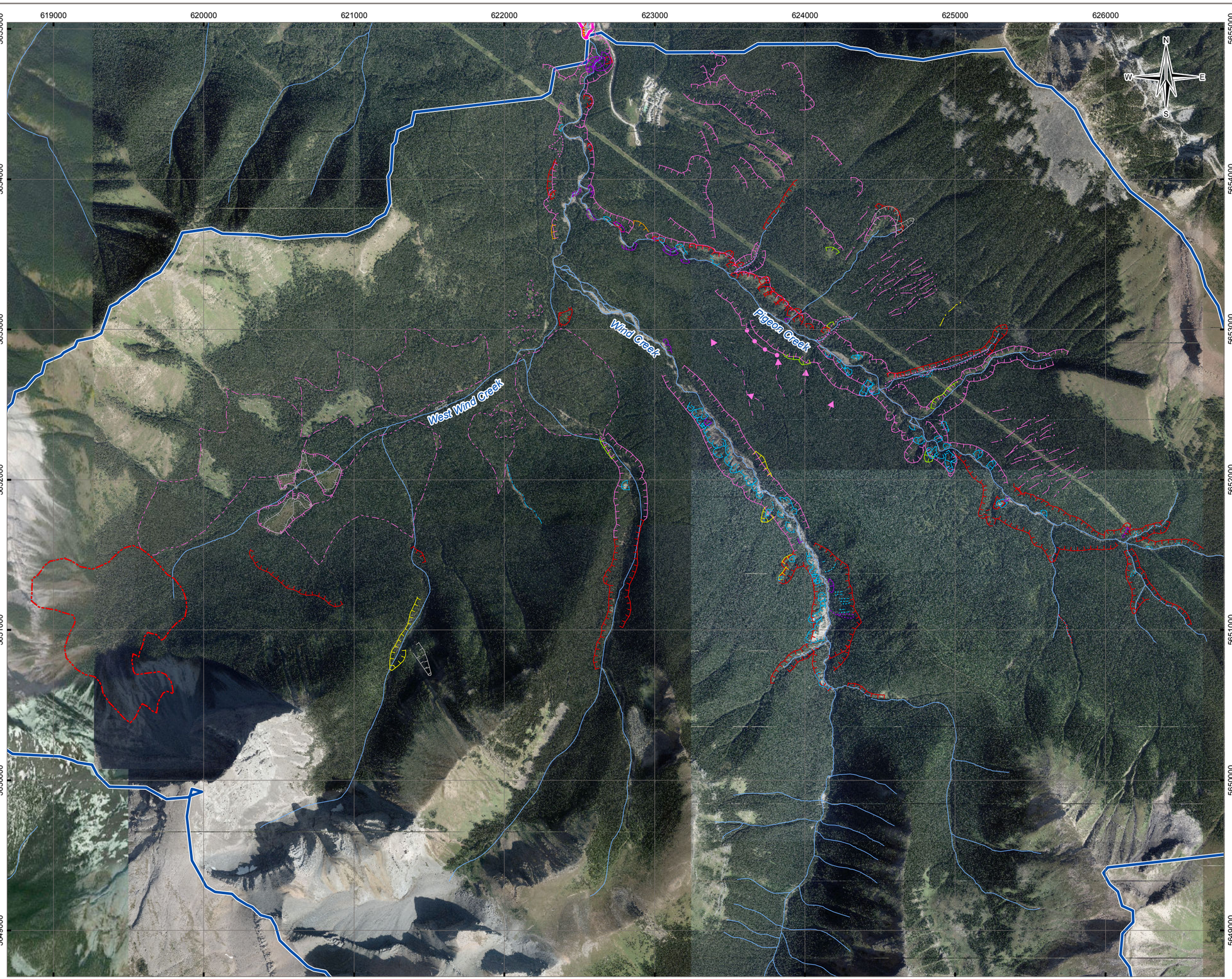

LEGEND

- Pigeon Creek Fan
- Pigeon Creek Watershed
- Watercourse

Geomorphic Feature

- Cleared Area
- Colluvial Blanket
- Colluvial Cone
- Debris Flood
- Debris Flow
- Debris Slide
- Deep-Seated Failure
- Drainage Path
- Log Jam
- Rill
- Rockfall
- Slide Block
- Tension Crack
- Wetland

Year

- 1950
- 1962
- 1972
- 1984
- 1997
- 2008
- 2013
- 2014

NOTES
1. Features identified through air photo interpretation and fieldwork.
Base data source:
Imagery provided by Colbert Tam.

STATUS
ISSUED FOR USE

PIGEON CREEK HAZARD ASSESSMENT

Geomorphic Features in the Watershed

PROJECTION UTM Zone 11	**DATUM** NAD83		**CLIENT** Town of CANMORE
Scale: 1:25,000 (400 200 0 400 Metres)			TETRA TECH EBA
FILE NO. V13203145-01_Figure05-1_WatershedGeomorph.mxd			
PROJECT NO. V13203145-01	**DWN** SL / **CKD** MEZ / **APVD** JS / **REV** 0		Figure 4.4
OFFICE Tt EBA-VANC	**DATE** December 2016		

Q:\Vancouver\GIS\ENGINEERING\V132\V13203145-01_PigeonCreek\Maps\HazardAssessment\V13203145-01_Figure05-1_WatershedGeomorph.mxd modified 12/8/2014 by stephanie.leusink

621500 622000 622500 623000

5656500 5656000 5655500 5655000

Pigeon Creek

N W E S

LEGEND

- Pigeon Creek Fan
- Pigeon Creek Watershed
- Watercourse

Geomorphic Feature

- Bow River Inundation Limit
- Cleared Area
- Debris Slide
- Deep-Seated Failure
- Fan Sediments
- Gravel Dyke
- New Road
- Old Channel
- Rockfall
- Slide Block

Year

- 1947
- 1950
- 1962
- 1972
- 1984
- 1997
- 2008
- 2013
- 2014

NOTES
1. Features identified through air photo interpretation and fieldwork.
Base data source:
Imagery provided by Colbert Tam.

STATUS
ISSUED FOR USE

PIGEON CREEK HAZARD ASSESSMENT

Geomorphic Features on the Fan

PROJECTION UTM Zone 11		**DATUM** NAD83		**CLIENT** Town of CANMORE
Scale: 1:7,000 — 100 50 0 100 — Metres				TETRA TECH EBA
FILE NO. V13203145-01_Figure05-2_FanGeo_RevA.mxd				
PROJECT NO. V13203145-01	**DWN** SL	**CKD** MEZ	**APVD** JS	**REV** 0
OFFICE Tt EBA-VANC	**DATE** December 2016			Figure 4.5

Q:\Vancouver\GIS\ENGINEERING\V132\V13203145-01_PigeonCreek\Maps\HazardAssessmentRevised\V13203145-01_Figure05-2_FanGeo_RevA.mxd modified 26/03/2015 by stephanie.leusink

621500 622000 622500

5656000 5655500 5655000

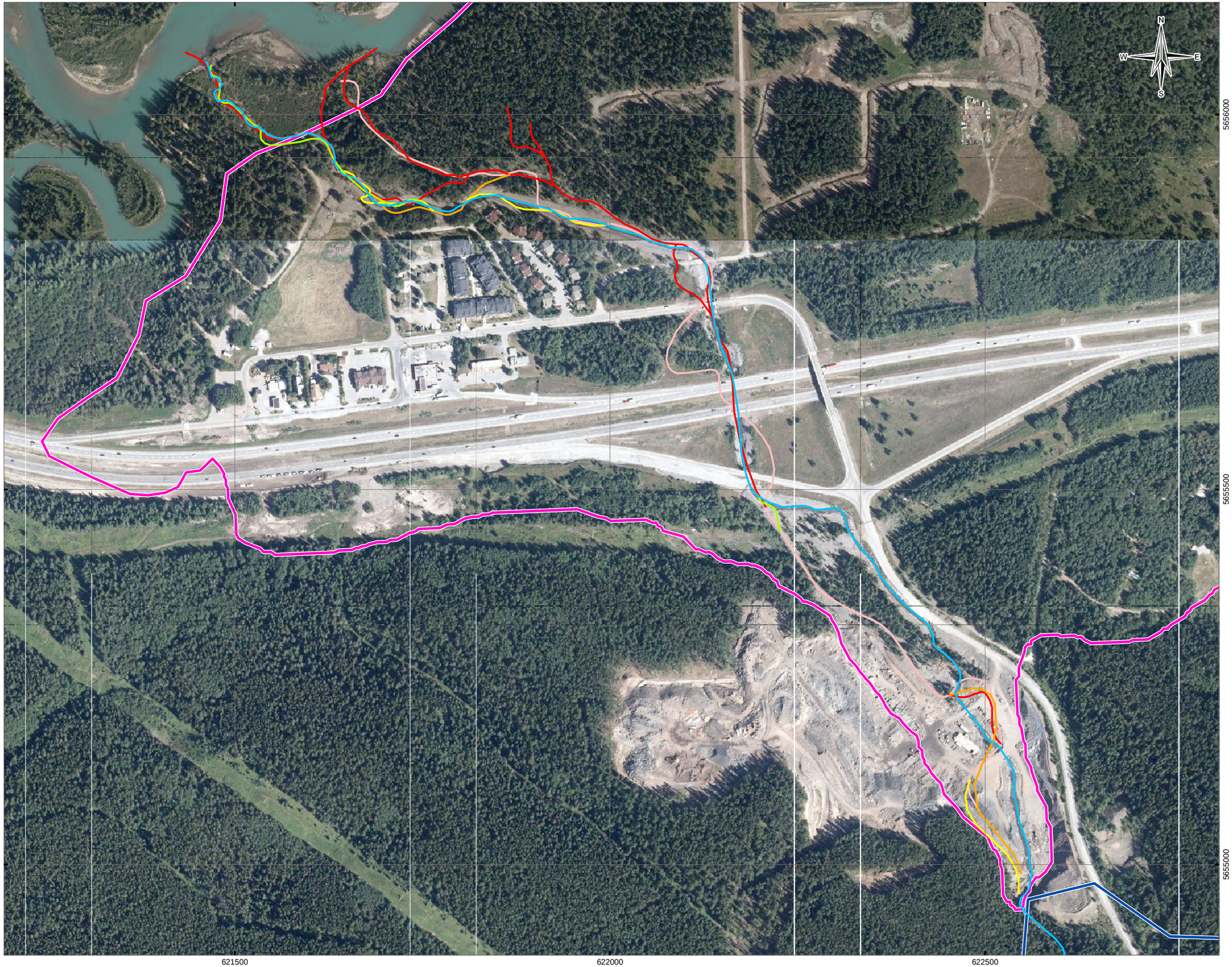

LEGEND

- Pigeon Creek Fan
- Pigeon Creek Watershed

Pigeon Creek Location

- 1947 (Pre Trans-Canada Hwy)
- 1962
- 1972
- 1984
- 1997
- 2013 (Post Flood)

NOTES

1. Features identified through air photo interpretation and fieldwork.
Base data source:
Imagery provided by Colbert Tam.

STATUS
ISSUED FOR USE

PIGEON CREEK HAZARD ASSESSMENT

Historic Alignments of Pigeon Creek on the Fan

PROJECTION UTM Zone 11			**DATUM** NAD83		**CLIENT** Town of CANMORE
Scale: 1:5,000 100 50 0 100 Metres					TETRA TECH EBA
FILE NO. V13203145-01_Figure05-3_PigeonCrk_RevA.mxd					
PROJECT NO. V13203145-01	**DWN** SL	**CKD** MEZ	**APVD** JS	**REV** 0	Figure 4.6
OFFICE Tt EBA-VANC	**DATE** December 2016				

O:\Vancouver\GIS\ENGINEERING\V132\V13203145-01_PigeonCreek\Maps\HazardAssessment\Revised\V13203145-01_Figure05-3_PigeonCrk_RevA.mxd modified 26/03/2015 by stephanie.leusink

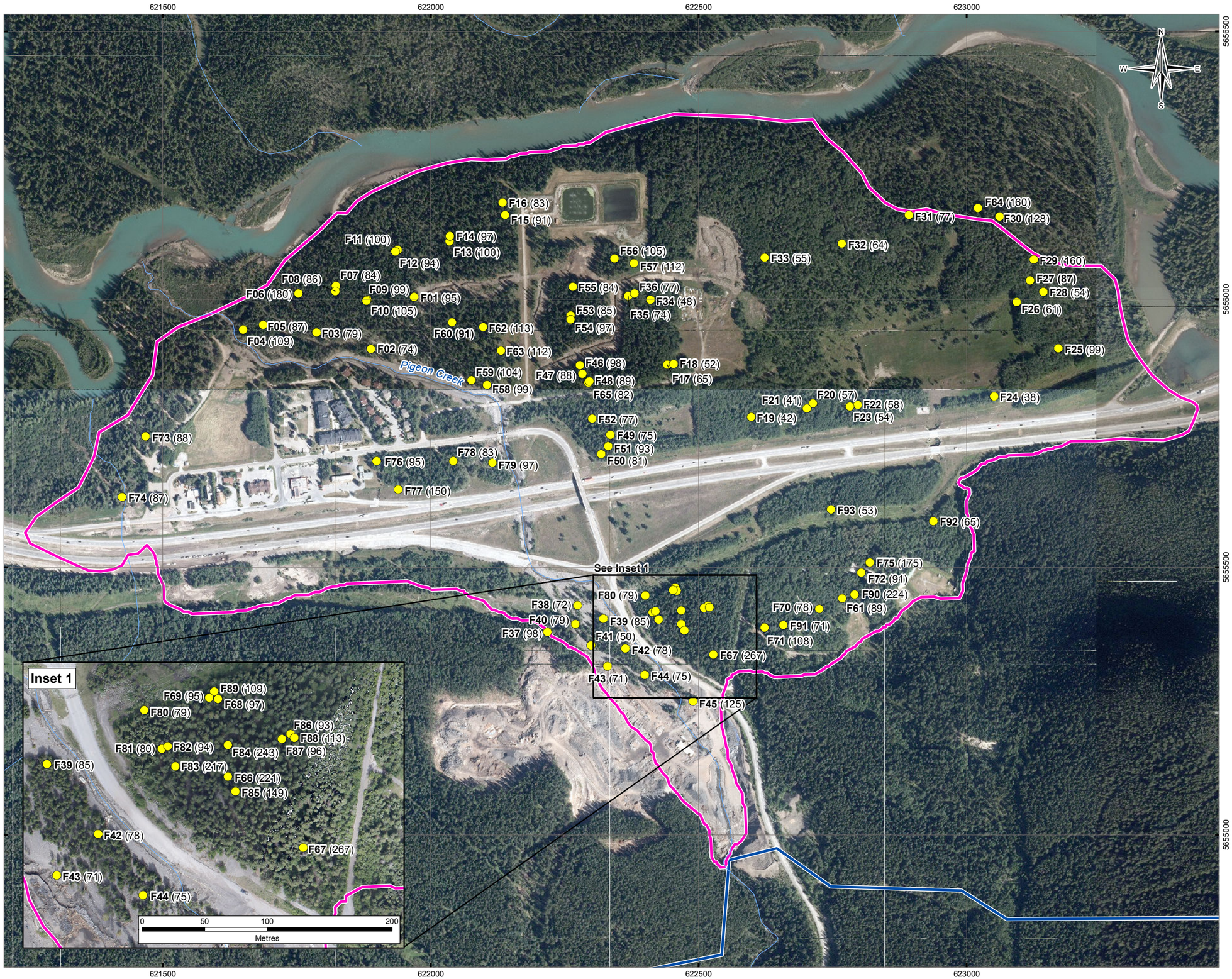

LEGEND

- Fan Tree Core (Age in years)
- Pigeon Creek Fan
- Pigeon Creek Watershed
- Watercourse

NOTES
Base data source:
Imagery provided by Colbert Tam.

STATUS
ISSUED FOR USE

PIGEON CREEK HAZARD ASSESSMENT

Tree Core Locations and Age on the Fan

PROJECTION	DATUM	CLIENT
UTM Zone 11	NAD83	Town of CANMORE

Scale: 1:7,000
100 50 0 100
Metres

TETRA TECH EBA

FILE NO.				
V13203145-01_Figure05-7_FanTreeCores.mxd				
PROJECT NO.	DWN	CKD	APVD	REV
V13203145-01	SL	MEZ	JS	0
OFFICE	DATE			
Tt EBA-VANC	December 2016			

Figure 4.7

Q:\Vancouver\GIS\ENGINEERING\V132\V13203145-01_PigeonCreek\Maps\HazardAssessment\V13203145-01_Figure05-7_FanTreeCores.mxd modified 12/8/2014 by stephanie.leusink

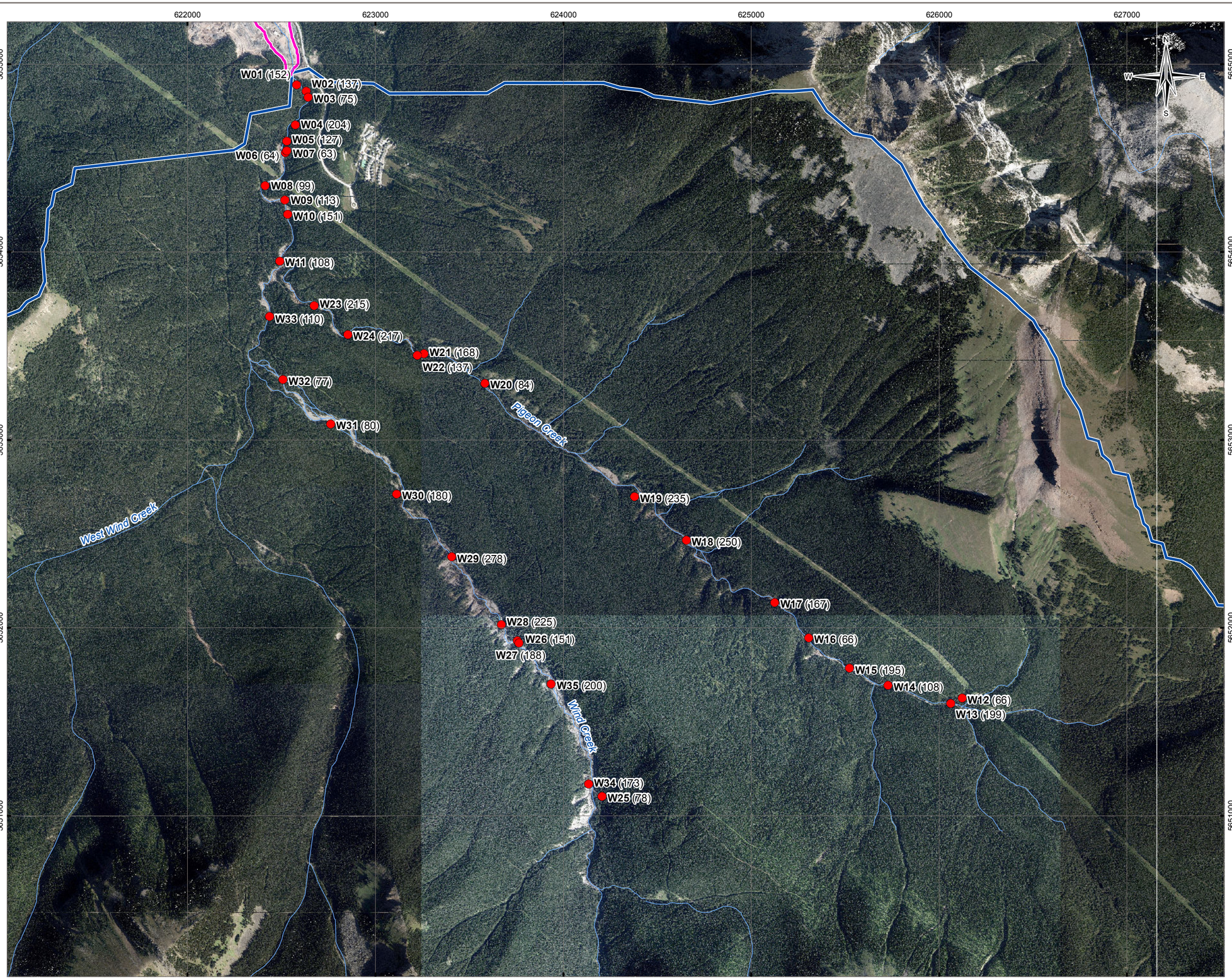

LEGEND

- Watershed Tree Core (Age in years)
- Pigeon Creek Fan
- Pigeon Creek Watershed
- Watercourse

NOTES
Base data source:
Imagery provided by Colbert Tam.

STATUS
ISSUED FOR USE

PIGEON CREEK HAZARD ASSESSMENT

Tree Core Locations and Age in the Watershed

PROJECTION UTM Zone 11	**DATUM** NAD83	**CLIENT** Town of CANMORE
Scale: 1:20,000 (400 200 0 400 Metres)		TETRA TECH EBA
FILE NO. V13203145-01_Figure05-8_WatershedTreeCores.mxd		
PROJECT NO. V13203145-01	**DWN** SL / **CKD** MEZ / **APVD** JS / **REV** 0	Figure 4.8
OFFICE Tt EBA-VANC	**DATE** December 2016	

Q:\Vancouver\GIS\ENGINEERING\V13\V13203145-01_PigeonCreek\Maps\HazardAssessment\V13203145-01_Figure05-8_WatershedTreeCores.mxd modified 12/8/2014 by stephanie.leusink

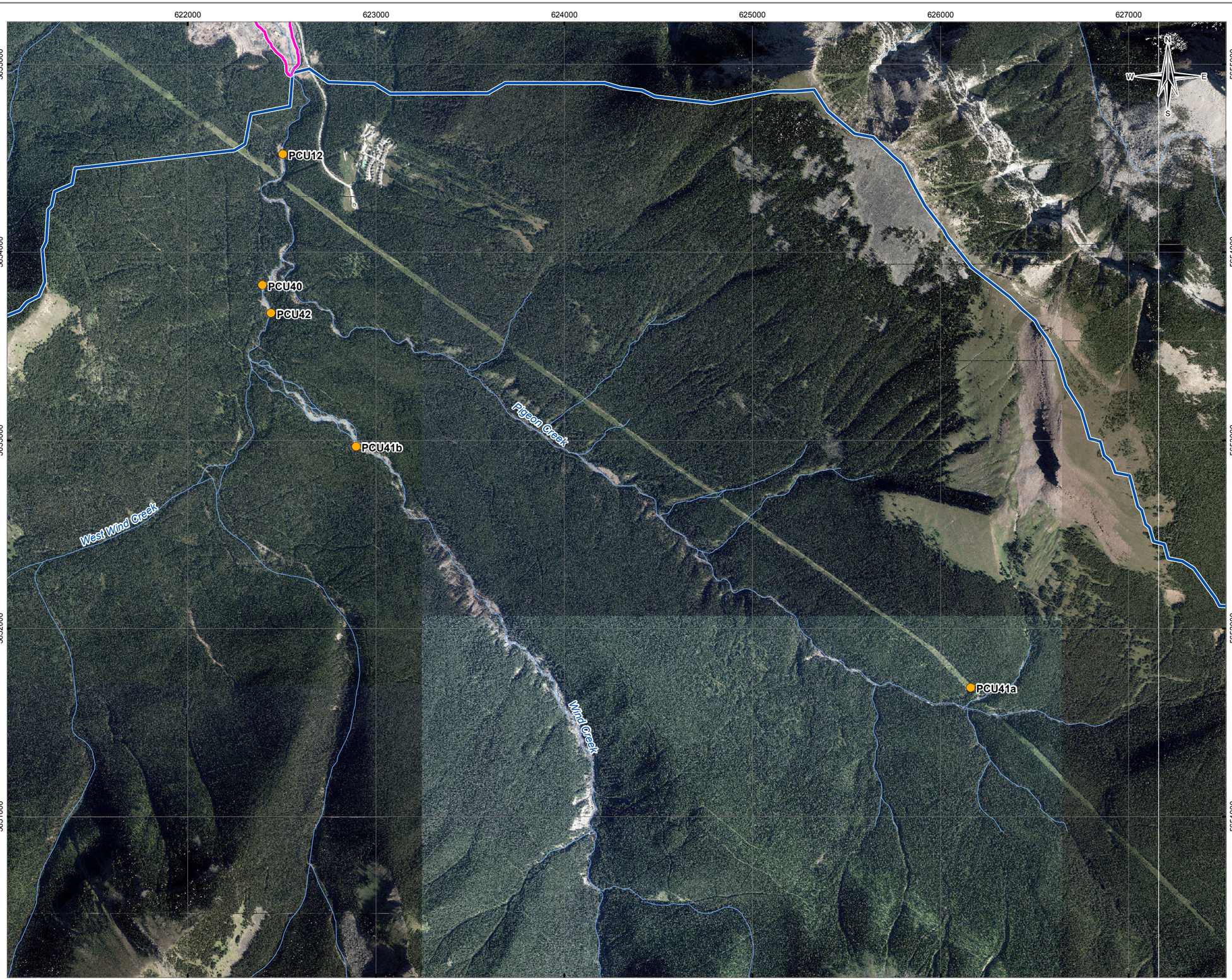

LEGEND

- Test Pit
- Pigeon Creek Fan
- Pigeon Creek Watershed
- Watercourse

NOTES
Base data source:
Imagery provided by Colbert Tam.

STATUS
ISSUED FOR USE

PIGEON CREEK HAZARD ASSESSMENT

Sampled Natural Exposure Site Locations in the Watershed

PROJECTION UTM Zone 11	**DATUM** NAD83	**CLIENT** Town of CANMORE
Scale: 1:20,000 — 400 200 0 400 Metres		TETRA TECH EBA
FILE NO. V13203145-01_Figure05-4_WatershedTestPits.mxd		
PROJECT NO. V13203145-01	**DWN** SL / **CKD** MEZ / **APVD** JS / **REV** 0	Figure 4.11
OFFICE Tt EBA-VANC	**DATE** December 2016	

Q:\Vancouver\GIS\ENGINEERING\V13\V13203145-01_PigeonCreek\Maps\HazardAssessment\V13203145-01_Figure05-4_WatershedTestPits.mxd modified 12/8/2014 by stephanie.leusink

621500 622000 622500 623000

5656500 5656000 5655500 5655000

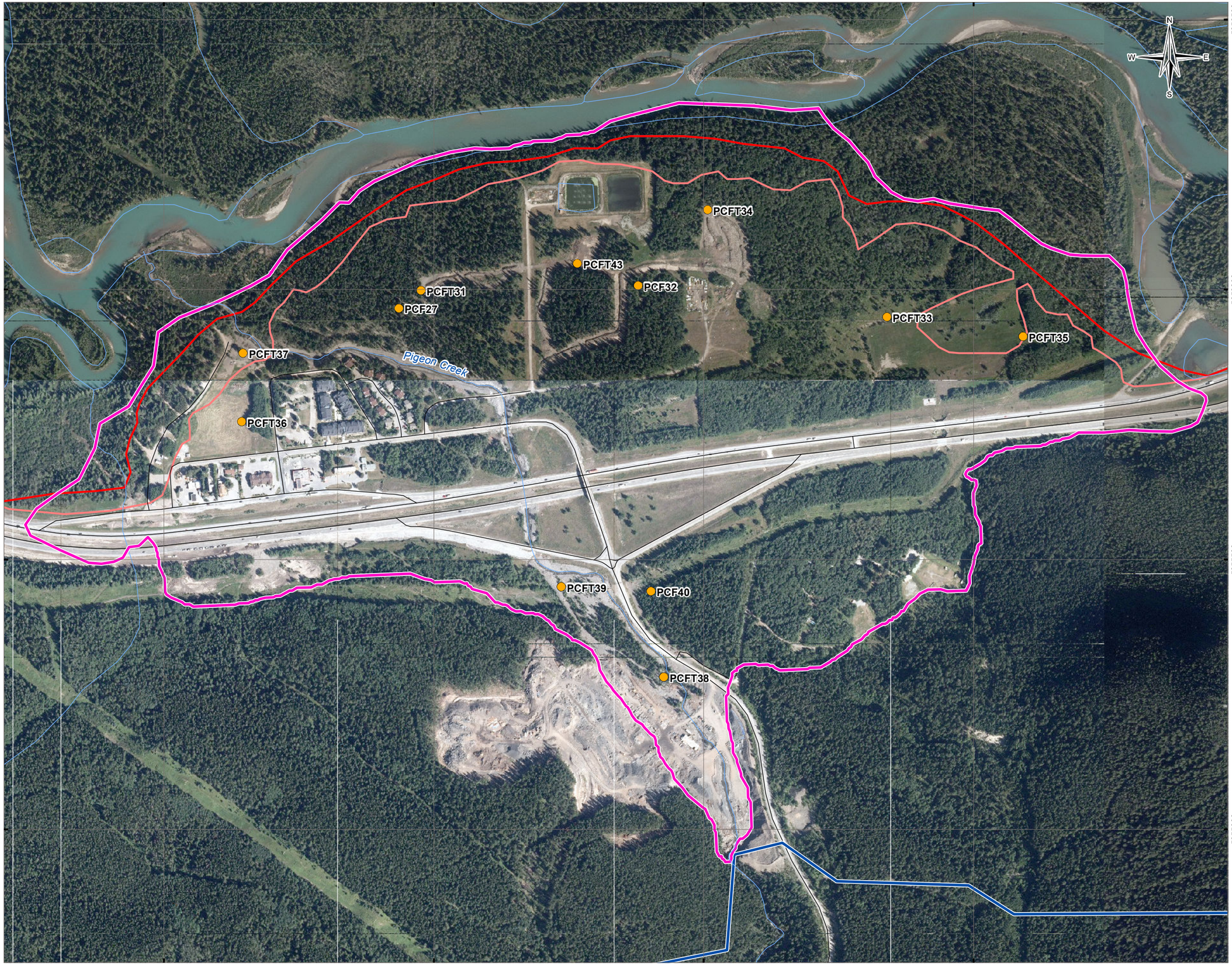

LEGEND

- Test Pit
- Pigeon Creek Fan
- Pigeon Creek Watershed
- Bow River Flood Fringe
- Bow River Floodway
- Road
- Watercourse
- Waterbody

Flood Fringe: The portion of the flood hazard area outside of the floodway. Water in the flood fringe is generally shallower and flows more slowly than in the floodway. New development in the flood fringe may be permitted in some communities and should be flood-proofed.

Floodway: The portion of the flood hazard area where flows are deepest, fastest and most destructive. The floodway typically includes the main channel of a stream and a portion of the adjacent overbank area. New development is discouraged in the floodway.

NOTES
Base data source:
Floodway and Flood Fringe are digitized from http://esrd.alberta.ca/water/programs-and-services/flood-hazard-identification-program/flood-hazard-mapping.aspx/
Imagery provided by Colbert Tam.

STATUS
ISSUED FOR USE

PIGEON CREEK HAZARD ASSESSMENT

Sampled Test Pit and Exposure Locations on the Fan

PROJECTION UTM Zone 11		**DATUM** NAD83		**CLIENT** Town of CANMORE
Scale: 1:7,000 100 50 0 100 Metres				TETRA TECH EBA
FILE NO. V13203145-01_Figure05-5_FanTestPits.mxd				
PROJECT NO. V13203145-01	**DWN** SL	**CKD** MEZ	**APVD** JS	**REV** 0
OFFICE Tt EBA-VANC	**DATE** December 2016			Figure 4.12

Q:\Vancouver\GIS\ENGINEERING\V13203145-01_PigeonCreek\Maps\HazardAssessment\V13203145-01_Figure05-5_FanTestPits.mxd modified 12/8/2014 by stephanie.leusink

621000 621500 622000 622500 623000 623500 624000

5656500 5656000 5655500 5655000 5654500 5654000

Sample	Depth (m bgs)	Age (^{14}C Yrs)
PCFTR34a	1.26	1820 +/- 30 BP

Sample	Depth (m bgs)	Age (^{14}C Yrs)
PCFTR43a	1.61	880 +/- 30 BP
PCFTR43b	2.18	1260 +/- 30 BP

Sample	Depth (m bgs)	Age (^{14}C Yrs)
PCFTR33b	3.69	3280 +/- 30 BP
PCFTR33d	4.81	3430 +/- 30 BP

Sample	Depth (m bgs)	Age (^{14}C Yrs)
PCFTR31b	1.25	520 +/- 30 BP
PCFTR31c	4.1	870 +/- 30 BP

Sample	Depth (m bgs)	Age (^{14}C Yrs)
PCFR27	0.83	210 +/- 30 BP

Sample	Depth (m bgs)	Age (^{14}C Yrs)
PCFTR36b	1.58	850 +/- 30 BP
PCFTR36c	4.06	14380 +/- 50 BP

Sample	Depth (m bgs)	Age (^{14}C Yrs)
PCFTR35a	2.25	2520 +/- 30 BP
PCFTR35b	2.47	3780 +/- 30 BP
PCFTR35c	2.57	2510 +/- 30 BP
PCFTR35d	5.99	2890 +/- 30 BP

Sample	Depth (m bgs)	Age (^{14}C Yrs)
PCFTR38	2.51	modern

Sample	Depth (m bgs)	Age (^{14}C Yrs)
PCUR13	1.17	90 +/- 30 BP

Sample	Depth (m bgs)	Age (^{14}C Yrs)
PCUR40	1.32	2010 +/- 30 BP

PCFT34 PCFT43 PCFT31 PCF27 PCFT33 PCFT35 PCFT36 PCFT38 PCU12 PCU40

Pigeon Creek

N W E S

LEGEND

- Radiocarbon Sample Site
- Pigeon Creek Fan
- Pigeon Creek Watershed
- Watercourse
- XXX Sites with Possible Coal Contamination
- XXX Sites Where Charcoal was Dated

NOTES
Base data source:
Imagery provided by Colbert Tam.

STATUS
ISSUED FOR USE

PIGEON CREEK HAZARD ASSESSMENT

Radiocarbon Samples on the Fan and Watershed

PROJECTION UTM Zone 11	**DATUM** NAD83			**CLIENT** Town of CANMORE
Scale: 1:12,000 — 200 100 0 200 Metres				TETRA TECH EBA
FILE NO. V13203145-01_Figure05-6_Radiocarbon.mxd				
PROJECT NO. V13203145-01	**DWN** SL	**CKD** MEZ	**APVD** JS	**REV** 0
OFFICE Tt EBA-VANC	**DATE** December 2016			Figure 4.13

Q:\Vancouver\GIS\ENGINEERING\V132\V13203145-01_PigeonCreek\Maps\HazardAssessment\V13203145-01_Figure05-6_Radiocarbon.mxd modified 12/8/2014 by stephanie.leusink

621500 622000 622500 623000

5656500 5656000 5655500 5655000

CeF - 04
CeF - 16
CeF - 05
CeF - 06
ChF - 18
ChF - 03
Pigeon Creek
CeF - 17
CeF - 07
CeF - 08
DEF - F15
DEF - 13
DEF - F14
EF - F12
EF - F10
EF - F11
EF - F09
ChF - F01
WF - 20
WF - 19
WF - 02
Qds - 02
Qds - 01
Qds - 13
Qds - 14
Qds - 12
Qs-10
Qs-07
Qs-03
Qs-08
Qs-09
Qs-11
Qs-04
Qs-06
Qs-05

N W E S

LEGEND

Difference Area Zone Polygon

Pigeon Creek Fan 2009-2013 Difference - (m)

- -10.01318359 - -8
- -7.99 - -4
- -3.99 - -2
- -1.99 - -1
- -0.99 - -0.7
- -0.7 - -0.5
- -0.5 - -0.4
- -0.4 - -0.3
- -0.3 - -0.25
- -0.25 - -0.2
- -0.2 - -0.15
- -0.15 - -0.1
- -0.09 - -0.05
- -0.05 - 0.05
- 0.05 - 0.1
- 0.10 - 0.15
- 0.15 - 0.2
- 0.2 - 0.25
- 0.25 - 0.3
- 0.3 - 0.4
- 0.4 - 0.5
- 0.5 - 0.7
- 0.7 - 1
- 1.01 - 2
- 2.01 - 4

Pigeon and Other Creek Location

- Pigeon Creek Floodplain, 1950
- Pigeon Creek delta, 1950
- Pigeon Creek delta, 1962
- Pigeon Creek delta, 1984
- Pigeon Creek delta, 2013
- Pigeon Creek, 1950
- Pigeon Creek, 1962
- Pigeon Creek, 1972
- Pigeon Creek, 1984
- Pigeon Creek, 1997
- Pigeon Creek, 2013
- other creek, 1972
- other creek, 2013
- other creek, 2014
- Pigeon Creek Fan
- Pigeon Creek Watershed

NOTES

Base data source:
1.Imagery provided by Colbert Tam.
2.2008 (Issued 2009) elevation data created from a compilation of xyz point cloud LiDAR data provided by Julia Eisl from theTown of Canmore, and 0.5m contour line CAD data provided by the Municipal District of Bighorn.
3.2013 elevation data created from single source of xyz point cloud LiDAR. The data encompassed both the boundaries of the Pigeon Creek Fan and Watershed.

STATUS
ISSUED FOR USE

PIGEON CREEK HAZARD ASSESSMENT

LiDAR derived DEM Elevation Difference Between 2008 and 2013 of Pigeon Creek Fan

PROJECTION	DATUM	CLIENT
UTM Zone 11	NAD83	TOWN OF CANMORE

Scale: 1:7,000
100 50 0 100
Metres

TETRA TECH EBA

FILE NO.
V13203145-01_Figure06-6_LiDAR_Comparison.mxd

PROJECT NO.	DWN	CKD	APVD	REV
V13203145-01	YL	MEZ	JS	0

OFFICE: Tt EBA-VANC
DATE: December 2016

Figure 5.14

Q:\Vancouver\GIS\ENGINEERING\V13203145-01_PigeonCreekMaps\HazardAssessment\V13203145-01_Figure06-6_LiDAR_Comparison.mxd modified 5/12/2015 by york.law

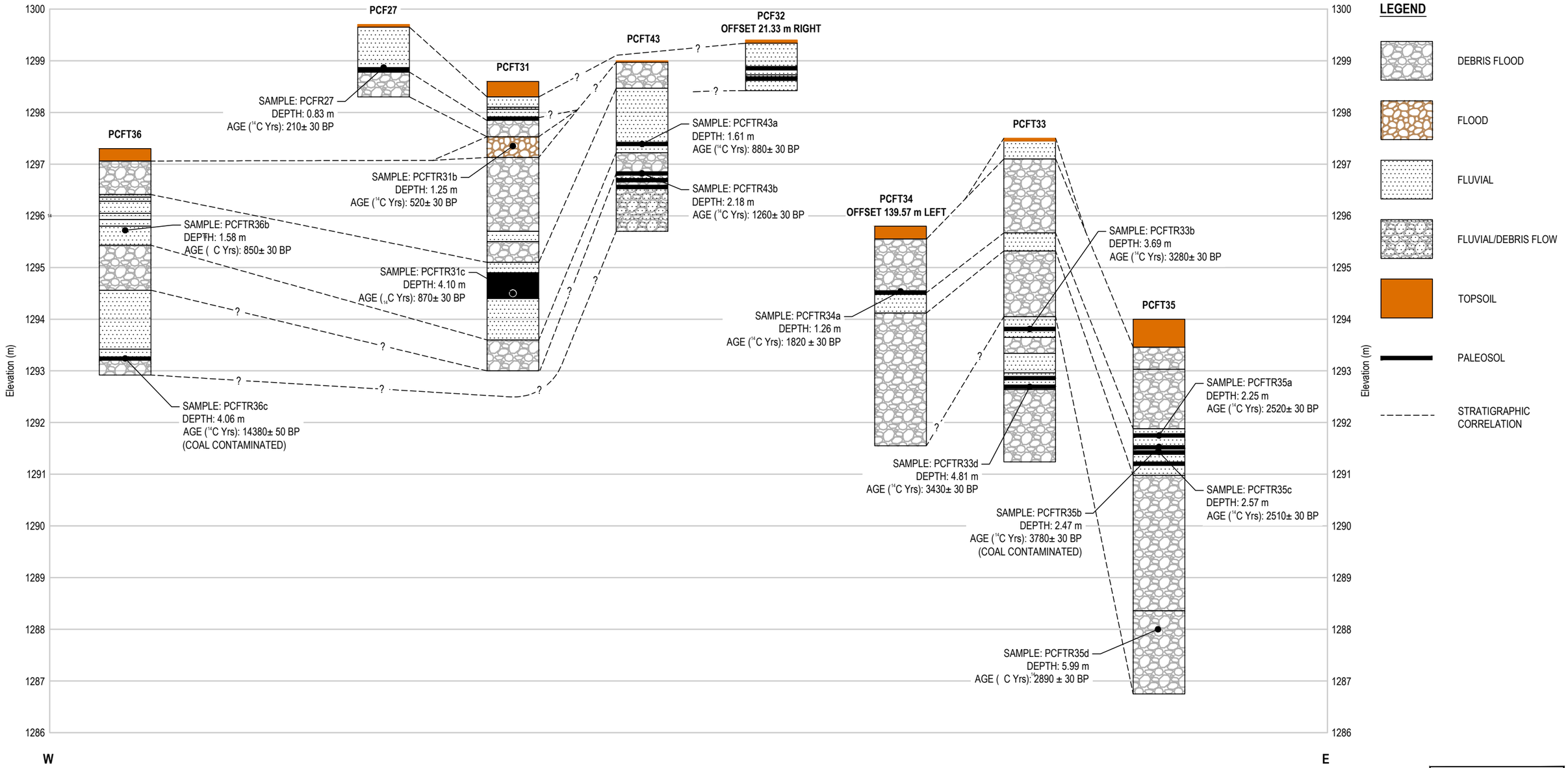

LOWER FAN PROFILE

ISSUED FOR USE

LEGEND

NOTES

NUM	DATE	DWN	CKD	APR	DESCRIPTION
0	25/03/15	JDM	MB	MB	ISSUED FOR REVIEW

REVISIONS

PROFESSIONAL SEAL

CLIENT

Town of CANMORE

TETRA TECH EBA

PIGEON CREEK HAZARD ASSESSMENT
MUNICIPAL DISTRICT OF BIGHORN, AB

TEST PIT PROFILES ON THE FAN
LOWER FAN

PROJECT NO.	OFFICE	DES	CKD	REV	DRAWING
V13203145	VANC	SM	SM	1	Figure 5.15
DATE	SHEET No.	DWN	APP	STATUS	
December 2016	3 of 3	JDM/MM	MB	-	

\\eba.local\corp\VancouverEngineering\V132\Projects\V13203145 Pigeon Cr Hazard and Risk\CAD\V13203145 - Pigeon Creek Test Pit Profiles_R1.dwg [FIGURE 5.7] April 15, 2015 - 9:26:56 am (BY: MARSH, MAUREEN)

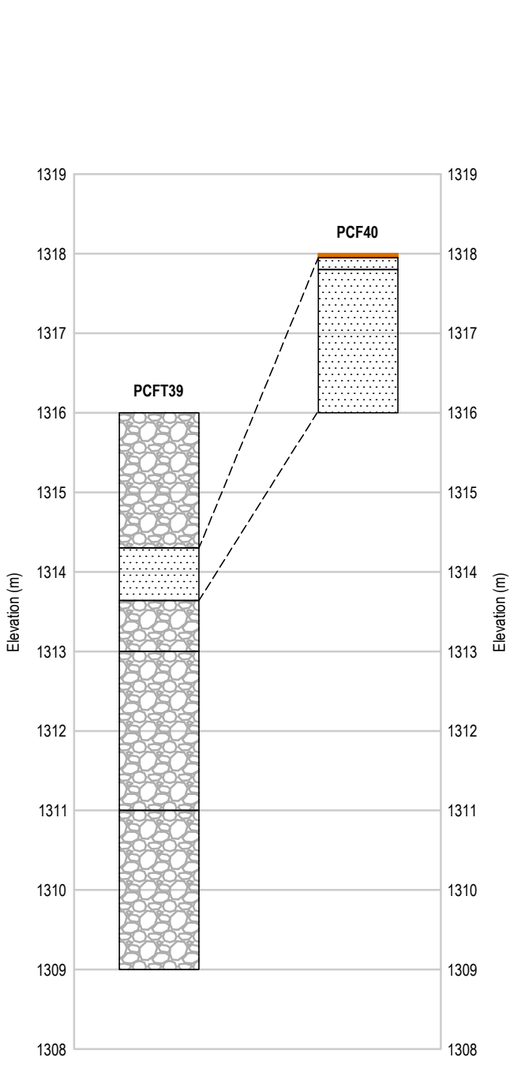

UPPER FAN PROFILE

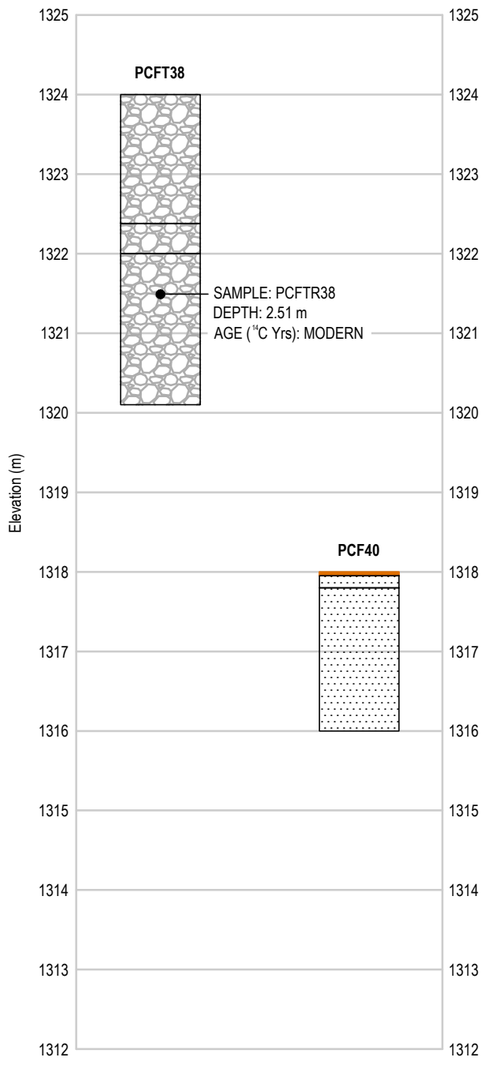

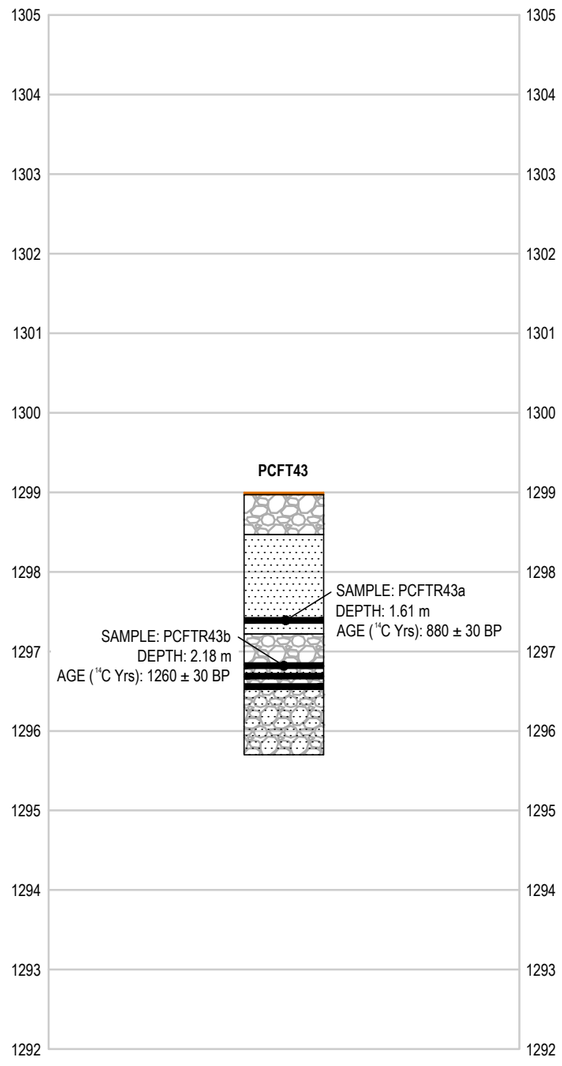

NORTH - SOUTH PROFILE

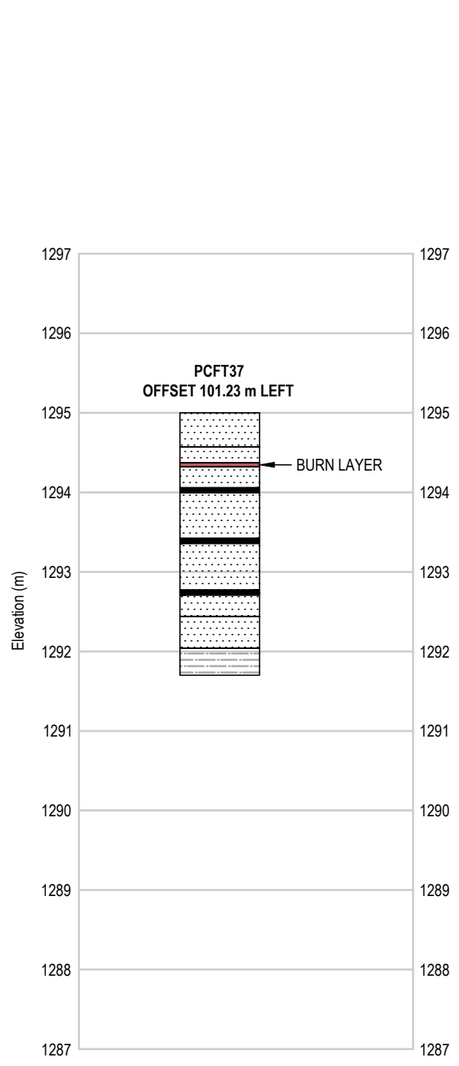

BOW RIVER DEPOSITS

LEGEND

- DEBRIS FLOOD
- FLUVIAL
- FLUVIAL/DEBRIS FLOW
- GLACIOLACUSTRINE
- TOPSOIL
- PALEOSOL
- STRATIGRAPHIC CORRELATION

ISSUED FOR USE

LEGEND

NOTES

NUM	DATE	DWN	CKD	APR	DESCRIPTION
0	25/03/15	JDM	MB	MB	ISSUED FOR REVIEW

REVISIONS

PROFESSIONAL SEAL

CLIENT

Town of CANMORE

TETRA TECH EBA

PIGEON CREEK HAZARD ASSESSMENT
MUNICIPAL DISTRICT OF BIGHORN, AB

TEST PIT PROFILES ON THE FAN
UPPER FAN & NORTH - SOUTH

PROJECT NO.	OFFICE	DES	CKD	REV	DRAWING
V13203145	VANC	SM	SM	1	Figure 5.16
DATE	SHEET No.	DWN	APP	STATUS	
December 2016	2 of 3	JDM/MM	MB	-	

\\eba.local\corp\Vancouver\Engineering\V132\Projects\V13203145 Pigeon Cr Hazard and Risk\CAD\V13203145 - Pigeon Creek Test Pit Profiles_R1.dwg [FIGURE 5.8] April 15, 2015 - 9:22:30 am (BY: MARSH, MAUREEN)

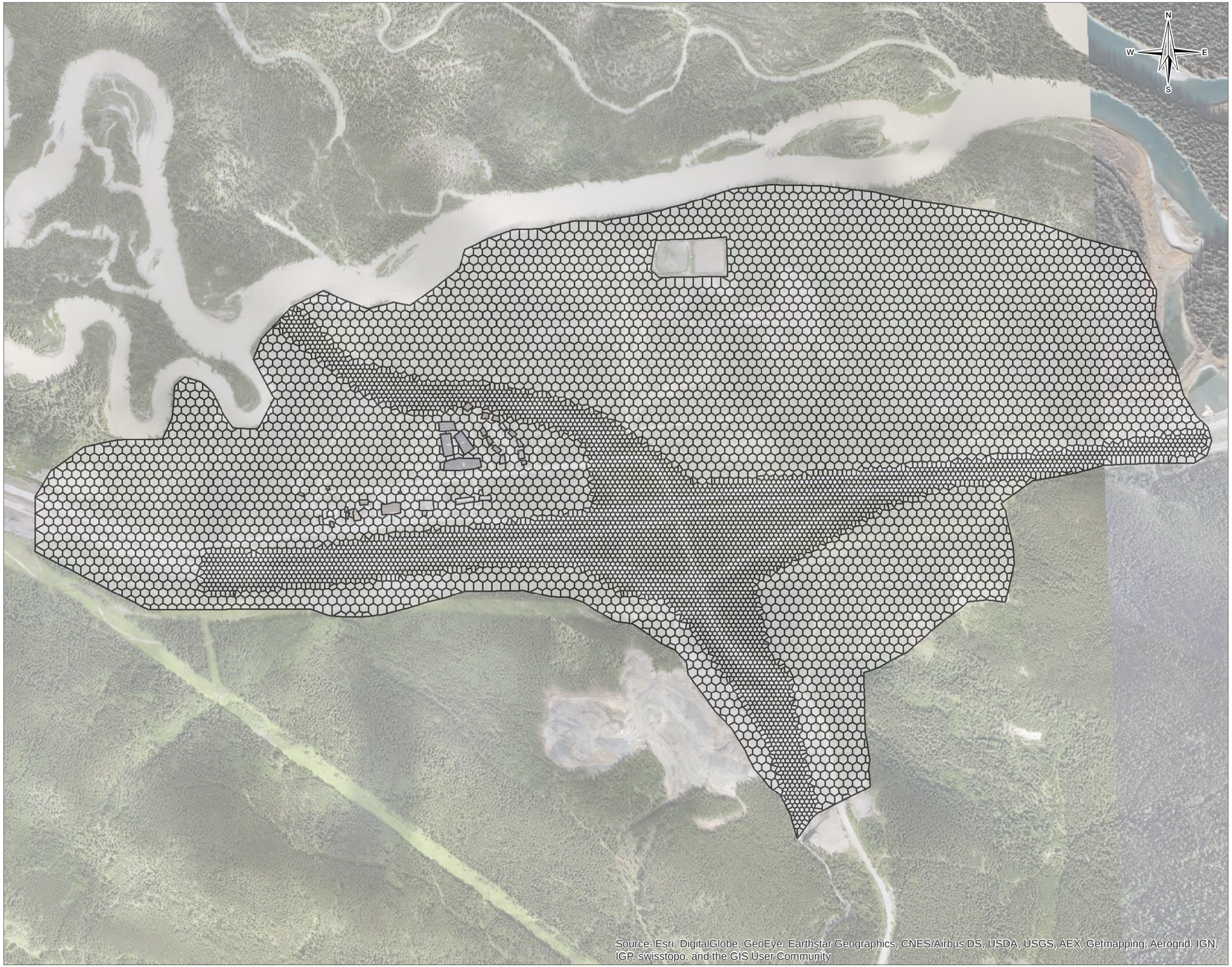

Mesh Grid

Mesh Grid

NOTES
1. Features identified through air photo interpretation and fieldwork.
Base data source:
Imagery provided by Colbert Tam.

STATUS
ISSUED FOR USE

PIGEON CREEK HAZARD ASSESSMENT

Mesh Grid used for Two-Dimensional Modeling

PROJECTION UTM Zone 11	**DATUM** NAD83	**CLIENT** Town of CANMORE
Scale: 1:8,000 — 100 50 0 100 — Metres		TETRA TECH EBA
FILE NO. V13203145-01_Figure9.1_2D-grid-PCSWMM.mxd		
PROJECT NO. V13203145-01	**DWN** MH / **CKD** MEZ / **APVD** DJ / **REV** 0	**Figure 9.1**
OFFICE Tt EBA-VANC	**DATE** December 2016	

Q:\Vancouver\Engineering\V132\Projects\V13203145 Pigeon Cr Hazard and Risk\GIS\Report Figures\V13203145-01_Figure9.1_2D-grid-PCSWMM.mxd modified 1/31/2016 by mauricio.herrera

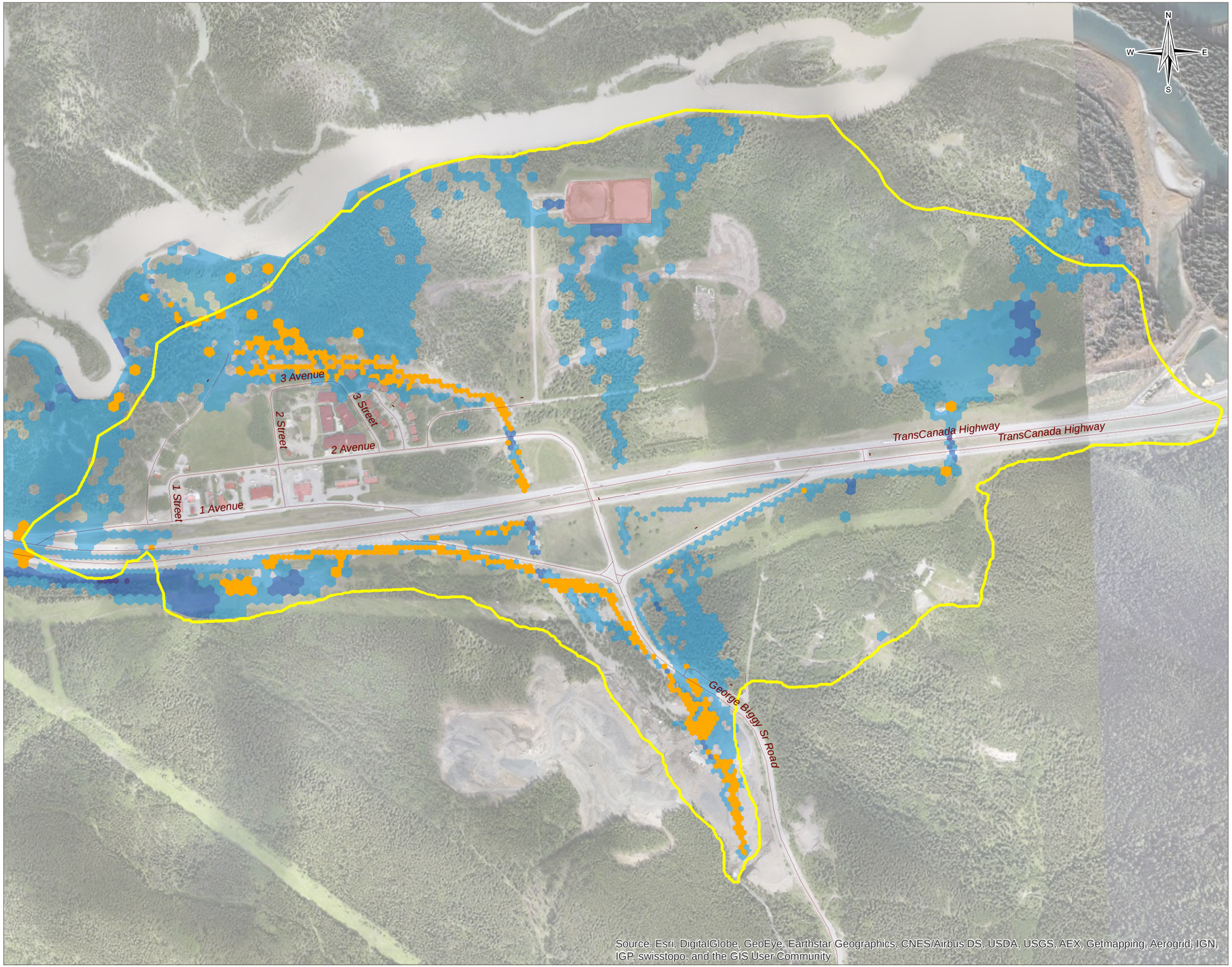

Flood Intensity (m²/s) (v>1m/s)

- Moderate
- High
- Extreme

Maximum Flow Depth (m) (v<1m/s)

- <1
- 1 - 2.5
- >2.5
- Pigeon Creek Fan
- Roads
- Buildings/Structures

STATUS
ISSUED FOR USE

PIGEON CREEK HAZARD ASSESSMENT

Flood Intensity and Flood Depth 10-30-yr Return Period

PROJECTION: UTM Zone 11	DATUM: NAD83			CLIENT: Town of CANMORE
Scale: 1:6,896 (100 50 0 100 Metres)				TETRA TECH EBA
FILE NO.: V13203145-01_Figure9.2_10-30yr flood intensity.mxd				
PROJECT NO.: V13203145-01	DWN: MH	CKD: MEZ	APVD: DJ	REV: 0
OFFICE: Tt EBA-VANC	DATE: December 2016			Figure 9.2

Q:\Vancouver\Engineering\V132\Projects\V13203145 Pigeon Cr Hazard and Risk\GIS\Report Figures\V13203145-01_Figure9.2_10-30yr flood intensity.mxd modified 1/31/2016 by mauricio.herrera

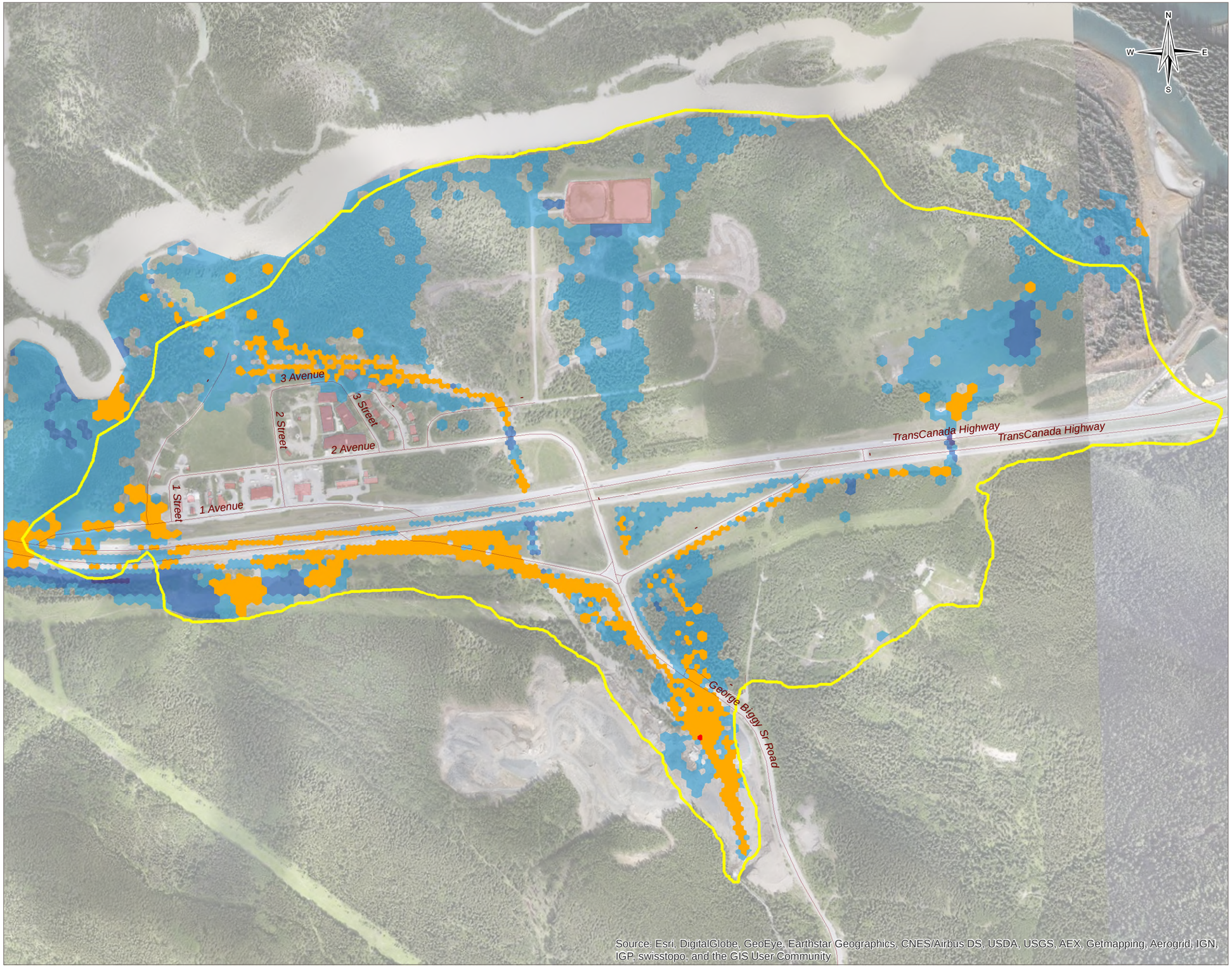

Flood Intensity (m²/s) (v>1m/s)

- Moderate
- High
- Extreme

Maximum Flow Depth (m) (v<1m/s)

- <1
- 1 - 2.5
- >2.5
- Pigeon Creek Fan
- Roads
- Buildings/Structures

STATUS
ISSUED FOR USE

PIGEON CREEK HAZARD ASSESSMENT

Flood Intensity and Flood Depth 30-100-yr Return Period

PROJECTION: UTM Zone 11				DATUM: NAD83	CLIENT: Town of CANMORE
Scale: 1:6,896 (100 50 0 100 Metres)					TETRA TECH EBA
FILE NO.: V13203145-01_Figure9.3_30-100yr flood intensity.mxd					
PROJECT NO.: V13203145-01	DWN: MH	CKD: MEZ	APVD: DJ	REV: 0	Figure 9.3
OFFICE: Tt EBA-VANC	DATE: December 2016				

Q:\Vancouver\Engineering\V132\Projects\V13203145 Pigeon Cr Hazard and Risk\GIS\Report Figures\V13203145-01_Figure9.3_30-100yr flood intensity.mxd modified 1/31/2016 by mauricio.herrera

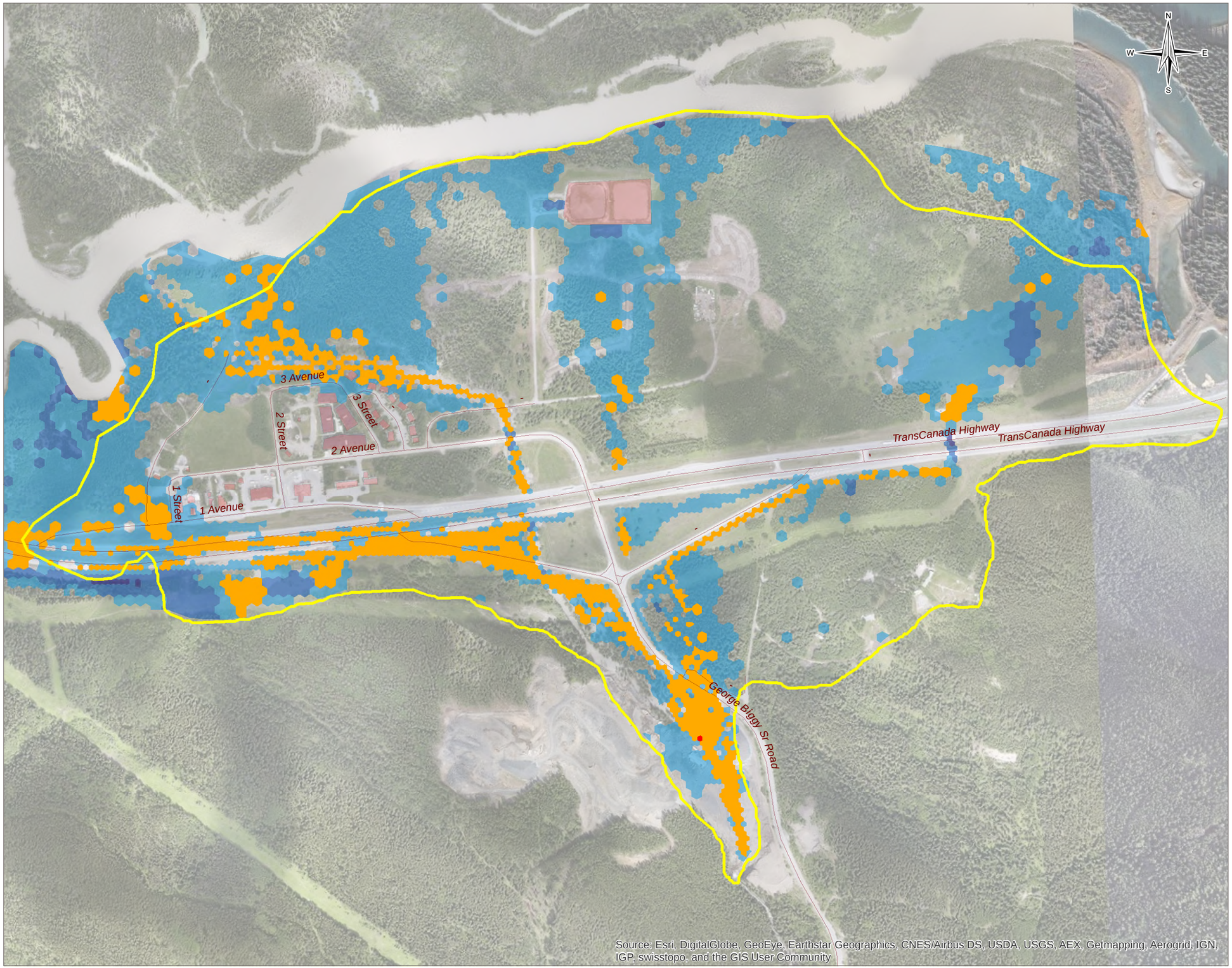

Flood Intensity (m²/s) (v>1m/s)

- Moderate
- High
- Extreme

Maximum Flow Depth (m) (v<1m/s)

- <1
- 1 - 2.5
- >2.5
- Pigeon Creek Fan
- Roads
- Buildings/Structures

STATUS
ISSUED FOR USE

PIGEON CREEK HAZARD ASSESSMENT

Flood Intensity and Flood Depth 100-300-yr Return Period

PROJECTION: UTM Zone 11	DATUM: NAD83			CLIENT: Town of CANMORE
Scale: 1:6,896 (100 50 0 100 Metres)				TETRA TECH EBA
FILE NO.: V13203145-01_Figure9.4_100-300 flood intensity.mxd				
PROJECT NO.: V13203145-01	DWN: MH	CKD: MEZ	APVD: DJ	REV: 0
OFFICE: Tt EBA-VANC	DATE: December 2016			Figure 9.4

Q:\Vancouver\Engineering\V132\Projects\V13203145 Pigeon Cr Hazard and Risk\GIS\Report Figures\V13203145-01_Figure9.4_100-300 flood intensity.mxd modified 1/31/2016 by mauricio.herrera

Flood Intensity (m²/s) (v>1m/s)

- Moderate
- High
- Extreme

Maximum Flow Depth (m) (v<1m/s)

- <1
- 1 - 2.5
- >2.5
- Pigeon Creek Fan
- Roads
- Buildings/Structures

STATUS
ISSUED FOR USE

PIGEON CREEK HAZARD ASSESSMENT

Flood Intensity and Flood Depth 300-1000-yr Return Period

PROJECTION: UTM Zone 11				DATUM: NAD83	CLIENT: Town of CANMORE
Scale: 1:6,896 (100 50 0 100 Metres)					TETRA TECH EBA
FILE NO.: V13203145-01_Figure9.5_300-1000yr flood intensity.mxd					
PROJECT NO.: V13203145-01	DWN: MH	CKD: MEZ	APVD: DJ	REV: 0	Figure 9.5
OFFICE: Tt EBA-VANC	DATE: December 2016				

Q:\Vancouver\Engineering\V132\Projects\V13203145 Pigeon Cr Hazard and Risk\GIS\Report Figures\V13203145-01_Figure9.5_300-1000yr flood intensity.mxd modified 1/31/2016 by mauricio.herrera

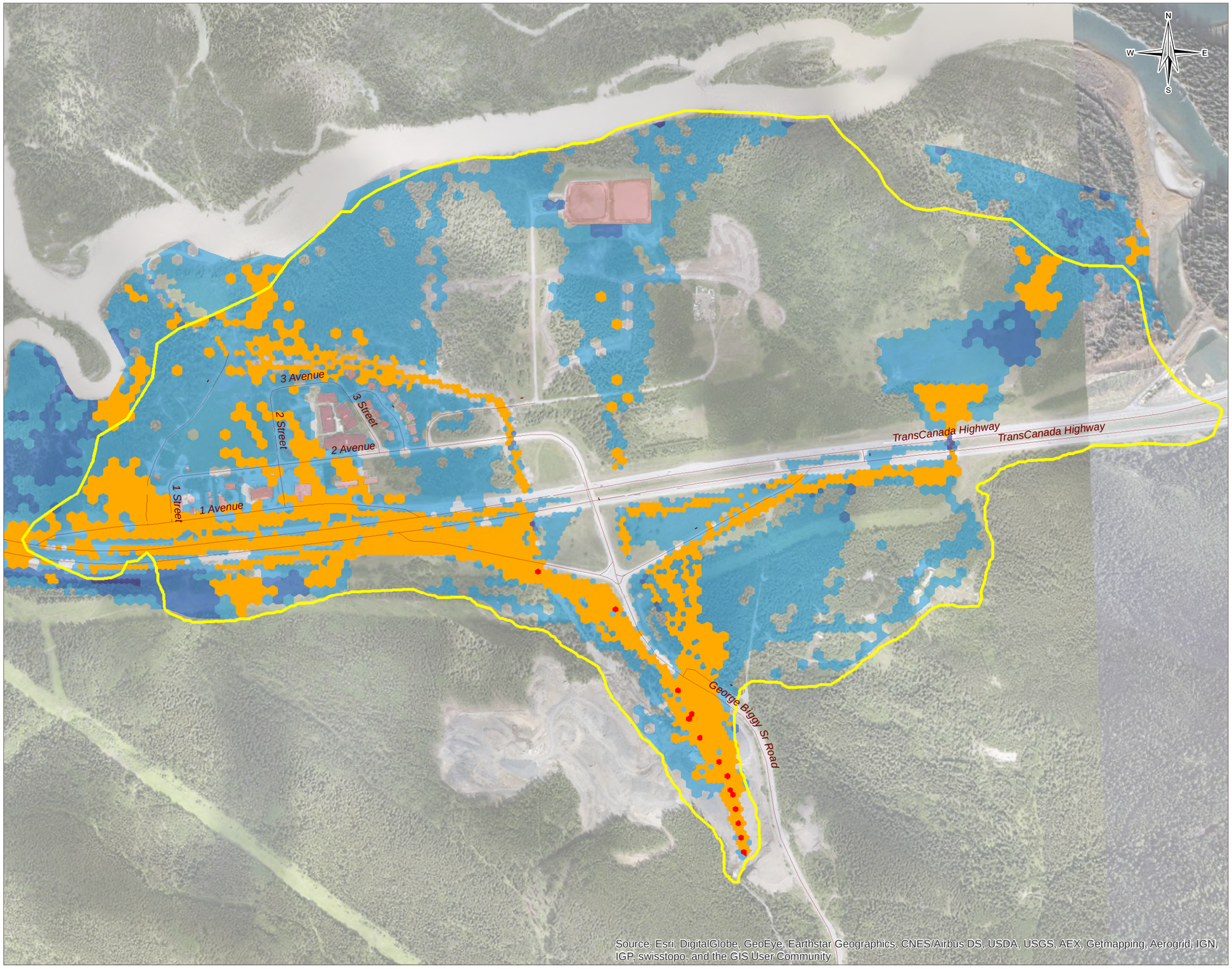

Flood Intensity (m²/s) (v>1m/s)

- Moderate
- High
- Extreme

Maximum Flow Depth (m) (v<1m/s)

- <1
- 1 - 2.5
- >2.5
- Pigeon Creek Fan
- Roads
- Buildings/Structures

STATUS
ISSUED FOR USE

PIGEON CREEK HAZARD ASSESSMENT

Flood Intensity and Flood Depth 1000-3000-yr Return Period

PROJECTION: UTM Zone 11	DATUM: NAD83				CLIENT: Town of CANMORE
Scale: 1:6,896 (100 50 0 100 Metres)					TETRA TECH EBA
FILE NO.: V13203145-01_Figure9.6_1000-3000yr flood intensity.mxd					
PROJECT NO.: V13203145-01	DWN: MH	CKD: MEZ	APVD: DJ	REV: 0	Figure 9.6
OFFICE: Tt EBA-VANC	DATE: December 2016				

Q:\Vancouver\Engineering\V132\Projects\V13203145 Pigeon Cr Hazard and Risk\GIS\Report Figures\V13203145-01_Figure9.6_1000-3000yr flood intensity.mxd modified 1/31/2016 by mauricio.herrera

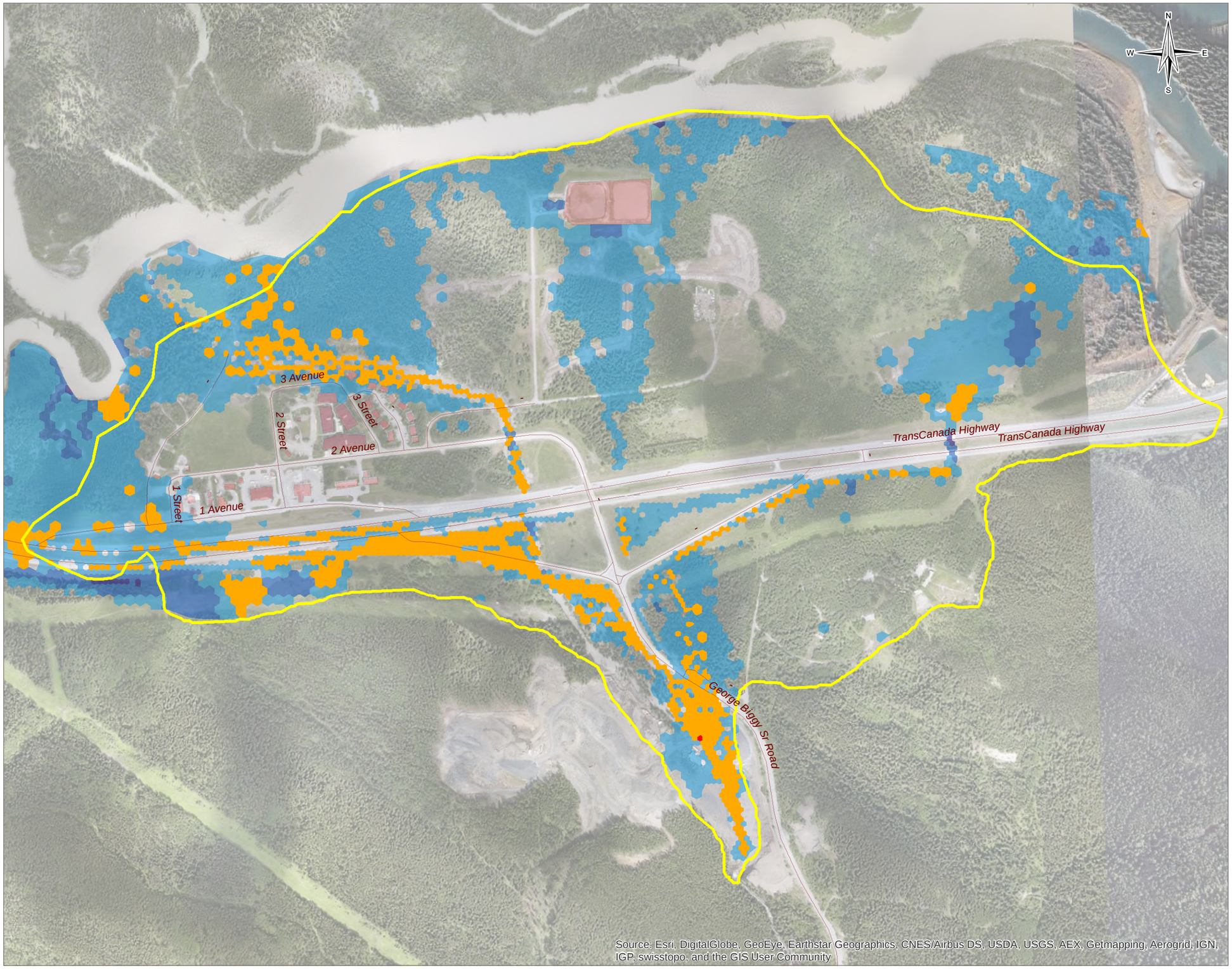

Flood Intensity (m²/s) (v>1m/s)

- Moderate
- High
- Extreme

Maximum Flow Depth (m) (v<1m/s)

- <1
- 1 - 2.5
- >2.5
- Pigeon Creek Fan
- Roads
- Buildings/Structures

STATUS
ISSUED FOR USE

PIGEON CREEK HAZARD ASSESSMENT

Flood Intensity and Flood Depth Event of June 19-21, 2013

PROJECTION: UTM Zone 11	DATUM: NAD83			CLIENT: Town of CANMORE
Scale: 1:6,896 (100 50 0 100 Metres)				TETRA TECH EBA
FILE NO.: V13203145-01_Figure9.7_2013 flood intensity.mxd				
PROJECT NO.: V13203145-01	DWN: MH	CKD: MEZ	APVD: DJ	REV: 0
OFFICE: Tt EBA-VANC	DATE: December 2016			Figure 9.7

Q:\Vancouver\Engineering\V132\Projects\V13203145 Pigeon Cr Hazard and Risk\GIS\Report Figures\V13203145-01_Figure9.7_2013 flood intensity.mxd modified 1/31/2016 by mauricio.herrera

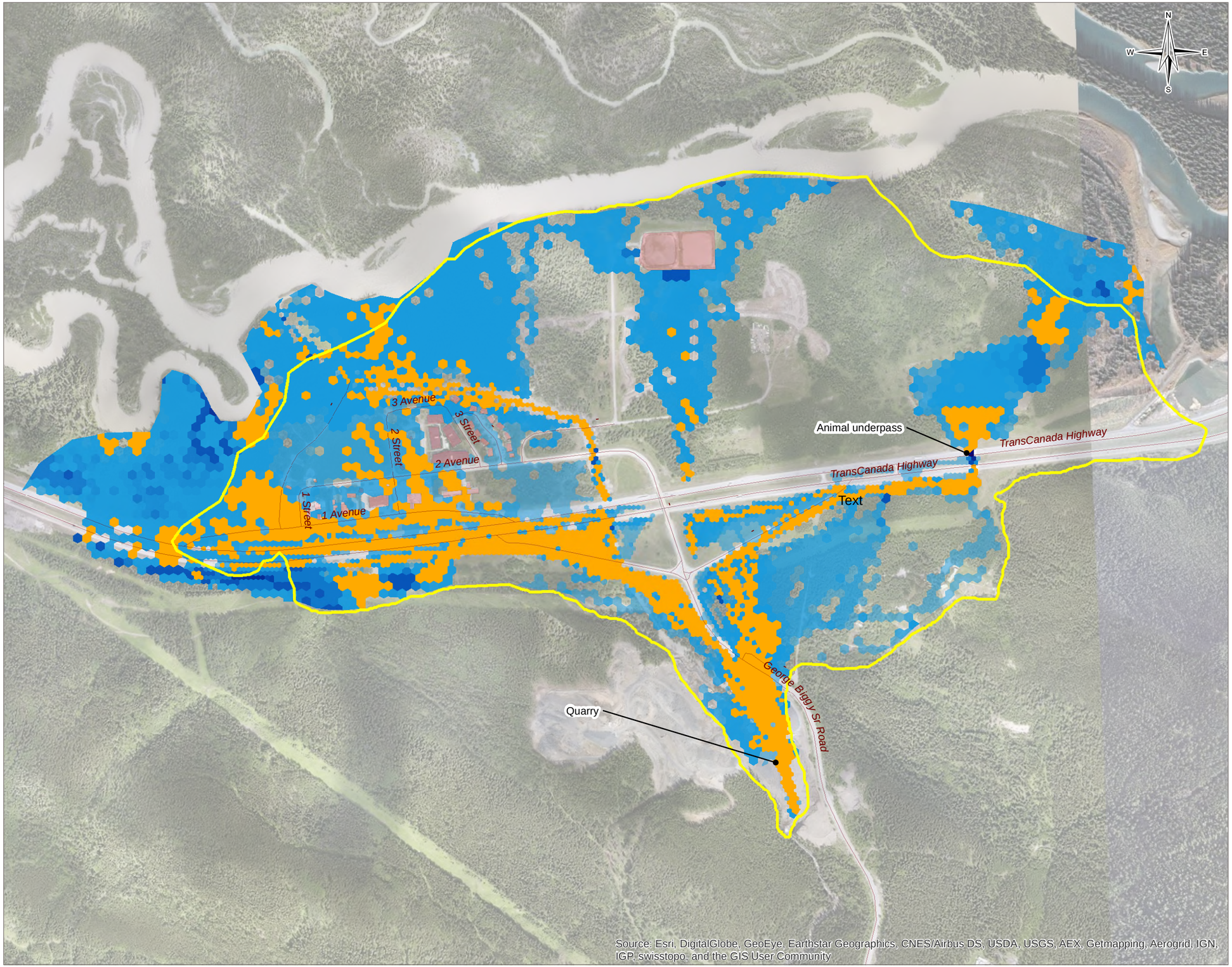

Flood Intensity

(m²/s) (v>1m/s)

- Moderate
- High
- Extreme

Maximum Flow Depth

(m) (v<1m/s)

- <1
- 1 - 2.5
- >2.5

STATUS
ISSUED FOR USE

PIGEON CREEK HAZARD ASSESSMENT

Composite Flood Intensity and Flood Depth

PROJECTION UTM Zone 11		DATUM NAD83				CLIENT Town of CANMORE
Scale: 1:8,000 100 50 0 100 Metres						TETRA TECH EBA
FILE NO. V13203145-01_Figure9.8_composite flood intensity.mxd						
PROJECT NO. V13203145-01	DWN MH	CKD MEZ	APVD DJ	REV 0		Figure 9.8
OFFICE Tt EBA-VANC	DATE December 2016					

Q:\Vancouver\Engineering\V132\Projects\V13203145 Pigeon Cr Hazard and Risk\GIS\Report Figures\V13203145-01_Figure9.8_composite flood intensity.mxd modified 1/31/2016 by mauricio.herrera

APPENDIX A
ENGINEERING REPORTS REVIEW

1.0 BGC 2013 MEMORANDUM

A preliminary hazard assessment for Pigeon Creek was provided by BGC Engineering Inc. (BGC 2013). The following is a summary of the report.

BGC conducted a visual inspection by helicopter as well as a limited foot traverse of the fan. They located and categorized damaged areas and did a preliminary debris flood frequency analysis by interpreting aerial photography from several years. Data from these studies was used to prepare conceptual risk reduction options for property damage and loss of life due to possible future debris floods.

The June 2013 flood event was categorized as a flood above the waterfall (which is located immediately south of Thunderstone limestone quarry) and a debris flood below it, mainly because aggregate from the quarry added to the flood's sediment load. Most of the damage to infrastructure occurred in the debris flood portion of the flood (in other words, on the fan). Sediment grain size was found to generally decrease downstream, but coarser deposits were identified in the larger fan channels.

The Pigeon Creek watershed provides abundant erodible sediment to the creek, which is incised into thick Pleistocene sediments above the waterfall. These sediments likely comprise till and glaciofluvial deposits, possibly underlain by glaciolacustrine units, as noted at Cougar Creek. Gully erosion, rotational slumps, skin flows and shallow translational slides are common in the watershed area. Extreme rainstorms are thus expected to continue to produce debris floods in the future.

The 2013 debris flood caused damage to quarry buildings, erosion of stockpiled aggregate due to straightening of the creek route, erosion of a fill slope at the edge of George Biggy Sr. Road, possible pipeline damage, ponding on the south side of the highway, damage of a bridge due to culvert blockage, and damage to a house by channel avulsion.

The air photo analysis showed that the waterfall formed because of gravel removal in the quarry after 1975 and that former channel positions that pre-date 1949 are evident. A large debris flood is suspected to have occurred during the 1923 flood event. The creek remained in a stable position after 1962, until the 2013 flood event. Deadman's Flat became developed between 1962 and 2008; infrastructure now includes residential areas, a campground, a resort, a sewage treatment plant and a small ski hill.

Mitigation options proposed include:

- Restoration of the original creek channel downstream of the quarry.
- Re-establishment of culvert capacity.
- Discouraging quarry operators from stockpiling aggregate on the creek floodplain or re-establishing the two 90º bends they created in the creek for this purpose.
  - Protect current stockpiles with riprap.
- Construction of a debris barrier or a series of debris flow nets upstream of the waterfall.
- Construction of a geomechanically reinforced soil berm within Thunderstone Quarry.
- Construction of setback dykes that allow for wider flood flow on the lower fan.

BGC also suggests that a detailed hazard assessment be conducted to determine flood/debris flood frequency and magnitude, followed by a risk assessment. This is the focus of the present study.

2.0 HELICOPTER RECONNAISSANCE, M. MILES AND ASSOCIATES

One day of aerial reconnaissance and two days of ground fieldwork were performed in snow conditions from November 30 to December 2, 2013 (Miles 2014a, 2014b). The objective of the study was to develop short term remediation options for the damage caused by the June 2013 flood. Photos from the ground work are shown in Miles (2014a), Volumes 1 and 2, while helicopter survey photos can be found in Miles (2014b).

The helicopter survey photos are of limited use due to the snow cover on the ground. The ground photos show the debris and damage in more detail.

2.1 Volume 1

Volume 1 contains a preface that gives an overview of what was found by all the studies. The following paragraph summarizes the preface.

The helicopter reconnaissance showed that slope instabilities and bank erosion were common in the upper watershed area. Sediment and woody debris blocked two culverts under the eastbound Highway 1 off-ramp, causing water to pond along the south side of the highway. It then flowed north across the highway into the western end of Deadman's Flats. Water also flowed under the eastern part of Highway 1 and spread laterally across the fan. One house in the west was damaged and the proposed River's Bend subdivision was flooded. Evidence of larger past floods on the fan highlights the need for protective structures in developed areas.

The ground reconnaissance in Volume 1 covers Pigeon Creek, extending from Bow River to Highway 1.

Sediments and woody debris fine downstream, from sandy pebble, cobble and boulder gravel and logs upstream of the pedestrian bridge to sticks and sandy pebble/cobble gravel, to fine sand, silt and wood chips near the confluence with the Bow River. Winter water flow in the channel appears to decrease downstream as well. Clasts appear to be very angular to subround in the photos. Wooden pallet and other industrial debris within the flood sediments have probably come from the limestone quarry.

Woody debris and sediment plastered on and around trees show flood water levels. Overbank flows were 0.3 to 0.5 m deep, less than 1 m near the pedestrian bridge, about 1 m upstream of the bridge and in the constructed berm area, and 2 m near the yellow house and the condominium development.

An older channel east of the constructed berm contains 1 to 1.5 m of flood deposits. Lichen-covered rocks show that the last flood event here was some time ago and that it was also a fairly large event.

There was a large, constructed berm near the housing and condo developments, which is evidently too small. Bends near housing and condos are riprapped. Bank erosion upstream of the proposed development exposes older sediments consisting of what appears to be sandy pebble/cobble gravel and sand beds. Eroded berm banks contain woody debris in places.

The wooden road bridge that survived the flood needs to be raised as flood sediments are quite close to the base of it. Near the highway and the reconstructed washed out road, riprap has been placed on the constructed berm; however more is needed. The washed out road has been rebuilt and two large, multi-plate culverts placed beneath it. The channel above the road repair has been excavated and the two culverts under Highway 1 were still being excavated at the time of fieldwork. Flood deposits were observed on top of the culvert outlet and on the highway median.

2.2 Volume 2

Volume 2 covers the area south of the highway to the waterfall, as well as an area immediately north of the highway on the western portion of the fan.

The Volume 2 ground photos show sediment-choked culverts, overtopped culverts, channel shifts, debris accumulations, undermined fence lines, eroded banks, a channel breach on the south side of the highway, and the eroded portions of George Biggy Senior Road. It is noted that woody debris is an important factor in the clogging of culverts.

An old channel east of George Biggy Sr. Road carried flood water about 1 m deep and passed under the highway via a culvert.

Just north of the highway, a fence shows a 1 m high water line and a 0.75 m debris line. Water from the south side highway diversion area appears to have flowed across the highway to this area as well as through the culverts. From there, it flowed through the campground before rejoining Pigeon Creek.

The majority of the sediment south of the highway is not quarry rock (Rundle Stone), but quarry rocks (crushed rock aggregate and spoil pile material) become more common in the flood deposits that are closer to the quarry. The flood deposits appear to comprise very angular to subround pebble to boulder gravel with some sand, as well as large pieces of woody debris (as shown in the photos). Within the quarry area, boulders up to 3 m in diameter and large trees have been moved.

Sediment ranges from 0.3 to 2 m thick, and is over 2 m thick immediately downstream of the waterfall. It is about 0.5 m thick in the quarry area.

One building in the quarry area has been heavily damaged by debris and a large spoil/overburden pile has been eroded. By December, 2013, a fair volume of spoil pile material had been replaced.

The waterfall itself sits in a water-carved bedrock channel. Wood and pebble, cobble and boulder gravel are abundant near its base. The flood deposits (with the exception of quarry rocks) appear to be derived from sources upstream of the waterfall.

2.3 Remedial Options

2.3.1 Short term

The main remediation option suggested is construction of an 800 m long channel on the fan. It should be protected with riprap between the two bridges, and raising the left berm to better protect existing houses would be a good option.

Other options include the following:

- Add riprap to some banks.
- Raise some banks.
- Clean out culverts.
- Excavate flood deposits in some areas.
- Do more detailed hazard investigations for River's Bend subdivision.
- Protect or move spoil bank.

2.3.2 Long term

For the long term, construction of at least one upstream sediment detention basin in the quarry area and/or the valley bottom south of Highway 1 is recommended. Mapping the flood deposits and calculating their volume will be necessary to estimate the appropriate size for the detention basin.

Other options include the following:

- Install debris control structures at some culverts.
- Reconfigure channels and re-establish pre-flood main channel alignment.
- Replace and raise bridge.
- Construct riprapped dyke at River's Bend subdivision.
- Move George Biggy Senior Road to the east, add riprap to bank.

APPENDIX B
TEST PIT NATURAL/MANMADE EXPOSURE LOGS

Test Pit	Date Completed	Method	UTM Coordinates		Elevation[1] (m asl)[2]	Max Depth[3] (m bgs)[4]
			Northing	Easting		
PCU12	20-Aug-14	Trowel	5654522	622504	1373	1.73
PCF27	21-Aug-14	Trowel	5655965	621935	1299	1.4
PCFT31	10-Sept-14	Excavator	5655998	621976	1299	5.6
PCF32	10-Sept-14	Shovel, Trowel	5656007	622378	1300	0.98
PCFT33	11-Sept-14	Excavator	5655949	622839	1297	6.26
PCFT34	11-Sept-14	Excavator	5656148	622507	1296	4.25
PCFT35	11-Sept-14	Excavator	5655905	623102	1294	7.25
PCFT36	12-Sept-14	Excavator	5655755	621644	1297	4.38
PCFT37	12-Sept-14	Excavator	5655882	621647	1295	3.3
PCFT38	12-Sept-14	Excavator	5655282	622426	1324	3.9
PCFT39	12-Sept-14	Excavator	5655449	622236	1317	7.0
PCF40	12-Sept-14	Shovel	5655441	622402	1316	2.0
PCU40	12-Sept-14	Trowel	5653825	622395	1398	1.42
PCU41a	13-Sept-14	Natural	5651687	626159	1705	3.4
PCU41b	13-Sept-14	Trowel	5652968	622893	1461	1.93
PCU42	14-Sept-14	Trowel	5653676	622441	1402	1.3
PCFT43	15-Sept-14	Excavator	5656048	622266	1299	3.3

Sample Legend[5]
◆ Organic

Notes:
1. Elevations are from LiDAR data
2. m asl – meters above sea level
3. Depth of trench or thickness of natural or manmade exposure
4. m bgs – meters below ground surface
5. Radiocarbon sample locations indicated on test trench and exposure photos are approximate and may not represent the actual location of the samples. Not all samples are shown in the photos.
6. *Pxxxx* – photo number

EXPOSURE PCU12

Date: 20 August, 2014
Location: 5654522 N 622504 E
Datum: UTM NAD 83
Elevation: 1373 m asl
Equipment: Trowel
Logged by: Shirley McCuaig, Jamie Stirling
Total Depth: 1.7 m (not recorded, approximate)

Depth From (m bgs)	Depth To (m bgs)	Lithologic Description
0	0.05	UNIT 1: TOPSOIL Forest floor and topsoil
0.05	0.9	UNIT 2: FLUVIAL Fine, medium and coarse sand laminations and thin beds
0.9	0.91	UNIT 3: PALEOSOL[1] Organic layer, contains needles, possibly tiny leaves; Sample PCUR12a
0.91	1.11	UNIT 4: FLUVIAL Beds of fine and coarse sand
1.11	1.12	UNIT 5: PALEOSOL Organic layer, same as above; Sample PCUR12b
1.12	1.17	UNIT 6: FLUVIAL Beds of fine and coarse sand
1.17	1.18	UNIT 7: PALEOSOL Organic layer, same as above; Sample PCUR12c; Sample PCUR13 is from a burnt log in wood-rich layer equivalent to this paleosol about 60 m to the south and at approximately same depth in exposure
1.18	1.5	UNIT 8: FLUVIAL Medium sand, thinly bedded
1.5	1.7	UNIT 9: DEBRIS FLOOD Pebble/cobble/boulder gravel

[1]Although listed as paleosols, most of these units are organic layers, not soils. They are listed as paleosols for ease of stratigraphic correlation.

Sample	Depth (m bgs)	Age (^{14}C Yrs)
PCUR13	1.17	90 +/- 30 BP

EXPOSURE PCF27

Date: 21 August, 2014
Location: Road cut exposure in new road area
Datum: UTM NAD 83
Elevation: 1299 m asl
Equipment: Trowel, shovel
Logged by: Shirley McCuaig, Jamie Stirling
Total Depth: 1.4 m (not recorded, approximate)

Depth From (m bgs)	Depth To (m bgs)	Lithologic Description
0	0.05	UNIT 1: TOPSOIL Forest floor
0.05	0.83	UNIT 2: FLUVIAL Well bedded sandy pebble gravel and fine sand
0.83	0.92	UNIT 3: PALEOSOL Layer containing at least four pieces of burnt wood. No evidence of fire or burnt wood in modern forest. Sample PCFR27 – wood and charcoal
0.92	1.4	UNIT 4: DEBRIS FLOOD Sandy pebble gravel

Sample	Depth (m bgs)	Age (^{14}C Yrs)
PCFR27	0.83	210 +/- 30 BP

TEST PIT PCFT31

Date: 10 September, 2014
Location: 5655998 N 621976 E
Datum: UTM NAD 83
Elevation: 1299 m asl
Equipment: Excavator
Logged by: Shirley McCuaig, Jamie Stirling, Mike Harvey, Renee Vandermause
Total Depth: 5.6 m (not recorded, approximate)

Depth From (m bgs)	Depth To (m bgs)	Lithologic Description
0	0.3	UNIT 1: TOPSOIL Forest floor and topsoil
0.3	0.5	UNIT 2: FLUVIAL Silty fine sand, sharp contact[2]
0.5	0.54	UNIT 3: FLUVIAL Sandy pebble gravel, matrix supported, sharp contact, subrounded to angular, Dmax=2 cm, Davg=1 cm
0.54	0.7	UNIT 4: FLUVIAL Fine sand, well sorted
0.7	0.74	UNIT 5: PALEOSOL Charcoal layer; Sample PCFTR31a
0.74	1.07	UNIT 6: DEBRIS FLOOD Sandy gravel, massive, matrix supported, 80% rounded to subrounded, sharp contact, Dmax=6 cm, Davg=2 cm
1.07	1.47	UNIT 7: FLOOD Sandy gravel, mainly clast supported, crudely bedded, some imbrication, irregular contact; 2 bone fragments at 1.25 m depth; SamplePCFTR31b
1.47	2.9	UNIT 8: DEBRIS FLOOD Sandy pebble to boulder gravel, matrix supported, coarse sand matrix, massive, Dmax=25 cm, clasts range from 3 to 25 cm, irregular contact
2.9	3.1	UNIT 9: FLUVIAL Sand, fine to medium grained
3.1	3.5	UNIT 10: DEBRIS FLOOD Sandy gravel, matrix supported, some clast support, rounded to angular, mostly subangular, sharp contact, Dmax=7 cm, Davg=2 cm
3.5	3.7	UNIT 11: FLUVIAL Silty fine sand, disseminated organics, silt/sand beds near base, sharp contact
3.7	4.2	UNIT 12: PALEOSOL Silt, organic with charcoal and wood fragments near top; Sample PCFTR31c

[2] All contacts described are lower contacts

4.2	5	UNIT 13: FLUVIAL Sand, silty, fine-grained, coarse-grained in upper 10 cm
5	5.6	UNIT 14: DEBRIS FLOOD Sandy gravel, matrix supported, rounded to subrounded, Dmax=3 cm, Davg=1 cm

Sample	Depth (m bgs)	Age (^{14}C Yrs)
PCFTR31b	1.25	520 +/- 30 BP
PCFTR31c	4.1	870 +/- 30 BP

EXPOSURE PCF32

Date: 10 September, 2014
Location: 5656007 N 622378 E
Datum: UTM NAD 83
Elevation: 1300 m asl
Equipment: Shovel and trowel
Logged by: Shirley McCuaig, Jamie Stirling, Mike Harvey, Renee Vandermause
Total Depth: 0.98 m (not recorded, approximate)

Depth From (m bgs)	Depth To (m bgs)	Lithologic Description
0	0.06	UNIT 1: TOPSOIL Forest floor moss
0.06	0.58	UNIT 2: FLUVIAL Silt, light and dark brown beds, 1 cm thick organic layer at 0.5; SamplePCFTR32a – a few bits of charcoal
0.58	0.67	UNIT 3A: FLUVIAL Fine sand, layer of 30% pebbles (Dmax=2 cm) in upper 3 cm
0.67	0.71	UNIT 3B: FLUVIAL Silt, medium brown
0.71	0.74	UNIT 4: PALEOSOL Paleosol, dark brown at top, pink brown below, a few burrows showing subaerial exposure, some charcoal; SamplePCFTR32b – paleosol: soil and some charcoal
0.74	0.98	UNIT 5: FLUVIAL Silt

TEST PIT PCFT33

Date: 11 September, 2014
Location: 5656007 N 622378 E
Equipment: Excavator
Elevation: 1297m asl
Logged by: Shirley McCuaig, Renee Vandermause
Total Depth: 6.26 m (not recorded, approximate)

Depth From (m bgs)	Depth To (m bgs)	Lithologic Description
0	0.05	UNIT 1: TOPSOIL
0.0	0.4	UNIT 2: FLUVIAL Silty fine sand, vague undulating bedding, lower 10 cm silt
0.4	1.83	UNIT 3: DEBRIS FLOOD Sandy gravel, matrix supported, clast supported lenses make up about 10% of unit, sharp contact, subrounded to angular, mainly subangular, 70% clasts, vague horizontal bedding, some imbrication, abundant pea gravel, Dmax=30 cm *P1364,5*
1.83	2.18	UNIT 4: FLUVIAL Silt, some sand (2 m wide lens up to 35 cm thick) *P1365 scale in lens unit*
2.18	3.45	UNIT 5: DEBRIS FLOOD Sandy gravel, same as Unit 2, 50% clasts, Dmax=15
3.45	3.85	UNIT 6: FLUVIAL/PALEOSOL Silt lens with trace clay, a few lenses of fine sand, thin organic layer at 3.62 m, Sample PCFTR33a; 1 cm thick organic layer at 3.69 m, Sample PCFTR33b, with burrows in soil above sampled material *(P1367-8)*
3.85	4.16	UNIT 7: DEBRIS FLOOD Sandy gravel, matrix supported, some clast support, 80% clasts, Dmax=10 cm, subrounded to subangular
4.16	4.54	UNIT 8: FLUVIAL Sand, fine to medium grained, crossbedded
4.54	4.86	UNIT 9: FLUVIAL/PALEOSOL Beds of clay, silt, fine sand, paleosols at 4.61 and 4.81 m; Samples PCFTR33c and d, respectively *(P1371-6)*
4.86	6.26	UNIT 10: DEBRIS FLOOD Sandy gravel, matrix supported, some clast support, subrounded to subangular, Dmax=30 cm, Davg=10 cm, hit water table *(P1377)*

Sample	Depth (m bgs)	Age (^{14}C Yrs)
PCFTR33b	3.69	3280 +/- 30 BP
PCFTR33d	4.81	3430 +/- 30 BP

GSA
CM
IN
mm
09.11.2014

09.11.2014

TEST PIT PCFT34

Date: 11 September, 2014
Location: 5656148 N 622507 E; upper pit is 8 m away from lower pit
Equipment: Excavator
Elevation: 1296 m asl
Logged by: Shirley McCuaig, Renee Vandermause
Total Depth: 4.25 m (not recorded, approximate)

Depth From (m bgs)	Depth To (m bgs)	Lithologic Description
0	0.25	UNIT 1: TOPSOIL Forest floor and topsoil, *could not identify nearest channel on ground*
0.25	1.25	UNIT 2: DEBRIS FLOOD Sandy gravel, Dmax=30 cm, Davg=8 cm, rounded to angular, mainly subrounded to subangular, loose, poorly sorted *P1386*
1.25	1.68	UNIT 3: FLUVIAL/PALEOSOL Silty clay and clayey silt layers, some charcoal in a layer at 1.26 m; SamplePCFTR34a *P1387*
1.68	4.25	UNIT 4: DEBRIS FLOOD Sandy cobble/boulder gravel, matrix supported, vague horizontal bedding, rounded to angular, mostly subangular, *sharp contact*, Dmax=18 cm, Davg=8 cm *P1392-95*

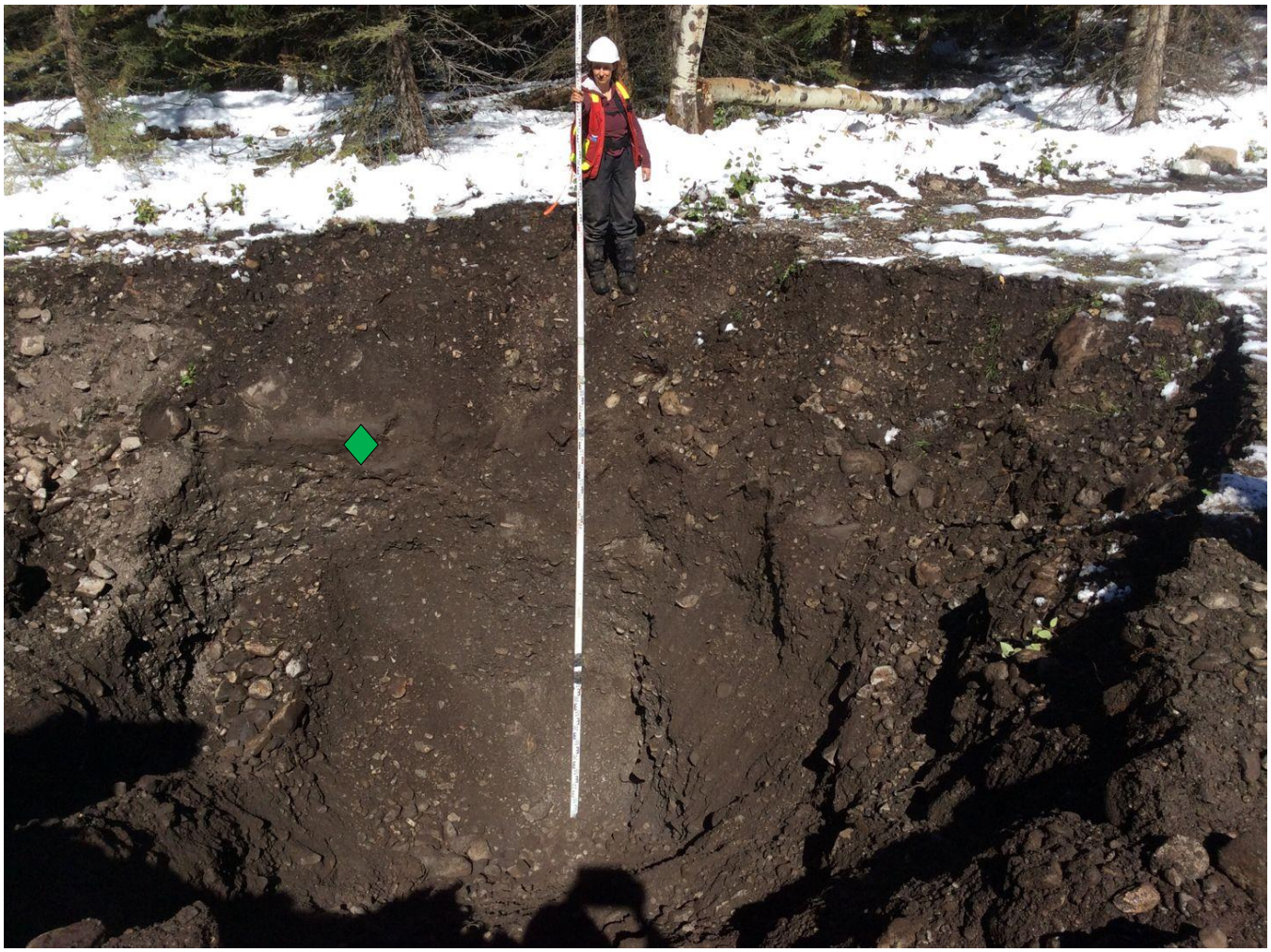

Sample	Depth (m bgs)	Age (^{14}C Yrs)
PCFTR34a	1.26	1820 +/- 30 BP

Possible coal found in Sample PCFTR34a by Beta Analytic – may be some coal contamination despite dating the pieces that most resembled charcoal

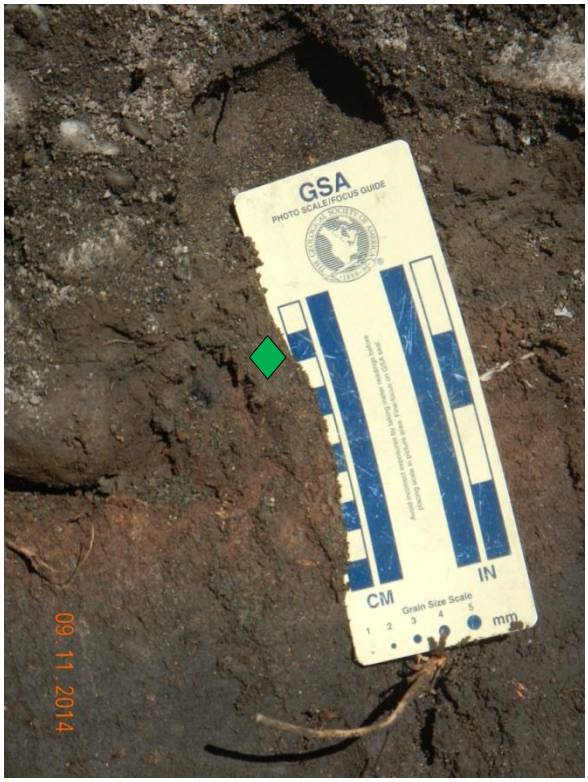
GSA
PHOTO SCALE/FOCUS GUIDE
CM
IN
Grain Size Scale
mm
09. 11. 2014

TEST PIT PCFT35

Date: 11 September, 2014
Location: 5655905 N 623102 E
Equipment: Excavator
Elevation: 1294 m asl
Logged by: Shirley McCuaig, Renee Vandermause
Total Depth: 7.25 m (not recorded, approximate)

Depth From (m bgs)	Depth To (m bgs)	Lithologic Description
0	0.54	UNIT 1: TOPSOIL Upper portion of excavation) Grass over organic silt
0.54	0.97	UNIT 2: DEBRIS FLOOD Sandy gravel, matrix supported, medium to coarse sand matrix, sharp contact, subrounded to angular in about equal amounts, Dmax=10 cm *P1405*
0.97	2.12	UNIT 3: DEBRIS FLOOD Sandy cobble gravel, fine to coarse sand matrix, lens of medium sand and silt, vaguely bedded, rounded to angular, mainly subrounded, Dmax=10 cm, medium brown colour
2.12	3.02	UNIT 4: FLUVIAL/PALEOSOL Silt/fine sand/coarse sand beds and laminations, paleosol with dark brown charcoal at 2.25 m, organic layer at 2.47 m; Sample PCFTR35a at 2.25 m; Sample PCFTR35b at 2.47 m; paleosol at 2.57 m, includes fragile charcoal, good sample, Sample PCFTR35c; organic layer (paleosol?) at 2.79 m, contains dark brown charcoal; small pocket of dark disseminated material (charcoal?) at 2.8-3.02 m
3.02	5.64	UNIT 5: DEBRIS FLOOD (Lower portion pit) Sandy pebble gravel, matrix supported, sharp contact, subrounded to angular, mainly subangular, irregular bedding, Dmax=6 cm, Davg=2 cm *P1398-99*
5.64	7.25	UNIT 6: DEBRIS FLOOD Sandy pebble/cobble gravel, matrix supported, 10% clast supported, rounded to subangular, mostly subangular, Dmax=10 cm, hit water table at 7.23 m *(P1400-01),* lens of fine sand/silt beds (20 cm maximum thickness) at 5.89 m, contains disseminated charcoal Sample PCFTR35d at 5.99 m

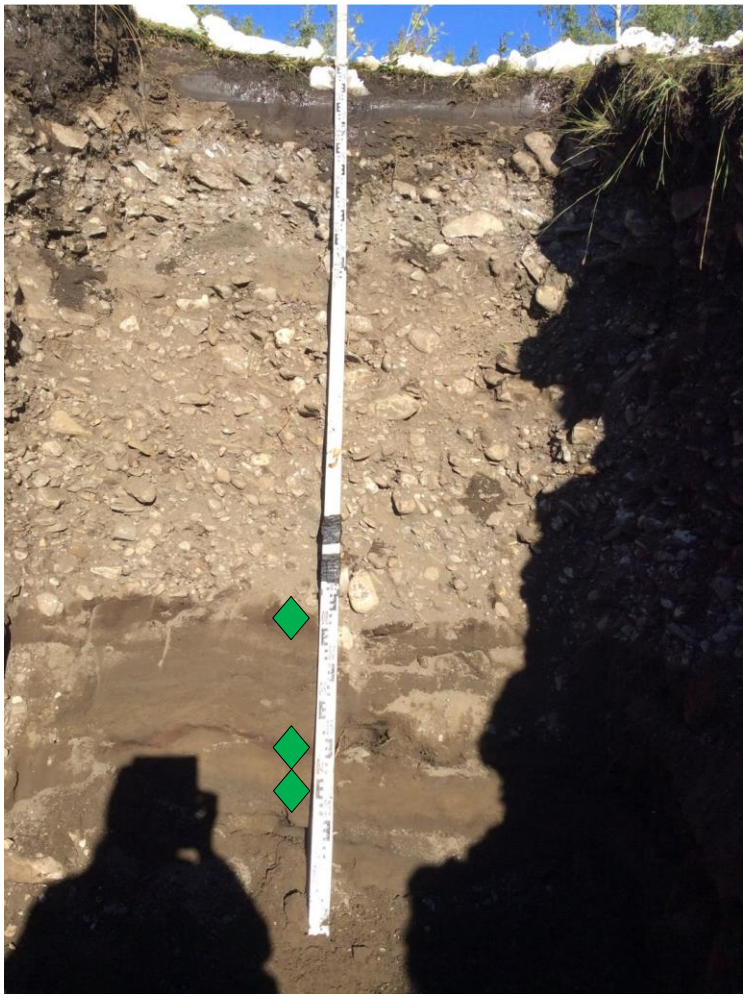

Sample	Depth (m bgs)	Age (^{14}C Yrs)
PCFTR35a	2.25	2520 +/- 30 BP
PCFTR35b	2.47	3780 +/- 30 BP
PCFTR35c	2.57	2510 +/- 30 BP
PCFTR35d	5.99	2890 +/- 30 BP

Possible coal found in sample PCFTR35b by Beta Analytic – “looked to be either some obsidian or perhaps coal flakes[3]”, therefore there may be some coal contamination despite dating the pieces that most resembled charcoal.

[3] Email from Ron Hatfield, Beta Analytic

TEST PIT PCFT36

Date: 12 September, 2014
Location: 5655755 N 621644 E
Equipment: Excavator
Elevation: 1297 m asl
Logged by: Mike Harvey, Renee Vandermause
Total Depth: 4.38 m (not recorded, approximate)

Depth From (m bgs)	Depth To (m bgs)	Lithologic Description
0	0.24	UNIT 1: TOPSOIL Grass, forest floor, organic silt
0.24	0.89	UNIT 2: DEBRIS FLOOD Sandy pebble/cobble gravel, matrix supported, fine to medium sand matrix, white (carbonate?) coating on clasts, loose, crude horizontal bedding, Dmax=13 cm
0.89	0.94	UNIT 3A: FLUVIAL Sandy silt
0.94	1.02	UNIT 3B: FLUVIAL Coarse sand, fine gravel
1.02	1.25	UNIT 3C: FLUVIAL Beds of very fine, fine to medium and silty sand, 2-15 cm thick
1.25	1.37	UNIT 3D: FLUVIAL Fine sand, ripple marks
1.37	1.5	UNIT 3E: FLUVIAL Medium to coarse sand and fine gravel
1.5	1.87	UNIT 4: FLUVIAL/PALEOSOL Medium to coarse sand and silty fine sand beds; Sample PCFTR36a; Sample PCFTR36b: wood
1.87	2.74	UNIT 5: DEBRIS FLOOD Sandy gravel, matrix supported, fine to medium sand matrix, some carbonate coating on gravel clasts, subrounded to subangular, crude bedding, sharp contact, Dmax=13 cm, Davg=25 cm
2.74	3.88	UNIT 6: FLUVIAL Beds of fine sand, silty sand, medium to coarse sand and fine gravel
3.88	4.08	UNIT 7: FLUVIAL/PALEOSOL Silty sand, sharp contact; Sample PCFTR36c at base of unit
4.08	4.38	UNIT 8: DEBRIS FLOOD Sandy cobble gravel, matrix supported, one layer of small boulders, Dmax=30 cm

Sample	Depth (m bgs)	Age (^{14}C Yrs)
PCFTR36b	1.58	850 +/- 30 BP
PCFTR36c	4.06	14380 +/- 50 BP

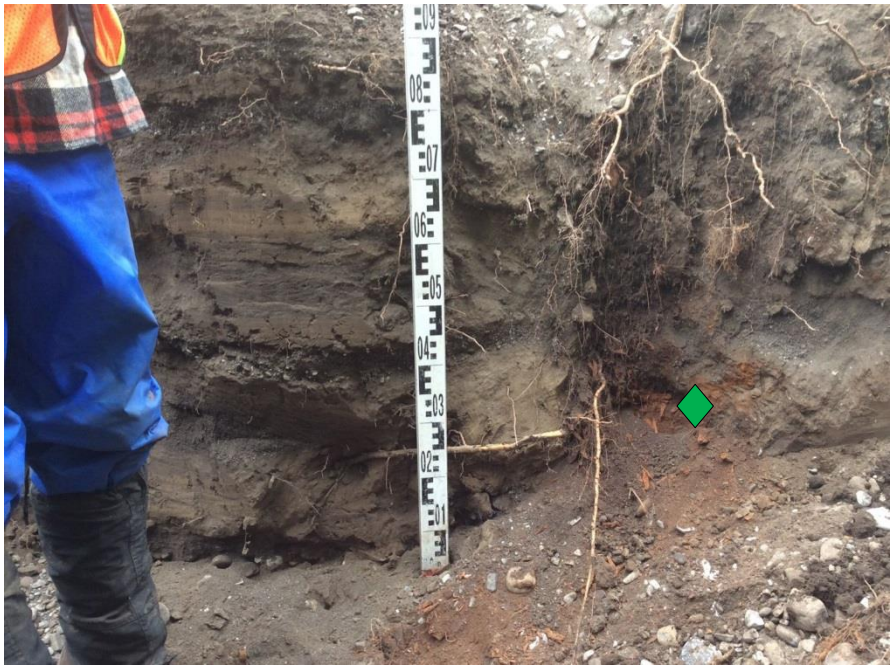

No evidence of contamination was identified in Sample PCFTR36c; however, this was the only Sample not containing wood or charcoal; therefore organic sediment was dated. Could contain microscopic coal.

TEST PIT PCFT37

Date: 12 September, 2014
Location: 5655882 N 621647 E
Equipment: Excavator
Elevation: 1295 m asl
Logged by: Shirley McCuaig, Jamie Stirling, Mike Harvey, Renee Vandermause
Total Depth: 3.3 m (not recorded, approximate)

Depth From (m bgs)	Depth To (m bgs)	Lithologic Description
0	0.43	UNIT 1A: FLUVIAL Fine sand, pebble lens, medium grey, Dmax=9 cm
0.43	0.63	UNIT 1B: FLUVIAL Very fine sandy silt, trace pebbles, dark brown
0.63	0.68	Burn layer
0.68	2.26	UNIT 2: FLUVIAL/PALEOSOL Beds of fine silty sand and silt; Sample PCFTR37aa at 0.97m; Sample PCFTR37a at 1.61 m in charcoal pocket; Sample PCFTR37b at 2.26 m (charcoal)
2.26	2.56	UNIT 3A: FLUVIAL Medium to coarse sand, clean
2.56	2.96	UNIT 3B: FLUVIAL Fine sand, silty, saturated, hit water table at 2.96 m
2.96	3.3	UNIT 4: GLACIOLACUSTRINE Clay

TEST PIT PCFT38

Date: 12 September, 2014
Location: 5655282 N 622426 E
Equipment: Excavator
Elevation: 1324 m asl
Logged by: Shirley McCuaig
Total Depth: 3.9 m (not recorded, approximate)

Depth From (m bgs)	Depth To (m bgs)	Lithologic Description
0	1.62	UNIT 1: 2013 DEBRIS FLOOD Sandy gravel, matrix supported, a few clast supported lenses, vaguely horizontally bedded to dipping beds, clasts mainly subround to subangular, but some very angular (VA ones are limestone clasts from the quarry which make up about 30% of deposit). Rock types include sandstone, limestone, limestone conglomerate, red sandstone and siltstone. Dmax=15 cm. Contains large and small trees and roots at various levels within unit. One is upright and in situ, with a root structure indicative of creekside location. Forest floor litter identified at 1.47 m. These indicate the old floodplain surface at 1.47 to 1.62 m.
1.62	2.0	UNIT 2: DEBRIS FLOOD Silty fine sand lens, well sorted, measured at point of maximum thickness. Contains small woody bits and some charcoal at approximately same level as tree – may be the old creek bank. Wood appears older than the modern wood.
2.0	3.9	UNIT 3: DEBRIS FLOOD Sandy gravel as in Unit 1, but more boulders, indistinct undulating beds, medium to coarse sand matrix, clasts rounded to angular but angular and rounded very minor, some rusty stained crumbling siltstone clasts. Dmax=25 cm. At 2.51 m, a piece of older looking solid wood; Sample PCFTR38. Roots in this zone are less than 0.5 cm in diameter; wood is 4X4X11 cm. There are a number of other wood fragments in this layer, which is about 15 cm thick.

Sample	Depth (m bgs)	Age (^{14}C Yrs)
PCFTR38	2.51	modern

TEST PIT PCFT39

Date: 12 September, 2014
Location: 5655449 N 622236 E
Equipment: Excavator
Elevation: 1317 m asl
Logged by: Shirley McCuaig, Jamie Stirling, Mike Harvey, Renee Vandermause
Total Depth: 7 m (not recorded, approximate)

Depth From (m bgs)	Depth To (m bgs)	Lithologic Description
0	1.7	UNIT 1: DEBRIS FLOOD Sandy pebble/cobble gravel, matrix supported, sand matrix, angular to subround, mostly angular, Dmax=16 cm (up to 1 m on surface), Davg=4 cm
1.7	2.36	UNIT 2: FLUVIAL Lens of coarse sand and fine gravel grading up to medium to coarse sand, vaguely bedded
2.36	3.0	UNIT 3: DEBRIS FLOOD Sandy pebble/cobble gravel, same as Unit 1
3.0	5.0	UNIT 4: DEBRIS FLOOD Sandy pebble/cobble gravel, matrix supported, coarse sand matrix, with fine gravel lens, possible disturbance between 3.0 and 3.7 m from initial excavation for pit
5.0	7.0	UNIT 5: DEBRIS FLOOD Sandy pebble/cobble/boulder gravel, matrix supported, beds of fine gravel and gravel, subangular but becoming more rounded towards base, Dmax=36 cm but few boulders and most are less than 18 cm

EXPOSURE PCF40

Date: 12 September, 2014
Location: 5655441 N 622402 E
Equipment: Shovel
Elevation: 1316 m asl
Logged by: Shirley McCuaig, Jamie Stirling
Total Depth: 2 m (not recorded, approximate)

Depth From (m bgs)	Depth To (m bgs)	Lithologic Description
0	0.05	UNIT 1: TOPSOIL Topsoil
0.05	0.2	UNIT 2: FLUVIAL Organic silt
0.2	2.0	UNIT 3: FLUVIAL Beds of silty sand and sand

EXPOSURE PCU40

Date: 12 September, 2014
Location: 5653825 N 622395 E
Equipment: Trowel
Elevation: 1398 m asl
Logged by: Shirley McCuaig, Jamie Stirling
Total Depth: 1.42 m (not recorded, approximate)

Depth From (m bgs)	Depth To (m bgs)	Lithologic Description
0	0.05	UNIT 1: TOPSOIL Topsoil
0.05	1.12	UNIT 2: DEBRIS FLOOD Sandy gravel, matrix supported, poorly sorted, pebbles, cobbles and occasional boulders, clasts subround to angular, mainly subangular
1.12	1.42	UNIT 5: FLUVIAL/PALEOSOL Undulating beds of silt and sand, 1 to 2 cm thick dark brown organic layers at 1.15 m, 1.27 m and 1.32 m. Sample PCUR40: charcoal with some sand and silt, from 1.32 m.

Sample	Depth (m bgs)	Age (^{14}C Yrs)
PCUR40	1.32	2010 +/- 30 BP

EXPOSURE PCU41a

Date: 13 September, 2014
Location: 5651687 N 626159 E
Equipment: None, natural exposure
Elevation: 1705 m asl
Logged by: Shirley McCuaig, Jamie Stirling
Total Depth: 3.4 m (not recorded, approximate)

Depth From (m bgs)	Depth To (m bgs)	Lithologic Description
0	0.15	UNIT 1: TOPSOIL Moss
0.15	3.4	UNIT 2: DEBRIS SLIDE/DEBRIS FLOW 3 m high vertical headscarp of recent slide in tributary valley with no stream at present: Till, matrix supported, clasts mostly angular, Dmax = 1 m, 40% clasts, matrix silty sand with some clay, mostly limestone, some siltstone, minor sandstone, 5% striated clasts. Debris flow below formed in gully from debris slide material above, moss covered cutbank downstream from this location suggests site is an old flow path.

EXPOSURE PCU41b

Date: 13 September, 2014
Location: 5652968 N 622893 E
Equipment: Natural exposure, trowel for sampling
Elevation: 1461 m asl
Logged by: Shirley McCuaig, Jamie Stirling
Total Depth: 1.93 m (not recorded, approximate)

Depth From (m bgs)	Depth To (m bgs)	Lithologic Description
0	0.25	UNIT 1: TOPSOIL Forest floor litter
0.25	0.55	UNIT 2: FLOOD Pebble-cobble gravel, clast supported, moderately well sorted, 90% clasts, subround to subangular, mainly subround, coarse sand bed at base
0.55	0.63	UNIT 3: PALEOSOL Silt, dark brown organic layer at 0.59. Sample PCUR41: organic silt.
0.63	1.93	UNIT 4: DEBRIS FLOOD Mainly matrix supported but about 10% clast supported, subround to subangular, mainly subround, moderately sorted, Dmax=110+ cm, Davg=8 cm

EXPOSURE PCU42

Date: 14 September, 2014
Location: 5653676 N 622441 E
Elevation: 1402 m asl
Equipment: Trowel, shovel
Logged by: Shirley McCuaig, Jamie Stirling
Total Depth: 1.3 m (not recorded, approximate)

Depth From (m bgs)	Depth To (m bgs)	Lithologic Description
0	0.04	UNIT 1: TOPSOIL Moss
0.4	1.0	UNIT 2: DEBRIS FLOOD Sandy gravel, matrix supported, poorly sorted, vaguely horizontally bedded, pebbles, cobbles and occasional boulders, clasts subround to subangular, mainly subangular; some lenses of fine to medium sand
1.0	1.2	UNIT 3: FLUVIAL/PALEOSOL Bedded fine and medium sand, dark brown organic layer at 1.15. Sample PCUR42: organic silt with some charcoal.
1.2	1.3	UNIT 4: FLUVIAL Bedded sandy gravel and coarse sand

TEST PIT PCFT43

Date: 15 September, 2014
Location: 5656048 N 622266 E
Elevation: 1299 m asl
Equipment: Excavator
Logged by: Shirley McCuaig, Jamie Stirling
Total Depth: 3.3 m (not recorded, approximate)

Depth From (m bgs)	Depth To (m bgs)	Lithologic Description
0	0.03	UNIT 1: TOPSOIL Forest floor litter
0.03	0.53	UNIT 2: DEBRIS FLOOD Sandy gravel, matrix supported, coarse sand matrix, clasts subround to very angular, Dmax=30 cm, Davg= 5 cm
0.53	1.78	UNIT 3: FLUVIAL/PALEOSOL Silt with interbedded sand of various sizes; black, brown and pink paleosol at 1.61 m; Sample PCFTR43a
1.78	2.18	UNIT 4: DEBRIS FLOOD Large lens of same material as Unit 2
2.18	3.3	UNIT 5: FLUVIAL/DEBRIS FLOW/PALEOSOL Same silt/sand as above, with a few thin beds of Unit 2 sandy gravel, two organic layers and a black and pink paleosol from 2.18 to 2.33; Sample PCFTR43b is from upper organic layer which is immediately below the debris flow layer. Some charcoal present.

Sample	Depth (m bgs)	Age (14C Yrs)
PCFTR43a	1.61	880 +/- 30 BP
PCFTR43b	2.18	1260 +/- 30 BP

APPENDIX C
PHOTOGRAPHS

Photo 36(1): Gravel from 2013 event on floor of old channel and log jam showing minimum water level, looking north.

Photo 34(1): Gravel and tree debris in old channel at same location as above, looking south.

Photo 111(1): 2003 flood deposition near present position of Pigeon Creek. Flow velocity decreased here as flow spread laterally, depositing a thin layer of gravel between the trees.

Photo 7125: Looking upstream at aggraded channel.

Photo 7137: Damage to George Biggy Senior Road.

Photo 43(1): New position of Pigeon Creek in Thunderstone Quarry, near apex waterfall, looking north. Note limestone block riprap placed on west bank by Thunderstone Quarry operator.

Photo 46(1): Pigeon Creek, immediately south of apex waterfall, looking north toward falls. Creek has eroded down to bedrock and approximate height of maximum flood is shown by bare bedrock areas.

Photo 45(3): Flood damage to older tree, just south of location above. This damage is older than the 2013 event.

Photo 213(2): Log jam against trees and flood damage on trees above jam. The logs and damage are from the 2013 event and show the minimum flood level above the current creek surface. Looking north with waterfall drop off in background.

Photo 56(1): Looking downstream showing debris on banks.

Photo 117(1): Older flood damage in upper Pigeon Creek area. Note pebbles held in place by healed bark.

Photo 71(1): Large log jam on Pigeon Creek floodplain, southeast of confluence of Pigeion and West Wind creeks.

Photo 74(1): Aggraded channel.

Photo 221(3): Clast supported boulders and matrix supported finer material in creek exposure.

Photo 87(1): Very friable shale of the Fernie Group overlain by till; both eroded by the 2013 debris flood and therefore both contributing material to it.

Photo 224(1): Youngest debris flood deposit pre-dating the 2013 event.

Photo 93(1): Large log jam on West Wind Creek near its confluence with Pigeon Creek

Photo 155(4): We probably have a better pic of this from the air. will have a look at my photos.

Photo 123(3): Log jam downstream of large debris slide area in upper Pigeon Creek valley

Photo 126(1): Aggraded channel.

Photo 132(1): Log jam in central Pigeon Creek valley.

Photo 180(2): Tree debris derived directly from debris slide in background. Looking southwest, central Wind Creek.

Photo 185(1): Tree debris derived directly from debris slide in background. Looking west, central Wind Creek.

Photo 189(4): Sediment wedge from 2013 event, burying coniferous trees on Wind Creek floodplain, just northwest of the steeply sloped Wind Creek valley.

Photo 198(5): Debris flood deposits on wider part of Wind Creek floodplain, southeast of its confluence with West Wind Creek, looking west.

Photo 199(1): Debris flood deposits on wider part of Wind Creek floodplain, closer to the confluence with West Wind Creek, looking northwest.

Photo 136(2): Debris at toe of slide.

Photo 139(1): Aggraded channel.

Photo 154(1): Coring an older tree among younger ones, northwestern reach of Pigeon Creek.

Photo 167(2): Thick till exposure formed by debris slide processes, central Wind Creek valley.

Photo 168(4): Debris at toe of slide.

Photo 171(11): Thick till deposit downstream of image above, and sediment wedge from 2013 event on left.

Photo 171(6): Debris slide exposing thick till unit, central Wind Creek valley.

Photo 171(9): Small log jam and sediment wedges in same location as above two images.

Photo 173(1): Debris slide in till, with fallen trees from slope resting at base of slide, central Wind Creek valley.

Photo 176(1): Aggraded channel.

Photo 178(1): Gully slide in tributary.

Photo 179(1): Failed slope in creek.

Photo 157(1): Slope failure.

Photo 157(3): Slope failure.

Photo 157(6): Aggraded channel.

Photo 157(8): Large debris slide exposing thick till unit, upper Wind Creek valley, looking west.

Photo 158(4): Log jam immediately downstream of large slide shown in Photo 157 (8).

Photo 158(5): Log jam immediately downstream of large slide shown in Photo 157 (8).

Photo 159(1): Log jam still further downstream from slide shown in Photo 157(8).

Photo 167(3): Aggraded channel.

Photo 165(3): Aggraded channel.

Photo 7130: Looking downstream at the inlet of the upstream pair of Highway 1 culverts.

APPENDIX D
BEDLOAD TRANSPORT ANALYSIS

BEDLOAD TRANSPORT CALCULATIONS - EVENT OF JUNE 2013

densitity of fluid (ton/m3)	1
S	0.14
S'	0.050577396
n	0.035
ntot	0.069
D50 (mm)	25
D90(mm)	1000
exp	1.5
W (m)	3

Critical Discharge to Mobilize Sediment

$q_c = 0.065(s-1)^{1.67}\sqrt{g}D_{50}^{1.5}S^{-1.12}$

qc (d50)	0.016786927

Observed	116,000.00	116,000.00
Ratio Com	1.192193867	1.034770839
	1.034770839	1.034770839

Pigeon Creek Mainstem

	FLOW	Qb	Uncorrected Loadings for Energy						Corrected Loadings for Energy					
IDs:	100_28	100_28	$q_b = 1.5(q-q_c)S^{1.5}$		$q_b = 5.8(q-q_c)S^2$		$q_b = 1.5(q-q_c)S^{1.5}$	$q_b = 5.8(q-q_c)S^2$	$q_b = 1.5(q-q_c)S^{1.5}$		$q_b = 5.8(q-q_c)S^2$		$q_b = 1.5(q-q_c)S^{1.5}$	$q_b = 5.8(q-q_c)S^2$
Date/Time	Flow	Flow												
M/d/yyyy	m³/s	m³/s	qb (m³/s)	qb (kg/s)	qb (m³/s)	qb (kg/s)	636,886.77	921,431.34	qb (m³/s)	qb (kg/s)	qb (m³/s)	qb (kg/s)	138,294.49	120,033.42
6/19/2013 14:19	8.725918	2.908639333												
6/19/2013 15:00	8.681882	2.893960667	0.67822	1797.283259	0.981231	2600.263031			0.147269666	390.26461	0.12871771	341.1019		
6/19/2013 16:00	8.544328	2.848109333	0.667412	1768.64132	0.965594	2558.824613	6418664.243	9286357.758	0.144922741	384.04526	0.128064356	339.3705	1393757.779	1224850.452
6/19/2013 17:00	8.526532	2.842177333	0.666014	1764.93578	0.963571	2553.463532	6360438.78	9202118.661	0.144619108	383.24064	0.126023491	333.9623	1381114.62	1211999.029
6/19/2013 18:00	8.557087	2.852362333	0.668414	1771.298041	0.967045	2562.668287	6365220.877	9209037.275	0.145140433	384.62215	0.125759455	333.2626	1382153.011	1201004.653
6/19/2013 19:00	8.942207	2.980735667	0.698675	1851.488972	1.010825	2678.686457	6521016.623	9434438.54	0.15171129	402.03492	0.126212794	334.4639	1415982.718	1201907.629
6/19/2013 20:00	13.22236	4.407453333	1.034987	2742.71627	1.497393	3968.091109	8269569.437	11964199.62	0.224738591	595.55727	0.131926752	349.6059	1795665.935	1231325.633
6/19/2013 21:00	20.86435	6.954783333	1.635455	4333.956139	2.366134	6270.25588	12738010.34	18429024.58	0.35512503	941.08133	0.195430626	517.8912	2765949.474	1561494.689
6/19/2013 22:00	27.67056	9.22352	2.170252	5751.167194	3.139864	8320.640255	18153222	26263613.04	0.471251521	1248.8165	0.308813481	818.3557	3941816.149	2405244.389
6/19/2013 23:00	33.90999	11.30333	2.660514	7050.361484	3.849163	10200.28102	23042751.62	33337658.3	0.5777077	1530.9254	0.409796017	1085.959	5003535.485	3427767.304
6/20/2013 0:00	34.35471	11.45157	2.695458	7142.96252	3.899718	10334.25381	25547983.21	36962162.7	0.585295443	1551.0329	0.502369337	1331.279	5547524.995	4351028.738
6/20/2013 1:00	33.0363	11.0121	2.591864	6868.438927	3.749842	9937.080162	25220522.6	36488401.15	0.562800938	1491.4225	0.508967569	1348.764	5476419.739	4824077.044
6/20/2013 2:00	33.42755	11.14251667	2.622606	6949.906267	3.794319	10054.94501	24873021.35	35985645.3	0.569476384	1509.1124	0.489406553	1296.927	5400962.828	4762244.564
6/20/2013 3:00	31.66849	10.55616333	2.484388	6583.629106	3.594349	9525.024664	24360363.67	35243945.41	0.539463578	1429.5785	0.49521146	1312.31	5289643.619	4696627.923
6/20/2013 4:00	30.4348	10.14493333	2.387451	6326.746185	3.454103	9153.373084	23238675.52	33621115.95	0.518414552	1373.7986	0.469112598	1243.148	5046078.677	4599825.756
6/20/2013 5:00	31.28983	10.42994333	2.454635	6504.783296	3.551303	9410.952581	23096753.07	33415786.2	0.53300294	1412.4578	0.450808557	1194.643	5015261.435	4388023.909
6/20/2013 6:00	34.74311	11.58103667	2.725976	7223.836424	3.943872	10451.26009	24711515.5	35751982.8	0.591922263	1568.594	0.463494486	1228.26	5365893.22	4361225.517
6/20/2013 7:00	42.79964	14.26654667	3.359016	8901.393152	4.859738	12878.30586	29025413.24	41993218.71	0.729381519	1932.861	0.514730192	1364.035	6302619.041	4666131.713
6/20/2013 8:00	57.14947	19.04982333	4.486551	11889.36116	6.491027	17201.22085	37423357.75	54143148.09	0.974216075	2581.6726	0.634263504	1680.798	8126160.521	5480699.927
6/20/2013 9:00	76.25542	25.41847333	5.987798	15867.66385	8.662991	22956.9265	49962645	72284665.23	1.300198807	3445.5268	0.847169397	2244.999	10848958.98	7066434.935
6/20/2013 10:00	85.82645	28.60881667	6.739839	17860.57466	9.751026	25840.21843	60710829.31	87834860.87	1.463498224	3878.2703	1.130641002	2996.199	13182834.84	9434155.599
6/20/2013 11:00	79.37601	26.45867	6.232997	16517.44319	9.01774	23897.01048	61880432.12	89527012.04	1.353441825	3586.6208	1.272644683	3372.508	13436804.04	11463672.72
6/20/2013 12:00	63.47858	21.15952667	4.98386	13207.22891	7.21052	19107.8779	53504409.77	77408799.08	1.08220236	2867.8363	1.176940644	3118.893	11618022.77	11684522.01
6/20/2013 13:00	44.90788	14.96929333	3.524671	9340.377702	5.099403	13513.41738	40585691.89	58718331.5	0.76535198	2028.1827	0.941073284	2493.844	8812834.202	10102926.44
6/20/2013 14:00	30.17762	10.05920667	2.367244	6273.195333	3.424867	9075.897095	28104431.46	40660766.05	0.514026587	1362.1705	0.665543088	1763.689	6102635.764	7663560.094
6/20/2013 15:00	21.40036	7.133453333	1.677572	4445.565874	2.427068	6431.729965	19293770.17	27913728.71	0.364270349	965.31642	0.446992823	1184.531	4189476.383	5306796.297
6/20/2013 16:00	16.53422	5.511406667	1.295216	3432.322469	1.873885	4965.795558	14180199.02	20515545.94	0.281245029	745.29933	0.316766167	839.4303	3079108.352	3643130.381
6/20/2013 17:00	18.70963	6.236543333	1.466148	3885.293373	2.121186	5621.142171	13171708.51	19056487.91	0.318361534	843.65807	0.244568107	648.1055	2860123.307	2677564.487
6/20/2013 18:00	27.6695	9.223166667	2.170168	5750.946477	3.139744	8320.320928	17345231.73	25094633.58	0.471233435	1248.7686	0.276844281	733.6373	3766368.006	2487137.093
6/20/2013 19:00	32.58933	10.86311	2.556743	6775.369388	3.69903	9802.429555	22547368.56	32620950.87	0.555174806	1471.2132	0.40978029	1085.918	4895967.311	3275199.202
6/20/2013 20:00	38.73088	12.91029333	3.039314	8054.182788	4.397201	11652.58378	26693193.92	38619024	0.659960972	1748.8966	0.482774938	1279.354	5796197.659	4257488.436
6/20/2013 21:00	36.85879	12.28626333	2.892215	7664.370155	4.184382	11088.61292	28293395.3	40934154.05	0.628019665	1664.2521	0.573896031	1520.824	6143667.636	5040320.52
6/20/2013 22:00	28.4481	9.4827	2.231347	5913.069087	3.228255	8554.875735	24439390.63	35358279.58	0.484517787	1283.9721	0.546120162	1447.218	5306803.645	5342477.238
6/20/2013 23:00	26.35409	8.784696667	2.06681	5477.047553	2.990208	7924.051035	20502209.95	29662068.19	0.448790116	1189.2938	0.42133224	1116.53	4451878.696	4614747.958
6/21/2013 0:00	35.07547	11.69182333	2.752091	7293.041498	3.981654	10551.3842	22986160.29	33255783.43	0.597592938	1583.6213	0.390263784	1034.199	4991247.165	3871313.034
6/21/2013 1:00	41.8561	13.95203333	3.284878	8704.926202	4.752476	12594.06255	28796341.86	41661804.16	0.713282987	1890.1999	0.519661358	1377.103	6252878.16	4340342.927
6/21/2013 2:00	39.1824	13.0608	3.074792	8148.199743	4.44853	11788.60508	30335626.7	43888801.73	0.667664735	1769.3115	0.620264368	1643.701	6587120.635	5437445.712
6/21/2013 3:00	34.48796	11.49598667	2.705928	7170.708266	3.914866	10374.39564	27574034.42	39893401.29	0.587568934	1557.0577	0.580595153	1538.577	5987464.603	5728099.913
6/21/2013 4:00	32.14109	10.71369667	2.521523	6682.035406	3.648074	9667.396359	24934938.61	36075225.6	0.547527005	1450.9466	0.510944576	1354.003	5414407.629	5206644.507

6/21/2013 5:00	36.37036	12.12345333	2.853837	7562.667681	4.128858	10941.4724	25640465.56	37095963.78	0.619686149	1642.1683	0.47612448	1261.73	5567606.742	4708319.399
6/21/2013 6:00	41.5466	13.84886667	3.260559	8640.481112	4.717292	12500.82506	29165667.83	42196135.43	0.708002346	1876.2062	0.538873412	1428.015	6333074.12	4841539.948
6/21/2013 7:00	42.33706	14.11235333	3.322669	8805.073249	4.807152	12738.95271	31401997.85	45431599.99	0.721489051	1911.946	0.615672371	1631.532	6818673.965	5507183.385
6/21/2013 8:00	42.72579	14.24193	3.353214	8886.015866	4.851343	12856.0584	31843960.41	46071020.01	0.728121502	1929.522	0.627400286	1662.611	6914642.336	5929456.573
6/21/2013 9:00	38.46894	12.82298	3.018732	7999.640794	4.367424	11573.67383	30394181.99	43973518.01	0.655491792	1737.0532	0.633167804	1677.895	6599835.412	6012909.792
6/21/2013 10:00	35.61919	11.87306333	2.794814	7406.256635	4.043465	10715.18094	27730615.37	40119938.58	0.606869803	1608.205	0.570009673	1510.526	6021464.812	5739156.568
6/21/2013 11:00	37.27637	12.42545667	2.925026	7751.320013	4.231853	11214.40973	27283637.97	39473263.21	0.635144349	1683.1325	0.527728436	1398.48	5924407.509	5236210.779
6/21/2013 12:00	43.98809	14.66269667	3.452399	9148.856054	4.994841	13236.3288	30420316.92	44011329.36	0.749658667	1986.5955	0.552315723	1463.637	6605510.388	5151810.635
6/21/2013 13:00	52.4328	17.4776	4.11594	10907.24088	5.954836	15780.31458	36100974.48	52229958.09	0.893740989	2368.4136	0.651896327	1727.525	7839016.357	5744091.475
6/21/2013 14:00	53.8855	17.96183333	4.230086	11209.72677	6.119979	16217.94336	39810541.76	57596864.29	0.918526729	2434.0958	0.777188997	2059.551	8644517.013	6816736.994
6/21/2013 15:00	54.4432	18.14773333	4.273907	11325.85287	6.183378	16385.9516	40564043.34	58687010.93	0.928042119	2459.3116	0.79874245	2116.667	8808133.405	7517193.004
6/21/2013 16:00	53.41523	17.80507667	4.193134	11111.80563	6.066518	16076.27358	40387785.29	58432005.33	0.910503056	2412.8331	0.807016947	2138.595	8769860.484	7659472.324
6/21/2013 17:00	50.57444	16.85814667	3.96992	10520.28715	5.743577	15220.47991	38937767	56334156.29	0.862033941	2284.3899	0.791765137	2098.178	8455001.473	7626190.541
6/21/2013 18:00	48.27286	16.09095333	3.789073	10041.04472	5.481934	14527.12433	37010397.36	53545687.65	0.822764743	2180.3266	0.749616838	1986.485	8036489.721	7352392.023
6/21/2013 19:00	47.49412	15.83137333	3.727884	9878.892958	5.393407	14292.52735	35855887.82	51875373.04	0.809478003	2145.1167	0.715468702	1895.992	7785797.895	6988458.027
6/21/2013 20:00	48.6179	16.20596667	3.816185	10112.89006	5.521158	14631.06833	35985209.44	52062472.22	0.828651761	2195.9272	0.703914674	1865.374	7813878.973	6770458.706
6/21/2013 21:00	44.97975	14.99325	3.530318	9355.342706	5.107573	13535.06836	35042818.98	50699046.04	0.766578215	2031.4323	0.720588	1909.558	7609246.985	6794877.755
6/21/2013 22:00	36.28815	12.09605	2.847377	7545.549649	4.119512	10916.70648	30421606.24	44013194.71	0.618283494	1638.4513	0.666609411	1766.515	6605790.352	6616931.648
6/21/2013 23:00	28.28977	9.429923333	2.218906	5880.101102	3.210256	8507.178506	24166171.35	34962992.97	0.481816385	1276.8134	0.537653677	1424.782	5247476.426	5744334.929
6/22/2013 0:00	23.61258	7.87086	1.851397	4906.201476	2.678553	7098.165664	19415344.64	28089619.51	0.402014901	1065.3395	0.418983126	1110.305	4215875.234	4563157.55
6/22/2013 1:00	21.54202	7.180673333	1.688703	4475.062778	2.443172	6474.405323	16886275.66	24430627.78	0.36668733	971.72142	0.349588484	926.4095	3666709.639	3666086.58
6/22/2013 2:00	19.04029	6.346763333	1.49213	3954.144468	2.158775	5720.754157	15172573.04	21951287.07	0.324003204	858.60849	0.318867951	845.0001	3294593.843	3188537.197
6/22/2013 3:00	17.10776	5.702586667	1.340282	3551.746822	1.939085	5138.57563	13510604.32	19546793.62	0.291030679	771.2313	0.281750225	746.6381	2933711.619	2864948.701
6/22/2013 4:00	15.69642	5.23214	1.229386	3257.873043	1.778644	4713.406632	12257315.76	17733568.07	0.266950616	707.41913	0.253077619	670.6557	2661570.778	2551128.816
6/22/2013 5:00	14.41683	4.80561	1.128843	2991.432676	1.63318	4327.927585	11248750.3	16274401.59	0.245118452	649.5639	0.232137817	615.1652	2442569.455	2314477.628
6/22/2013 6:00	13.43372	4.477906667	1.051595	2786.726333	1.52142	4031.763732	10400686.22	15047444.37	0.228344783	605.11367	0.213152766	564.8548	2258419.629	2124036.079
6/22/2013 7:00	12.87947	4.293156667	1.008045	2671.318606	1.458413	3864.794811	9824480.889	14213805.38	0.218888256	580.05388	0.198566536	526.2013	2133301.594	1963901.072
6/22/2013 7:47	12.99848	4.332826667	1.017396	2696.099253	1.471942	3900.646811	9661352.145	13977794.92	0.220918786	585.43478	0.190343227	504.4096	2097879.589	1855099.573

APPENDIX E

PIGEON CREEK: AIRBORNE LIDAR CHANGE DETECTION ANALYSIS, BGC ENGINEERING INC

BGC ENGINEERING INC.
AN APPLIED EARTH SCIENCES COMPANY
Suite 600 - 372 Bay Street, Toronto, ON Canada M5H 2W9
Telephone (416) 644-1216 Fax (416) 649-0335

Project Memorandum

To:	**Town of Canmore**	**Doc. No.:**	
Attention:	**Julia Eisl**	**cc:**	
From:	**Matthew Lato and Matthias Jakob**	**Date:**	**July 04, 2016**
Subject:	**Pigeon Creek: Airborne LiDAR Change Detection Analysis - FINAL**		
Project No.:	**1261014**		

1.0 INTRODUCTION

At the request of the Town of Canmore, BGC Engineering Inc. (BGC) carried out a topographic change detection analysis of the Airborne LiDAR Scanning (ALS) datasets of the Pigeon Creek region acquired by the Alberta government and the Town of Canmore in 2009 and 2013, respectively. BGC's change detection aimed to identify areas and calculate volumes of erosion and accumulation along the creek on the fan. It is expected that most of the erosion and accumulation detected in this analysis was caused by the debris flood event that occurred between June 18 to 21 2013. This memorandum summarizes the methods and results.

This work was authorized by Julia Eisl from the Town of Canmore and was completed under the Town of Canmore/BGC Master Consulting Agreement dated July 15, 2013.

2.0 ALS CHANGE DETECTION METHODOLOGY

Analysis of Airborne Laser Scanning (ALS) datasets for spatial change consists of four main steps: (i) a refined spatial alignment of the datasets; (ii) the spatial analysis of change between the datasets; (iii) filtering results; and (iv) calculating volumes. The initial step of re-aligning the ALS data removes georeferencing errors resulting from poor GPS or ground control at the time of data collection, maximizing the ability to detect change between datasets. The Limit of Detectable change (LoD) between datasets is a function of the alignment, data quality, and resolution. The LoD is typically set to two times the standard deviation of the mean error and is written as $LoD_{95\%}$.

2.1. Step 1: Data Re-Alignment

The 2009 and 2013 ALS datasets used in this analysis were supplied to BGC by data registered in UTM Zone 11. The georeferenced accuracy of the ALS data is controlled by the GPS coverage at the time of data collection, and the quantity and accuracy of ground survey control points. The georeferenced accuracy is a measure of the absolute spatial position of the point cloud data, referred to as the network accuracy. The accuracy of each point relative to neighbouring points within the ALS dataset, referred to as local accuracy, is controlled by the accuracy of the LiDAR

sensor and various other onboard navigation sensors. Local accuracy controls the ability to detect relative change between datasets because network accuracies are lower than local accuracies.

The first step in the analysis of the ALS data is to remove local errors through an iterative closest point (ICP) re-alignment process (Besl and McKay 1992). In this analysis, the 2009 ALS point cloud is set as the 'baseline' dataset to which the 2013 datasets are aligned. The ICP alignment minimizes the local errors between the datasets while maintaining the network accuracy of the 2009 dataset. This process is optimized by omitting data points from the 2009 dataset that are known or suspected to have deformed between 2009 and 2013; in this project, all points along the creek and the fan where deposition occurred were removed.

The corrected spatial alignment has a mean error of -0.03 m and a standard deviation of 0.06 m. The $LoD_{95\%}$ is set at 0 +/- 0.15 m.

2.2. Step 2: Spatial Change Detection

The second step in the process uses a point-to-surface analysis for the spatial change detection. The point-to-surface analysis is conducted by converting the 2009 baseline ALS dataset from a 3D point cloud to a 3D surface model; the resultant surface model is used as the baseline to assess the 2013 datasets for change. Any change in excess of the $LoD_{95\%}$ to the topography, as represented by the ALS data, will be identified by the algorithm and interpreted as change.

Changes in the topography can be positive or negative with respect to the baseline dataset (Figure 2-1). Positive change represents zones of accumulation with respect to the baseline surface, e.g. deposition of material on the fan. Conversely, negative change represents zones of ablation with respect to the baseline surface, e.g. erosion of creek banks (blue zone in Figure 2-1).

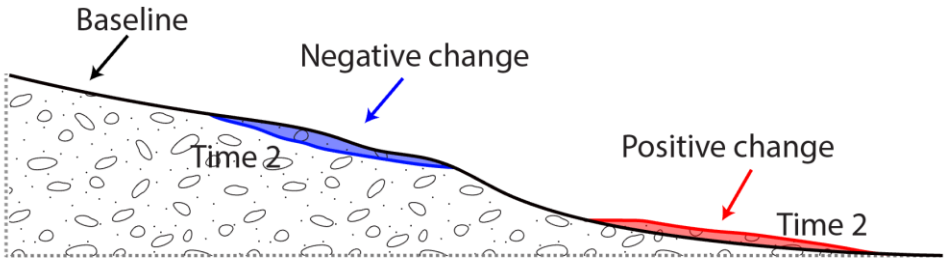

Figure 2-1. Schematic of change detection analysis illustrating zones of loss and accumulation

3.0 RESULTS

For the assessment of volumetric change along Pigeon Creek the region was separated into regions of suspected change and stable regions. This was done through visual examination of the datasets, orthophotos, site specific knowledge, and expert judgement. Figure 3-1 identifies the region in which the change detection analysis was completed. The combined area of the region mapped for change is approximately 165,000 m^2.

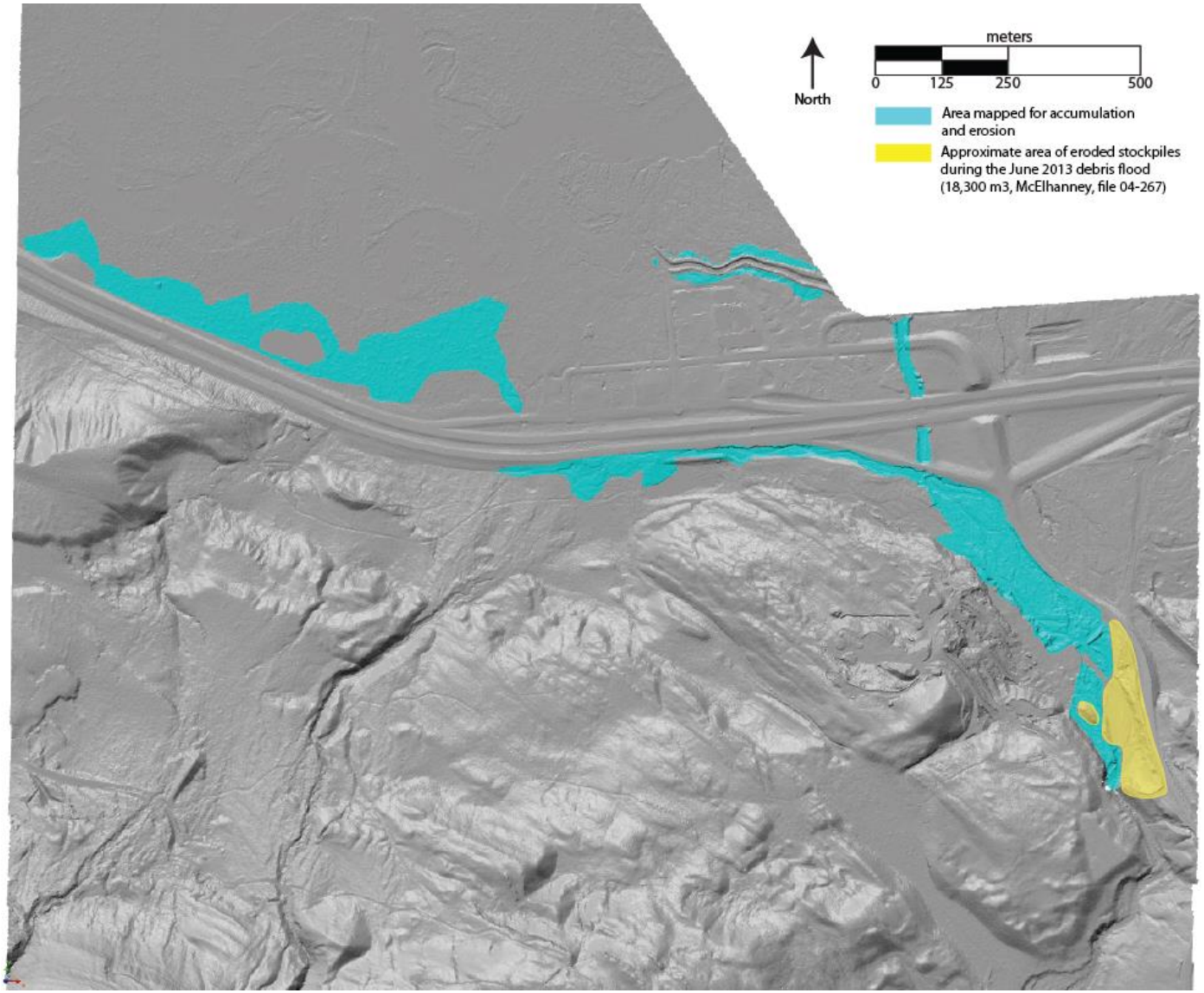

Figure 3-1. Isolated regions used for the calculation of material accumulation and erosion. LiDAR information is absent for the top (northern edge of the fan)

The calculation of material sourced from the Pigeon Creek channel upstream of the fan apex and deposited on the fan is summarized as:

Volume of Accumulation – Volume of Loss – Material Eroded from the quarry

The results of the shortest distance change detection results are reported as an isopach map in Figure 3-2 and numerically in Table 3-1. The material from the quarry's stockpiles were subtracted from the net change because the stockpile had not been included in the delineation of the areas for change detection which underwent erosion and deposition. Since quarry stockpile material was eroded and subsequently deposited downstream, it is part of the 107,000 m^3 of accumulation volume that was determined from the analysis and reported in Table 3-1.

Table 3-2. Volumetric change detection results and error analysis

Change Type	Measurement
Positive (accumulation)	107,000 m^3
Negative (erosion)	21,500 m^3
Material from Quarry*	18,300 m^3
Area	165,000 m^2
Net Change	**67,200**
+/- (to one standard deviation)	**9,900**

***McElhanney File 04-267**

3.1. Limitations

There are three main sources of limitation in the analysis of the ALS data for spatial change:

1. Time delay between the collection of the 2009 ALS data and the flood event. Any material accumulated or removed on the fan post the 2009 ALS data collection and prior to the 2013 debris flood are indistinguishable from material accumulation or erosion due to the debris flood event.
2. Time delay between the 2013 flood event the collection of the 2013 ALS dataset. Any material transported off site post the 2013 debris flood but prior to the 2013 ALS data collection would reduce the amount of accumulated material in the analysis.
3. Material deposited underwater cannot be assessed with ALS. Therefore, the finer-grained sediment that discharged into Bow River, are not included in this analysis. Given the distal nature of the confluence of Pigeon Creek with Bow River, BGC believes that this is likely a small percentage of the total sediment transport.

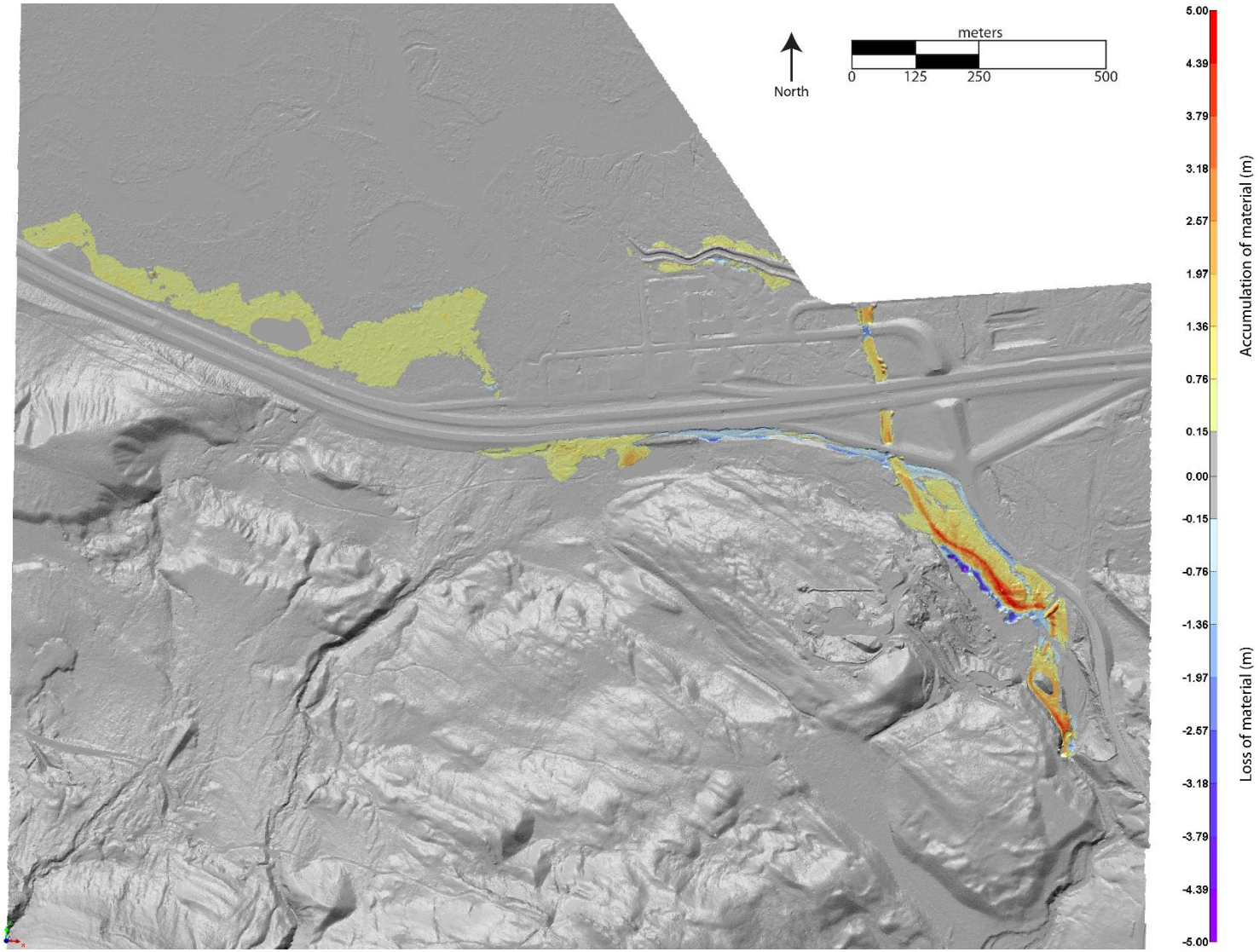

Figure 3-2. Isopach of material accumulation (warm colours) and material erosion (cool colours)

4.0 CLOSURE

BGC Engineering Inc. (BGC) prepared this document for the account of the Town of Canmore. The material in it reflects the judgment of BGC staff in light of the information available to BGC at the time of document preparation. Any use which a third party makes of this document or any reliance on decisions to be based on it is the responsibility of such third parties. BGC accepts no responsibility for damages, if any, suffered by any third party as a result of decisions made or actions based on this document.

As a mutual protection to our client, the public, and ourselves, all documents and drawings are submitted for the confidential information of our client for a specific project. Authorization for any use and/or publication of this document or any data, statements, conclusions or abstracts from or regarding our documents and drawings, through any form of print or electronic media, including without limitation, posting or reproduction of same on any website, is reserved pending BGC's written approval. A record copy of this document is on file at BGC. That copy takes precedence over any other copy or reproduction of this document.

Yours sincerely,

BGC ENGINEERING INC.
per:

Matthew Lato, Ph.D. Eng., P.Eng. (ON, BC, NL)
Senior Geotechnical Engineer

Matthias Jakob, Ph.D. P.Geo. (BC, AB)
Principal Geoscientist

Reviewed by:

Michael Porter, M.Eng., P.Eng (BC, AB)

ML/MJ/mjp/md

APPENDIX F
TETRA TECH EBA'S GENERAL CONDITIONS

GENERAL CONDITIONS

HYDROTECHNICAL

This report incorporates and is subject to these “General Conditions”.

1.1 USE OF REPORTS AND OWNERSHIP

This report pertains to a specific site, a specific development, and a specific scope of work. The report may include plans, drawings, profiles and other supporting documents that collectively constitute the report (the “Report”).

The Report is intended for the sole use of TETRA TECH’s Client (the “Client”) as specifically identified in the TETRA TECH Services Agreement or other Contract entered into with the Client (either of which is termed the “Services Agreement” herein). TETRA TECH does not accept any responsibility for the accuracy of any of the data, analyses, recommendations or other contents of the Report when it is used or relied upon by any party other than the Client, unless authorized in writing by TETRA TECH.

Any unauthorized use of the Report is at the sole risk of the user. TETRA TECH accepts no responsibility whatsoever for any loss or damage where such loss or damage is alleged to be or, is in fact, caused by the unauthorized use of the Report.

Where TETRA TECH has expressly authorized the use of the Report by a third party (an “Authorized Party”), consideration for such authorization is the Authorized Party’s acceptance of these General Conditions as well as any limitations on liability contained in the Services Agreement with the Client (all of which is collectively termed the “Limitations on Liability”). The Authorized Party should carefully review both these General Conditions and the Services Agreement prior to making any use of the Report. Any use made of the Report by an Authorized Party constitutes the Authorized Party’s express acceptance of, and agreement to, the Limitations on Liability.

The Report and any other form or type of data or documents generated by TETRA TECH during the performance of the work are TETRA TECH’s professional work product and shall remain the copyright property of TETRA TECH.

The Report is subject to copyright and shall not be reproduced either wholly or in part without the prior, written permission of TETRA TECH. Additional copies of the Report, if required, may be obtained upon request.

1.2 ALTERNATIVE REPORT FORMAT

Where TETRA TECH submits both electronic file and hard copy versions of the Report or any drawings or other project-related documents and deliverables (collectively termed TETRA TECH’s “Instruments of Professional Service”), only the signed and/or sealed versions shall be considered final. The original signed and/or sealed version archived by TETRA TECH shall be deemed to be the original. TETRA TECH will archive the original signed and/or sealed version for a maximum period of 10 years.

Both electronic file and hard copy versions of TETRA TECH’s Instruments of Professional Service shall not, under any circumstances, be altered by any party except TETRA TECH. TETRA TECH’s Instruments of Professional Service will be used only and exactly as submitted by TETRA TECH.

Electronic files submitted by TETRA TECH have been prepared and submitted using specific software and hardware systems. TETRA TECH makes no representation about the compatibility of these files with the Client’s current or future software and hardware systems.

1.3 STANDARD OF CARE

Services performed by TETRA TECH for the Report have been conducted in accordance with the Services Agreement, in a manner consistent with the level of skill ordinarily exercised by members of the profession currently practicing under similar conditions in the jurisdiction in which the services are provided. Professional judgment has been applied in developing the conclusions and/or recommendations provided in this Report. No warranty or guarantee, express or implied, is made concerning the test results, comments, recommendations, or any other portion of the Report.

If any error or omission is detected by the Client or an Authorized Party, the error or omission must be immediately brought to the attention of TETRA TECH.

1.4 ENVIRONMENTAL AND REGULATORY ISSUES

Unless expressly agreed to in the Services Agreement, TETRA TECH was not retained to investigate, address or consider, and has not investigated, addressed or considered any environmental or regulatory issues associated with the project.

1.5 DISCLOSURE OF INFORMATION BY CLIENT

The Client acknowledges that it has fully cooperated with TETRA TECH with respect to the provision of all available information on the past, present, and proposed conditions on the site, including historical information respecting the use of the site. The Client further acknowledges that in order for TETRA TECH to properly provide the services contracted for in the Services Agreement, TETRA TECH has relied upon the Client with respect to both the full disclosure and accuracy of any such information.

1.6 INFORMATION PROVIDED TO TETRA TECH BY OTHERS

During the performance of the work and the preparation of this Report, TETRA TECH may have relied on information provided by persons other than the Client.

While TETRA TECH endeavours to verify the accuracy of such information, TETRA TECH accepts no responsibility for the accuracy or the reliability of such information even where inaccurate or unreliable information impacts any recommendations, design or other deliverables and causes the Client or an Authorized Party loss or damage.

1.7 GENERAL LIMITATIONS OF REPORT

This Report is based solely on the conditions present and the data available to TETRA TECH at the time the Report was prepared.

The Client, and any Authorized Party, acknowledges that the Report is based on limited data and that the conclusions, opinions, and recommendations contained in the Report are the result of the application of professional judgment to such limited data.

The Report is not applicable to any other sites, nor should it be relied upon for types of development other than those to which it refers. Any variation from the site conditions present at or the development proposed as of the date of the Report requires a supplementary investigation and assessment.

It is incumbent upon the Client and any Authorized Party, to be knowledgeable of the level of risk that has been incorporated into the project design, in consideration of the level of the hydrotechnical information that was reasonably acquired to facilitate completion of the design.

The Client acknowledges that TETRA TECH is neither qualified to, nor is it making, any recommendations with respect to the purchase, sale, investment or development of the property, the decisions on which are the sole responsibility of the Client.

1.8 JOB SITE SAFETY

TETRA TECH is only responsible for the activities of its employees on the job site and was not and will not be responsible for the supervision of any other persons whatsoever. The presence of TETRA TECH personnel on site shall not be construed in any way to relieve the Client or any other persons on site from their responsibility for job site safety.